

Molecular mechanisms driving prostate cancer neuroendocrine differentiation

Submitted by
Joseph Edward Sutton

Supervisory team:
Dr Amy Poole (DoS)
Dr Jennifer Fraser
Dr Gary Hutchison

A thesis submitted in partial fulfilment of the requirements of
Edinburgh Napier University, for the award of Doctor of Philosophy.

October 2019

School of Applied Sciences
Edinburgh Napier University
Edinburgh

Declaration

It is hereby declared that this thesis is the result of the author's original research. It has been composed by the author and has not been previously submitted for examination which has led to the award of a degree.

Signed:



Dedication

This thesis is dedicated to my grandfather William 'Harry' Russell, who died of stomach cancer in 2014. Thank you for always encouraging me to achieve my ambitions, believing in me and for retaining your incredible positivity and sense of humour, even at the very end of your life.

Acknowledgements

First of all, I would like to acknowledge my parents, who dedicated so much effort and energy into helping me to achieve my lifelong ambition of becoming a scientist. From taking me to the Natural History and Science Museums in London as a child, to tolerating my obsession with Jurassic Park and continuing to support me in both of your unique yet equally important ways, thank you.

I would also like to thank my PhD supervisors Dr Amy Poole and Dr Jenny Fraser, not only for their excellent scientific guidance but also for their great banter and encouragement along the way. Thank you for seeing some potential in me, taking a chance on me and for helping me to continue my scientific journey. Thank you also to Dr Gary Hutchison and Dr Sharon Vass for their words of wisdom and encouragement.

Thank you to my amazing friends at Edinburgh Napier who are too numerous to mention all by name, in particular Lee Curley, Dave Lawson, Liam Ralph and Alva Smith who are the best friends that anyone could ask for. Thank you all (you know who you are) for making these the best years of my life, I will always remember the impromptu barbecues on the meadows, the PGR conferences, the pub quiz victories and of course the times Lewis climbed the Christmas tree and Lee almost lost his hand. Thank you also to the amazing support staff at Napier, especially Tracy for always wishing us a good day and making sure there was always a hot haggis roll waiting on those freezing winter mornings, it makes a difference. I would also like to acknowledge Gareth Southgate for making us believe that one day, football is coming home. Thanks also to Thom, Jonny, Colin, Ed, Phil and Nigel for the company during long writing sessions and weekends in the lab.

Finally, and most of all, thank you to Sasha Pereira for all of your love, support, patience and belief during these difficult and often uncertain times.

Abstract

Annually, 11,500 men in the UK die of prostate cancer (PCa). PCa tumours are initially dependent upon androgen receptor (AR) signalling and androgen deprivation therapy (ADT) is highly effective in restricting tumour growth. However, ADT resistance and progression to castrate-resistant prostate cancer (CRPC) is inevitable, usually occurring within three years. CRPC is considerably more aggressive, and metastatic CRPC remains incurable. One mechanism of ADT resistance is neuroendocrine differentiation (NED). NED is common in PCa tumours treated with ADT (30% of cases) and is associated with poorer survival. Prevalence of NED is rising and can be induced by other therapeutics including radiotherapy and chemotherapeutics. However, the precise molecular events underlying NED remain poorly understood. Therefore, an in-depth molecular investigation of NED was conducted using an in vitro system.

The first objective was to establish a robust, in vitro model of ADT-induced NED using the PCa cell line, LNCaP. Extensive molecular analysis by qRT-PCR, Western blotting and confocal microscopy revealed the transcription factor, human achaete-scute homolog-1 (hASH1) as a potential key driver of NED. hASH1 localisation shifted from exclusively cytoplasmic to nuclear upon acquisition of NED morphology, concurrent with increased expression of the clinical biomarker neuron specific enolase (NSE) and decreased expression of prostate-specific antigen (PSA).

Next, the effects of intermittent (I)ADT on the NED pathway were investigated. AD arrest resulted in reacquisition of epithelial morphology and resurgence of PSA expression. Interestingly, hASH1 was retained in the nucleus alongside NSE upregulation, indicating emergence of a potential 'hybrid' phenotype. After a second AD cycle, cells regained NED morphology and maintained hASH1 nuclear localisation. As hASH1 drives the development of GABAergic neurons and GABA has previously been implicated in PCa growth and invasion, a comprehensive characterisation of GABA receptor subunit expression in PCa cells was undertaken. Differential expression between androgen-sensitive and androgen resistant cells was discovered and indicated PCa GABAergic signalling may be modulated by androgen availability.

Abbreviations

°C - Celsius
AD - Androgen deprived
AD1 - 1st AD cycle
AD2 - 2nd AD cycle
ADT - Androgen deprivation therapy
ANOVA - Analysis of variance
AR - Androgen Receptor
ARE - Androgen response element
ATCC - American type culture collection
BLAST - Basic local alignment search tool
BPH - Benign prostate hyperplasia
BSA - Bovine serum albumin
BZ - Benzodiazepine
C - Control
cAD - Constant AD
CCC - Cation-chloride co-transporters
cDNA - Complimentary DNA
CgA - Chromogranin-A
CREB - cAMP response element-binding protein
CNS – Central nervous system
CRPC - castrate-resistant prostate cancer
CS-FBS - Charcoal stripped fetal bovine serum
CSC - Cancer stem cell
Ctrl - Control
DEPC - diethylpyrocarbonate
DHT - Dihydrotestosterone
DMSO - dimethyl sulphide
DNA - Deoxyribonucleic acid
DRE - Digital rectal examination
ECM - Extracellular matrix
EDTA - Ethylenediaminetetraacetic acid
EGF - Epidermal growth factor
EGFR - Epidermal growth factor receptor

ELISA - Enzyme-linked immunosorbent assay
EMT - Epithelial to mesenchymal transition
ER - Estrogen receptor
FBS - Foetal bovine serum
GABA - γ -aminobutyric acid
GABA-T - GABA transaminase
GABARs - GABA receptors
GAD1 - Glutamate decarboxylase 1
GAD2 - Glutamate decarboxylase 2
GBP – Gabapentin
GRP – Gastrin releasing peptide
H&E - Haematoxylin and eosin
H₂O - Water
hASH1 - Human achaete-scute homolog-1
IADT - Intermittent androgen deprivation
IGF-1 - Insulin-like growth factor 1
IHC - Immunohistochemistry
KCC - K⁺-Cl⁻ co- transporters
KDa - Kilodalton
LSB - loading sample buffer
mAb - monoclonal antibody
MMP - Matrix metalloproteinase
mRNA - messenger RNA
MTT - 3-(4,5-dimethylthiazol-2-yl)-2,5-diphenyltetrazolium bromide
MW - molecular weight
NB - Neuroblastoma
NE - Neuroendocrine
NED - Neuroendocrine differentiation
NEPC - Neuroendocrine Prostate Cancer
NICE - National Institute for Health and Care Excellence
NKCC - Na⁺-K⁺-2Cl⁻ co-transporters
NSE - Neuron specific enolase
PBS - Phosphate buffered saline

PBS-T - Phosphate buffered saline-Tween
PCa - Prostate Cancer
PCPT – Prostate Cancer Prevention Trial
PDX - Patient Derived Xenograft
PNS – Peripheral nervous system
PSA - Prostate specific antigen
PTEN - Phosphatase and tensin homolog
PTOV1 - Prostate Tumour Overexpressed 1
qRT-PCR - Quantitative reverse transcription-polymerase chain reaction
REST - RE1-silencing transcription factor
RIN - RNA integrity number
RNA - Ribonucleic Acid
RNAi - Ribonucleic acid interference
RPMI - Roswell park memorial institute
SCLC - Small cell lung cancer
SDS - Sodium Dodecyl Sulphate
SDS-PAGE - Sodium Dodecyl Sulphate Polyacrylamide gel electrophoresis
SRD5A2 - steroid-5 α -reductase, α -polypeptide 2
TAPS - Total androgen program suppression
TEMED - N,N,N',N'-Tetramethyl-ethylenediamine
TIMP – Tissue inhibitor of metalloproteinase
UK – United Kingdom
VFTD - Venus fly trap domain
VGCCs - Voltage-gated calcium channels

CONTENTS

Page No.

1. Introduction	1
1.1 Prostate cancer epidemiology	1
1.1.1 Endogenous and exogenous risk factors.....	2
1.1.2 Androgen steroidogenesis	3
1.1.3 Anti-androgen therapeutic targets and total androgen blockade.....	3
1.1.4 Prostate anatomy and physiology.....	4
1.1.5 Androgen dependent growth of healthy prostate	6
1.1.6 Neuroendocrine cells in benign and malignant prostate	7
1.1.7 Prognostic factors and diagnostic tools	8
1.1.8 Current treatment strategies	10
1.2 Progression to castrate-resistant prostate cancer	15
1.2.1 Molecular mechanisms of castrate-resistant prostate cancer	15
1.2.1.1 Androgen receptor	15
1.2.1.2 Hypersensitive pathway	16
1.2.1.3 Promiscuous pathway	16
1.2.1.4 Outlaw pathway	17
1.2.1.5 Endogenous androgen synthesis.....	18
1.2.1.6 Constitutively active androgen receptor splice variants	18
1.2.2 Tumour evolution.....	20
1.2.3 Metastasis and invasion of prostate cancer.....	21
1.2.4 Cancer stem cells	22
1.3 Neuroendocrine differentiation	23
1.3.1 Potential interplay between PCa CSC's, epithelial PCa cells and NED PCa cells	25
1.3.2 Known inducing factors of NED	26
1.3.3 Previous developed models of ADT-induced NED	27

1.3.4 This studies proposed pathway of AD-induced NED	28
1.3.5 hASH1 mediated canonical neurogenesis	29
1.3.6 hASH1 ability to act as a pioneer factor in neurogenesis and cancer	29
1.3.7 hASH1 activity in SCLC	30
1.3.8 hASH1 in PCa	31
1.4 Structure and function of GABA _A and GABA _B receptors	31
1.4.1 GABA _A receptors	33
1.4.2 GABA _B receptors	33
1.4.3 CCC regulation of 1.4.1 GABA _A receptor activity	34
1.4.4 Previous GABA _A R and GABA _B R studies in prostate cancer	36
1.4.5 GABA is implicated in increased growth and aggression of prostate cancer	37
1.4.6 Previous GABA _A R and GABA _B R studies in prostate cancer	37
1.5 Summary	39
1.6 Hypothesis and aims	40
2. Materials and methods	42
2.2 Cell culture techniques	42
2.1.1 Cell lines	42
2.1.2 Cell culture conditions	42
2.1.3 Passaging cell lines	42
2.1.4 Counting cells	43
2.1.5 Cryopreservation of cell lines	43
2.1.6 Reviving cells from liquid nitrogen storage	43
2.1.7 androgen deprivation of prostate cancer cell lines	44
2.1.8 Synthetic androgen treatment	44
2.1.9 Muscimol, baclofen and gabapentin drug treatments	45
2.1.10 Harvesting cells	45
2.1.11 Alamar blue cell viability assay	46
2.2 RNA isolation	46

2.2.1 Preparation of nuclease free water	46
2.2.2 RNA isolation.....	46
2.2.3 Quantification of RNA by spectrophotometry (Nanodrop 2000).....	47
2.2.4 Quantification of RNA by microfluidic analysis (Bioanalyser 2100).....	47
2.2.5 Reverse transcription of RNA / cDNA synthesis	48
2.3 Quantification of gene expression	49
2.3.1 Oligonucleotide design and preparation	49
2.3.2 qRT-PCR.....	53
2.3.3 Identification of reference genes	54
2.3.4 Data analysis / quantification of fold change in gene expression.....	54
2.4 Protein analysis.....	56
2.4.1 Protein extraction.....	56
2.4.2 Bradford analysis of protein concentration	56
2.4.3 Cell protein lysate preparation	57
2.4.4 Sodium dodecyl sulphate polyacrylamide gel electrophoresis (SDS-PAGE)	57
2.4.5 Immunoblotting	58
2.4.6 Scratch assays	58
2.5 Immunofluorescence	61
2.5.1 Fixing cells.....	61
2.5.2 Immunofluorescent staining of cells.....	62
2.5.3 Confocal microscopy	62
2.5.4 Neurite outgrowth staining kit	63
2.5.5 Neurite outgrowth analysis	63
2.6 Analysis of statistical significance.....	64

3. Elucidating the molecular mechanisms of neuroendocrine differentiation of prostate cancer cells	65
3.1 Introduction	65
3.1.1 Characterisation of PCa cell lines.....	65
3.1.2 Castrate-resistant prostate cancer and study justification ..	66

3.1.3 Hypothetical NED pathway	69
3.1.4 Study aim and research questions	70
3.2 Results	71
3.2.1 Characterisation of prostate cancer cell lines	71
3.2.2 Molecular characterisation of PCa and CRPC cells.....	71
3.2.2.1 Androgen receptor and prostate specific antigen expression	72
3.2.2.2 Prostate cancer stem-like cell marker expression.	74
3.2.2.3 Initial analysis of core protagonists in the NED pathway; biomarker, repressor and neurotransmitter synthesis ..	76
3.2.3.1 Androgen-sensitive LNCaP cells display significantly slower growth in scratch assays compared to CRPC cell lines.....	79
3.2.4.1 Androgen-deprivation triggers a neuroendocrine differentiation program in androgen-sensitive prostate cancer cells	81
3.2.4.2 Analysis of neurite growth.....	83
3.2.4.3 Molecular changes resulting from androgen deprivation of LNCaP cells	85
3.2.4.4 Visualisation of hASH1 and NSE expression and localisation before and after AD-induced NED	87
3.2.5 Validation of AD mediated effects using synthetic androgen	89
3.2.5.1 Effect on cell viability of synthetic androgen R1881	89
3.2.5.2 Further refinement of AD experiment design	91
3.2.5.3 Androgen-sensitive LNCaP cells display altered morphology during androgen deprivation	91
3.2.5.4 Validating the effect of AD on NED related genes in LNCaP cells.....	92
3.2.5.5 Protein expression in response to androgen deprivation.....	95
3.2.6 Conclusions	97
3.3 Discussion	98

3.3.1	Characterisation of prostate cancer cell lines	98
3.3.2	Androgen receptor signalling in androgen-sensitive and CRPC cell lines	100
3.3.3	Advantages and disadvantages of different androgen- deprivation stimulation methods.....	101
3.3.4	Neuroendocrine gene expression signatures of prostate cancer cells	103
3.3.5	Androgen-deprivation triggers neuronal-like morphological changes in androgen-sensitive LNCaP prostate cancer cells	104
3.3.6	Molecular characterisation reveals neuronal-like signature of androgen deprived LNCaP cells.....	105
3.3.7	Morphological changes are associated with hASH1 nuclear localisation and activation of canonical neurogenesis pathway.....	106
3.3.8	Neuronal-like molecular profile is preventable by androgen receptor signalling	107
3.3.9	Neuronal-like morphological changes are prevented and reversed by androgen receptor signalling	109
3.3.10	Disruption of Notch1 signalling may promote aberrant cell fates	110
3.3.11	hASH1 as a therapeutic target.....	110
3.4	Conclusions.....	111
3.5	Limitations, weaknesses and future experiments	112

4. Molecular reversibility of neuroendocrine differentiation in prostate

4.	Molecular reversibility of neuroendocrine differentiation in prostate cancer cells	114
4.1	Introduction	114
4.1.1	Clinical use of intermittent ADT	115
4.1.2	Potential implication of NED reversibility	116
4.1.3	Previous NED reversibility studies.....	117
4.1.4	Development of an IAD model.....	118
4.1.5	Investigating the molecular and morphological reversibility of NED.....	119
4.1.6	Study aim and research questions	120

4.2 Results	121
4.2.1 Reversibility of neuroendocrine morphology.....	121
4.2.2 Molecular reversibility of NED.....	122
4.2.3 hASH1 retains nuclear localisation upon reintroduction of androgen	125
4.2.4 Investigating the reversibility of NED and effects of IAD ..	129
4.2.5 Effect of IAD on LNCaP cellular morphology	130
4.2.6 Molecular analysis of the effect of IAD on AR signalling...	131
4.2.7 Molecular analysis of the effect of IAD on NED pathway..	133
4.2.8 Analysis of hASH1 localisation throughout IAD	137
4.3 Discussion.....	139
4.3.1 Research objectives and key findings	139
4.3.2 Morphological NED reversal and the relationship between form and function	141
4.3.3 Molecular reversibility of NED.....	142
4.3.4 Retention of nuclear hASH1 and the potential for hybrid phenotypes and heterogeneity	143
4.3.5 Effects of IAD on the proposed NED pathway	146
4.3.6 hASH1 as a potential therapeutic target	147
4.4 Conclusions.....	148
4.5 Limitations, weaknesses and future experiments.....	148

5. Preliminary investigation of GABAergic signalling in prostate cancer

.....	150
5.1 Introduction	150
5.1.1 background and rationale for study	150
5.1.2 Clinical use of gabapentin in prostate cancer patients.....	151
5.1.3 Study aim and research questions	154
5.2 Results	155
5.2.1 Expression of GABAR subunits in PCa cell lines.....	155
5.2.2 Quantification of GABA _A R and GABA _B R subunit expression in PCa cell lines.....	157

5.2.3 Quantification of the effect of IAD on the expression of GABA _A and GABA _B receptor subunits in LNCaP cells.....	158
5.2.4 Assessment of the effect of intermittent (I)AD on GABA _A R subunit expression in LNCaP cells	163
5.2.5 Expression of CCCs during IAD	167
5.2.6 The effects of AD and IAD on GABA _B R expression.....	169
5.2.7 GABA synthesis and metabolism pathways during IAD ...	173
5.2.8 Effect on cell viability of GABA _A R and GABA _B R agonists.	175
5.2.9 Effects of muscimol and baclofen on NED LNCaP gene expression.....	176
5.2.10 Effect of Gabapentin on NED pathway associated genes in LNCaP cells	178
5.3 Discussion.....	184
5.3.1 Presence of GABA _A R and GABA _B R subunits in PCa cell lines.....	184
5.3.2 Expression of GABA _A R and GABA _B R subunits in PCa cell lines.....	187
5.3.3 Effect of AD on GABA _A R and GABA _B R subunit expression	188
5.3.4 The effect of IAD on expression of GABA _A R subunits	189
5.3.5 Expression of selected CCCs during IAD	190
5.3.6 Expression of GABA _B R subunits during AD and IAD.....	192
5.3.7 Expression of genes involved in GABA synthesis and metabolism during IAD	194
5.3.8 The effect of muscimol and baclofen on a key panel of genes in AD LNCaP cells	195
5.3.9 The effect of gabapentin on LNCaP cells	196
5.3.10 Future functional GABAR experiments.....	197
5.3.11 GABA results in relation to previous studies.....	198
5.4 Conclusions of GABAR studies	199
5.5 Limitations, weaknesses and future experiments.....	201

6. General discussion and future directions	203
6.1 Summary of findings.....	203
6.1.1 hASH1 is a likely key driver of Ad-induced NED in PCa...	203
6.1.2 The molecular reversibility of AD-induced NED is established for the first time	204
6.1.3 The effects of intermittent AD on PCa NED were investigated for the first time	204
6.1.4 The first comprehensive assessment of GABAR subunit expression in PCa cell lines and the effect of IAD and GABAR agonists on their expression	205
6.2 hASH1 as a potential therapeutic target in NED PCa.....	207
6.3 Clinical implications of the effects of IAD and PCa NED	208
6.4 Limitations and weaknesses of this study	208
6.5 Future work	211
6.4.1 Further investigations of hASH1 activity in PCa and validation as a therapeutic target	211
6.4.2 Investigating the paracrine signalling potential of NED PCa cells.....	213
6.4.3 Investigating the role of GABARs and CCCs in NED PCa	214
7. References	215
8. Appendix 1: Investigation of possible androgen receptor splice variants induced by AD	248

List of Figures

Page No.

Figure 1.1: Diagram displaying the zonal model of prostate anatomy.....	4
Figure 1.2: Progression of prostate cancer to metastatic castrate-resistant prostate cancer	15
Figure 1.3: pathways facilitating androgen receptor activation in an androgen deprived environment	19
Figure 1.4: The origin and involvement of the neuroendocrine niche in CRPC progression	24
Figure 1.5: Structural diagram illustrating the composition of a typical GABA _A R and GABA _B R.....	35
Figure 1.6: The expression and activity of CCCs determines the activity of GABA _A Rs.....	36
Figure 3.1: Schematic diagram illustrating the enrichment of neuroendocrine phenotype cells in some prostate cancer tumours treated with androgen deprivation therapy	67
Figure 3.2: Androgen receptor (AR) and prostate specific antigen (PSA) expression in androgen-sensitive LNCaP and castrate-resistant DU-145 and PC-3 prostate cancer cells.....	73
Figure 3.3: Expression of cancer stem cell (CSC) markers in androgen-sensitive LNCaP and castrate-resistant DU-145 and PC03 prostate cancer cells	75
Figure 3.4: Expression of neuroendocrine differentiation (NED)-related genes in androgen-sensitive and castrate-resistant prostate cancer cells	77
Figure 3.5: Analysis of basal expression of key prostate cancer markers.....	78
Figure 3.6: Wound closure and migration of prostate cancer cell lines	80
Figure 3.7: Schematic diagram indicating the experiment design for androgen deprivation experiments.....	81
Figure 3.8: Androgen-sensitive LNCaP cells undergo morphological change in response to androgen deprivation.....	82

Figure 3.9: Effect of androgen deprivation on PSA and androgen receptor expression	83
Figure 3.10: Androgen deprivation triggers significant morphological changes in LNCaP cells	84
Figure 3.11: Androgen deprivation dramatically downregulates PSA expression and activates the canonical neurogenesis pathway	86
Figure 3.12: Androgen deprivation downregulates PSA expression and expression of NSE in markedly increased	87
Figure 3.13: Androgen deprivation triggers neuronal-like changes in LNCaP morphology associated with hASH1 nuclear localisation	88
Figure 3.14: Toxicity assessment of synthetic androgen R1881 and DMSO vehicle in prostate cancer cell lines.....	90
Figure 3.15: Visual representation of experiment design for androgen deprivation experiments.....	91
Figure 3.16: Presence of androgen prevents neuroendocrine differentiation...	92
Figure 3.17: Androgen supplementation prevents activation of the canonical neurogenesis pathway	94
Figure 3.18: Androgen supplementation prevents activation of the canonical neurogenesis pathway	96
Figure 3.19: Schematic summary of chapter 3 results in relation to the proposed model of AD induced PCa NED	97
Figure 4.1: Schematic diagram depicting proposed interactions between neuroendocrine differentiation in prostate cancer cells and the tumour microenvironment	116
Figure 4.2: Schematic diagram detailing the experiment design for androgen deprivation cessation experiments.....	118
Figure 4.3: Reintroduction of androgen reverses neuroendocrine differentiation morphology	121
Figure 4.4: Molecular changes associated with reversal of neuroendocrine differentiation via androgen reintroduction	123

Figure 4.5: Neurogenesis promoter hASH1 retains nuclear localization despite a reversal of neuroendocrine morphology	125
Figure 4.6: Retention of nuclear hASH1 is widespread and neurite-like processes containing hASH1 are lost	127
Figure 4.7: Schematic diagram showing the experimental design for investigation of IAD, including two 15-day cycles of AD separated by a 15-day intermediate period of androgen reintroduction	129
Figure 4.8: Morphological changes of LNCaP cells throughout IAD	130
Figure 4.9: Expression of androgen receptor and prostate specific antigen in LNCaP cells after two AD cycles.....	132
Figure 4.10: Expression of key NED associated genes during IAD	133
Figure 4.11: Expression of key neuroendocrine associated proteins during IAD	135
Figure 4.12: Schematic diagram detailing the experiment design for androgen deprivation cessation experiments assessing hASH1 localisation	137
Figure 4.13: hASH1 localisation throughout IADT and 10 days into a second AD cycle.....	138
Figure 4.14: Schematic diagram illustrating the shift in transcription factor activity between LNCaP in the presence, absence and reintroduction of androgen.....	144
Figure 5.1: Chemical structures of GABA and gabapentin.....	152
Figure 5.2: Quantitative relative expression of GABA _A R subunits in brain and PCa cells.....	157
Figure 5.3: Relative expression of GABA _A R subunits in LNCaP cells subjected to androgen deprivation	160
Figure 5.4: Expression of GABA _A R subunits in LNCaP cells cultured in AD conditions or in the presence of 1 nM or 10 nM synthetic androgen (R1881) .	161
Figure 5.5: Expression of GABA _A R subunits in LNCaP cells subjected to IAD	165
Figure 5.6: Expression of KCCs and NKCCs in LNCaP cells subjected to IAD	168
Figure 5.7: Expression of GABA _B R subunits in LNCaP cells subjected to AD	170

Figure 5.8: Expression of GABA _B R subunits in LNCaP cells subjected to IAD	171
Figure 5.9: Expression of GABA synthesis and metabolism genes GAD1, GAD2 and GABA-T in PCa cells subjected to AD or IAD.....	173
Figure 5.10: Assessment of muscimol, baclofen and ethanol vehicle on LNCaP cell viability.....	175
Figure 5.11: Effect of muscimol and baclofen on LNCaP gene expression ...	177
Figure 5.12: Effect of gabapentin on LNCaP cell AR and PSA expression in LNCaP cells not subjected to AD	179
Figure 5.13: Effect of gabapentin on key NED related genes in LNCaP cells not subjected to AD.....	180
Figure 5.14: Effect of gabapentin on key GABA synthesis and metabolism related genes in LNCaP cells not subjected to AD.....	182
Figure 5.15: Effect of gabapentin on GABA _B R subunit gene expression in LNCaP cells not subjected to AD	183
Figure 8.1: Diagram displaying known androgen receptor splice variants and their exon composition	249

List of Tables

Page No.

Table 2.1: Oligonucleotides used in this study for qRT-PCR analysis, relevant accession numbers are provided	51
Table 2.2: List of oligonucleotides used in this study for GABA _A and GABA _B receptor subunit expression	52
Table 2.3: Primary antibodies used in this study for immunoblotting and immunofluorescence	60
Table 2.4: Secondary antibodies used in this study for immunoblotting and immunofluorescence	61
Table 5.1: Assessment of GABA _A R and GABA _B R subunit expression in LNCaP, DU-145 and PC-3 PCa cells	155
Table 5.2: Presence and absence assessment of GABAR subunits during intermittent AD	164

1. Introduction

1.1 Prostate Cancer Epidemiology

Prostate cancer is the second most common cancer in men and the second most common cause of cancer-related death in men in the UK (Nelson *et al.*, 2014). Each year, 11,500 men die from prostate cancer in the UK alone. The incidence of prostate cancer continues to rise, in part due to better detection techniques and increasing adoption of serum prostate specific antigen (PSA) tests to diagnose prostate cancer. UK population ageing also contributes to increased incidence of prostate cancer, with age remaining the biggest risk factor for all cancers (Jahn, Giovannucci, & Stampfer, 2015).

In addition, it must be considered that at autopsy, 80% of men aged 80 years or older displayed sub-clinical signs (non-symptomatic and unlikely to be diagnosed) of prostate cancer. Importantly, 50% of 50-year-old men also display sub-clinical prostate cancer. In addition, 36% of Caucasians and 51% of African-Americans aged 70-79 had prostate cancer tumours discovered upon autopsy (Jahn *et al.*, 2015). Therefore, it is likely that even with advances in prostate cancer care, incidence is likely to continue to rise in the foreseeable future. The vast majority (>85%) of prostate cancer patients are diagnosed over the age of 65 and the average age of prostate cancer sufferers is between 70-75 years old (Cancer Research UK statistics). For men diagnosed with locally confined disease, radical prostatectomy is often curative. However, in many cases the disease recurs, often due to occult metastases, which can be difficult to detect using current imaging techniques due to their strong bone tropism (Bill-Axelsson *et al.*, 2014). In addition, many patients only experience serious symptoms after the disease has spread beyond the prostate gland, rendering radical prostatectomy ineffective.

The seminal work of Charles Huggins, first identified that almost all prostate cancers are initially dependent upon androgen for their growth and survival (Huggins, 1941). Androgen deprivation therapy (ADT) triggers regression of prostate tumours, however, resistance to ADT usually develops within 3 years and is termed castrate-resistant prostate cancer (CRPC) (Karantanos, Corn, &

Thompson, 2013). Once CRPC has become metastatic, no curative therapeutic options currently exist and patients usually succumb to the disease within 18 months. Gaining a greater understanding of the mechanisms facilitating progression to CRPC is vital to the identification of novel therapeutic strategies and targets.

1.1.1 Endogenous and Exogenous Risk Factors

Analysis of data from several large scale studies has shown family history to be highly informative on the relative risk of developing prostate cancer second only to PSA screening (Madersbacher *et al.*, 2011). Males with a father or brother with prostate cancer display a 2-fold increased likelihood of developing the disease with the risk increasing substantially for every additional first degree family member with prostate cancer (Steinberg *et al.*, 1990). As with all cancer types, risk increases dramatically with age and current European Urologic Association guidelines suggest that PSA screening should begin between age 40 and 45 (Glass, Cary & Cooperberg, 2013; Heidenreich *et al.*, 2013). The incidence of prostate cancer is also correlated to race, with black populations at the highest risk and often presenting at earlier ages with higher grade disease (Glass, Cary & Cooperberg 2013). Caucasian individuals have the second highest risk, whilst Asian populations make up the lowest risk group. Germ-line mutations to either *BRCA1* or *BRCA2* also confers a 3-fold higher risk of developing prostate cancer and are associated with more aggressive forms of the disease (Castro *et al.*, 2013).

In addition to endogenous risk factors, exogenous factors such as the western diet and obesity have been linked to prostate cancer development. Westernisation of diet in Japan appears to have influenced a gradual increase in prostate cancer diagnoses (Gathirua-Mwangi & Zhang, 2014; Satoh *et al.*, 2014). Tobacco consumption is associated with increased prostate cancer-specific morbidity, as well as increased rate of disease recurrence, however this risk returns to that of non-smokers after 10 years of abstention (Kenfield *et al.*, 2011). Perhaps the greatest exogenous risk factor is chronic inflammation of the prostate gland (prostatitis), caused by infection (Palapattu *et al.*, 2005).

1.1.2 Androgen Steroidogenesis

In males, testosterone is synthesised in the testes and the adrenal glands, with the testes comprising 95% of androgen production (Mooradian *et al.*, 1987). Conversion of testosterone to DHT, which is a considerably more potent agonist of the AR, can occur in the prostate, liver, brain and skin. The production of androgens first requires the conversion of cholesterol into progestogens which are then further modified into androgen precursors and finally to testosterone (Marks, 2004). Cholesterol side-chain cleavage enzyme CYP11A1 converts cholesterol into pregnenolone, a pre-cursor to a wide range of steroids including mineralocorticoids, glucocorticoids, estrogens and androgens. The outputs of steroidogenesis are tightly regulated by the activity of specific enzymes for each group of steroids, 17 β -HSD and 5 α -reductase (androgens), aromatase (estrogens) 11 β -hydroxylase (glucocorticoids and aldosterone synthase (mineralocorticoids) (Miller & Auchus, 2011). For androgen synthesis, pregnenolone is either converted directly to 17 α -hydroxy pregnenolone, or first converted to progesterone by 3 β -HSD before being converted to 17- α -hydroxyprogesterone by 17 α -hydroxylase. These are then converted by 17,20 lyase to dehydroepiandrosterone or androstenedione respectively. At this stage, androstenedione can be directly converted to testosterone by 17 β -HSD, whereas dehydroepiandrosterone must first be converted to androstenediol by 17 β -HSD and then into testosterone by 3 β -HSD. Once testosterone has been synthesised, its conversion to DHT is performed by the 5 α -reductase enzyme (Chang *et al.*, 2013).

1.1.3 Anti-androgen therapeutic targets and total androgen blockade

Anti-androgens are able to disrupt androgen receptor signalling through either direct targeting of the AR or by inhibiting the production of AR ligands. In the treatment of prostate cancer, two most frequently used AR antagonists are bicalutamide and enzalutamide (Hoffman-Censits & Kelly, 2013). In order to inhibit the production of androgens, both from the testes and the adrenal cortex, the CYP17A1 inhibitor abiraterone acetate can be used (Koninckx *et al.*, 2019). Combining both of these approaches results in total androgen blockade, which can be effective against resistance mechanisms to each approach (Arora *et al.*,

2013). For example, where treatment with enzalutamide has resulted in increased androgen production or where AR becomes overexpressed, hypersensitive or promiscuous to other ligands to adapt to the low androgen availability caused by abiraterone treatment (Attard *et al.*, 2014). In addition, 5α -reductase inhibitors such as finasteride have been investigated as a potential preventative treatment for prostate cancer. The recent Prostate Cancer Prevention Trial (PCPT) found finasteride to be effective in this role (Unger *et al.*, 2018), although its use remains controversial as it could lead to underdiagnoses by significantly decreasing PSA production. This risk was highlighted in the PCPT study which found although risk of developing PC fell 25%, in the men that did develop PCa there was a 68% increase in the likelihood of this being a high grade Gleason score 7-10 tumour (Unger *et al.*, 2018).

1.1.4 Prostate Anatomy and Physiology

Although there has been considerable debate over differing models of prostate anatomy, it has become generally recognised that McNeal's 'zonal' description (McNeal, 1968) remains more accurate and clinically relevant than the Tisell and Salandar 'lobular' model (Myers, 2000; Tisell & Salander, 1975).

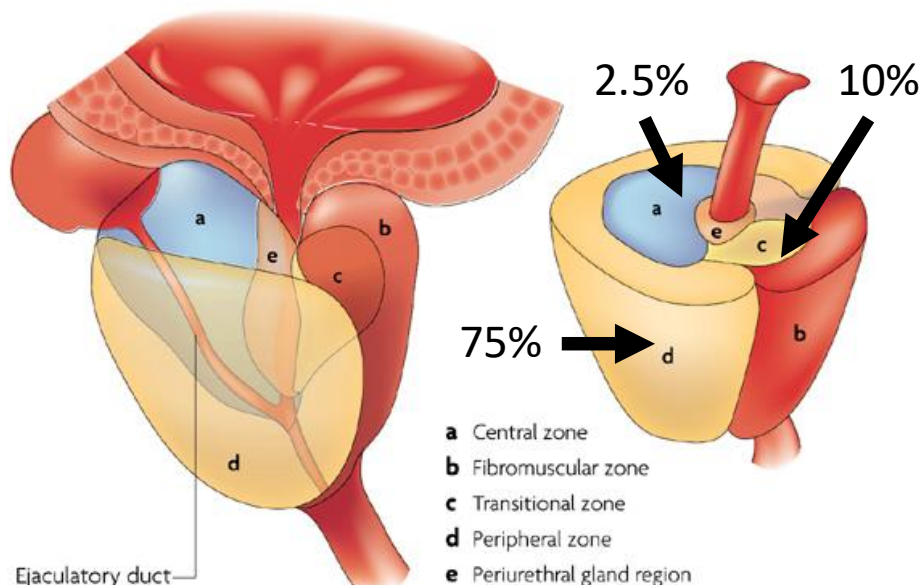


Figure 1.1 Diagram displaying the zonal model of prostate anatomy. Adapted from (De Marzo *et al.*, 2007).

The human prostate is comprised of 3 major zones, the peripheral zone, the central zone and the transition zone. Of these zones, it is the peripheral zone that is the most common site of carcinogenesis, the transition zone which is the primary location for benign hyperplasia and the central zone that is the most resistant to disease (McNeal, 1968). Despite the physiological differences between the different zones of the prostate, it should be noted that other factors are more statistically significant for prognosis than location alone (Cohen *et al.*, 2008).

The peripheral zone (the largest zone of the prostate) surrounds the distal urethra and approximately 75% of tumours arise from this zone (Shen & Abate-Shen, 2010). Due to its positioning, the peripheral zone is easily screened for potential carcinoma via a digital rectal examination (DRE) making early diagnosis considerably easier than other zones. However, early stage tumour growth in this zone rarely impinges on the function of the urethra. This means that without a medical diagnostic procedure such as DRE or a PSA test, a patient is unlikely to present clinically until the disease has progressed further (Myers, 2000; Verma *et al.*, 2014).

The Central zone surrounds the ejaculatory ducts. A study of 2,494 tumours found that only 2.5% of tumours originated in the central zone. Although rare, a tumour in the central zone is usually considerably more aggressive with a higher likelihood for metastasis given the close proximity to the seminal vesicles and ejaculatory ducts allowing invasive cells to leave the prostate gland. A compounding factor in the poor prognosis of central zone prostate tumours is that the central zone is often avoided during prostate gland biopsy, often preventing early diagnosis and treatment (Cohen *et al.*, 2008).

The transition zone surrounds the proximal urethra and accounts for approximately 5% of the prostate gland at puberty with 10% of prostate tumours arising from this zone. In addition, this zone continues to grow throughout the life of the individual and is the site of benign prostate hyperplasia (BPH) (Shen & Abate-Shen, 2010). Either malignant or benign growth in this zone of the prostate

is highly likely to cause obstruction of the urethra and associated symptoms (Lee & Kuo, 2017).

1.1.5 Androgen Dependent Growth of Healthy Prostate

The androgen receptor (AR) is critical for growth and development of the prostate in response to androgens (Gao *et al.*, 2013; Parimi *et al.*, 2014). The primary mechanism for activation of AR is through uptake of circulating testosterone into the cell, which is then converted by steroid-5 α -reductase, α -polypeptide 2 (SRD5A2) into dihydrotestosterone (DHT). Upon androgen receptor activation, heat-shock proteins HSP90 and HSP70 dissociate from the AR causing the AR protein to dimerise and translocate into the nucleus (Chang *et al.*, 2011; Foley & Mitsiades, 2016).

Androgen receptor signalling is able to control and maintain the differentiation and proliferation of prostate tissue via androgen response elements (AREs) in the promoter regions of specific genes (Dutt & Gao, 2009). Prostate specific antigen (PSA) is known to contain an ARE and is expressed in response to androgen receptor signalling (Dutt & Gao, 2009; Kim & Coetzee, 2004). Prostate cancer tumours are initially dependent upon androgens for their growth and express PSA, which has been utilised as a biomarker of prostate cancer growth (Feldman & Feldman, 2001; Gudmundsson *et al.*, 2010).

It is also important to consider that AR signalling can occur in a non-genomic fashion. In this pathway, binding of androgens to the AR can result in increased cell proliferation and survival through direct activation of the mitogen-activated protein kinase (MAPK) and protein kinase B (AKT) pathways (Leung & Sadar, 2017; Migliaccio *et al.*, 2000; Zarif *et al.*, 2015) facilitated by the interaction of the AR with non-receptor tyrosine kinase Src (Leung & Sadar, 2017; Migliaccio *et al.*, 2000; Migliaccio *et al.*, 2007). This non-genomic signalling mechanism is active at very low androgen concentrations (0.1 nM) up to concentrations that are approaching physiological levels (10 nM) (Leung & Sadar, 2017; Unni *et al.*, 2004).

1.1.6 Neuroendocrine cells in benign and malignant prostate tissue

Neuroendocrine (NE) cells make up >1% of benign prostate tissue (Parimi *et al.*, 2014) and are able to influence surrounding cells via paracrine secretions and dendritic-like extensions to support the growth and development of the gland (Hu *et al.*, 2002). NE cells are terminally differentiated, non-proliferating and primarily found within the basal compartment of the prostate (Lang, Frame, & Collins, 2009). NE cells of the prostate are differentiated from epithelial stem cells, as opposed to the neural crest which is the source of NE cells in the pituitary and adrenal glands (Cox *et al.*, 1999). Although the functions of NE cells are relatively well understood in the development of the prostate, the role of these cells in adult prostate tissue is less clear (Cox *et al.*, 1999).

NE cells also contain synaptic vesicles that can secrete neurotransmitters, including gamma aminobutyric acid (GABA), glutamate and glycine. These secretions are regulated by cAMP, cGMP and calcium (Parimi *et al.*, 2014). In addition, NE cells are very challenging to identify via haematoxylin and eosin (H&E) staining and immunohistochemistry (IHC) is the preferred method of identifying NE cells. To achieve this, there are four commonly utilised clinical biomarkers of NE cells, neuron-specific enolase (NSE), synaptophysin (SYP), chromogranin A (CgA) and CD56 (Altree-Tacha, Tyrrell, & Li, 2017; Kamiya *et al.*, 2003; Kaufmann, Georgi, & Dietel, 1997). NSE is considered a high sensitivity marker of neuronal as well as NE cells, however it is not highly specific to only these two cell types (Marangos & Schmechel, 1987; Schmechel, Marangos, & Brightman, 1978.; Seshi *et al.*, 1988). Synaptophysin is a marker both of NE cells and of neurons that participate in synaptic transmission (Chang *et al.*, 2017; Gupta *et al.*, 2013; Zhu *et al.*, 2014). CgA is present in and secreted by NE cells (Cox *et al.*, 1999; Danza *et al.*, 2012; Esposito *et al.*, 2015), however it is highly unspecific (Gut *et al.*, 2016). CD56 is also considered a highly specific marker for primary NEPC (Altree-Tacha *et al.*, 2017; Kaufmann *et al.*, 1997).

Despite being non-proliferative themselves, enrichment of the NE cell niche during prostate cancer progression is associated with poor prognosis (Yuan, Veeramani, & Lin, 2007). These cells are inherently androgen-independent, and are resistant to most PCa therapeutics such as ADT, radiotherapy and most chemotherapeutics. In addition, previous evidence has demonstrated that the epithelial cells surrounding NE cells display increased proliferation, perhaps due to paracrine activity of NE cells (Noordzij *et al.*, 1995).

Neuroendocrine prostate cancer (NEPC) arising de novo is extremely rare, accounting for less than 2% of malignancies (Shen & Abate-Shen, 2010). It is usually diagnosed as carcinoid or small-cell carcinoma due to difficulty in identification via haematoxylin and eosin staining (Parimi *et al.*, 2014; Grignon, 2004). However, following administration of ADT, neuroendocrine differentiation (NED) becomes common place and is observed in the majority of advanced prostate adenocarcinomas (Terry & Beltran, 2014), evidenced by enrichment of neuroendocrine markers (Nouri *et al.*, 2014a; Shen & Abate-Shen, 2010). These neuroendocrine-like cells are non-proliferative and genetic analysis suggests that they originate via transdifferentiation of adenocarcinoma cells, rather than differentiation of pluripotent stem cells (Sauer *et al.*, 2006). Once transdifferentiated to a neuroendocrine phenotype, these cells become highly treatment resistant and support growth and recurrence of tumours in a paracrine manner (Terry & Beltran, 2014; Wu *et al.*, 2014; Chevalier *et al.*, 2002).

1.1.7 Prognostic Factors and diagnostic tools

The only currently approved prognostic factors for prostate cancer are tumour stage, grade and serum PSA (Rapa *et al.*, 2008). The standard method for many decades of assessing the prognosis of PCa is the Gleason grading system (Humphrey, 2004) which was last reviewed and updated by the International Society of Urological Pathology in 2014 (Epstein *et al.*, 2015). The Gleason grading system uses a scale of 2-10 (1 and 2 are not considered malignant) which is a composite of the primary and secondary pattern grades. Pathologists analyse samples of the biopsied prostate tissue and determines the pattern of the tumour from 1 (resembles normal prostate tissue) to 5 (little to no recognisable glands). The primary and secondary patterns present in the sample are graded (1-5) and

their sum forms the overall Gleason Score (Humphrey, 2004). It should be noted that even at the same Gleason score there can be differences in the prognoses given since the same score can be attained from different combinations of primary and secondary scores. For example, an individual with a primary score of 3 and a secondary score of 4 would have a more favourable prognosis than a patient with primary score 4 and secondary score 3 as the majority of the latter's tumour is at a higher grade despite both having an overall Gleason score of 7 (Humphrey, 2004). The latest update to Gleason grading system aimed to address this through the addition of grade groups, which lists Gleason 3+4 as lower grade than Gleason 4+3 and has been accepted by the World Health Organization in 2016 (Berney *et al.*, 2016; Epstein *et al.*, 2015) Gleason scores between 3-6 are considered to be low risk and are ideal for active surveillance, 7 is moderate and scores of 8-10 have the fastest progression (Penney *et al.*, 2013). A large statistical study of many cohorts found that it was rare for the Gleason score of a tumour to change and that the aggressiveness of the tumour may be determined early on in its development (Penney *et al.*, 2013).

From a patient's perspective, it is unlikely that clear symptoms will be experienced during the early stages of the disease. Occasionally, difficulty in urination and the onset of erectile dysfunction will present alongside tumour growth (Hamilton *et al.*, 2006). In addition, patients often initially present due to symptoms of bone pain caused by metastases in later stages of the disease (Gater *et al.*, 2011). Unfortunately, the non-specificity of these symptoms and their frequent occurrence in old age often mean that they are ignored by patients. Therefore, accurate and sensitive techniques for the diagnosis of prostate cancer are vital to discovering early stage, curable disease.

The primary low invasiveness tests for PCa are the digital rectal exam (DRE) and serum PSA concentration, whilst these methods lend themselves very well to a convenient, economic and low-risk way to mass screen large populations, these methods are not considered to have high specificity for prostate cancer (Verma *et al.*, 2014). This method of screening inevitably results in a large amount of false-positive diagnoses, leading to many patients undergoing unnecessary and invasive biopsies often impacting negatively upon potency and continence. In a

cohort of 521 men referred for biopsy in 2011, only 57% were ultimately diagnosed with prostate cancer (Verma *et al.*, 2014).

This raises an interesting dilemma, in that current methods of mass screening are frequently resulting in unnecessary biopsies, yet if screening based on PSA-serum and DRE were abandoned, many cases of prostate cancer would be detected later and with lower likelihood of survival. Whilst serum PSA remains a useful predictor of prostate cancer, it is important that this value be considered in the context of several other factors (such as family history and genetic disposition) and not as the 'magic bullet' as initially hoped (Boccon-Gibod, 2007). One approach to improving the accuracy of PSA screening is to test at-risk individuals earlier in life and to consider the rise in PSA concentration relative to the individual's basal level, rather than defining a universal threshold (Gudmundsson *et al.*, 2010).

1.1.8 Current Treatment Strategies

Radical prostatectomy involves the removal of the entire prostate gland. Whilst radical prostatectomy can be curative for men with prostate confined disease, to benefit from this treatment a patient is expected to have a future life expectancy greater than 10 years (Bill-Axelson *et al.*, 2014). Radical prostatectomy is the preferred option for men with intermediate and high risk disease (Gleason score >7 and Stage 2 or higher). A limitation of this treatment is that often men present with disease which has already progressed beyond the prostate gland (Bill-Axelson *et al.*, 2014).

Androgen deprivation therapy (ADT) was first described as an effective treatment for prostate cancer by Charles Huggins in 1941. The first method of achieving androgen deprivation (AD) was bilateral orchiectomy, the effects of which were soon able to be mimicked using GnRH agonists in order to force a downregulation of GnRH receptors, making surgical removal of the testes rare in the modern era (Perlmutter & Lepor, 2007). It should also be considered that even after orchiectomy, small amounts of androgen can be produced from the adrenal glands (Chang, Ercole, & Sharifi, 2014; Perlmutter & Lepor, 2007). Evolution of GnRH agonists focussed upon increasing their potency by substituting the sixth

amino acid of LHRH to achieve downregulation sooner and at lower dosages to avoid cardiotoxicity (Perlmutter & Lopor, 2007). The key limitation of GnRH agonists is that time to achieve maximal AD is around 30 days, during which patients experience the 'flare' phenomenon whereby production of testosterone dramatically increases in response to the down regulation of GnRH receptors resulting in brief but rapid tumour growth which can prove paralytic or even fatal in patients with spinal metastasis (Crawford & Hou, 2009; Perlmutter & Lopor, 2007).

Combined therapy of GnRH agonists with non-steroidal anti-androgens such as flutamide and bicalutamide have been approved since 1989 and are able to prevent the androgen flare by acting directly on the androgen receptor to prevent the binding of testosterone or DHT (Perlmutter & Lopor, 2007). From 2008 GnRH agonists have been effectively superseded by novel GnRH antagonists that not only achieve maximal AD far sooner, but also do not require the use of an anti-androgen to prevent the 'flare' response (Crawford & Hou, 2009).

The latest additions to ADT therapy abiraterone (Ryan *et al.*, 2015) and enzalutamide (Tran *et al.*, 2009) have been demonstrated to extend the time frame that ADT can control a tumour via targeting other tissue sources of androgen production and blocking androgen receptor nuclear co-localisation respectively. Each of these drugs demonstrated a 5-month extension to overall survival in Phase III clinical trials (Merseburger *et al.*, 2015; Ryan *et al.*, 2015). These pharmacological advances in ADT have undoubtedly contributed to an extension of survival for metastatic prostate cancer patients, unfortunately all forms of ADT place a strong selective pressure upon prostate tumours to adopt a castrate-resistant phenotype, usually occurring within 3 years of treatment (Karantanos *et al.*, 2013; Nouri *et al.*, 2014).

Given that a significant proportion of patients with suspected PCa are advanced in age and with slow disease progression, a strategy of 'watchful waiting' rather than immediate treatment is sometimes adopted. Under watchful waiting, patients are given no treatment until symptoms begin to develop. If symptoms develop, patients receive palliative treatments (Bill-Axelson *et al.*, 2014; Klotz *et al.*, 2010).

To avoid unnecessary treatments and their associated negative side-effects, men with low-moderate risk disease can be closely monitored via their serum PSA level and a series of prostate biopsies, a strategy termed 'active surveillance' (Klotz *et al.*, 2010). If disease progression is detected, treatment begins immediately. For low risk patients, active surveillance has an almost 100% 5-year survival rate. The method of delaying treatment also has the additional benefit of delaying the onset of resistance to treatments such as ADT (Klotz *et al.*, 2010).

It is well established that PCa tumours treated with ADT often display increased NED (Shen *et al.*, 1997; Terry & Beltran, 2014). As such, intermittent (I)ADT has long been touted as a solution to delaying the development of CRPC in response to ADT (Feldman & Feldman, 2001). The intermittent use of radio and chemotherapeutics clinically is well accepted, primarily because poorly tolerated toxicity necessitates discontinuous use (Canil & Tannock, 2004; Cash *et al.*, 2018). Whereas, in the case of ADT, intermittent treatment is proposed to delay hormone therapy resistance, improve patient quality of life and reduce financial costs (Shore & Crawford, 2010). Indeed, it has been argued that IADT should be the standard of care for PCa (Seruga & Tannock, 2008). However, European Association of Urology guidelines continue to mandate that ADT be constant and do not support the use of IADT clinically (Heidenreich *et al.*, 2014).

Clinical trials evaluating IADT have been conducted from as early as 1986. These early trials focussed on the quality of life enhancements offered by IADT and were very favourable (Klotz *et al.*, 1986). Unfortunately, the small sample size (n=20) makes it impossible to draw accurate conclusions on overall survival or disease progression. Higher powered studies (n=3040 and n=1386) focussing on overall survival, found that IADT was at best non-inferior to constant ADT (cADT) or performed considerably worse than cADT (Crook *et al.*, 2012; Hussain *et al.*, 2013; Mottet *et al.*, 2012). Unfortunately, all of these trials suffer from a lack of molecular stratification of these tumours, meaning that it is not possible to infer if IADT reduced NED or benefitted/harmed patients with high NED compared to cADT. This lack of stratification, to account for tumour heterogeneity, could also explain the inconclusive findings of IADT clinical trials to date (Hussain., 2017).

Evidently, before more structured clinical trials can investigate the effects of IADT on NED, a greater understanding of the molecular drivers of NED is required.

Following the failure of ADT to contain tumour progression to symptomatic CRPC, chemotherapeutics become the first line treatment. Until recently, there was very little evidence to support the use of chemotherapy before this point, either as an adjuvant or neoadjuvant treatment for localised prostate cancer (Canil & Tannock, 2004). However, the latest results from the STAMPEDE clinical trial demonstrate that starting docetaxel chemotherapy alongside ADT or even before ADT can improve survival by an average of 10 months, one of the largest life extension margins in the modern era (James *et al.*, 2016, 2017; Vale *et al.*, 2016).

The primary chemotherapeutic strategy used to treat CRPC is docetaxel in combination with immuno-suppressant prednisone (Heidenreich *et al.*, 2014; James *et al.*, 2016). Docetaxel (approved in 1999) acts by binding to Beta-Tubulin, resulting in induction of apoptosis. Docetaxel has succeeded mitoxantrone (a topoisomerase II inhibitor approved for use since 1987) as the first line of chemotherapeutic treatment for CRPC, providing a modest 2-month improvement to overall survival (Petrylak *et al.*, 2004).

For patients where the disease continues to progress after treatment with Docetaxel, the final clinical chemotherapeutic option currently available is cabazitaxel. Cabazitaxel has been demonstrated to provide a median progression free survival increase compared to mitoxantrone but a significant increase in grade 3 and 4 adverse effects, most notably neutropenia leaving patients at increased risk of infection (Basch *et al.*, 2014).

Despite next generation chemotherapeutics such as docetaxel and cabazitaxel becoming available and approved for use in CRPC, the increase in life extension has been poor with overall survival still under 2 years. The use of chemotherapeutics for metastatic CRPC has to date been an exercise in palliative rather than curative care and their use must be carefully weighed against potential quality of life impacts on patients (Basch *et al.*, 2014; Canil & Tannock, 2004; Petrylak *et al.*, 2004). Currently, the only clinically available response to

PCa NED is the use of platinum based chemotherapeutics (Aparicio *et al.*, 2013). However, these therapeutics, such as cisplatin, do not specifically target mechanisms of NED mediated survival and drug resistance. The life extension and anti-tumour effects of these platinum based agents is modest, usually securing around 8-months life extension (Aparicio *et al.*, 2013; Hager *et al.*, 2016; Vlachostergios & Papandreou, 2015).

Brachytherapy is suitable for men with low-intermediate risk disease and involves either the permanent implantation of radioactive beads into the prostate (low dose rate) or the insertion of radioactive wires into the prostate for several hours (high dose rate). For patients with higher risk disease, brachytherapy is often combined with external beam radiotherapy (EBRT), although EBRT can also be used independently for all patients or used in conjunction with ADT in patients with more advanced disease (Krause *et al.*, 2014; Lu-Yao *et al.*, 2009; von Amsberg *et al.*, 2014).

Immunotherapy is a rapidly emerging area of oncological research which can broadly be defined as any therapeutic designed to invoke an immune or auto-immune response (Hammerstrom *et al.*, 2011). There are three main strategies for immunotherapy including vaccines, monoclonal antibodies and immunomodulatory agents. In 2010 Sipuleucel-T became the first approved therapeutic vaccine for CRPC in patients with minimally symptomatic disease (Hammerstrom *et al.*, 2011). Sipuleucel-T is able to induce an auto-immune response against prostate tumours via *in vitro* modification of a patient's own dendritic cells to present prostatic acid phosphatase on their surface (Fernández-García *et al.*, 2014).

1.2 Progression to Castrate-Resistant Prostate Cancer

Prostate cancer is the second most common cause of cancer-related death in males (Karantanos, Corn, & Thompson, 2013). It is initially androgen dependent and tumours are responsive to ADT (Mooso *et al.*, 2012). However, long-term AD induces prostate cancers to transition to a more aggressive androgen-independent phenotype, resulting in poor prognosis and limited treatment options (Di Lorenzo *et al.*, 2010; Karantanos *et al.*, 2013). These hormone refractory tumours, termed castrate-resistant prostate cancer (CRPC) are able to progress with serum levels of testosterone below 200ng/L (Gomella, 2009) and are incurable once metastasised (Fernández-García *et al.*, 2014). Combined treatment with docetaxel and prednisone is the standard of care for metastatic CRPC (Fig. 1.2) providing only a modest 18-month life extension (Karantanos *et al.*, 2013).

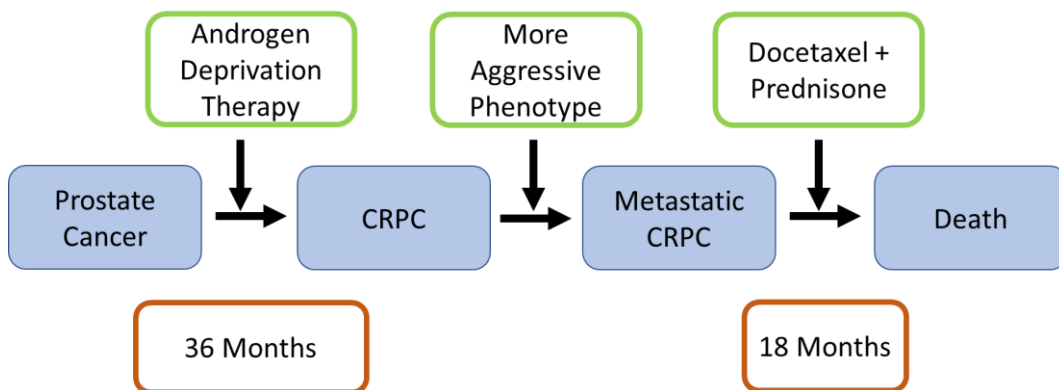


Figure 1.2. Progression of prostate cancer to metastatic castrate-resistant prostate cancer (mCRPC).

1.2.1 Molecular Mechanisms of Castrate Resistant Prostate Cancer

1.2.1.1 Androgen Receptor

The androgen receptor (AR) is critical for the growth and development of the prostate in response to androgens (Gao *et al.*, 2013). The primary mechanism for activation of AR is through the uptake of circulating testosterone which is then converted by SRD5A2 into DHT which has five times greater affinity for the AR than testosterone. Upon activation by DHT, heat-shock proteins HSP90 and HSP70 disassociate causing the AR protein to translocate into the nucleus, form

dimers and to influence gene transcription by binding to androgen responsive elements (AREs) (Cottard *et al.*, 2013; Niu *et al.*, 2008; Zhu *et al.*, 2013).

Removal of the AR ligands testosterone and dihydrotestosterone via ADT is initially effective, however there are a multitude of mechanisms by which AR signalling can persist in the AD environment (Feldman & Feldman, 2001). Although serum levels of androgen are almost entirely ablated by ADT, aberrant androgen receptor (AR) activation via alternative mechanisms or auto/paracrine sources of androgen remains an important consideration, hence these cancers are more accurately described as castrate-resistant rather than androgen-independent (Crawford & Petrylak, 2010). Mutations and expression of different splice variants of the AR gene can facilitate the circumvention of ADT in several ways (Fig. 1.3), including becoming hypersensitive to the remaining androgen, promiscuous activation by non-androgen ligands, direct phosphorylation, alternative pathways for androgen synthesis or upregulation of various AR coactivators (Dehm *et al.*, 2011; Jones *et al.*, 2015; Jones *et al.*, 2017; Kong *et al.*, 2015).

1.2.1.2 Hypersensitive Pathway

Despite ADT, trace levels of serum androgen remain, in response prostate cancer cells often become hypersensitive. One of the most common early events following ADT treatment is amplification of the AR gene allowing for continued AR signalling even at castrate levels of testosterone (Bubendorf *et al.*, 1999; Gundem *et al.*, 2015). The presence of excess AR protein may also be achieved via an upregulation in transcription or enhanced half-life of the protein due to inhibition of its degradation (Katsogiannou *et al.*, 2015). In addition, sensitivity to remaining androgen may be heightened due to increase in 5 α -reductase enzyme activity, thus converting more testosterone to the more potent DHT. (Dutt & Gao, 2009).

1.2.1.3 Promiscuous Pathway

Mutations in the AR gene T877A and L701H change the structure of the AR protein ligand binding domain, resulting in loss of specificity and facilitating promiscuous activation (van de Wijngaart *et al.*, 2010). Of particular interest is

mutant AR T877A which was found to be activated by flutamide, an anti-androgen routinely used in ADT, with flutamide withdrawal proving beneficial to prognosis and resulting in decreased PSA level (Scher & Kelly, 1993). Furthermore, androgen receptor splice variant AR-V7 produces a truncated protein lacking the ligand binding domain entirely and can bind the AREs in the absence of any ligand (Dehm *et al.*, 2011; Jones *et al.*, 2015; Jones *et al.*, 2017; Kong *et al.*, 2015).

1.2.1.4 Outlaw Pathway & Paracrine Signalling

The outlaw pathway removes the necessity of an AR ligand entirely. In this pathway, the AR is directly phosphorylated by AKT/MAPK (Feldman & Feldman, 2001) facilitated by upstream deregulation of growth factors such as EGF or Src (Ishikura *et al.*, 2010). Therefore, mechanisms allowing for modulation of these growth factors may facilitate the outlaw AR mechanism. It has previously been demonstrated that Src can directly phosphorylate the AR and drive its transcriptional activity in low androgen conditions (Guo *et al.*, 2006; Asim *et al.*, 2008; Cai *et al.*, 2011). Interestingly, treatment of PCa cell lines LNCaP and PC-3 with GABA and GABA_A receptor agonists has been shown to increase levels of phospho-Src and resulted in increased proliferation (Wu *et al.*, 2014). Furthermore, elevated phospho-Src was found to be specific to invasive PCa cells co-expressing the GABA_A receptor α 1 subunit (Wu *et al.*, 2014). These previous findings would suggest that GABA is a potential mediator of outlaw AR signalling.

A potential source of GABA is paracrine signalling from NED PCa cells, which have been demonstrated in mouse models, to overexpress the GABA synthesis enzyme GAD1 and possess increased levels of GABA compared to normal NE cells of the prostate (Hu *et al.*, 2002). LNCaP cells have also been shown to secrete GABA vesicles when treated with AR siRNA (Solorzano *et al.*, 2018). In addition to its potential direct role as a facilitator of outlaw AR signalling, paracrine GABA signalling may also indirectly support AR outlaw pathways by inducing the expression of other neuropeptides such as gastrin-releasing peptide (GRP) which is linked to increased invasiveness and resistance to chemotherapeutics in PCa cell lines (Solorzano *et al.*, 2018; Salido, Vilches & Lopez, 2002; Nagakawa *et*

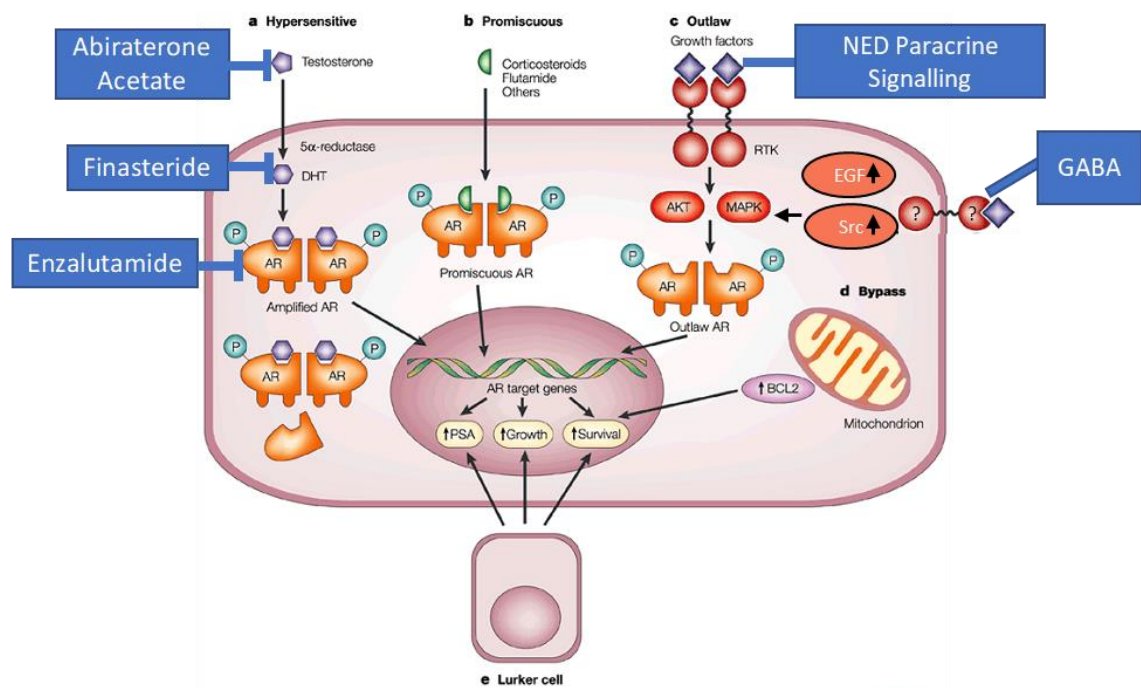
et al., 2008). Treatment of LNCaP cells in low androgen culture conditions with GRP has previously been shown to induce expression of AR target genes specifically in AR⁺ PCa cells (Lee *et al.*, 2001). This evidence suggests that the paracrine GABA signalling via GABA_B receptors effects of NED PCa cells can facilitate a version of the outlaw AR mechanism.

1.2.1.5 Endogenous Androgen Synthesis

Synthesis of dihydrotestosterone (DHT) from testosterone by prostatic cells is facilitated by isoenzyme SRD5A (Chang *et al.*, 2011). Isoform SRD5A2 is constitutively expressed, however, during CRPC progression SRD5A1 expression is induced and becomes dominant. SRD5A1 is able to convert androstenedione to 5 α -androstenedione, allowing for endogenous DHT production in the absence of serum testosterone (Chang *et al.*, 2011). This pathway is active in six different PCa cell lines as well as primary human tissue (Chang *et al.*, 2011)

1.2.1.6 Constitutively active androgen receptor splice variants

It is important to consider that CRPC is not necessarily androgen receptor independent, it is merely independent of AR ligands. Some splice variants of the androgen receptor, such as AR-V7 are known to lack the ligand binding domain, but retain transcriptional activity (Beltran *et al.*, 2016), making them resistant to enzalutamide and abiraterone (Hu *et al.*, 2012). These AR splice variants (including AR-V7 and ARV567es) are known to be upregulated by AD and crucially, these AR splice variants have unique transcriptional profiles that are enriched for cell cycle genes and depleted of genes implicated in cellular differentiation (Hu *et al.*, 2012). Therefore, the emergence of AR splice variants after application of ADT is a key driver of therapeutic resistance and alters the transcriptional landscape of CRPC cells (Jones *et al.*, 2015; Jones *et al.*, 2017; Kong *et al.*, 2015).



Nature Reviews | Cancer

Figure 1.3 Pathways facilitating androgen receptor activation in an androgen deprived environment. Adapted from Feldman and Feldman (2001). (A) Increased production of androgen receptor (AR) and increased conversion of testosterone to DHT results in hypersensitivity to remaining androgen. (B) The ligand specificity of the AR is reduced via mutations, allowing for promiscuous binding and activation of the AR to non-androgens. (C) The androgen receptor is directly phosphorylated by protein kinase B or mitogen- activated protein kinase allowing ligand independent activation. (D) Expression of oncogenes, such as BCL2, prevents apoptosis due to lack of AR signalling. (E) Prostate cancer stem cells and neuroendocrine cells are inherently androgen independent and can facilitate downstream activation of growth and survival pathways through differentiation and paracrine secretions (Feldman & Feldman, 2001). The drug targets of Abiraterone acetate (testosterone synthesis via CYP17A1 inhibition), Finasteride (5α -reductase inhibitor) and Enzalutamide (AR antagonist) are also indicated, as is the proposed mechanism by which PCa NED may utilise the outlaw pathway via secretion of neuropeptides such as GABA in a paracrine manner, although the receptor by which GABA may mediate upregulation of EGF and Src remains unknown (Wu *et al.*, 2014).

1.2.2 Tumour Evolution

The tumour microenvironment places selective pressures upon cancerous cells which influences their evolutionary route towards a more aggressive and metastatic phenotype (Gundem *et al.*, 2015). Although initially highly effective in limiting tumour growth, ADT becomes the prevailing selective pressure upon androgen sensitive tumours, driving them to become castrate-resistant (Dago *et al.*, 2014; Nouri *et al.*, 2014b; Harris *et al.*, 2009). The chronology of mutations facilitating castrate-resistance is variable and multiple mechanisms of CRPC progression have been characterised. However, transition to CRPC is synonymous with mutations to Phosphatase and tensin homolog (PTEN) and TP53 tumour suppressor genes, followed by transient amplification of the androgen receptor (AR) and genes facilitating androgen receptor signalling such as FOXA1 (Gundem *et al.*, 2015).

Although there are uniting carcinogenic events that appear frequently in prostate cancer, it is proposed that both the sub-type of cells these mutations first arise in, as well as the specific microenvironment, is key to determining the evolutionary course of the tumour and its ultimate phenotype (Tu & Lin, 2012). This high level of heterogeneity both between patients and within tumours demonstrates that there is no single root pathway of prostate carcinogenesis or castrate resistance, but rather a complex relationship between multiple distinct mechanisms (Palapattu *et al.*, 2005).

One of the earliest and common events in the natural history of prostate cancer is the fusion of the TMPRSS2 and ERG genes, occurring in the majority of prostate cancers (Esgueva *et al.*, 2010; Gundem *et al.*, 2015; Yu *et al.*, 2010). Transcription of the TMPRSS2 gene is upregulated by androgen receptor signalling, whilst ERG is an oncogene that has been demonstrated to increase cell invasion in prostate cancer through upregulation of MMP-3 and MMP-9 (Tomlins *et al.*, 2008; Yu *et al.*, 2010). In addition to its ability to increase the aggressiveness of prostate cancer, ERG is a multifunctional repressor of androgen receptor signalling, thus TMPRSS2-ERG gene fusion can act to disrupt the canonical androgen mediated differentiation of prostate cells. Furthermore, TMPRSS2-ERG repression of androgen receptor signalling, may constitute an

intracellular selective pressure, driving epigenetic changes facilitating androgen independent growth (Katsogiannou *et al.*, 2015; Tomlins *et al.*, 2008; Yu *et al.*, 2010).

1.2.3 Metastasis and Invasion of Prostate Cancer

Once metastasised, CRPC becomes incurable, therefore understanding mechanisms of metastasis and how these metastases differ from primary tumours is a key area of prostate cancer research (Karantanos *et al.*, 2013; Saad *et al.*, 2015). Matrix metalloproteinase 9 (MMP-9) is a zinc metalloproteinase enzyme which is primarily involved in degradation of extracellular matrix, giving it important roles in tissue remodelling, wound healing as well as facilitating the invasion of cancer cells in a pathological setting (Nagase & Woessner, 1999). Interestingly, evidence shows that GABA(B) receptor activity can promote MMP expression in PCa cells (Abdul *et al.*, 2008; Ippolito *et al.*, 2006). Due to the potentially destructive activity of MMP's, they are produced as inactive zymogens and their activity is tightly regulated by the binding of tissue inhibitors of metalloproteinases (TIMPS) (Ramos-DeSimone *et al.*, 1999; Nagase & Woessner, 1999). In the case of MMP-9, the enzyme is produced as pro-MMP-9 and is inhibited by TIMP-1 (Roderfeld *et al.*, 2009). Activation of pro-MMP-9 and the release of TIMP-1 is a two-step process, requiring the activation of MMP-3 by plasmin, which then allows for MMP-3 to activate MMP-9 (Christensen & Shastri, 2015; Ye *et al.*, 1996). However, it should also be considered that MMP-9 has been shown to be activatable by other enzymes under different conditions, including MMP-2, MMP-7, MMP-10, MMP-13, plasmin, cathepsin G and cathepsin K, however MMP-3 remains the most effective activator of MMP-9 (Christensen & Shastri, 2015). MMP-9 has been strongly associated with metastatic and invasive activity in numerous different types of cancer including cervical (Kato, Yamashita, & Ishikawa, 2002), colorectal (Baker & Leaper, 2002), liver and pancreatic (Nagakawa *et al.*, 2002). Prostate cancer tumours with Gleason scores above 8 had significantly higher MMP-9 mRNA and protein levels than those with a Gleason score of 6 or less ($p = 0.01$) (Cardillo, Di Silverio, & Gentile, 2006). In addition, when the prostate cancer cell line LNCaP was transfected with a pcDNA6-MMP-9 expression plasmid, invasive activity was significantly increased (Aalinkeel *et al.*, 2004).

1.2.4 Cancer Stem Cells

Cancer stem cells (CSCs) have been implicated in a wide range of cancer types due to their self-renewal properties, high potential for differentiation and resistance to chemotherapeutics (Chen *et al.*, 2013; Hu *et al.*, 2009; Klarmann *et al.*, 2009). Although treatments such as ADT, docetaxel and radiotherapy are effective against the majority of prostate cancer cells, an underlying sub-population of CSCs are refractory to treatment and can re-establish the tumour mass (Zhang & Waxman, 2010). This is of particular clinical interest in prostate cancer where the AD state of the patient creates a strong selective pressure upon the CSCs, inducing an androgen independent tumour phenotype (Chen *et al.*, 2013; Gudem *et al.*, 2015). It is important to distinguish that even within a CSC population there is considerable heterogeneity and sub-types (Chen *et al.*, 2013). An effective way to characterise these is through analysis of co-expression patterns of CSC surface markers such as CD44, CD133, CD166 and $\alpha 2\beta 1$ -integrin (Mizrak, Brittan, & Alison, 2008; Patrawala *et al.*, 2006; Reyes *et al.*, 2013; Smith *et al.*, 2012; Tu & Lin, 2012).

The presence and activity of CD44⁺ CSCs would appear to be a strong evidence in support of the lurker cell theory given that they are AR⁻ but are able to differentiate into AR⁺ tumour cells. CD44⁺ cells were also found to have higher rates of proliferation and metastatic ability than CD44⁻ prostate cancer cells and appear to co-express several other genes native to stem cells such as Oct-3/4, Bmi, beta-catenin and SMO. (Patrawala, *et al.*, 2006)

CD133⁺ cells have been shown to make up around 5% of the population of prostate cancer cell lines and they fit the usual criteria of CSCs in that they are able to self-renew, proliferate indefinitely and are able to differentiate (Reyes *et al.*, 2013). AC133 is a glycosylated epitope of CD133 and cells with expression profile AC133⁺/CD34⁺ showed greater proliferation than AC133⁻/CD34⁺ cells indicating that AC133 is a more specific target for the identification of CD133 stem cells. (Mizrak, Brittan, & Alison, 2008). CD166 has been demonstrated to be highly expressed in the prostates of developing human fetuses as well as in both

human and mouse CRPC cells, making it a likely CSC marker (Smith *et al.*, 2012).

1.3 Neuroendocrine Differentiation

Neuroendocrine differentiated (NED) tumour cells are thought to transdifferentiate from adenocarcinoma cells (Fig. 1.4), a theory supported by genetic analysis (Sauer *et al.*, 2006). Neuroendocrine-like (NE) cells have been implicated in the progression of PCa to CRPC because of the role of NE cells in healthy prostate tissue in stimulating the growth of surrounding cells in a paracrine manner (Terry & Beltran, 2014). NE-like cells are non-proliferative, making them resistant to many chemotherapeutics, and able to resist apoptosis by overexpression of survivin (Xing *et al.*, 2001), allowing continued paracrine support of regional cancerous cells through expression of proliferative and angiogenic growth factors (Chevalier *et al.*, 2002).

Increased NED is closely associated with PCa disease progression whilst under the selective pressure of ADT, which can be seen both histologically and in increased NED markers such as NSE and CgA in patient serum (Isgro, Bottoni, & Scatena, 2015; Kamiya *et al.*, 2003; Rech *et al.*, 2006). NED is becoming a more prevalent issue in prostate cancer treatment, which has coincided with the introduction of more potent ADT therapeutics. In addition, the proportion of patients experiencing NED is increasing as patients are living longer with prostate cancer, giving more time for NED to occur (Bluemn *et al.*, 2017).

Given that ADT is a known inducer of NED both *in vitro* (Rapa *et al.*, 2013) and *in vivo* (Zhang *et al.*, 2018), that PCa resistance to ADT and progression to CRPC is inevitable in patients (Beltran *et al.*, 2011) and that CRPC and mCRPC tumours show greatly increased NED with disease progression (Borromeo *et al.*, 2016), it is clear that NED may be a core facilitating feature of progression and maintenance of CRPC. In this study we aim to investigate how androgen deprivation of androgen sensitive PCa cells can trigger NED, the extent to which this is reversible and whether there is potential for paracrine (e.g. GABAergic)

signalling in PCa NED cells using an *in vitro* model. Previous studies have demonstrated that the androgen sensitive PCa cell line LNCaP is amenable to NED in response to a variety of treatments including AD, radiotherapy, chemotherapeutics and hypoxia (Bang *et al.*, 1994; Cox *et al.*, 1999; Zhu *et al.*, 2014; Deng *et al.*, 2011; Farach *et al.*, 2016; Komiya *et al.*, 2009; Rapa *et al.*, 2008, 2013; Danza *et al.*, 2012; Liang *et al.*, 2014; Lin *et al.*, 2016; Sarkar *et al.*, 2011; Yadav *et al.*, 2017), making it a practical and robust basis of a model to study the effects of AD and intermittent AD in the context of PCa NED.

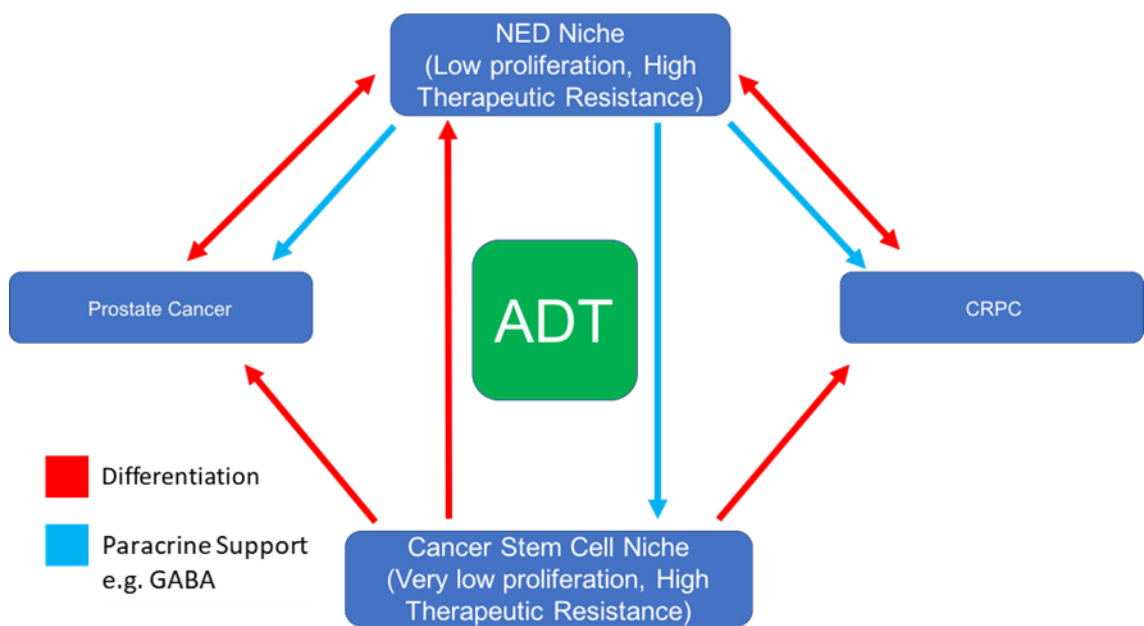


Figure 1.4 The origin and involvement of the NE niche in CRPC progression.

The cancer stem cell (CSC) niche can contribute to disease recurrence and progression through classical tumour reseeded (Chang, 2016). The CSC niche has low proliferation and high therapeutic resistance, meaning that after the application of therapeutic regimens such as androgen deprivation therapy (ADT), CSCs can remain (Lang *et al.*, 2009), these cells can then contribute to disease progression by repopulating the tumour with castrate-resistant or androgen-independent cells (Lang *et al.*, 2009). The less differentiated state of CSCs grants increased ability to adapt under the selective pressure of applied therapeutics (Chang, 2016; Lang *et al.*, 2009). It is a possibility that the NED niche may also be able to fulfil a similar role, by becoming treatment resistant (Hu *et al.*, 2015) and later transdifferentiating back into an epithelial PCa (Shen *et al.*, 1997) or

castrate-resistant prostate cancer (CRPC) phenotype. Furthermore, the enrichment of the NED niche within tumours could have the potential to exert effects upon surrounding PCa and CRPC cells, as well as influencing the differentiation of existing CSCs through modulation of the tumour microenvironment (Chevalier *et al.*, 2002; Hu *et al.*, 2015; Terry & Beltran, 2014; Xing *et al.*, 2001).

1.3.1 Potential interplay between PCa CSCs, epithelial PCa cells and NED PCa cells.

When describing the potential implications of PCa NED it is important to consider that within a tumour, the NED niche is also accompanied by the cancer stem cell population, androgen sensitive epithelial PCa cells and potentially CRPC cells. Although NED PCa cells are known to have a slower proliferative rate than epithelial PCa cells (Grigore *et al.*, 2015) the effects that these NED cells may have upon the other subpopulations of PCa cells via paracrine signalling may contribute to the poorer outcomes observed clinically in tumours with high NED (Komiya *et al.*, 2013). The precise mechanisms of interplay between the NED niche and other PCa tumour subpopulations remains poorly understood. However, the ability of NED PCa cells to secrete neuropeptides and growth factors is well established including NSE, chromogranin-A, bombesin and synaptophysin which are clinically utilised NED markers. Recently, the possibility that NED PCa cells could be secreting or be sensitive to GABA has been a growing area of research interest (Ippolito & Piwnica-Worms, 2014; Wu *et al.*, 2014). In addition, several other secreted factors of NED PCa cells have been reported in the literature including: adrenocorticotrophic hormone, antidiuretic hormone, α -human chorionic gonadotrophin, calcitonin, cholecystokinin, glucagon, parathyroid hormone-related protein, serotonin, somatostatin and thyroid-stimulating hormone (Bok and Small, 2002; Cussenot *et al.*, 1998, Abrahamsson., 1999; Ather *et al.*, 2000).

Considering the plethora of secreted paracrine factors produced by NED PCa cells, it is possible that this modification of the tumour microenvironment could influence the activity and differentiation of PCa CSCs into proliferative PCa or

CRPC cells (Fig 1.4). Such mechanisms could enhance the ability of the PCa CSC niche to contribute to tumour reseeding, therapeutic resistance and disease recurrence under ADT. For example, NED PCa cells have been linked to the activation of EGFR pathway in surrounding cells (Wu *et al.*, 2014) and this is a key driver of CSC self-renewal (Rybak *et al.*, 2013; Conteduca *et al.*, 2014). The ability of PCa CSCs to facilitate tumour recurrence by differentiation into resistant and proliferative phenotypes is well established (Chang, 2016; Lang *et al.*, 2009).

The ability of PCa cells to undergo NED as a resistance mechanism to ADT, radiotherapy and several chemotherapeutics could provide a similar 'resevoir' of highly resistant cells that are able to return to a proliferative epithelial phenotype similar to the CSC niche (Deng *et al.*, 2011; Hu *et al.*, 2015; Wang *et al.*, 2018; Yadav *et al.*, 2017). This studies proposed pathway for PCa NED is described in section 1.3.4. In addition, the secreted factors of the NED subpopulation are thought to facilitate the growth and survival of PCa epithelial cells in low androgen conditions (Ippolito *et al.*, 2006; Ippolito & Piwnica-Worms, 2014; Komiya *et al.*, 2009; Wu *et al.*, 2014).

1.3.2 Known inducing factors of NED

NED has been demonstrated to be inducible in LNCaP cells by a variety of stimuli, including cAMP (Bang *et al.*, 1994; Cox *et al.*, 1999), IL-6 (Zhu *et al.*, 2014), ionising radiation (Deng *et al.*, 2011), ADT (Farach *et al.*, 2016; Komiya *et al.*, 2009; Rapa *et al.*, 2008, 2013), hypoxia (Danza *et al.*, 2012; Liang *et al.*, 2014; Lin *et al.*, 2016), chemotherapeutics such as docetaxel (Sarkar *et al.*, 2011) and most recently, tyrosine-kinase inhibitors such as dovitinib (Yadav *et al.*, 2017). Importantly, there are no existing therapeutics which directly target NED PCa cells or the NED process. Evidently, the wide range of endogenous and therapeutic stimuli that can induce PCa NED is of concern clinically and highlights a need to better understand NED as a mechanism of therapeutic resistance and progression to CRPC. Interestingly, the morphological features induced by all of these stimuli and the increased expression of a core set of NED biomarkers (NSE, CgA and synaptophysin) appear to be present in all these types of NED induction. There are also some known molecular drivers of NED that appear to be shared across at least two inducing factors, for example the reduction in RE-

1 silencing transcription factor (REST) expression (the canonical repressor of neurogenesis) has previously been implicated in both IL-6 and hypoxia mediated PCa NED (Liang *et al.*, 2014; Zhu *et al.*, 2014). However, considering PCa NED research has only recently increased in volume and that this research is fragmented between studies investigating a wide array of different inducing factors, each with their own models, it remains unclear which components of the PCa NED pathway are shared or required. In contrast, study of lung cancer NED has progressed relatively rapidly, partly due to NED being a feature mainly observed in small cell lung cancer (SCLC) (Meder, *et al.*, 2016). The molecular mechanisms by which these known inducers can trigger NED can be distinct. For example IL-6 is implicated in activation of PI3K and STAT3 pathways (Deeble *et al.*, 2001). Meanwhile, cAMP induction of NED is thought to arise from activation of the PKA/CREB signalling pathway (Cox *et al.*, 1999). Furthermore, a recent study demonstrated that canonical neurogenesis promoter human achaete-scute homolog-1 (hASH1) is essential for NED in SCLC in both human SCLC cell lines and in a mouse model (Borromeo *et al.*, 2016)

1.3.3 Previously developed models of ADT induced NED

The focus of this project is to investigate AD as an inducing factor of PCa NED, which required the development and characterisation of a model of ADT induced NED using androgen-sensitive LNCaP cells. Several models are previously published in the literature and can broadly be categorised into two branches; models which utilise current ADT therapeutics to target the AR directly and ones in which androgens are depleted from the cell culture media. This can be achieved through charcoal-stripping the fetal bovine serum (CS-FBS), which preferentially, but not specifically, removes hormones from the media and/or by reducing the overall concentration of FBS in the media, typically from 10% to 5%, which uniformly decreases all factors within the FBS (Farach *et al.*, 2016; Komiya *et al.*, 2009; Rapa *et al.*, 2008, 2013).

The vast majority of existing ADT induced NED models for PCa utilise the LNCaP cell line, however LuCaP cells are occasionally used as an *in vivo* xenograft model (Xiaotun Zhang *et al.*, 2015). Models using charcoal-stripping and

reduction of FBS in the cell culture media usually use either 10% (Rapa *et al.*, 2013; Shen *et al.*, 1997), 5% (Yuan *et al.*, 2006) or 0% (Juarranz *et al.*, 2001; Martín-Orozco *et al.*, 2007) CS-FBS. Under these conditions, LNCaP cells have been cultured for up to 4 days in 0% FBS, up to 9 days using 5% CS-FBS and 15 days with 10% CS-FBS (Juarranz *et al.*, 2001; Martín-Orozco *et al.*, 2007; Rapa *et al.*, 2013; Yuan *et al.*, 2006). Some studies have also directly used ADT therapeutics to create models of NED using LNCaP cells (Bishop *et al.*, 2017).

1.3.4 This studies proposed pathway of AD-induced NED

Notch1 is selectively expressed in the basal epithelial cells of the adult prostate where it regulates and maintains cell differentiation and is highly expressed in prostate progenitor cells during development (Belandia *et al.*, 2005; Wang *et al.*, 2004). One function of the Notch1 signalling cascade is the negative regulation of hASH1 (a promoter of neurogenesis) through upregulation of bHLH transcriptional repressor genes Hes1 and Hey1 (Axelson, 2004; Ishibashi *et al.*, 1995). PTOV1 acts as a negative regulator of Notch1 signalling by interacting with the Notch repressor complex, thus facilitating increased expression of hASH1 leading to NED. This mechanism is further evidenced by the co-localisation of PTOV1 with NED marker chromogranin-A (Alaña *et al.*, 2014) and the correlation between AD and increased hASH1 expression (Rapa *et al.*, 2008)

Notch signalling via Hey1 also acts as a repressor of AR signalling in the absence of testosterone, therefore loss of Notch signalling may allow continued expression of androgen responsive genes even in an AD state (Belandia *et al.*, 2005). Patients with PCa showed a complete lack of Hey1 localised in the nucleus whereas those with benign prostate hyperplasia retained Hey1 in the nucleus (Belandia *et al.*, 2005). These findings suggest that abnormalities in Notch1 signalling and the resulting exclusion of Hey1 from the nucleus could contribute to androgen independence. This hypothesis was supported by a previous study demonstrating the tumour suppressive qualities of Notch and Hey1 in the prostate and that PTOV1 may be responsible for the breakdown of Notch signalling during PCa progression (Alaña *et al.*, 2014). In order to prevent activation of pro-neural development pathways in non-neuronal tissues, and to preserve the adult neural stem cell pool, REST recruits corepressors CoREST and mSin3a to the

chromatin for prevent the expression of target genes including hASH1 (Gao *et al.*, 2011). Therefore, a reduction in REST expression or activity is likely necessary to allow for hASH1 mediated NED and has been previously found to be essential for hypoxia-induced NED of PCa (Lin *et al.*, 2016).

1.3.5 hASH1 mediated canonical neurogenesis

Transcription factor hASH1 is critical to neuroblast differentiation and helps to maintain lateral inhibition by increasing the expression of Delta-like ligands. Although originally discovered in drosophila studies, the mechanism of hASH1 mediated neurogenesis has been found to be conserved in all animals (Henke *et al.*, 2009; Nelson *et al.*, 2009) and is particularly important in the development of GABAergic neurons (Guillemot & Hassan, 2017; Casarosa, Fode & Guillemot, 1999). hASH1 is expressed in neuronal pre-cursor cells of both the central (CNS) and peripheral nervous system (PNS). Gain and loss of function experiments have demonstrated that hASH1 is required for neurogenesis and able to independently drive neurogenesis (Bertrand *et al.*, 2002; Wilkinson *et al.*, 2013). Knock down of hASH1 in mouse models *in vivo* results in a lethal phenotype due to improper formation of the CNS and PNS (Axelson *et al.*, 2004). The ability for hASH1 to induce neurogenesis has also been demonstrated in fibroblasts, pericytes and astrocytes (Raposo *et al.*, 2015; Vierbuchen *et al.*, 2010). hASH1 is able to drive deployment of neuronal transcriptional programs by binding to its putative consensus site 'CAGCTGC', where hASH1 targets gene pathways responsible for neurotransmitter biosynthesis, notch signalling regulation, axon guidance, regulation of cell cycle and cell fate commitment and cell projection morphogenesis amongst others as assessed by ChIP-chip and Gene Ontology analysis results (Castro *et al.*, 2011).

1.3.6 hASH1 ability to act as a pioneer factor in neurogenesis and cancer

The powerful ability of hASH1 to trigger neurogenesis both in neural precursor and non-neuronal cells relies on its ability to act as a pioneer factor and facilitate the accessibility of closed chromatin (Raposo *et al.*, 2015). The pioneer factor activity of hASH1 is likely the reason that it is a required factor for neurogenesis, as it allows subsequent transcription factors to access chromatin and drive expression of their target genes (Raposo *et al.*, 2015; Zaret & Carroll, 2011).

Furthermore, the chromatin remodelling and genome wide transcriptional activity of pioneer factors such as hASH1 make them a strong candidate for roles in NED of PCa cells and hASH1 has been strongly implicated in NED of small cell lung cancer (SCLC) (Borromeo *et al.*, 2016). Importantly, hASH1 is unique in its ability to trigger neuronal differentiation in non-neuronal tissues (Guillemot & Hassan, 2017).

hASH1 activity in cancer has been most thoroughly studied in neuroblastoma (NB) (Gillotin, Davies & Philpott, 2018; Wylie *et al.*, 2015). During canonical neurogenesis, hASH1 is expressed transiently, increasing in expression in non-proliferating differentiating cells until neurogenesis is complete and then receding as cells re-enter the cell cycle (Raposo *et al.*, 2015). However, in the NB setting, hASH1 expression fails to decrease and remains high even in proliferating NB cells (Wylie *et al.*, 2015), it is thought that the phosphorylated hASH1 is able to maintain NB cells in a proliferative state, potentially through interactions with N-MYC (Wylie *et al.*, 2015). Therefore, hASH1's role in NB is converse to its reported role in non-neuronal cancers such as SCLC and PCa. In the NB setting high hASH1 expression prevents the final stage of differentiation, maintaining the plasticity of NB precursor cells, whereas in SCLC and PCa hASH1 could effectively 'de-differentiate' epithelial cancer cells, driving NED and increased plasticity by contributing to further repression of notch signalling (Somasundaram *et al.*, 2005).

1.3.7 hASH1 activity in SCLC

In addition to neuroblastoma, hASH1 has also been extensively studied in the context of SCLC NED and has been identified as a potential therapeutic target (Augustyn *et al.*, 2014; Borromeo *et al.*, 2016; Demelash *et al.*, 2012; Nishikawa *et al.*, 2011; Osada *et al.*, 2008, 2005). Recent studies have demonstrated that hASH1 is the only required and sufficient factor to induce SCLC NED and that the target genes of hASH1 in SCLC include several GABAergic pathway genes including GAD2 which synthesizes GABA and GABA_A receptor subunit GABRB3 (Borromeo *et al.*, 2016). In addition, it is known that hASH1 drives expression of Delta-like ligands and research into hASH1 activity in SCLC has led to the development of rovalpituzumab, a DLL3 inhibitor which is currently in phase III

clinical trials (ClinicalTrials.Gov; NCT03033511). This previous literature provides a strong basis that hASH1 is able to induce NED in non-neuronal tissue cancer types and further demonstrates the pioneer factor activity of hASH1 facilitating NED in already differentiated cells making hASH1 a logical candidate for driving PCa NED as well.

1.3.8 hASH1 in PCa

Previous studies examining PCa NED have demonstrated that transduction of hASH1 is associated with increased expression of NED markers chromogranin-A and synaptophysin (Rapa *et al.*, 2013). Furthermore, hASH1 staining has previously been found in the nuclei of human PCa samples co-expressing chromogranin-A (Rapa *et al.*, 2008). However, no studies have previously examined the response of hASH1 localisation to androgen deprivation and whether these responses are persistent or reversible during intermittent androgen deprivation or whether hASH1 triggers a GABAergic phenotype.

1.4 Gamma aminobutyric acid is implicated in increased growth and aggression of prostate cancer

Although originally thought to only be present in the central and peripheral nervous system, it is now well established and accepted that both GABA_A and GABA_B receptors are present and functional in many healthy non-neuronal tissues, albeit in much lower abundance (Takehara *et al.*, 2007; Hedblom & Kirkness 1997; Tyagi *et al.*, 2007). Therefore, and perhaps unsurprisingly, GABARs have also been detected in multiple cancer types including PCa where a previous study detected GABA_ARs in 95% of prostate cancer specimens by immunohistochemistry (Abdul, McCray & Hoosein, 2007). Whilst much is still unknown about their oncogenic activity, activation of both the GABA_A and GABA_B receptors in cancer has been demonstrated to modulate growth, invasion and metastasis of cancer cells (Young & Bordey, 2009; Bugar *et al.*, 2016; Wu *et al.*, 2014). Given that hASH1 has previously been associated with increased prostate cancer NED (Rapa *et al.*, 2008; Rapa *et al.*, 2013) and that hASH1 is known to drive the differentiation of GABAergic neurons (Guillemot & Hassan, 2017; Casarosa, Fode & Guillemot, 1999), this has led to investigations into the potential activity of GABA and GABARs in PCa NED.

Presence of NE-like cells in prostate cancers and enrichment of this cell niche via ADT induced transdifferentiation has prompted researchers to analyse the gamma aminobutyric acid (GABA) axis as a possible novel mechanism of castrate resistance (Ippolito & Piwnica-Worms, 2014; Nouri *et al.*, 2014; Wu *et al.*, 2014). Recent studies have demonstrated that GAD1, a gene encoding GAD67 enzyme, critical for production of GABA, is upregulated in CPRC (Ippolito & Piwnica-Worms, 2014). Furthermore, it has also been demonstrated that treatment of prostate cancer cells with GABA upregulated transcription of epidermal growth factor and resulted in increased activation of EGFR and Src (Wu *et al.*, 2014), which would implicate GABA as potentially modulating PCa growth via the outlaw pathway (Figure 1.3).

GABA production is dependent upon GAD65 and GAD67 encoded by the GAD2 and GAD1 genes respectively (Hu, *et al.*, 2002). Expression of the mouse variant of hASH1, mASH1, is known to induce production of GAD67 in mice (Fode, *et al.*, 2000) and hASH1 is also known to drive the development of GABAergic neurons (Castro *et al.*, 2011; Peltopuro *et al.*, 2010; Wang *et al.*, 2017). Immunohistochemistry analysis of PCa previously found that the expression of hASH1 correlated with NE differentiation and that hASH1 expression was co-localised with NE marker chromogranin-A (Hu, *et al.*, 2002).

Activation of GABA_A receptors (GABA_ARs) by GABA has been demonstrated to result in activation of the EGFR and Src in both LNCaP and PC-3 PCa cell lines. These pathways are strongly associated with tumour growth, therefore, it is suggested that transdifferentiation of PCa cells to NE-like cells can provide PCa tumours with an androgen independent pathway for growth and survival via the paracrine signalling of NE transdifferentiated cells (Wu, *et al.*, 2014). In addition, activation of the GABA_A receptor has been demonstrated to increase the growth of four PCa cell lines, whilst the same study found GABA_B receptor agonism had no effect on growth (Abdul, McCray & Hoosein, 2007). Meanwhile, activation of the GABA_B receptor has been demonstrated to increase the invasive abilities of PCa cells through upregulation of MMP-9, an effect which was not observed after treatment with GABA_A receptor agonists (Azuma *et al.*, 2003). This suggests that the oncogenic activity of GABA_ARs in PCa is potentially synergistic, with GABA_AR

activation implicated in increased growth and GABA_BR with invasive potential. Finally, GABA has previously been shown to increase androgen production in rat testicular tissue (Ritta, Campos, & Calandra, 1987). It is already established that prostate cancer tumours are capable of producing DHT from androgen precursors (Chang, Ercole, & Sharifi, 2014; Chang *et al.*, 2011) and this might be a mechanism of ADT resistance.

1.4.1 Structure and function of GABA_A and GABA_B receptors

There are two classes of GABARs, the ionotropic GABA type A receptors (GABA_ARs) and the metabotropic type B receptors (GABA_BRs). The GABA_AR family also includes the GABA type C (GABA_CRs), however, these are generally confined to the retina (Lukasiewicz, 1996; Qian, 1995) and are not considered in this study. The structure and function of GABA_ARs and GABA_BRs is very different, GABA_ARs are ligand-gated ion channels, whereas GABA_BRs are G-protein coupled receptors. As such, GABA_ARs usually mediate rapid responses to the endogenous ligand GABA (Barnard *et al.*, 1998), whilst GABA_BRs mediate slower responses to GABA (Bowery *et al.*, 2002). Although, it should be noted that some GABA_ARs can mediate slow responses, which is believed to be mediated by the $\alpha 5$ subunit (Zarnowska *et al.*, 2009).

1.4.2 GABA_A Receptors

The structure of the GABA_AR is considerably more complex than that of the GABA_BR, with the full crystal structure only recently resolved (Miller & Aricescu, 2014). Therefore, when studying GABA_AR subunits, especially in novel contexts such as PCa and NED PCa, all subunits must be considered. In a physiological setting, a GABA_AR usually comprises two α , two β and one other subunit (generally a γ subunit) (Sigel & Steinmann, 2012). The $\alpha\beta\gamma$ receptors are generally synaptic, where they mediate phasic transmission, $\alpha\beta\delta$ receptors are mainly extrasynaptic where they mediate tonic inhibition (Dixon *et al.*, 2014; Serwanski *et al.*, 2006; Zheleznova *et al.*, 2009). The most common combination of subunit is $\alpha 1$, $\beta 2$ and $\gamma 2$ (Whiting, McKernan, & Wafford, 1995), which is usually arranged $\gamma 2\beta 2\alpha 1\beta 2\alpha$ around the central pore of the receptor (Baumann *et al.*, 2002; Baur *et al.*, 2006; Tretter *et al.*, 1997). In addition to $\alpha 1-6$, $\beta 1-3$ and $\gamma 1-3$

there are also the δ , ϵ , θ and π subunits, which can substitute for the γ subunit with various effects upon the receptors activity and pharmacology (Jacob et al., 2008; Montori et al., 2012). Also of interest, is that five $\beta 3$ subunits have the ability to form functional GABA_ARs, independently of other subunits (Miller & Aricescu, 2014). GABA binds to GABA_ARs at the interface of the α and β subunits and activation occurs when two GABA molecules bind simultaneously (Puthenkalam *et al.*, 2016). Upon GABA binding, a conformational switch forms, which opens the ion channel resulting in Cl⁻ ion flow into the cell causing membrane hyperpolarisation and thereby inhibiting neurotransmitter release (Miller & Smart, 2010).

The GABA_AR subtype has thus far shown to be of particular importance in the progression of CRPC as its activation has many downstream proliferative and mitogenic effects including upregulation of EGF and activation of Src which activates both the MAPK and STAT pathways (Wu *et al.*, 2014). When studying the effects of GABA_AR activation, the specific agonist muscimol is frequently utilised in the literature (Johnston, 2014).

1.4.3 GABA_B Receptors

In comparison to GABA_A receptors which can be formed from 16 different subunits, GABA_B receptors are heterodimers composed of just 2 subunits (Bormann, 2000), GABA_{B1} and GABA_{B2}. The GABA_{B1} subunit also has two isoforms, GABA_{B1a} and GABA_{B1b} encoded by the GABBR1 gene, although the effects of each isoform appear to be indistinguishable (Gassmann & Bettler, 2012). GABA_BRs, like GABA_ARs, are also typically inhibitory to neurotransmitter release (Benarroch, 2012; Hill & Bowery, 1981). The GABA_{B1} subunit contains an arginine-rich endoplasmic reticulum-retention signal, which is obstructed when bound to GABA_{B2}, ensuring that only these heterodimers are able to leave the endoplasmic reticulum and reach the cell surface (Gassmann & Bettler, 2012). The GABA_{B1} subunit contains the GABA binding site, whilst the GABA_{B2} subunit is responsible for activation of the G protein (Gassmann & Bettler, 2012). Binding of GABA to GABA_BRs results in the closure of the Venus fly trap domain (VFTD) of GABA_{B1}, causing it to interact with the VFTD of GABA_{B2}, resulting in activation

of the G protein (Gassmann & Bettler, 2012). Synthetic selective GABA_BR agonist baclofen is employed ubiquitously in the previous literature examining the effects of GABA_BR activation (Hill & Bowery, 1981).

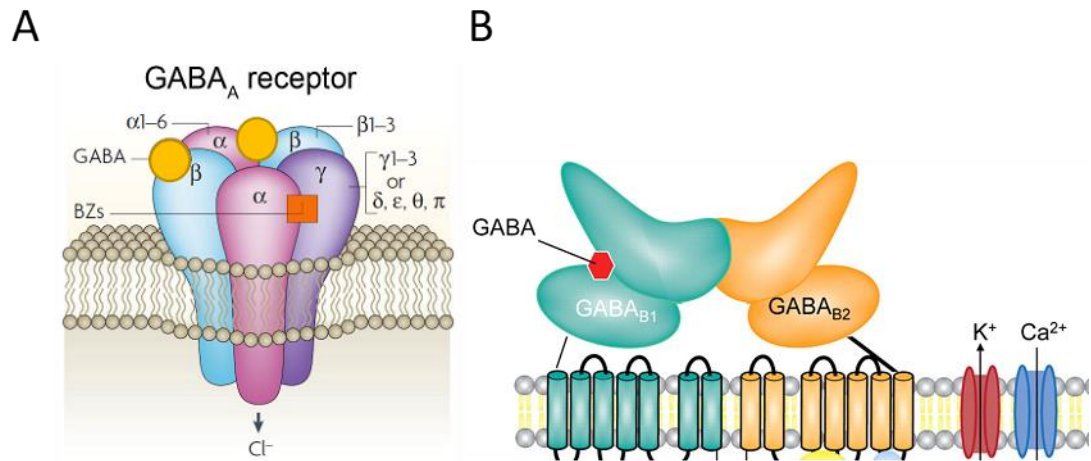


Figure 1.5 Structural diagram illustrating the composition of a typical GABA_AR and GABA_BR. (A) GABA_ARs are heteropentameric and can be formed from 16 unique subunits. The endogenous ligand GABA binds at the interface of α and β subunits and activation of the receptor requires the simultaneous binding of two GABA molecules. Upon activation, the central pore of the receptor opens and allows the influx of Cl^- ions. Many clinically important pharmacological agents also bind to GABA_ARs, including benzodiazepines (BZs on image). **(B)** GABA_BRs are obligate heterodimers of just two subunits (GABA_{B1} and GABA_{B2}), the GABA_{B1} subunit comprises the GABA binding site and is retained in the endoplasmic reticulum until bound to the GABA_{B2} subunit, which is responsible for the activation of the G protein. GABA_BRs are indirectly coupled to K^+ ion channels and when activated they open K^+ ion channels and decrease influx of Ca^{2+} ions (Olsen & DeLorey, 1999). Image of GABA_AR adapted from (Jacob, Moss, & Jurd, 2008) and image of GABA_BR adapted from (Benarroch, 2012).

1.4.4 CCC regulation of GABA_A receptor activity

The chloride gradient across the cell membrane is a key determinate of whether GABA_AR activity is inhibitory or excitatory. Therefore, the activity of cation-chloride co-transporters (CCCs) ultimately influences the effects of GABA_AR signalling.

Despite GABA's role as the most prevalent inhibitory neurotransmitter in the human central nervous system, when neuronal chloride concentration is high, the activation of GABA_A receptors by GABA and other clinically-important ligands can act in an excitatory rather than inhibitory manner (Li & Xu, 2008). This process is determined by the chloride gradient of the cell and this is regulated by CCC transport proteins (Kahle *et al.*, 2008; Li & Xu, 2008).

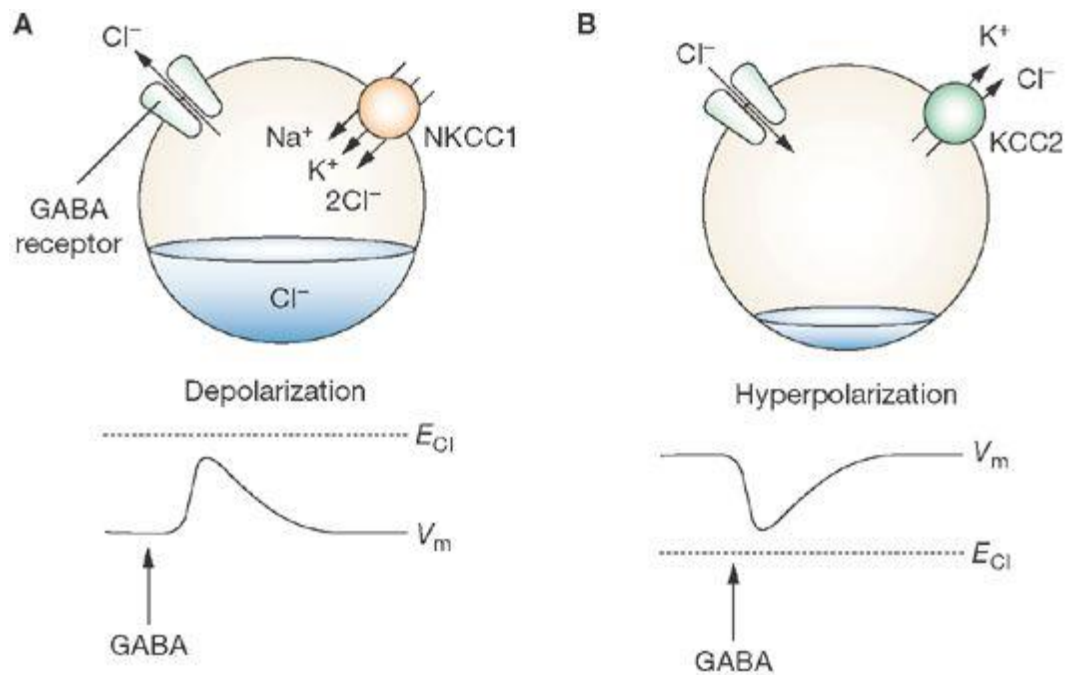


Figure 1.6 The expression and activity of CCCs determines the activity of GABA_ARs. (A) Na-K-2Cl cotransporter NKCC1 is the predominantly expressed CCC during neonatal neuronal development and usually has high activity, whilst KCC2 expression and activity is very low during development, therefore the [Cl⁻]_i is high meaning that activation of the GABA_AR and therefore opening of the CCCs results in chloride efflux, causing neuronal excitation via depolarization (Li & Xu, 2008; Succol *et al.*, 2012). (B) In mature neurons, KCC2 expression and activity increases whilst NKCC1 decreases (Hartmann & Nothwang, 2014; Li & Xu, 2008). This results in a lower [Cl⁻]_i, therefore,

activation of the GABA_A receptor results hyperpolarization (neuronal inhibition) due to chloride influx, adapted from Kahle *et al.*, (2008). Also important to note is that the composition of the GABA_AR subunits can be influenced by the chloride gradient, therefore, certain subunit assemblies can be indicative of excitatory or inhibitory activity (Succol *et al.*, 2012).

The chloride gradient of cells and the nature of GABA_A receptor activity is primarily governed by CCCs. These can be categorised into Na⁺-K⁺-2Cl⁻ co-transporters (NKCC1-2) and K⁺-Cl⁻ co- transporters (KCC1-4). The Cl⁻ concentration in neonatal cells is known to be higher (by 20-40 mM) than in adult neurons, a shift which determines whether GABA receptor activation is inhibitory (adult neurons, lower Cl⁻ concentration) or excitatory (immature neurons, higher Cl⁻ concentration) (Ben-Ari, 2002). NKCCs typically raise the neuronal [Cl⁻]_i by Cl⁻ influx, whilst KCCs mediate Cl⁻ efflux and lower neuronal [Cl⁻]_i (Ben-Ari, 2002). Thus, NKCC1 is upregulated during early CNS development, whilst KCC2 is responsible for the shift from excitatory to inhibitory action of GABA receptors and is a useful biomarker of mature neurons (Li & Xu, 2008), however NKCC1 is ubiquitous and not a specific neuronal marker (Ben-Ari, 2002; Li & Xu, 2008).

1.4.5 GABA Metabolism in cancer

In addition to its effects mediated through GABA_A and GABA_B receptors, some studies have proposed that metabolism of GABA could also be a pro-oncogenic pathway facilitating PCa NED and CRPC (Ippolito *et al.*, 2006; Ippolito *et al* 2014), a theory which has been previously demonstrated in other cancer types including breast cancer brain metastases (Neman *et al* 2014) and gastric cancer (Matuszek *et al.*, 2001). In addition, the prostate tissue is known to have one of the highest levels of GABA-T expression outside of the CNS (DepMap, Broad Institute), an enzyme that alongside SSADH can convert GABA into succinate and therefore input into the TCA cycle (Ippolito *et al.*, 2006).

1.4.6 Previous GABA_AR and GABA_BR studies in prostate cancer

GABARs have been found in a variety of tissue types and implicated in a multitude of disease states, including PCa (Nouri *et al.*, 2014; Wu *et al.*, 2014). Glutamate decarboxylase 1 (GAD1) which encodes the GAD67 enzyme, critical

for GABA synthesis and is upregulated in CPRC (Ippolito & Piwnica-Worms, 2014). Furthermore, treatment of PCa cells with GABA (10 nM) upregulated transcription of epidermal growth factor (EGF) and resulted in increased activation of epidermal growth factor receptor (EGFR) and Src (a non-receptor tyrosine kinase which transduces signals from the EGFR) (Wu *et al.*, 2014). Activation of EGFR and Src is closely associated with increased proliferation, treatment of LNCaP and PC-3 cells with 10 nM GABA significantly increased growth (Wu *et al.*, 2014). A possible mechanism for the initiation of EGFR and Src signalling is activation of the GABA_AR. Both androgen sensitive and insensitive cell lines (LNCaP and PC-3, respectively) show increased EGFR and Src expression when treated with GABA and other GABA_AR specific agonists (Wu, *et al.*, 2014). Recently, 3 α -diol (a metabolite of dihydrotestosterone (DHT)) was found to mediate increased EGF expression and growth in PC-3 cells in a GABA_AR dependent manner, independent of androgen receptor (AR) (Xia *et al.*, 2018). Furthermore, selective activation of GABA_B receptor using baclofen, increased the migration of PC-3 PCa cells (Xia *et al.*, 2017).

GABA production is dependent upon GAD65 and GAD67 encoded by the GAD2 and GAD1 genes respectively (Hu, *et al.*, 2002). Previously, mASH1 expression has been found to induce production of GAD67 in mice (Fode, *et al.*, 2000). Expression of the human ortholog of mASH1, hASH1, correlates with NED and hASH1 expression is co-localised with NE marker chromogranin-A (Hu, *et al.*, 2002). hASH1 expression is regulated via the highly conserved Notch signalling pathway (Sriuranpong *et al.*, 2002), which is also critical to the development of the prostate and maintenance of prostate epithelial cell fate (Wang *et al.*, 2006), which in turn is dependent upon androgens (He *et al.*, 2018). Therefore, it is possible that ADT is a mechanism of notch signalling disruption, increasing cell fate plasticity and facilitating expression of hASH1 to drive a NE-like transcriptional program. Therefore, it is suggested that transdifferentiation of PCa cells to NE-like cells can provide PCa tumours with an androgen-independent pathway for growth and survival via the paracrine signalling of NE transdifferentiated cells (Wu, *et al.*, 2014).

It has previously been shown that GABAR subunit expression changes during cellular differentiation and during development, which can result in altered sensitivity to GABA and pharmacological agents (Neelands, Zhang, & Macdonald, 1999.; Succol *et al.*, 2012), therefore, investigating the changes in GABAR subunit expression during NED and throughout IAD could help to elucidate the function of GABARs in these cells. Finally, gabapentinoids such as gabapentin are increasingly prescribed off label for management of PCa related pain. Gabapentin is a known ligand of the $\alpha 2\delta$ -2 subunit of voltage-gated calcium channels (VGCCs) (Warnier *et al.*, 2015; Zvejniece *et al.*, 2015) and is proposed to have an indirect effect upon levels of GABA through altering GABA secretion, uptake and metabolism (Lanneau *et al.*, 2001)

1.5 Summary

In summary, prostate cancer is a highly dichotomous disease which originates as a slow growing and often indolent malignancy that can be effectively controlled using ADT and curative surgical therapy is common (Bill-Axelson *et al.*, 2014). However, for patients whose disease progresses under ADT to CRPC, the disease becomes more aggressive with high metastatic potential (Katsogiannou *et al.*, 2015). Once metastasised, CRPC remains incurable and current treatment strategies only offer modest extension to life (Karantanos *et al.*, 2013). The tumour evolutionary paths that can lead to CRPC are varied and complex (Feldman & Feldman, 2001; Gundem *et al.*, 2015), however, NED appears to be enriched among CRPC patient tumours (Bluemn *et al.*, 2017) and is known to be directly inducible by almost all clinically used therapies, including ADT, radiotherapy and chemotherapeutics (Deng *et al.*, 2011; Hu *et al.*, 2015a; Wang *et al.*, 2018; Yadav *et al.*, 2017). NED is also increasing in prevalence, both due to the enhanced efficacy and potency of ADT drugs and the increasing life-span of PCa patients (Bluemn *et al.*, 2017).

Research into the mechanisms of ADT induced NED in PCa are critical to addressing an unmet clinical need. Currently, there are no targeted therapeutics to combat PCa NED, as such, it is vitally important that research identifying key components of the NED pathway are identified to facilitate the acquisition of novel

therapeutic targets. Finally, the ability to specifically target NED has the potential to increase the value of all existing therapeutic options, potentially extending the efficacy of ADT and delaying the necessity to apply chemotherapeutics to patients. Therefore, the primary goal of this study is to develop and characterise an *in vitro* model of PCa NED to study AD and intermittent AD to investigate the hypothesised NED pathway and potentially identify key drivers of the NED process.

1.6 Hypothesis and aims

The current literature, discussed in this chapter, highlights the challenges posed by NED of prostate cancer. Chief among which are the induction of NED by a variety of current therapeutic strategies, the high therapeutic resistance of PCa NED cells and potential for these NED cells to support the survival and growth of PCa tumours through paracrine activity. Although the correlation between NED and poorer clinical outcome is well established (Grigore *et al.*, 2015), the mechanisms by which NED contributes to this effect is largely unknown at a molecular level. The reversibility of PCa NED and the effects of intermittent AD have never previously been studied, particularly in regard to the molecular drivers of NED. Based upon the core hypothesis that NED is deleterious to the prognosis of prostate cancer, the aim of this study was to use a LNCaP based *in vitro* model to investigate the molecular drivers of prostate cancer NED in response to AD and identify mechanisms by which NED could contribute to poor outcome. Therefore, three projects were undertaken within this study to achieve these aims.

1. Characterisation of NED cells and identification of an AD-induced NED pathway

A model of AD-induced NED was established and extensively characterised. This allowed for the study of PCa NED morphology and the underlying molecular pathways driving NED.

2. An investigation into the effects of reintroduction of androgen on gene expression and cell morphology and a preliminary investigation into Intermittent AD.

To investigate the morphological and molecular reversibility of PCa NED, a model of intermittent ADT was developed and used to study the morphological and molecular changes caused by AD cessation and a second period of AD.

3. Investigation of the potential role of GABA receptors in PCa and NED PCa cells.

An assessment of GABA_AR and GABA_BR subunit expression in PCa cell lines was performed and the effects of AD and IAD on subunit expression was investigated. Finally, the effects of applying GABAergic compounds to these cells was also investigated.

2. Materials and Methods

2.1 Cell culture techniques

2.1.1 Cell lines

The human androgen-sensitive prostate cancer cell line LNCaP was purchased from American Type Culture Collection (ATCC) (CRL-1740). The adherent human castrate-resistant prostate cancer cell lines DU-145 and PC-3 were a generous gift from Professor Jim Ross at the University of Edinburgh, UK (Tissue Injury and Repair Group, Edinburgh Medical School). LNCaP cells were issued with STR genotype validation from ATCC. All cell lines were regularly assessed for expression of characteristic markers (AR, PSA), consistent morphology and growth rate and were subjected to mycoplasma testing.

2.1.2 Cell culture conditions

LNCaP, DU-145 and PC-3 cells were cultured in Roswell Park Memorial Institute (RPMI) 1640 medium containing 10% (v/v) heat-inactivated foetal bovine serum (FBS, Gibco, UK), 2 mM L-glutamine and 100 units/mL (v/v) penicillin and 100 µg/mL streptomycin (Gibco, UK) (complete medium). Cells were grown in T75 tissue culture flasks (Corning, UK) containing 12 mL of complete medium unless otherwise stated. Cells were cultured at 37 °C in a humidified incubator at an atmospheric pressure of 5 % (v/v) CO₂. The presence of mycoplasma contamination was routinely assessed using the Venor[®]GeM Classic Mycoplasma PCR Detection Kit (Cambio, UK).

2.1.3 Passaging cell lines

Cells were passaged at approximately 80% confluence. Cells were passaged by removing culture medium, washing with 10 mL 1 x phosphate buffered saline (PBS) and incubation with 2 mL 0.1 % (v/v) trypsin (Gibco, UK) in 0.9% (w/v) NaCl (Baxter, UK) for 2 minutes in a humidified incubator at 37 °C. Cells were observed by light microscopy (10 x magnification) to ensure dissociation from the tissue culture flask before the addition of 8 mL complete medium to deactivate the trypsin. Cells were transferred to 15 mL falcon tubes (total volume 10 mL) and centrifuged at 148 RCF for 5 minutes in a Universal 320R centrifuge (Hettich, Germany). The resultant cell pellet was resuspended in fresh medium and cells

were sub-cultured into sterile T75 tissue culture flasks at a ratio of 1:6 for LNCaP and 1:10 for DU-145 and PC-3 as per ATCC recommendations. All cell lines used for experiments were between passage 8 and 25 (number of times sub-cultured since acquisition).

2.1.4 Counting cells

Cells were trypsinised as previously described in section 2.1.3 and cell pellets were resuspended in 10 mL complete medium. A 10 μ L aliquot of cell suspension was pipetted into each chamber of a haemocytometer covered by a glass coverslip. Cells were visualised under light microscopy at 10 x magnification and cells residing in the middle square of the haemocytometer grid were counted. The mean count across both haemocytometer chambers was representative of 1×10^4 cells per millilitre and was used to calculate the total number of cells in the 10 mL suspension.

2.1.5 Cryopreservation of cell lines

Cryopreservation solution contained dimethylsulfoxide (DMSO; Sigma, UK) and foetal bovine serum (FBS; Gibco, UK) at 1:4 ratio. Cells at 80% confluency were trypsinised (see section 2.1.2) and centrifuged at 148 RCF for 5 minutes in a Universal 320R centrifuge (Hettich, Germany) to collect the cell pellet. Media was removed and the pellet was resuspended in 1 mL complete medium and 1 mL of cryopreservation solution was added and mixed by gentle pipetting. Cells were transferred in 500 μ L aliquots into 1.2 mL cryotubes and placed into a Mr Frosty (Nalgene) freezing container filled with isopropanol, and stored at -80 °C. For long term storage cells were transferred to storage in vapour phase liquid nitrogen.

2.1.6 Reviving cells from liquid nitrogen storage

Cells were thawed by addition of 1 mL warmed complete medium (37 °C) and gently resuspended by pipetting. Cell suspensions were transferred to a 15 mL falcon tube and the volume was adjusted to 10 mL with warmed medium. Cells were centrifuged at 148 RCF for 5 minutes in a Universal 320R centrifuge (Hettich, Germany) and cell pellets were resuspended in fresh complete medium

and transferred into a single T75 tissue culture flask. Cells were incubated at 37 °C until confluent.

2.1.7 Androgen deprivation of prostate cancer cells

AD was simulated using charcoal-stripped FBS (CS-FBS) in RPMI 1640 medium. LNCaP cells were seeded at 1×10^6 cells in 10 mL of medium in T75 flasks. Cells were also seeded into 12-well plates at a density of 2×10^4 cells in 1 mL medium. Cells were grown to approximately 50 % confluence over 48 hours. To simulate AD, culture medium was removed and cells were washed with 10 mL sterile saline before addition of phenol-red free RPMI 1640 medium supplemented with 10 % (v/v) heat inactivated CS-FBS, 2 mM L-glutamine, 100 units/mL (v/v) penicillin and 100 µg/mL streptomycin (CS-Complete Medium). Cells were cultured for a further 5-15 days depending on the experiment and culture medium was replaced every 3 days, for each timepoint in AD conditions a matched control flask was also seeded and cultured in normal media containing 10% FBS and harvested at the same timepoint as its matched AD flask. LNCaP cells grown in AD conditions were not passaged as this was not necessary, due to extremely low growth rate in AD conditions. LNCaP cells grown in control conditions and DU-145 and PC-3 cells grown in all conditions were passaged when approaching 90% confluency. The full media controls were seeded at lower densities to minimise the need to passage, when approaching confluence, the cells were split at ratios that would ensure they would be at similar confluence to the cells grown in CS-FBS. Furthermore, cells were never passaged within 72 hours of being harvested to minimise effects of cell stress on gene and protein expression.

2.1.8 Synthetic androgen treatment

R1881 (Sigma, UK) is a synthetic androgen and considered as the gold standard AR agonist, R1881 has extremely high affinity for the AR, R1881 has also been shown to bind to progesterone and glucocorticoid receptor (Ho-Kim *et al.*, 1981; Singh *et al.*, 2000). Stock concentrations were prepared at 10 µM in DMSO. Cells were seeded at 1×10^6 in 10 mL of medium in T75 flasks and cultured in the presence of 1 nM or 10 nM R1881 or 0.01 % (v/v) DMSO vehicle control (matched flasks for each timepoint) for 5, 10 and 15 days to observe the effect of R1881.

Cells were also cultured for 15 days in androgen-deprived culture conditions, then treated with R1881 or DMSO vehicle control for a further 15 days. For extended incubations (>3 days), culture medium containing R1881 or vehicle control was replaced every 3 days. When cells became confluent, they were passaged into medium containing R1881 by trypsinisation as described in section 2.1.3.

2.1.9 Muscimol, baclofen and gabapentin drug treatments

Muscimol is a potent selective agonist of the GABA_A receptor (Frolund *et al.*, 2002), whilst baclofen is a potent selective agonist of the GABA_B receptor (Woodward *et al.*, 1993). Gabapentin is a gabapentinoid which binds to the alpha2delta subunits of voltage-gated calcium channels, where it acts as an antagonist, but does not bind directly to either GABA_A or GABA_B receptors (Gale and Houghton., 2011; Calandre *et al.*, 2016). Stock concentrations of muscimol, baclofen (Sigma, UK) and gabapentin (GBP) (Tocris, UK) were prepared at 100 mM in ethanol. Cells were seeded at 1×10^6 in 10 mL of medium in T75 flasks, allowed to reach 50% confluence and then cultured 15 days in AD conditions with varying concentrations of muscimol (1, 10 or 100 μ M) or baclofen (10, 100, 500 μ M) added for the final 48 hours. For GBP experiments, cells were cultured in complete media to 50% confluence, then treated with GBP (2, 20, 166 μ M) for 48 hours.

2.1.10 Harvesting cells

Cells were harvested on ice. The culture medium was removed and cells were washed once with 10 mL ice-cold PBS. PBS was removed and 5 mL ice-cold PBS was added to the T75 flask. Adherent cells were dislodged from the flask surface using a rubber cell scraper (Corning, UK) and transferred into 15 mL falcon tubes before centrifugation at 148 RCF at 4 °C for 5 minutes in a Universal 320R refrigerated centrifuge (Hettich, Germany). Cell pellets were then resuspended in 1 mL ice-cold PBS and transferred to microfuge tubes and centrifuged at 835 RCF at 4 °C for 5 minutes in a 5415R refrigerated centrifuge (Eppendorf, Germany). The supernatant was aspirated and the cell pellets were stored at -80 °C for future experiments.

2.1.11 Alamar blue cell viability assay

To assess cell viability, cells were seeded at a density of 1×10^3 cells per well in 96-well plates in 100 μL complete culture medium and cultured at 37 °C. After 24 hours, medium was removed and replaced with 100 μL fresh medium containing drug treatments at the indicated concentrations. After a further 48 hours, 10 μL of Alamar Blue 10 x solution was added to each well and incubated for a further 24 hours at 37 °C protected from light. As a control, wells containing only Alamar blue and media were included in addition to wells containing only Alamar blue, media and cells as an untreated control. Media containing 2% v/v Triton-X (Sigma, UK) was used as a positive control for cell death. Plates were analysed by measuring the absorbance at 570 nm and a reference measurement at 600 nm using an LT-5000MS plate reader and Manta software (LabTech, UK). The raw data was processed by subtracting the absorbance of Alamar blue and media only from all readings. The control untreated cells were taken to be 100% viable and all other readings were expressed as a percentage of this.

2.2 RNA Isolation

2.2.1 Preparation of nuclease-free water

Nuclease-free water was prepared by treating distilled water with diethylpyrocarbonate (DEPC) (Sigma, UK). DEPC was added to distilled water at a final concentration of 0.1 %, mixed and incubated overnight at room temperature. The solution was autoclaved for 1 hour at 121 °C and 15 psi in order to deactivate the DEPC and allowed to cool to room temperature before use.

2.2.2 RNA isolation

Total RNA was extracted from cell pellets using TRIsure (Bioline, UK) according to manufacturer's protocol. RNA was extracted from cell pellets, which had been stored at -80 °C as previously described in section 2.1.7. TRIsure reagent (1 mL) was added to cell pellets and cell membrane disruption was aided by pipetting. Samples were incubated for 5 minutes at room temperature before 200 μL chloroform was added. Samples were shaken vigorously by hand for 15 seconds before a further 3-minute incubation at room temperature to allow for phase separation. Samples were centrifuged at 13000 RCF for 15 minutes at 4 °C in a

5415R refrigerated centrifuge (Eppendorf, Germany). The upper transparent phase containing RNA was transferred to a sterile microfuge tube and precipitated by the addition of 500 μ L ice-cold isopropanol (Sigma, UK). The mixture was incubated on ice for 30 minutes before samples were centrifuged at 13000 RCF for 10 minutes at 4 °C in a 5415R refrigerated centrifuge (Eppendorf, Germany) to form a pellet. RNA pellets were washed using 1 mL 75% (v/v) molecular grade ethanol (Sigma, UK) and gently vortexed before centrifugation at 9000 RCF for 5 minutes at 4 °C in a 5415R refrigerated centrifuge (Eppendorf, Germany). The supernatant was removed by pipetting and RNA pellets were allowed to air dry for 10 minutes at room temperature. RNA pellets were resuspended in 20 μ L DEPC-treated water and stored at -80 °C.

2.2.3 Quantification of RNA by spectrophotometry (Nanodrop 2000)

Extracted RNA was first analysed via spectrophotometry using NanoDrop 2000 (Thermo Fisher Scientific, UK) prior to microfluidic analysis to ensure samples assessed were within the optimal range of the Bioanalyzer 2100 (Agilent, UK) instrument (20-500 ng / μ L). DEPC-treated water (1 μ L) was used as a calibration 'blank' before 1 μ L RNA in DEPC-treated water was analysed via assessing absorbance at 260 nm. The absorbance at wavelengths 260/280 was used as an indication of RNA purity, with a ratio of 2.00 considered pure (Gallagher & Desjardins, 2006).

2.2.4 Quantification of RNA by microfluidic analysis (Bioanalyser 2100)

Extracted RNA was also quantified and the RNA integrity assessed by microfluidic analysis using a Bioanalyser 2100 (Agilent Technologies, UK). The 100 bp RNA 6000 NanoLadder was first prepared by heat denaturing at 70 °C for 2 minutes then cooled on ice. The Nano gel matrix was prepared by filtering 550 μ L of the gel through a spin filter column via centrifugation at 1500 RCF at room temperature for 10 minutes in a 5415R centrifuge (Eppendorf, Germany). Aliquots of 65 μ L of filtered gel were transferred to fresh microfuge tubes, stored at 4 °C and used within a maximum of 4 weeks. In order to prepare the gel for the chip, dye was added. RNA 6000 Nano dye concentrate was brought to room temperature, vortexed for 10 seconds and pulse centrifuged for 5 seconds in a

5415R centrifuge (Eppendorf, Germany) before 1 μL of the dye was added to a 65 μL aliquot of gel. Gel-Dye matrix was vortexed and then centrifuged at 13000 RCF for 10 minutes at room temperature in a 5415R centrifuge (Eppendorf, Germany).

RNA samples were diluted to the optimal range (20-500 $\text{ng}/\mu\text{L}$) with DEPC-treated H_2O . RNA 6000 Nano chips (Agilent Technologies, UK) were prepared by pipetting 9 μL gel-dye mix into the well marked 'G'. The gel was dispersed through the chip via gentle pressure using the chip priming station and the plunger was depressed for 30 seconds to achieve this. Next, 9 μL of the gel-dye mix was pipetted into the other 2 wells marked 'G' and 5 μL of RNA 6000 Nano marker was loaded into the sample and ladder wells on the chip. RNA samples (1 μL) were added to each sample well and 1 μL of RNA ladder was added to the appropriate ladder well on the chip. The prepared chip was then vortexed for 60 seconds at 2400 RPM using an IKA vortex mixer (Agilent, UK) and analysed via Bioanalyzer 2100, using Agilent 2100 Expert software, generating microfluidic gel images, electropherograms and RNA integrity numbers (RIN). Samples with RIN >9 were used in quantitative reverse transcription-polymerase chain reactions (qRT-PCRs) (Bustin *et al.*, 2009).

2.2.5 Reverse transcription of RNA / cDNA synthesis

Total RNA (2 μg) was reverse transcribed using the NanoScript 2 RT Premix kit (PrimerDesign, UK). Reactions were prepared containing 2 μg RNA in a final volume of 20 μL containing 1x RT Premix (including dNTPs, random octamers, and oligo dT) in 0.2 mL thin-walled reaction tubes. RNA was reverse transcribed at 42 $^\circ\text{C}$ for 20 minutes before the enzyme was heat inactivated at 72 $^\circ\text{C}$ for 10 minutes, using a programmed thermocycler (Applied Biosystems, UK). It was assumed that all reactions had 100% efficiency i.e. created 2 μg (c)DNA. The resultant complimentary (c)DNA was diluted to 5 $\text{ng}/\mu\text{L}$ using DEPC-treated H_2O before use in qRT-PCRs or stored at -20 $^\circ\text{C}$ for future use. Control reactions for qRT-PCR experiments were prepared by substituting RNA samples with an equal volume of DEPC-treated water in the reverse transcription reactions (no template control).

2.3 Quantification of gene expression

2.3.1 Oligonucleotide design and preparation

Oligonucleotides targeting genes of interest were designed to span exon boundaries to avoid genomic DNA amplification. They also had annealing temperature between 58-60 °C, 18-25 bp in length, 40-60 % guanine and cytosine content and amplicon sizes between 100-200 bp. Annealing temperatures were calculated using OligoCalc (Justbio, <http://www.justbio.com/index.php?page=oligocalc>) (Kibbe, 2007) and *in silico* analysis of oligonucleotide specificity was performed using the nucleotide basic local alignment search tool (BLAST; <https://blast.ncbi.nlm.nih.gov>) hosted by the National Centre for Biotechnology Information (NCBI; Altschul *et al.*, 1990). Alignments of transcript variants were performed using MultAlin (Corpet, 1988) (<http://multalin.toulouse.inra.fr/multalin/>) and where possible oligonucleotides were designed to target all known splice variants. For AR, oligonucleotides used in this study target transcript variants 1 and 2. The oligonucleotides used in this study are shown in Table 2.1 and 2.2.

Validation of qPCR primers involved rigorous *in silico* and empirical testing both during the design of oligonucleotides and after data acquisition. Oligonucleotide sequences were screened using NCBI Primer Blast tool in order to confirm that only the target gene would be targeted (Ye *et al.*, 2012), any oligonucleotides which had any off-target matches were redesigned to be target specific. Where possible, oligonucleotides were designed to target all known splice variants of the target gene, with the exception of AR for which only variants 1 and 2 were targeted (NM_000044.4 and NM_001011645.3, respectively). Initial testing and validation of oligonucleotides was performed in qPCR reactions using positive control cDNA, for example cDNA derived from human brain for GABA and neuronal related genes and LNCaP cells for androgen pathway genes. The majority of oligonucleotides were initially tested using end-point PCR where production of a PCR product at the expected amplicon size and absence of additional products or observable primer dimers on the gel was determined. After qPCR reactions had generated melt curves showing a single clear product, the melt temperature of this melt curve was cross-referenced with the *in silico*

predicted melt temperature for that gene product using the uMelt tool (Dwight *et al.*, 2011). Oligonucleotides which had been validated were then used in experiments, where positive and non-RT and water only controls were run alongside test samples. The melt curves of test samples were then compared to those of positive controls to ensure that the gene product peak was overlapping with the positive control. Oligonucleotides targeting GABA receptor subunits and CCCs were designed by Dr Amy V. Poole but were still subjected to the same extensive validation by Joseph E. Sutton.

Table 2.1: Oligonucleotides used in this study for qRT-PCR analysis, relevant accession numbers are provided

Target gene	Accession number	Oligo orientation	Sequence 5' – 3'
<i>AR</i>	NM_000044.4	Forward	CACTGCTACTCTTCAGCATTATTCC
		Reverse	ATGCAGCTCTCTCGCAATAGG
<i>GAD1</i>	NM_000817.2	Forward	AACGTACGATACCTGGTGCG
		Reverse	TTCTTGGAGGATTGCCTCTCC
<i>GAD2</i>	NM_000818.2	Forward	AAGGTGGCTCCAGTGATTAAAGC
		Reverse	AAGTCAATGTCTTGGTGAGTTGCC
<i>ASCL1</i>	NM_004316.3	Forward	AAGCAGGGTGATCGCACAAAC
		Reverse	ATGCCTCGCTTAGTTGGCG
<i>MMP-9</i>	NM_004994.2	Forward	GCACGACGTCTTCCAGTACC
		Reverse	CAGGATGTCATAGGTCACGTAGC
<i>NSE</i>	NM_001975.2	Forward	TATCCTGTGGTCTCCATTGAGG
		Reverse	TTGCACGCTTGGATGGCTTC
<i>PSA</i>	NM_001648.2	Forward	ATTGAACCAGAGGAGTTCTTGAC
		Reverse	AGCACACAGCATGAACTTGGTC
<i>PTOV1</i>	NM_017432.4	Forward	AACCTGGAGACCGACCAGTG
		Reverse	TCTCTGTTGGTGAAGTGGAAGT
<i>REST</i>	NM_005612.4	Forward	ATATGCGTACTCATTTCAGGTGAG
		Reverse	AATTGAACTGCCGTGGGTTTAC
<i>SYN</i>	NM_003179.2	Forward	TGTAGTCTGGTCAGTGAAGCC
		Reverse	ACTCAAGACTGGGCACCTAG
<i>CD44</i>	NM_000610.3	Forward	TTGAATATAACCTGCCGCTTTGC
		Reverse	CCTTCTATGAACCCATACCTGC
<i>CD166</i>	NM_001627.3	Forward	TTCTGCCTCTTGATCTCCGC
		Reverse	AGCCATCGGGCTTTTCATATTTT
<i>ITGA2</i>	NM_002203.3	Forward	ACCAGCTGCTCAAGAACAACC
		Reverse	CTACATCGCAGGCAACAGAC

Table 2.2: List of oligonucleotides used in this study for CCCs, GABA_A and GABA_B receptor subunit expression. GABRA = alpha, GABRB = beta, GABRG = gamma, GABRD = delta, GABRT = theta, GABRP = pi, GABBR = GABA_B Receptor.

Target gene	Accession number	Oligo orientation	Sequence 5' – 3'
GABRA1	NM_000806.5	Forward	ATCTTCAGCAAAGGAGCACG
		Reverse	AAAGACAGTCAGACAGACCTG
GABRA2	NM_000807.2	Forward	AGCCCATCGCTCCACGCTCTC
		Reverse	AGCAGGAATGCATGTTGTAAGATG
GABRA3	NM_000808	Forward	TTGGGAAGGCAAGAAGGTGC
		Reverse	CAACCTGGCCAAGGACACT
GABRA4	NM_000809	Forward	TGCGGAGTGTCCCATGAGA
		Reverse	CTAAGCTGGAAGACTCCTTCG
GABRA5	NM_000810	Forward	TGAAATTTGGCAGCTATGCGTAC
		Reverse	TGTATTCGCCTGTGCTGGTG
GABRA6	NM_000811	Forward	CAGGACATAATCTAAGACCACAAAC
		Reverse	TGCCTCAAGTCAGTCAGTAATCCAATAG
GABRB1	NM_000812.3	Forward	ATGGTCTGTTGTGCACACAGCAC
		Reverse	TCGTGAGCACTTCCGAGCC
GABRB2	NM_021911.2	Forward	TGATAATGCAGTAACAGGAGTAACG
		Reverse	ACGCAATAGACGATGTTGAAGAAG
GABRB3	NM_000814	Forward	GTCTCGAGGAATGTTGTCTCCG
		Reverse	AAGGACACCCACGACAGAATC
GABRG1	NM_173536.3	Forward	CATGGATGAACATTCCTGTCCAC
		Reverse	CTCACACGATCTCTGGGGATTA
GABRG2	NM_198904.2	Forward	ACAGGAAGCTCAGTCTACTCG
		Reverse	GCCAGAAATCTGATGATGACTATGA
GABRG3	NM_033223.4	Forward	TCCTCAAGATGGATTCTGAGC
		Reverse	CCTGTGTCTATGAGTGTCTGGAT
GABRD	NM_000815.4	Forward	TGTCTCTAGGCATCACCACG
		Reverse	TTCTGCTTCTTCTGTAGTCG

Table 2.2 Continued

Target gene	Accession number	Oligo orientation	Sequence 5' – 3'
<i>GABRE</i>	NM_004961.3	Forward	TTCTGAATGGCAATGTGGTGAGCC
		Reverse	TTGATACGAGGATGGCGGAGTTTAG
<i>GABRT</i>	NM_018558.3	Forward	TGGTAGAGAGCTATGGTTACACG
		Reverse	TAGACATACTCCAGCAAGGACAG
<i>GABRP</i>	NM_014211	Forward	TCCTTACAGCAGATGGCAGC
		Reverse	AGTGCTAGGACTTCTACACAGC
<i>GABBR1</i>	NM_001470.2	Forward	GACAGATATGGACACACCCAG
		Reverse	CCAGGTGAATCGAACGCCA
<i>GABBR2</i>	NM_005458	Forward	TAGGAAGCCAACCTTCCCTG
		Reverse	CACTGCCGCTTCTGGTTGT
<i>SLC12A1</i>	NM_001184832	Forward	AGTGCCAGTAATACCAATCGC
		Reverse	GCCTAAAGCTGATTCTGAGTCTT
<i>SLC12A2</i>	NM_001256461	Forward	TGGGTCAAGCTGGAATAGGTC
		Reverse	ACCAAATTCTGGCCCTAGACTT
<i>SLC12A4</i>	NM_001145963	Forward	CCTCATCGTGCTTATCTGCTG
		Reverse	GGCTGCTGCGAATGTTGTTC
<i>SLC12A5</i>	NM_001134771	Forward	AGGAAAGCAGTCCCTTCATCA
		Reverse	GCCTCTTCATGCTCCCTACTT
<i>SLC12A6</i>	NM_001042494	Forward	TCACAGTGATGACGCACTCAA
		Reverse	CCAAGATGGACACAATGACACA
<i>SLC12A7</i>	NM_006598	Forward	CTGGCGGGTCCTACTACATGA
		Reverse	AAAATCTCGATGGTCCCCAAAAT

2.3.2 qRT-PCR

qRT-PCR experiments contained 25 ng cDNA at a final concentration of 1.25 ng/μL, 300 nM forward and reverse oligonucleotide (MWG Eurofins, Germany) and 1 x PrecisionPLUS qRT-PCR master mix in a final volume of 20 μL. Reactions were prepared in BrightWhite 96-well plates in triplicate (PrimerDesign, UK). Transcripts were amplified and quantified using the StepOnePlus qRT-PCR system (Applied Biosystems, UK) using SYBR green

detection chemistry with the following instrument settings: 95 °C for 10 minutes followed by 40 cycles of; 95 °C for 15 seconds and 58-60 °C annealing temperature for 1 minute. Negative controls include a non-RT control and a reaction replacing cDNA with DEPC-treated water (template–ve). Amplification of a single PCR amplicon was determined by generating melt curves by heating the final PCR product from 60 °C to 95 °C in 0.3 °C increments followed by a final 15-second hold. Melt curves for test samples were compared to those of the positive control and no-template control in order to differentiate between the desired target gene product and unwanted primer oligomers or potential genomic DNA contamination.

2.3.3 Identification of reference genes

Analysis of candidate reference genes was performed using geNorm oligonucleotide kit (PrimerDesign, UK) and qBase+ software (Biogazelle, Belgium). A panel of 7 candidate reference genes (CYC1, UBC, ACTB, RPL13A, ATP5B, SDHA, EIF4A2) was screened against LNCaP, DU-145, PC-3 cells in triplicate and using a range of passage numbers. The reference gene with the most consistent expression across all cell lines and treatments (ACTB) was determined using qBase+ software geNorm M analysis (Biogazelle, Belgium).

2.3.4 Data analysis / quantification of fold change in gene expression

The expression of unknown target genes were analysed relative to the reference gene *ACTB* as an internal control, and fold change in gene expression was calculated using the $2^{(-\Delta\Delta Ct)}$ method (Livak & Schmittgen, 2001). Fold change values were calculated using Excel 2016 (Microsoft) as follows: experiments were analysed in biological triplicate with average Ct values of reference genes subtracted from the average Ct value of the gene of interest to give ΔCt values, followed by subtraction of the control group ΔCt from the treatment/comparison group ΔCt , these $\Delta\Delta Ct$ values were then expressed as $2^{(-\Delta\Delta Ct)}$ to give fold change values. The mean fold change values were then plotted as graphs using Graphpad Prism 7.0 (GraphPad Software Inc). Results are shown as the mean of three independent experiments \pm SEM. Unless otherwise stated, qPCR data was presented normalised to expression in untreated LNCaP cells (shown as 1) with the expression level of other samples shown relative to untreated LNCaP.

For time course experiments, each treatment had its own matched untreated control which were seeded and harvested at the same time and processed as part of the same batches during RNA extraction and cDNA synthesis.

2.4 Protein analysis

2.4.1 Protein extraction

Cell pellets were lysed in approximately 3 x the pellet volume of lysis buffer (50 mM Tris pH 8, 150 mM NaCl, 1 mM EDTA, 1 % (w/v) Triton-X and 1 % (v/v) Halt protease inhibitor cocktail (Thermo Fisher Scientific, UK)) on ice for 30 minutes. Lysates were clarified by centrifugation at 13000 RCF at 4 °C for 5 minutes in a 5415R refrigerated centrifuge (Eppendorf, Germany) and supernatant containing protein was transferred to a sterile, pre-cooled microfuge tube. Protein concentration was determined via Bradford assay (Bradford, 1976). Alternatively, samples were stored at -80 °C.

2.4.2 Bradford analysis of protein concentration

Bradford reagent was prepared by dissolving 50 mg of Coomassie Blue G250 in 50 mL methanol before adding 100 mL 85 % phosphoric acid. The solution was diluted to 1 L with dH₂O and filtered using a syringe filter to remove any precipitate and stored in the dark at 4 °C. Stock bovine serum albumin (BSA) solution was prepared at 10 mg/mL and serial dilutions of BSA were prepared in dH₂O at concentrations of 0.125, 0.250, 0.500, 0.750, 1.00 and 1.50 mg/mL. Cells lysates (section 2.4.1) were diluted by 1:5 by adding 1 µL of protein sample to 4 µL of dH₂O. Bradford reactions were prepared in a standard 96-well plate containing 200 µL of Bradford reagent per well and 1 µL of either BSA standards or diluted protein sample. Blank wells contained only Bradford reagent. BSA standards were prepared in a single replicate, whereas protein sample reactions were prepared in triplicate. All reactions were mixed thoroughly by pipetting and incubated for 5 minutes at room temperature. Samples were analysed using an LT-5000MS plate reader (LabTech, UK) using Manta software (LabTech, UK). Absorbance at 595 nm was measured and the blank sample background was subtracted from all samples. The protein concentration was calculated using a standard curve generated by using the bovine serum albumin standard concentrations between 0.125 and 1.5 mg/mL from the equation of the line ($y=mx+c$). Final protein concentrations were multiplied by the original dilution factor in order to obtain the final estimated concentration.

2.4.3 Cell protein lysate preparation

Protein lysates were prepared to a final concentration of 1 $\mu\text{g}/\mu\text{L}$ in 4 x Loading Sample Buffer (LSB) (20 % (w/v) glycerol, 200 mM Tris pH 6.8, 4 % (w/v) SDS, 10 mM EDTA, 1 % bromophenol blue supplemented with 10 % (v/v) β -mercaptoethanol) in microfuge tubes. Samples were denatured at 95 °C for 5 minutes in using a heat block before resolution by SDS-PAGE.

2.4.4 Sodium Dodecyl Sulphate Polyacrylamide Gel Electrophoresis (SDS-PAGE)

SDS-PAGE was performed using the method of Laemmli (1970), using the Biorad mini-protean electrophoresis system. The resolving gel contained 12 % (w/v) acrylamide (30% protogel) (Thermo Fisher Scientific, UK), 375 mM Tris pH 8.85, 0.1 % (w/v) SDS and 0.08 % (w/v) ammonium peroxidosulphate. The resolving gel was polymerised by addition of 0.005 % (w/v) N,N,N',N'-Tetramethyl-ethylenediamine (TEMED) and the mixture was pipetted between glass plates up to the level of the casting frame hinge. The resolving gel was covered in 2 mL isopropanol in order to polymerise the gel in the absence of oxygen. Once polymerised the isopropanol was removed and gel rinsed with distilled H₂O before the stacking gel was added.

The stacking gel contained 5 % (w/v) acrylamide, 130 mM Tris pH 6.8, 0.1 % SDS and 0.12 % (w/v) ammonium peroxidosulphate. Stacking gels were polymerised by addition of 0.01 % (w/v) N,N,N',N'-Tetramethyl-ethylenediamine (TEMED) and then pipetted onto the resolving gel and a gel comb was inserted into the stacking gel. After the stacking gel was fully polymerised, the cast gel was either stored at 4 °C wrapped in paper towel soaked in 1x Running buffer (25 mM Tris pH 8.3, 192 mM glycine and 0.1 % (w/v) SDS) or used immediately. Gels were submerged in electrophoresis running buffer and PageRuler Prestige protein ladder (2 μL) (Thermo Fisher Scientific, UK) was loaded onto the first well of the gel. Equal amounts of protein sample were then loaded into the SDS-PAGE gel, (typically 10 μg) and any vacant wells were filled with an equal volume of loading sample buffer to ensure even running of the samples through the gel. Protein samples and protein ladder were resolved on the gel via electrophoresis using

electrophoresis running buffer at 185 V for 50 minutes or until the loading sample buffer dye front reached the bottom of the gel.

2.4.5 Immunoblotting

Immunoblots were performed by the method of Towbin et al (1979). Resolved SDS-PAGE gels were assembled as follows: Sponge, 2 x 3MM paper, gel, nitrocellulose membrane, 2 x 3MM paper, sponge in a cassette whilst submerged in transfer buffer (25 mM Tris, 190 mM glycine and 20% (w/v) methanol). Air bubbles were removed by rolling the sandwich with a falcon tube. The Biorad Trans-Blot module was transferred to the electrophoresis tank and submerged in cool 1x transfer buffer (25 mM Tris, 190 mM glycine and 20% (w/v) methanol). A frozen cool block was also added to the tank to chill the buffer. Proteins were electrophoretically transferred onto nitrocellulose membrane at 100 V for 60 minutes in 1x transfer buffer at 4 °C.

After transfer membranes were blocked with 5 % (w/v) non-fat dried milk powder (Marvel) in PBS-Tween (0.1 % v/v) for 1 hour with shaking at room temperature. Primary antibodies were prepared in 5% Marvel at a dilution of 1:200-1:1000 and incubated with the membrane overnight at 4 °C. After 3 washes in PBS-Tween (0.1% v/v) for 5 minutes with shaking, membranes were incubated with IRDye-conjugated fluorescent secondary antibodies (LI-COR, UK) at 1:10000 in PBS-Tween containing 0.01% (w/v) SDS, and were protected from light. Membranes were washed again 3 times in PBS-Tween (0.1% v/v) for 5 minutes with shaking before being analysed using an Odyssey imaging system and ImageStudio 2.0 Software (LI-COR Biosciences, USA). Digital images of blots were captured using ImageStudio 2.0.

2.4.6 Scratch Assays

LNCaP, DU-145 and PC-3 were cultured in six well plates at a density of 5×10^5 cells/well in a total volume of 2 ml RPMI 1640 at 37 °C until a confluent monolayer was formed, typically 24 h for DU-145 and PC-3 and 48 h for LNCaP. Wounds were created by scratching a single line through the monolayer from the top to the bottom of each well with a 200 µl pipette tip. Media was replaced to remove cell debris. The wound site was observed by microscopy and images captured at

time points 0, 6, 24, 30, 48, 54, 72 and 96 h of one field of view at the vertical centre of the wound area (10 x magnification). The rate of wound healing was assessed using ImageJ software (Schneider, Rasband, & Eliceiri, 2012) to analyse the area of the wound (i.e. surface area in one field of view not covered by cells) at each time point. The area was then expressed as a percentage of the total original wound area (at 0 h). Each time point was performed with three biological replicates.

Table 2.3 Primary antibodies used in this study for immunoblotting and immunofluorescence.

Target Protein	Host species	Dilution factor	Source and Catalogue Number
Androgen Receptor (N-20)	Rabbit Polyclonal	1:1000	Santa Cruz Biotechnology (SC-816)
β -actin	Goat Polyclonal	1:1000	Santa Cruz Biotechnology
CD44	Mouse Monoclonal	1:1000	Cell Signalling Technology (5640)
hASH1	Rabbit Polyclonal	1:1000	Abcam (Ab74065)
NSE	Mouse Monoclonal (85F11)	1:1000	Abcam (Ab16808)
PSA	Goat Polyclonal	1:200	Santa Cruz Biotechnology (sc-7638)
REST	Rabbit Monoclonal	1:1000	Abcam (Ab75785)
GAD65/67	Rabbit Polyclonal	1:1000	Abcam (Ab11070)

Table 2.4 Secondary antibodies used in this study for immunoblotting and immunofluorescence.

Name	Species Reactivity	Dilution factor	Source and Cat. Number
Alexa Fluor 568	Goat anti-mouse	1:10000	Life Technologies (A11029)
Alex Fluor 488	Goat anti-rabbit	1:10000	Life Technologies (A11008)
IRDye 800CW	Goat anti-mouse	1:10000	LI-COR (926-32210)
IRDye 680LT	Donkey anti-goat	1:10000	LI-COR (926-68024)
IRDye 800CW	Goat anti-rabbit	1:10000	LI-COR (926-32211)
IRDye 680LT	Goat anti-rabbit	1:1000	LI-COR (926-68021)

2.5 Immunofluorescence

2.5.1 Fixing cells

Paraformaldehyde 4% (w/v) was prepared by adding 40 g of paraformaldehyde powder (Sigma, UK) to 800 mL PBS and dissolved using a heated stirring block and stirrer bar at 60 °C. To facilitate the dissolving of the paraformaldehyde powder, sodium hydroxide was added until the solution became clear and the total volume was adjusted to 1 L with 1x PBS. The solution was stored at 4 °C.

At day 15 of culture, LNCaP cells were fixed by removing medium and incubating with 800 µL 4 % paraformaldehyde for 20 minutes at room temperature. Cells were washed three times with PBS and incubated for 1 hour at room temperature with blocking buffer (20 % v/v Goat Serum in PBS) containing 0.2 % (v/v) Triton-X to block and permeabilise the cells.

2.5.2 Immunofluorescent staining of cells

Cells fixed on coverslips were washed three times with PBS then incubated with primary antibodies at a dilution of 1:1000 in PBS containing 2 % (v/v) goat serum and 0.2 % (v/v) Triton-X, overnight at 4 °C. Cells were then washed in PBS and incubated with Alexa Fluor secondary antibodies at 1:1000 dilution in PBS containing 2 % (v/v) goat serum and 0.2 % (v/v) Triton-X for one hour at room temperature in the dark. Cells were washed again in PBS before mounting face down on microscope slides using VECTASHIELD mounting reagent containing DAPI (Vector Laboratories, UK). Mounted coverslips were air dried for 10 minutes. Excess mounting medium was removed using paper towel and coverslips were sealed used nail varnish and allowed to set overnight at 4 °C. Prepared microscope slides were stored at 4 °C in the dark until being imaged on a Confocal LSM 880 microscope (Zeiss, UK).

2.5.3 Confocal microscopy

For confocal microscopy, cells were grown on glass coverslips as per section 2.5.1. Cells were visualised using an LSM 880 Confocal microscope (Zeiss, UK) operated using Zen Black software (Zeiss, UK) at 20 x magnification. Cells were imaged using 8x8 tile scan and these images were used to select several representative areas of the cell monolayer to image at higher resolution. Cells were then imaged at 63 x magnification using oil immersion. Settings for laser power and channel gain were optimised using positive samples to ensure saturation in each channel did not occur and these acquisition settings were applied when viewing each microscope slide to ensure consistency as per North, (2006). Representative images were captured at 1024 x 1024 resolution in .czi format and exported in .tiff format. Any brightness and contrast adjustments to aid visual presentation were made uniformly. Scale bars were generated using Zen Blue software from original captured images (Zeiss, UK).

2.5.4 Neurite outgrowth staining kit

To quantify the length of neurite-like projections from androgen-deprived LNCaP cells the Neurite Outgrowth Staining Kit (Thermo Fisher Scientific, UK) was utilised. LNCaP cells were seeded on 13 mm sterilised glass coverslips in 12-well plates (Corning, UK) at a density of 2×10^4 cells per well. Cells were grown for 48 hours at 37 °C in 5 % CO₂ to 50 % confluence before replacing complete medium with appropriate treatment medium. Control LNCaP cells were grown in phenol red-free RPMI1640 medium supplemented with 10% (v/v) FBS, whereas androgen-deprived LNCaP cells were grown in the same medium but supplemented with 10% CS-FBS (Sigma, UK). According to manufacturer's instructions, 1 x solution of Fix/Stain Solution was prepared by combining 10 µL cell viability indicator and 10 µL cell membrane stain in 10 mL 4 % (v/v) formaldehyde in PBS. Media was removed from wells; cells were washed with PBS and 800 µL of 1 x Fix/Stain Solution was added to each well and incubated for 20 minutes at room temperature. A 1 x solution of background suppression dye was prepared by adding 120 µL of the 100 x concentrate to 12 mL of PBS. The Fix/Stain Solution was removed and 800 µL of background suppression dye was added and incubated at room temperature for 10 minutes. Glass coverslips containing fixed and stained cells were removed from wells and washed 5 times in PBS, dried and mounted face down onto microscope slides using VECTASHIELD Mounting Media containing DAPI as per section 2.5.2.

2.5.5 Neurite outgrowth analysis

Prepared microscope slides were imaged using a Confocal LSM 880 microscope (Zeiss, UK). Representative images were captured using a 20x/0.8 objective using a 5 x 5 tile scan to capture 3 separate areas of the slide across 3 different slides for control and androgen-deprived samples. The average length of cell bodies was calculated by measuring 100 cell body lengths using Zen Blue 2.3 lite software (Zeiss, UK). Neurite-like projections were then measured using the same software package, measuring 100 neurites per tile scan image. Projections that were greater than twice the average cell body length were considered to be neurite-like (Wang *et al.*, 2012). Data was graphed and statistical analysis performed using Graphpad Prism 7.0 software (Graphpad software Inc.).

2.6 Analysis of statistical significance

Graphpad Prism 7.0 (Graphpad Software Inc) was used to perform statistical analysis for qRT-PCR and neurite outgrowth experiments. Results are shown as the mean of three independent experiments \pm SEM. SEM was used as it is descriptive of the expected variance in the mean of a specific determined value (e.g. fold change in gene expression), whereas the standard deviation would be more indicative of the range in which the individual values could occupy. Significance was determined using one-way ANOVA with Dunnett's correction ($p < 0.05$).

3. Elucidating the molecular mechanisms of neuroendocrine differentiation of prostate cancer cells

3.1 Introduction

3.1.1 Characterisation of PCa cell lines

Before investigating the effect of AD on PCa cell lines and the NED process, it was important to characterise and validate the cell lines used in this study and ensure that they displayed typical characteristics previously reported in the literature. Characterisation of the LNCaP, DU-145 and PC-3 cell lines involved the use of morphological analysis via microscopy, assessment of their growth and invasive potential using scratch assays and an assessment of key genes and proteins in an untreated state. This characterisation then continued to investigate the response of these cell lines to AD by culturing them in media containing charcoal-stripped FBS and determining responses at the morphological and molecular level.

Fluorescent microscopy was also used to assess for the growth of neurite-like projections in response to AD, a phenomenon which has previously been reported as a morphological marker of PCa NED *in vitro* (Rapa *et al.*, 2013; Farach *et al.*, 2016). Scratch assays allowed for an initial comparison of androgen-sensitive LNCaP to castrate-resistant DU-145 and PC-3 cells in terms of their ability to close the scratch area, giving an insight in the aggressive growth and invasive characteristics of these different cell lines.

On a molecular level, it was important to assess the expression of key genes and proteins that this study proposes as key drivers, readouts and effectors of NED and the potentially tumour modulatory mechanisms of PCa NED. This included an initial assessment of AR and PSA expression as these are extremely widely studied in these cell lines, thereby acting as an initial validation that LNCaP cells express the AR and have functional AR-signalling evidenced by PSA expression, whilst DU-145 and PC-3 are known to be AR and PSA negative. Next it was important to determine the expression of putative PCa cancer stem cell markers CD44, CD133 and CD166 in order to confirm previous reports that NED was

unlikely to be facilitated by a cancer stem cell niche (Sauer *et al.*, 2006). Characterisation of the proposed NED pathway was then a priority, seeking to establish the basal expression of the instigators (PTOV1, hASH1), the preventers (REST), the biomarkers (NSE), the potential for GABA synthesis (GAD1) and a proposed downstream effector of NED (MMP-9) across all three cell lines.

Having characterised these cell lines in a basal state, it was then important to verify their response to androgen deprivation. This was a two-stage process, first in assessing the morphological and molecular changes in response to AD at multiple time points (5, 10 and 15 d), then to establish whether these observed changes were specific to a reduction in androgen by culturing cells in AD conditions with the addition of a synthetic androgen (R1881) at concentrations used extensively throughout the literature (Bluemn *et al.*, 2018; Vander Griend *et al.*, 2014; DaSilva *et al.*, 2009). Finally, to further investigate the activity of the proposed PCa NED driver hASH1, confocal microscopy was used to determine the cellular localisation of transcription factor hASH1 throughout the NED process alongside expression of NED biomarker NSE. The experiments in this chapter were critical to the validation and characterisation of the LNCaP, DU-145 and PC-3 cell lines and provided both the confidence and foundational data to utilise the LNCaP cell line as a model of AD induced PCa NED. These experiments were also critical in identifying hASH1 as a potentially key transcription factor to the NED process.

3.1.2 Castrate-resistant prostate cancer and study justification

Long-term adjuvant and neo-adjuvant ADT is currently the standard of care for prostate cancer patients with locally advanced disease and is maintained throughout disease progression, including CRPC, in accordance with European Association of Urology guidelines (Heidenreich *et al.*, 2014). Therefore, investigating mechanisms by which prostate cancer is able to adapt to the selective pressure of ADT and become castrate-resistant is critically important. CRPC tumours possess a more aggressive phenotype and are incurable once they have metastasised (Beltran *et al.*, 2011). Elucidating the mechanisms facilitating resistance to ADT will allow for more informed ADT treatment strategies and contribute to identifying new therapeutic targets. Optimisation of ADT and

extending the window of ADT efficacy has the potential to extend patient survival times and improve quality of life (Karantanos *et al.*, 2013).

One mechanism by which prostate cancer cells can escape the efficacy of ADT is neuroendocrine differentiation (NED) (Bonkhoff, 2001). Neuroendocrine (NE) cells comprise around 1% of the healthy prostate (Parimi *et al.*, 2014) and are thought to have roles in regulating the secretory functions of the prostate gland, as well as guiding the differentiation and growth of epithelial prostate cells during development (Cox *et al.*, 1999; Yuan *et al.*, 2007). Neuroendocrine prostate cancer (NEPC) arising *de novo* is rare (Parimi *et al.*, 2014; Beltran *et al.*, 2011). However, features associated with NED, such as NED biomarkers neuron-specific enolase (NSE) and Chromogranin-A (CGA) become commonplace in advanced prostate cancer and are correlated with poor prognosis for disease progression and overall survival (Bonkhoff, 2001; Komiya *et al.*, 2009).

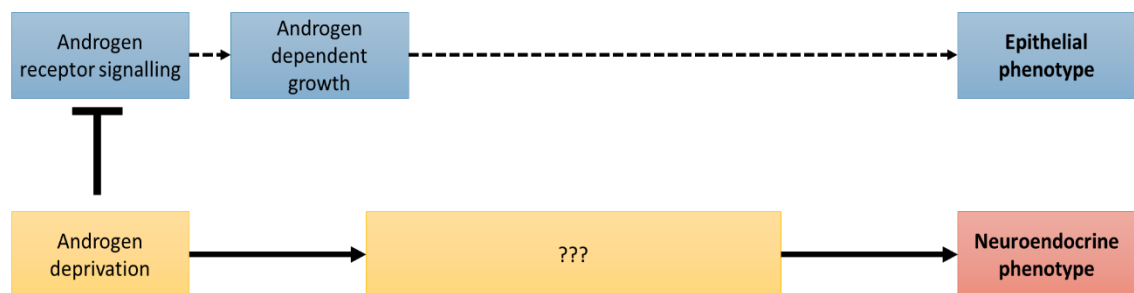


Figure 3.1 Schematic diagram illustrating the enrichment of neuroendocrine phenotype cells in some prostate cancer tumours treated with androgen deprivation therapy.

Enrichment of the NE cell niche is thought to arise through differentiation of epithelial prostate cancer cells, rather than from the prostate cancer (PCa) stem cell population or existing NE cells (Sauer *et al.*, 2006). In the developing prostate, androgen receptor (AR) signalling is vital for differentiation and maintenance of cells to the epithelial phenotype (Fig. 3.1) (Wilson, 2011). In the absence of AR signalling, healthy prostate cells undergo apoptosis, resulting in a vast reduction in size of the prostate gland (Wilson, 2011). However, some androgen-sensitive prostate cancer cells can survive and differentiate into a NE

phenotype in the absence of androgen (Fig 3.1) (Hu, Choo, & Huang, 2015). The precise molecular mechanisms facilitating this change, remain to be elucidated.

The phenomenon of prostate cancer NED in response to ADT has been known for over two decades. NED was first observed *in vivo* using haematoxylin and eosin (H&E) staining and immunostaining for chromogranin-A (Di Sant'Agnese, 1992) and also demonstrated *in vitro* in LNCaP prostate cancer cells (Shen *et al.*, 1997). The vast majority of research into NED in prostate cancer has focused upon identifying the treatment-based causes of NED, such as AD (Shen *et al.*, 1997) and ionizing radiation (Deng *et al.*, 2008). Tumour microenvironment causes of NED such as hypoxia (Danza *et al.*, 2012) and IL-6 secretion (Zhu *et al.*, 2014) have also been described. Several NED biomarkers have previously been evaluated such as neuron-specific enolase (NSE), chromogranin-A and synaptophysin and these are now widely used in PCa NED studies (Bonkhoff, 2001; Kamiya *et al.*, 2003).

In terms of research investigating the molecular pathways between the driver of NED and the resulting increase in NED biomarker expression and morphological change, there have been some studies investigating the roles of transcription factors snail family transcriptional repressor 1 (SNAI1) (McKeithen *et al.*, 2010) and human achaete-scute homolog-1 (hASH1) (Rapa *et al.*, 2008, 2013). These studies have demonstrated that transduction of hASH1 is associated with increased expression of NED markers chromogranin-A and synaptophysin (Rapa *et al.*, 2013). Furthermore, hASH1 staining has previously been found in the nuclei of human PCa samples co-expressing chromogranin-A (Rapa *et al.*, 2008).

PCa NED is induced by a variety of stimuli, including clinically-used therapies such as ADT and radiotherapy (Hu *et al.*, 2015). NE-like cells are also known to have increased resistance to ADT, radiotherapy and chemotherapeutic interventions (Hu *et al.*, 2015) and may be able to confer aspects of these advantages to other cell types within a PCa tumour through paracrine signalling. Therefore, research focus in this field has shifted to elucidating molecular pathways underpinning the NED process, which remains unclear, and could facilitate identification of potential biomarkers or novel therapeutic targets (Li,

Zhang, & Zhang, 2016). Finally, identifying the molecular components of the NED pathway could allow for earlier detection of NED. This could enable earlier selection of patients to receive non-AR targeting therapies, such as platinum chemotherapy, which are more effective against NED cancer cells (Beltran *et al.*, 2016).

3.1.3 Hypothetical NED pathway

Nuclear localisation of transcription factor Human achaete-scute homolog 1 (hASH1) is a critical step in the formation of neurons during canonical neurogenesis (Kasim *et al.*, 2016). Transduction of hASH1 to supraphysiological concentrations promotes an NE phenotype in prostate cancer cells (Axelson, 2004; Rapa *et al.*, 2008). Whilst expression of hASH1 is constitutively repressed in non-neuronal cells, aberrant expression of hASH1 could potentially be facilitated by Prostate Tumour Overexpressed 1 (PTOV1) overexpression, a common occurrence in prostate cancer carcinogenesis (Benedict *et al.*, 2001; Cánovas *et al.*, 2015). PTOV1 acts as a Notch1 signalling repressor (Alaña *et al.*, 2014). Since Notch1 signalling is fundamental to maintenance of cell fate (Lai, 2004), it is proposed that PTOV1 overexpression may allow prostate cancer cell fate to become increasingly malleable, allowing activation of different cell-differentiation programs.

The complete pathway facilitating NED remains to be clarified in an AD model at a molecular level. The extent of molecular reversibility of this proposed pathway in response to cessation of AD also remains unclear. The use of intermittent ADT (IADT) has long been touted as a possible clinical solution to the long-term effects of ADT, both to improve quality of life to patients by restoring sexual function and to delay onset of ADT resistance (CRPC) (Bruchovsky *et al.*, 2000; Grossfeld *et al.*, 2001; Klotz *et al.*, 1986; Goldenberg *et al.*, 1995; Oliver *et al.*, 1997). However, the effects of repeated bouts of ADT and therefore, potential differentiation events, have also not been studied in-depth at a molecular level. Furthermore, whilst hASH1 has been tentatively described as a potential therapeutic target for small cell lung cancer which shares many features with NED in PCa (Demelash *et al.*, 2012; Nishikawa *et al.*, 2011; Osada *et al.*, 2008; Osada, Tatematsu *et al.*, 2005), its utility in prostate cancer NED and role in AD

resistance remains to be proven. Providing insights into the NED pathway and its potential downstream effects is extremely valuable and could allow for clinicians to make more informed, evidenced-based choices in regards to ADT and IADT.

3.1.4 Study aim and research questions

Study aim: To establish and characterise an *in vitro* model of AD induced NED using androgen-sensitive LNCaP cells cultured in low androgen conditions to mimic the effects of ADT.

Research questions: **(1)** What are the key molecular components underpinning the NED process in response to AD? **(2)** To what extent are NED cells neuronal-like? **(3)** Can NED be induced specifically by AD?

3.2 Results

3.2.1 Characterisation of prostate cancer cell lines

In order to begin creating a model of prostate cancer disease progression, it was necessary to select and characterise a range of PCa cell lines which accurately recapitulate androgen-sensitive and castrate-resistant disease. In this study, LNCaP prostate cancer cells were used as a model of androgen-sensitive PCa and have been used previously for PCa NED studies (Farach *et al.*, 2016; Rapa *et al.*, 2013). In addition, the two classical prostate cancer cell lines DU-145 and PC-3 were used as a comparison and are well established models of castrate-resistant prostate cancer (Alimirah *et al.*, 2006).

The LNCaP cell line was originally derived from a lymph node metastasis (Horoszewicz *et al.*, 1983) and has become the prominent cell line used for androgen-sensitive prostate cancer research. PC-3 cells were first harvested from a bone metastasis (Kaighn *et al.*, 1979) and DU-145 cells were derived from a brain metastasis (Stone *et al.*, 1978) and as metastatic CRPC cells they are models of late-stage terminal disease (Karantanos *et al.*, 2013). The inclusion of these three prostate cancer cell lines in this study allowed for the comparison between an androgen-sensitive model of prostate cancer and two models of castrate-resistant prostate cancer. These cell lines were subjected to extensive molecular and morphological characterisation to assess the differences between androgen-sensitive and CRPC cells and their response to AD treatments.

3.2.2 Molecular characterisation of prostate cancer and CRPC cells

Exploratory analysis in CRPC cell lines was performed using end-point PCR (data not shown), in which an initial 'wide net' of genes was consolidated to a focussed selection of transcriptional programs including the androgen axis, cancer stem cell (CSC) markers and NED. These initial experiments also contributed to the optimisation of PCRs and the development of a robust array of highly specific oligonucleotides for the genes of interest for this study. Following these initial experiments and the validation of the oligonucleotides, a quantitative analysis of gene expression in CRPC cells and androgen-sensitive LNCaP cells was conducted using qRT-PCR.

3.2.2.1 Androgen receptor and prostate-specific antigen expression

AR expression was assessed in LNCaP, DU-145 and PC-3 cells via qRT-PCR (Fig. 3.2A) and AR expression was only detectable in LNCaP cells. Expression of AR protein was also only detected in LNCaP cells via immunoblot (Fig. 3.2C), bands visible on the immunoblot below 110 KDa are likely to be degraded forms of the AR protein or non-specific binding of the SC-816 antibody. PSA expression is driven by androgen receptor signalling as the kallikrein 3 (KLK3) gene which encodes PSA contains an androgen response element (ARE) (Luke and Coffey, 1994). This makes PSA expression a useful indicator of AR signalling (Kim & Coetzee, 2004). PSA expression was detected in androgen-sensitive LNCaP cells, but was undetectable in DU-145 and PC-3 via qRT-PCR and immunoblotting (Fig. 3.2 panels B and C). Analysis of AR and PSA expression confirmed that the LNCaP, PC-3 and DU-145 cells used in this study are consistent with the previously published literature on these cell lines (Yadav *et al.*, 2017).

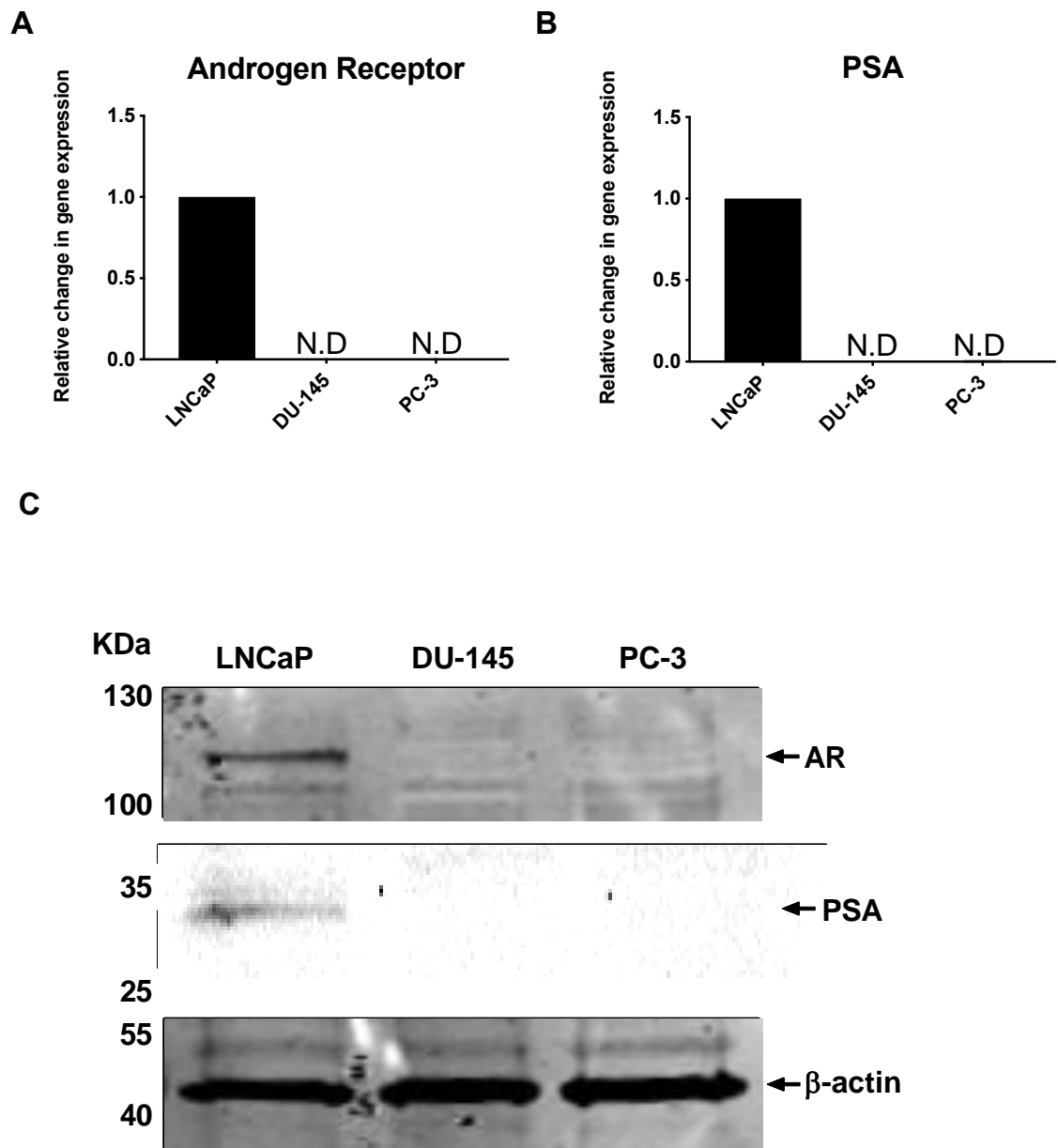


Figure 3.2. Androgen receptor (AR) and prostate specific antigen (PSA) expression in androgen-sensitive LNCaP and castrate-resistant DU-145 and PC-3 prostate cancer cells. A. Expression of **A. AR** and **B. PSA** in LNCaP, DU-145 and PC-3 prostate cancer cells was analysed by qRT-PCR and expressed as relative mRNA level normalised to *ACTB* ($2^{-\Delta\Delta Ct}$). Data presented as mean \pm SEM, (n=3), Not Detected (N.D). **C.** Representative immunoblot images of AR and PSA expression in LNCaP, DU-145 and PC-3 cells, β -actin was used as a loading control.

3.2.2.2 Prostate cancer stem-like cell marker expression

As PCa stem-like cells do not express androgen receptor, they are inherently resistant to AD (Tu & Lin, 2012) and expression of PCa stem-like cell biomarkers is associated with higher tumorigenic and metastatic ability (Patrawala *et al.*, 2006; Tu & Lin, 2012). CD44, CD166 and ITGA2 are putative biomarkers of PCa stem-like cells (Patrawala *et al.*, 2006; Reyes *et al.*, 2013; Tu & Lin, 2012; Zhang & Waxman, 2013).

Expression of CD44, CD166 and ITGA2 was assessed to investigate differences in the PCa CSC marker expression between androgen-sensitive LNCaP cells and CRPC cell lines, DU-145 and PC-3. Expression of *CD44*, *CD166* and *ITGA2* was significantly higher in CRPC cell line DU-145 compared to androgen-sensitive LNCaP cells (Fig. 3.3). Interestingly, PC-3 cells did not show significantly higher expression of the three PCa stem-like cell markers, despite also being a castrate-resistant cell line. Although DU-145 showed highest expression of CSC markers CD44, CD166 and ITGA2, expression in LNCaP and PC-3 was also robust. These findings indicate that expression of CSC markers is a feature of both androgen-sensitive and CRPC cell lines.

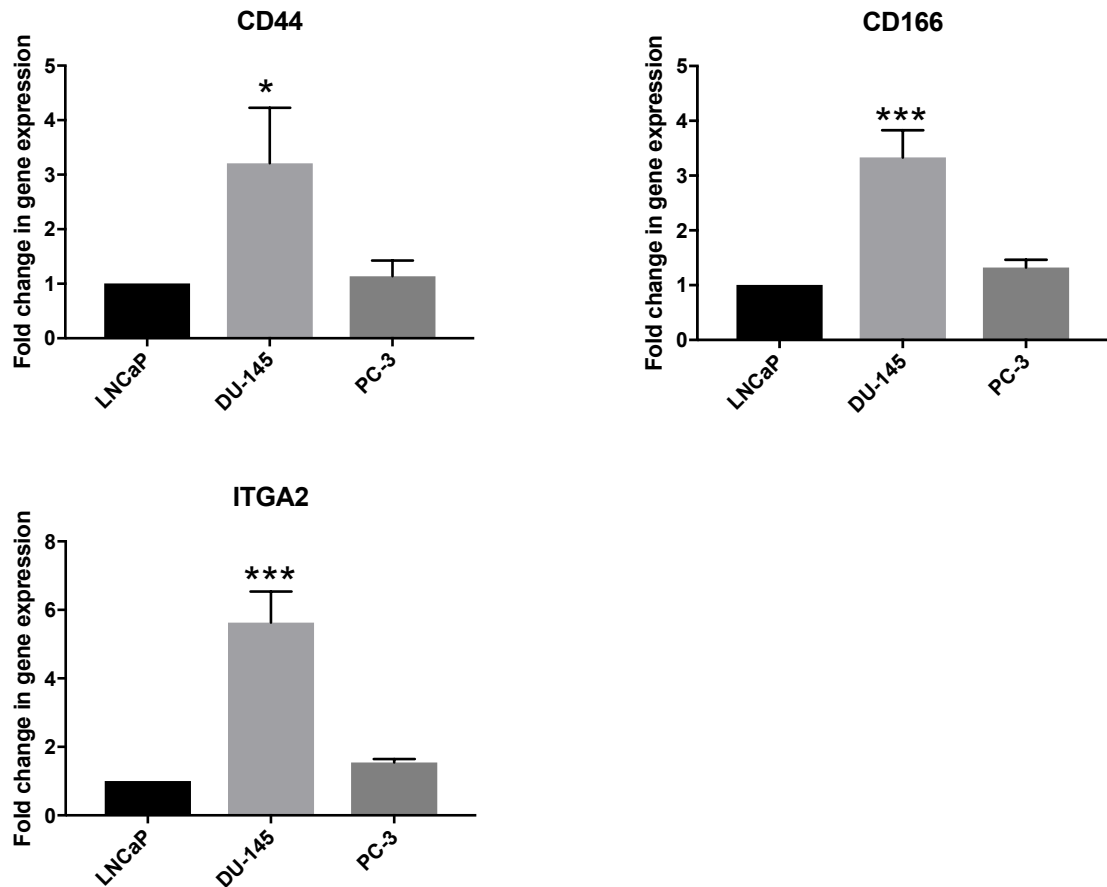


Figure 3.3. Expression of cancer stem cell (CSC) markers in androgen-sensitive LNCaP and castrate-resistant DU-145 and PC-3 prostate cancer cells. Expression of CD44, CD166 and ITGA2 mRNA in LNCaP, DU-145 and PC-3 cells were analysed by quantitative qRT-PCR and expressed as relative expression normalised to *ACTB* ($2^{-\Delta\Delta C_t}$). Data presented as mean \pm SEM, n=3. One-way ANOVA with Dunnett's correction was performed, $p < 0.05$ (*), $p < 0.01$ (**) and $p < 0.001$ (***).

3.2.2.3 Initial analysis of core protagonists in the NED pathway; biomarker, repressor and neurotransmitter synthesis.

As an initial investigation of the hypothetical NED pathway, three 'checkpoints' were assessed in androgen-sensitive (LNCaP) and CRPC cells (DU-145 & PC-3); A clinical biomarker of NED (NSE), a canonical repressor of neurogenesis (RE1-silencing transcription factor) and a neurotransmitter synthesis enzyme (GAD1).

NSE is a glycolytic metalloenzyme (Rech *et al.*, 2006). Expression of NSE occurs late into neuronal differentiation. It is therefore considered to be a marker of mature neurons (Isgro *et al.*, 2015). NSE is a clinical biomarker used to detect both primary NEPC and NED of PCa via immunohistochemistry (Isgro *et al.*, 2015; Komiya *et al.*, 2013). NSE is considered to be one of the best and most studied biomarkers for this disease state (Komiya *et al.*, 2013).

RE1-silencing transcription factor (REST) is a master negative regulator of neurogenesis which can control the expression of hundreds of neuronal genes (Gao *et al.*, 2011). Transcription factor hASH1 is a canonical promoter of neurogenesis and is a specific target gene of REST (Gao *et al.*, 2011). Glutamate decarboxylase 1 (GAD1) is involved in the synthesis of γ -aminobutyric acid (GABA) from L-glutamic acid (Ippolito & Piwnica-Worms, 2014). GABA has previously been implicated in increased aggressive and metastatic activity of prostate cancer (Azuma *et al.*, 2003) and decreased disease free survival (Ippolito & Piwnica-Worms, 2014). Expression of GAD1 has also been reported to be increased in castrate-resistant prostate cancer cells compared to androgen-sensitive prostate cancer cells (Ippolito & Piwnica-Worms, 2014). Therefore, to assess key points in the proposed NED pathway between androgen-sensitive and CRPC cells, expression of neuron-specific enolase (NSE), RE1-silencing transcription factor (REST) and glutamate decarboxylase 1 (GAD1) was investigated using qRT-PCR (Fig. 3.4).

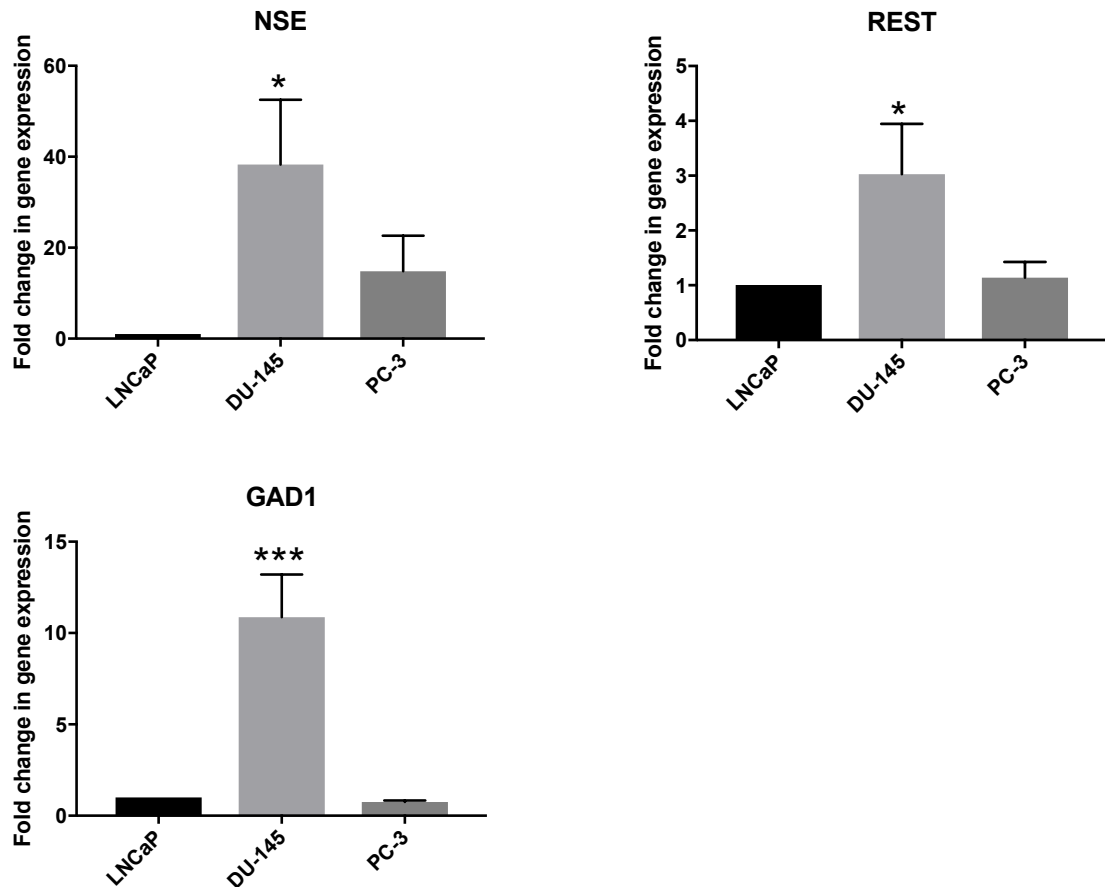


Figure 3.4. Expression of neuroendocrine differentiation (NED)-related genes in androgen-sensitive and castrate-resistant prostate cancer cells. Basal expression of neuron-specific enolase (NSE), RE1-silencing transcription factor (REST) and glutamate decarboxylase 1 (GAD1) mRNA in LNCaP, DU-145 and PC-3 cells were analysed by qRT-PCR and expressed as relative mRNA level normalised to *ACTB* ($2^{-\Delta\Delta Ct}$). Data presented as mean \pm SEM, (n=3). One-way ANOVA with Dunnett's correction was performed, $p < 0.05$ (*), $p < 0.01$ (**) and $p < 0.001$ (***).

Expression of the neuronal marker, NSE, was 38-fold higher in DU-145 cells when compared to LNCaP cells ($p = 0.02$), suggesting a higher degree of NED. Interestingly, expression of REST and GAD1 mRNA was also significantly higher in DU-145 cells, with 3-fold higher REST expression ($p = 0.03$) and 10-fold higher GAD1 expression ($p = <0.001$) compared to LNCaP cells. PC-3 cells displayed higher expression of NSE than LNCaP cells, although this was not statistically significant. Expression of REST and GAD1 was similar between LNCaP and PC-3 cells (Fig. 3.4). Higher expression of neuronal marker, NSE, and GABA

synthetic enzyme, GAD1 would appear to suggest that DU-145 cells display increased evidence of NED compared to androgen-sensitive LNCaP cells. Interestingly, gene expression of REST, which represses neurogenesis, was also higher in DU-145 cells which is converse to what would be expected, considering the higher expression of NSE. However, this result is consistent with that of Lin *et al.*, 2016 who found REST mRNA expression was unchanged after NED whereas REST protein was markedly downregulated. To support and validate the findings of qRT-PCR experiments, expression of key marker proteins in LNCaP DU-145 and PC-3 cells was analysed using immunoblotting (Fig. 3.5).

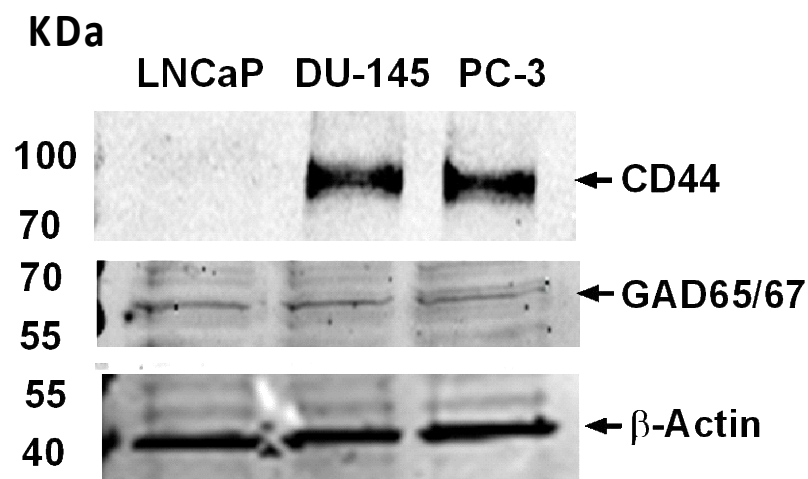


Figure 3.5. Analysis of basal expression of key prostate cancer markers. Representative immunoblots showing expression of CD44 and glutamate decarboxylase (GAD65/67) in LNCaP, DU-145 and PC-3 PCa cells. Beta actin was used as a loading control.

In contrast to qRT-PCR analysis of CD44 gene expression (Fig. 3.3), CD44 protein was only detected in CRPC cell lines DU-145 and PC-3 (Fig. 3.5). Interestingly, higher CD44 expression has also been previously found in prostate cancer cells co-expressing higher levels of NED markers NSE and Chromogranin-A (Hu *et al.*, 2015; Palapattu *et al.*, 2005). GAD65/67 protein was detected in all three cell lines (Fig. 3.5), in accordance with the qRT-PCR data (Fig. 3.4), suggesting that both androgen-sensitive LNCaP cells and CRPC cell lines may have γ -aminobutyric acid (GABA) synthesis potential (Ippolito &

Piwnica-Worms, 2014). Interestingly, the 10-fold higher relative GAD1 gene expression in DU-145 cells compared to LNCaP cells observed via qRT-PCR analysis was not reflected at a protein level (Fig. 3.5). In addition, CD44 was robustly expressed in both CRPC cell lines but undetectable in LNCaP, indicating that castrate-resistant cell lines display increased expression of at least one PCa stem cell marker. Furthermore, expression of GAD65/67 indicates that these cell lines may be able to synthesise GABA, a neurotransmitter previously demonstrated to increase the metastatic potential of prostate cancer cells (Azuma *et al.*, 2003).

3.2.3.1 Androgen-sensitive LNCaP cells display significantly slower growth in scratch assays compared to CRPC cell lines

A comparative assessment of growth and potential for migration of LNCaP, DU-145 and PC-3 cells was conducted using wound healing assays which were used to quantitatively assess the time taken to close a wound made in a confluent monolayer of cells. These experiments also allowed for the observation of cells migrating into the centre of a wound area via light microscopy. Images of the wound area were captured at regular time points (Fig 3.6A) and quantified using ImageJ (Fig 3.6B) (Schneider *et al.*, 2012). DU-145 cells displayed the fastest rate of wound closure, taking on average 24 h to fully close the original wound area. PC-3 cells took on average 96 h to close the original wound area and LNCaP cells displayed the slowest rate of wound closure, with 70% of original wound area still intact after 120 h. Images captured throughout the wound closure process showed that PC-3 cells consistently displayed greater migration into the centre of the wound at earlier time points than DU-145 cells despite an overall slower rate of wound closure. LNCaP cells showed minimal cellular migration into the centre of the wound area. The wound healing assay demonstrated the potentially more aggressive nature of castrate-resistant DU-145 and PC-3 cells which were considerably faster at wound closure than androgen-sensitive LNCaP cells.

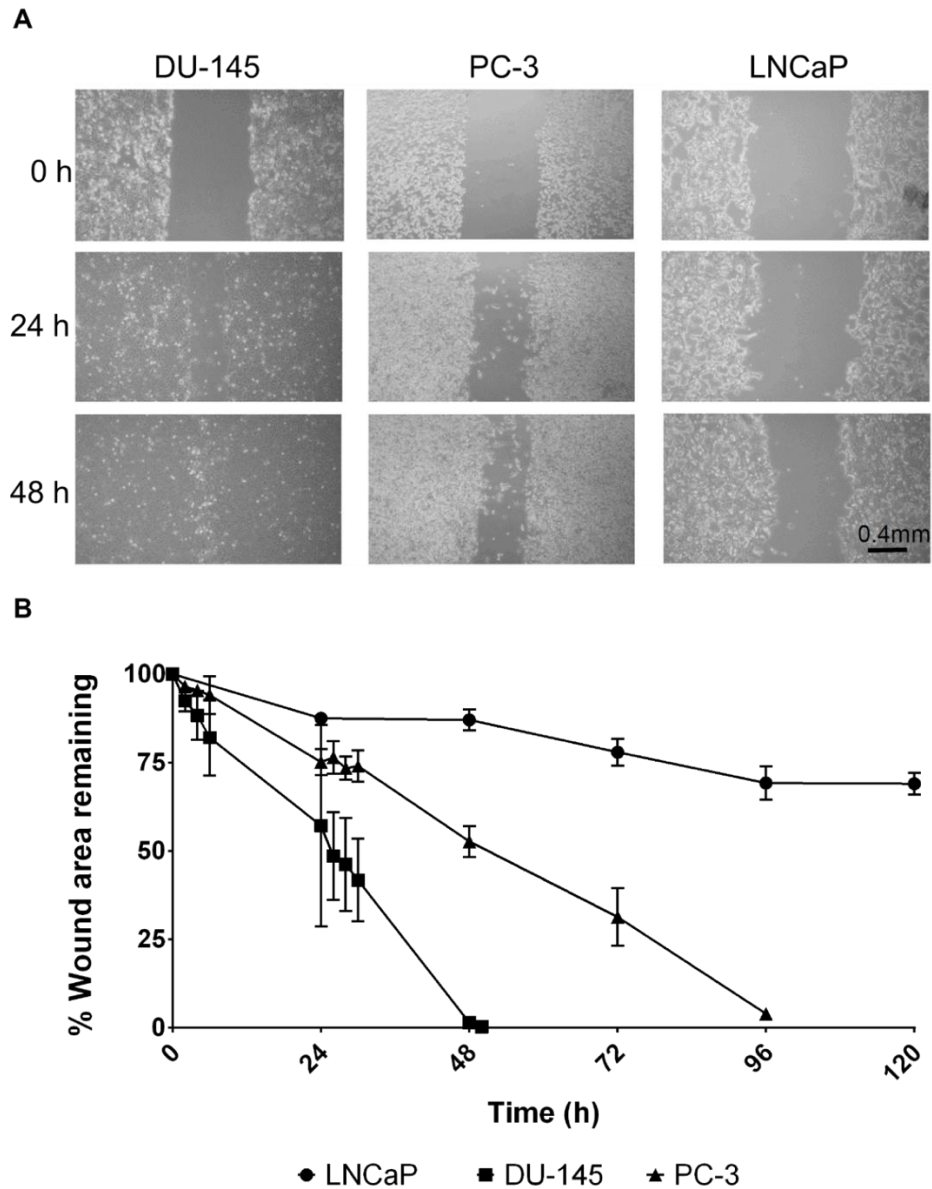


Figure 3.6. Wound closure and migration of prostate cancer cell lines assessed via scratch assays. A. Images captured at time points 0, 24 and 48 (h) of androgen-sensitive LNCaP and castrate-resistant DU145, PC-3 cells. As only LNCaP cells had remaining wound area at 120 h, measurements for DU-145 and PC-3 were not taken at this time point. **B.** Graph showing the percentage of wound healing over time of prostate cancer cell lines LNCaP, DU-145 and PC-3. Wound area was quantified at designated time points using ImageJ. Mean \pm SEM, (n=3). Images were captured of one field of view at the vertical centre of the wound area. The rate of wound healing was assessed using ImageJ software (Schneider, Rasband, & Eliceiri, 2012) to analyse the area of the wound (i.e. surface area in one field of view not covered by cells) at each time point. The area was then expressed as a percentage of the initial wound area.

3.2.4.1 Androgen deprivation triggers a neuroendocrine differentiation program in androgen-sensitive prostate cancer cells

To assess the morphological and molecular effects of AD on prostate cancer, LNCaP, DU-145 and PC-3 cells were cultured in either standard, complete RPMI 1640 media or, media containing charcoal-stripped FBS. Charcoal-stripped FBS contains a much lower level of androgen (Cao *et al.*, 2009) and was therefore used to simulate AD for 0, 5, 10 and 15-days (Fig. 3.7), the 15-day time span was chosen as this has previously been shown to result in well-established NED phenotype in LNCaP cells (Rapa *et al.*, 2013).

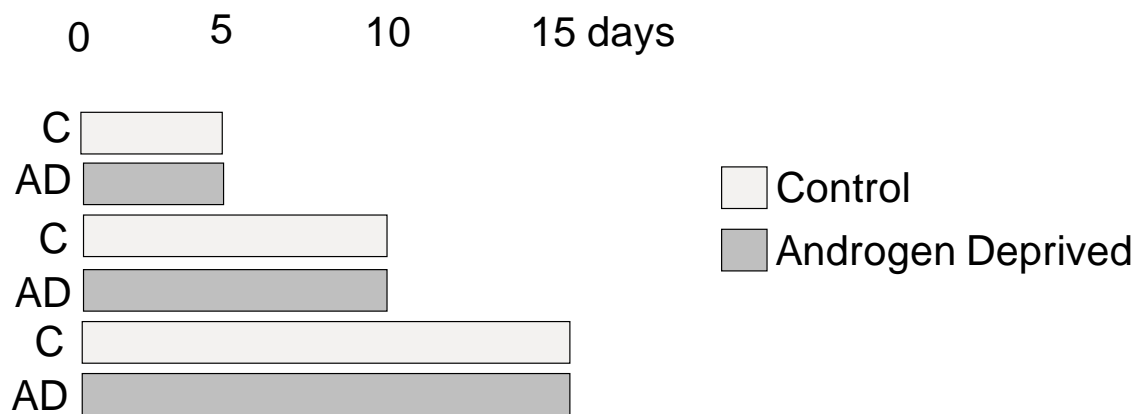


Figure 3.7. Schematic diagram indicating the experiment design for androgen deprivation experiments. LNCaP cells were cultured in either control media (C) or androgen deprived (AD) media which contained charcoal-stripped FBS, for 5, 10 and 15-days.

LNCaP, DU-145 and PC-3 cells were analysed by bright field microscopy (Fig. 3.8). At day zero LNCaP, DU145 and PC-3 display typical epithelial morphology with few outgrowths or projections from the cell membrane. By 5 d, androgen-sensitive LNCaP cells displayed noticeable changes in morphology, including development of short cytoplasmic protrusions (Fig. 3.8). These became extensive after 10 d in the absence of androgen by 15 d (indicated by black arrows in Fig. 3.8). The outgrowth of neurite-like processes from these cells supports the hypothesis that androgen-sensitive LNCaP cells become more neuronal-like in response to AD. In addition, the increasing length, complexity and inter-cellular contact of these neurite-like extensions over time suggests that these cells

become more mature in their neuronal differentiation (Mingorance-Le-Meur & O'Connor, 2009). Castrate-resistant cell lines, DU-145 and PC-3, did not display any observable morphological changes across 15 d AD, resembling untreated control cells throughout (Fig. 3.8). It must be acknowledged that images were not captured for LNCaP, DU-145 or PC-3 cells grown in control conditions at a 15 d timepoint, which is a clear limitation of this experiment, however they were for LNCaP in subsequent experiments (Fig. 3.10).

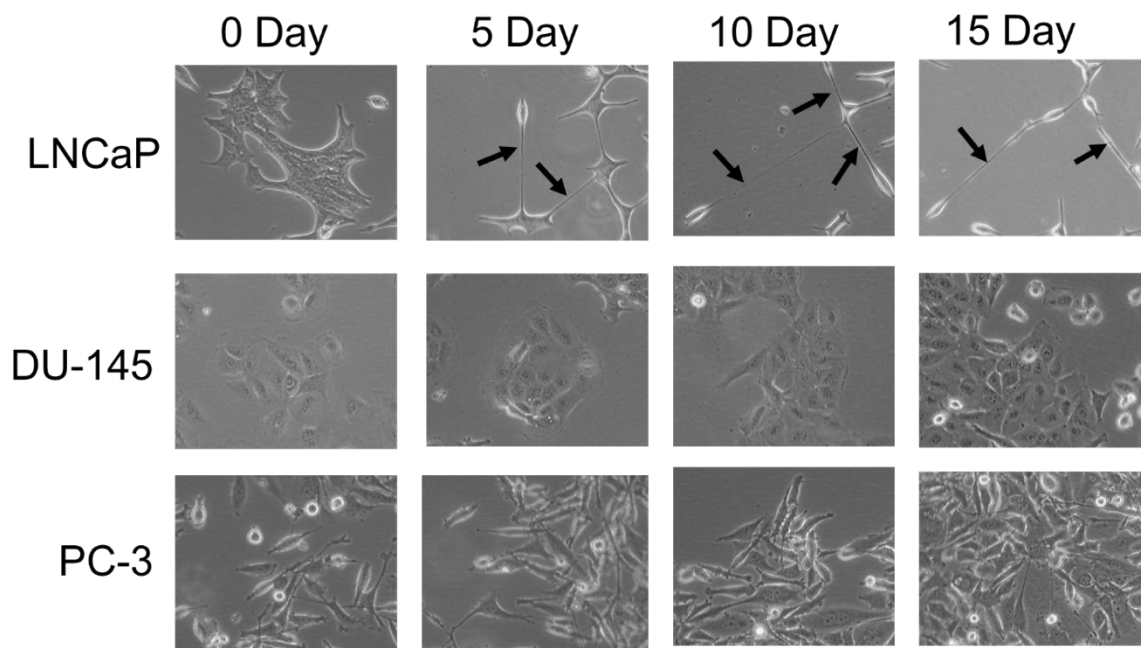


Figure 3.8, Androgen-sensitive LNCaP cells undergo morphological change in response to androgen deprivation. Representative images of LNCaP, DU-145 and PC-3 cells at 0 days (cells in control RPMI 1640 with 10% FBS) and 5, 10 and 15 d after culture in AD conditions (RPMI 1640 with 10% charcoal-stripped FBS). Cell morphology was recorded using bright field microscopy (20 × magnification). Arrows point to neurite-like extensions.

The impact of AD on AR signalling was also assessed by qRT-PCR (Fig. 3.9 panel A) and immunoblot (Fig 3.9 panel B). After 5 d of AD, qRT-PCR analysis revealed that expression of AR was slightly elevated (1.42-fold) in LNCaP cells, whilst PSA was down-regulated 14.23-fold compared to untreated LNCaP cells (Fig. 3.9). At 15 d, AR mRNA remained slightly elevated from basal levels (1.44-fold) and AR protein expression remained stable, whereas PSA mRNA expression was dramatically downregulated (50.97-fold; $p = <0.001$) and PSA

protein expression was no longer detectable. The results demonstrate that under AD conditions, AR signalling is greatly reduced as expression of PSA is dependent upon AR signalling mediated by androgen response elements in the PSA encoding gene (Luke and Coffey, 1994). These findings validate that the charcoal-stripped FBS model of AD used in this study prevents canonical AR signalling.

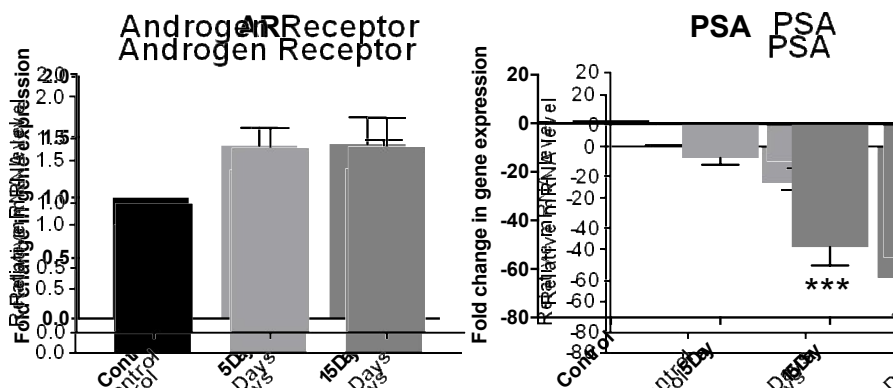


Figure 3.9. Effect of androgen deprivation on PSA and androgen receptor expression. A. Relative expression of AR, and PSA in LNCaP cells before and after 5 or 15 d androgen deprivation was analysed via qRT-PCR. Data is expressed as mean \pm SEM, where $n=3$ $p < 0.05$ (*), $p < 0.01$ (**) and $p < 0.001$ (***).

3.2.4.2 Analysis of neurite growth

The morphological changes observed in LNCaP cells following AD (Fig. 3.8) are typical of a more neuronal-like morphology (Rapa *et al.*, 2013). To confirm this, LNCaP cells were stained with a neurite outgrowth staining kit, which allowed for quantitative analysis of neurite length using a cell membrane stain to aid visualisation (Fig. 3.10). It should be noted that this neurite outgrowth kit is purely used to aid the visualisation of neurites and is in no way a cell-type specific dye. Analysis showed that after 15 d in AD conditions LNCaP cells acquired neurite-like protrusions, which were on average more than twice the length of the cell body they originated from. Thus, protrusions developed by LNCaP cells in response to AD meet the length criteria previously used to classify PC-12 cells as terminally differentiated, neuron-like cells (Wu *et al.*, 2012).

This finding suggests that if androgen-sensitive LNCaP cells acquire morphology consistent with neuronal cells when androgen deprived, it is possible that they may also gain some of the functions facilitated by neuronal morphology. This data also demonstrates that this model is robust and the morphology and gene expression changes associated with AD are consistent with the previous literature (Shen *et al.*, 1997). Therefore, this model was used to further investigate the molecular drivers of AD-induced NED of PCa cells.

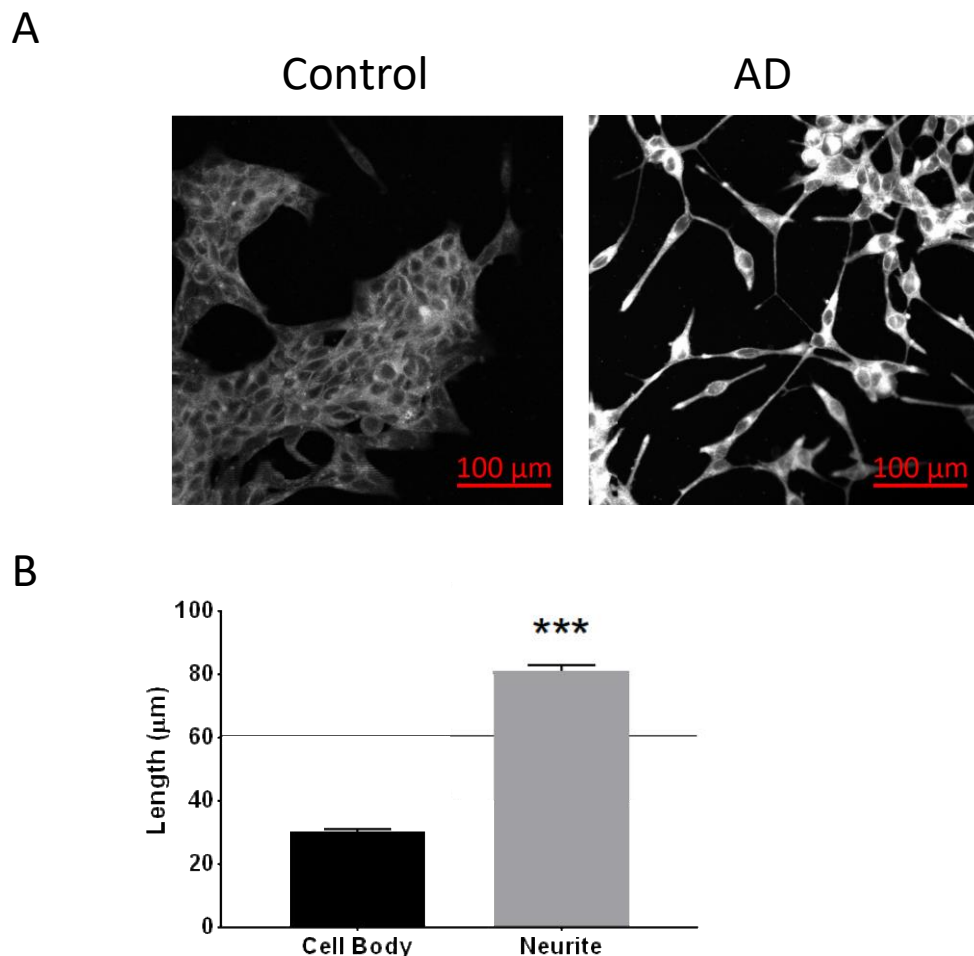


Figure 3.10. Androgen deprivation triggers significant morphological changes in LNCaP cells. **A.** Representative images of LNCaP cells cultured in media containing 10% (v/v) charcoal stripped FBS for 15 d and stained using neurite outgrowth staining kit. **B.** Cellular protrusions were analysed via fluorescent confocal microscopy (40 × magnification) and qualified as neurites when their length was greater than twice that of the cell body it originated from. Data was analysed using two-tailed t-test and expressed as mean ± SEM, where $n=3$ $p < 0.05$ (*), $p < 0.01$ (**) and $p < 0.001$ (***). Each biological replicate had 3

technical replicates, in which 100 neurite lengths were measured per technical replicate.

3.2.4.3 Molecular changes resulting from androgen deprivation of LNCaP cells

To assess molecular changes underpinning the shift to a neuronal-like morphology, expression of key genes and proteins relating to neurogenesis were assessed by qRT-PCR after 5 and 15 d AD periods (Fig. 3.11) and immunoblot at 5, 10 and 15 d AD periods (Fig. 3.12). Expression of AR remained highly stable throughout AD experiments whereas expression of PSA was greatly reduced under AD conditions, indicating a loss of AR signalling. PTOV1 is a Notch1 signalling repressor postulated to be critical to facilitating differentiation (Alaña *et al.*, 2014). PTOV1 was significantly upregulated after 5 d of AD and remained elevated at 15 d of treatment. hASH1 expression was upregulated 3.5-fold at 5 d of AD and this trend continued up to 15 d of treatment (Fig. 3.11). Gene expression of neuronal marker NSE was also significantly upregulated at 5 d of AD but returns to basal levels at 15 d of treatment (Fig. 3.11).

Immunoblot analysis revealed that AR expression remained stable throughout the 15 d AD period (Fig. 3.12). NSE expression appears to increase by 10 d and is highly pronounced by 15 d of AD (Fig. 3.12). Whilst expression of NSE protein steadily increased with longer periods of AD, LNCaP cells cultured in control media displayed a steady decrease in NSE expression between 5, 10 and 15 d AD periods. PSA expression was markedly downregulated by 5 d AD, declined further by 10 d and became undetectable by 15 d. Expression of hASH1 appears to remain unchanged by 5 d AD, however expression was increased compared to untreated control at 10 d and remained slightly elevated compared to the untreated control at 15 d. Overall, this data supports the hypothesis that AD activates a canonical neurogenesis pathway in LNCaP cells.

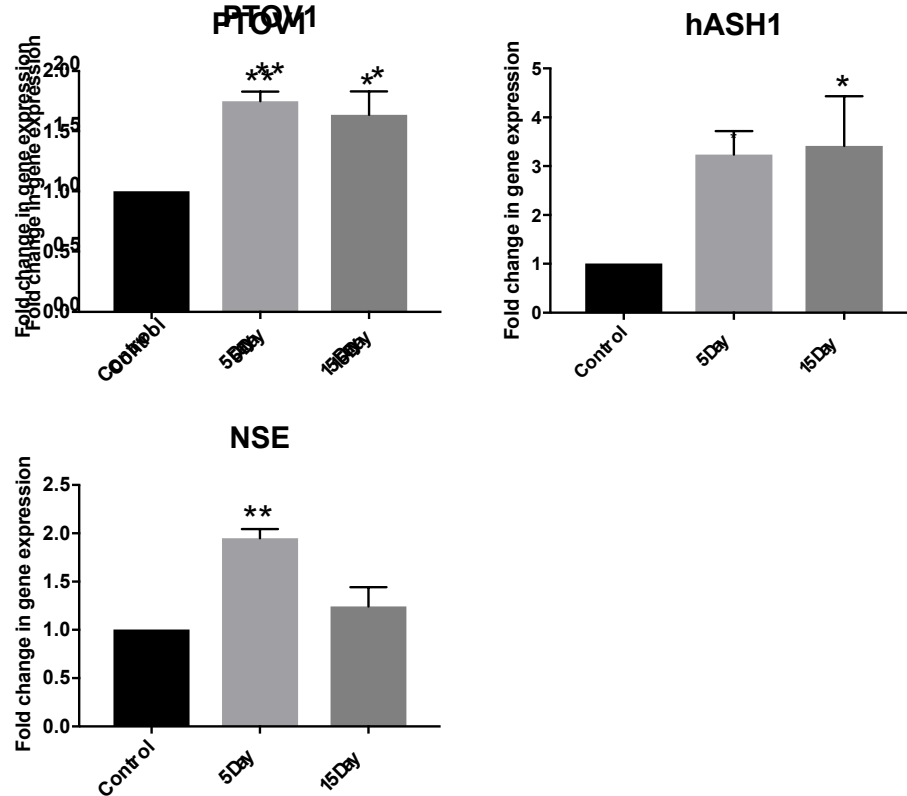


Figure 3.11. Androgen deprivation (AD) activates the canonical neurogenesis pathway. Relative expression of PTOV1, hASH1 and NSE in LNCaP cells before and after 5 or 15 d AD was analysed via qRT-PCR. Data is expressed as mean \pm SEM, where $n=3$ $p < 0.05$ (*), $p < 0.01$ (**) and $p < 0.001$ (***) as determined by one-way ANOVA with Dunnett's correction.

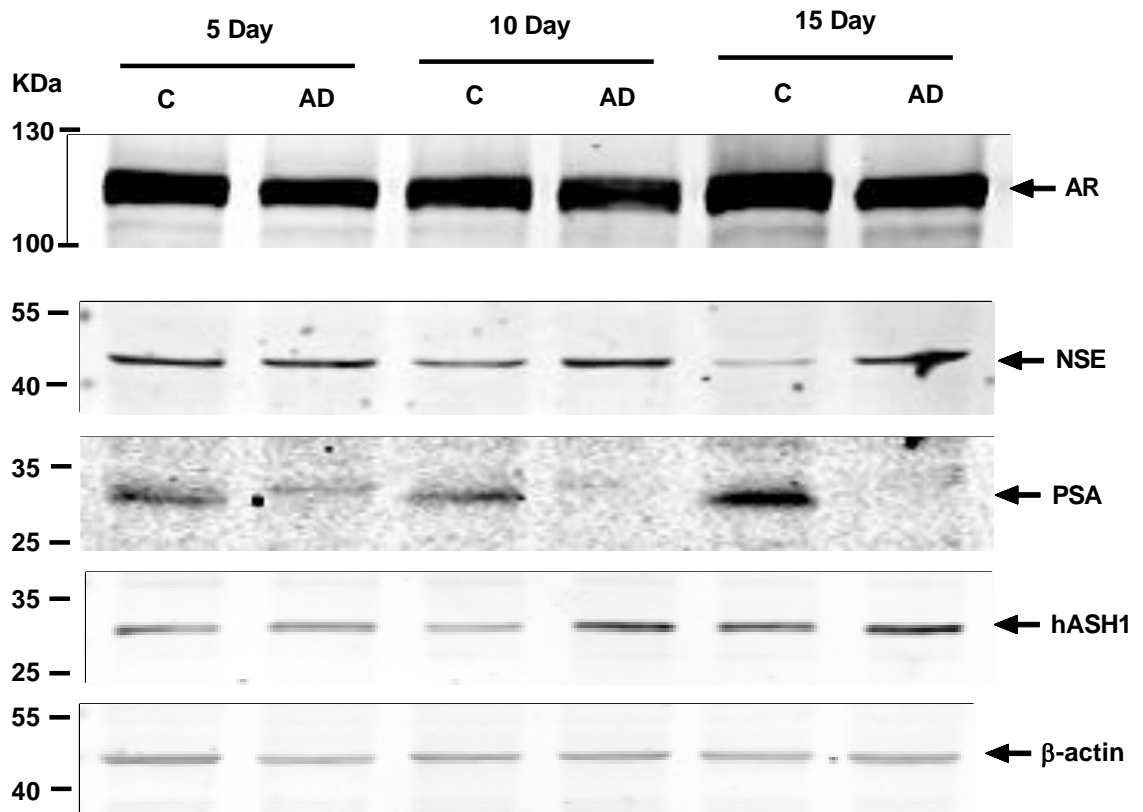


Figure 3.12. Androgen deprivation downregulates PSA expression and expression of NSE is markedly increased. Representative immunoblot analysis (n=3) of androgen receptor (AR), NSE, PSA and hASH1 in LNCaP cells at 5, 10 and 15 d of control or AD culture conditions. β -actin was used a control for equal loading.

3.2.4.4 Visualisation of hASH1 and NSE expression and localisation before and after AD induced NED

Nuclear localisation of hASH1 is a critical step in formation of neurons during canonical neurogenesis and transduction of hASH1 has previously been shown to promote a NE phenotype in prostate cancer cells (Axelson, 2004; Rapa *et al.*, 2008). In addition, hASH1 has also been described as a useful therapeutic target in lung cancer displaying NED (Osada *et al.*, 2005) and has more recently been demonstrated to have a function in increasing the migratory capacity of lung cancer cells (Demelash *et al.*, 2012; Osada *et al.*, 2008). Aberrant expression of hASH1 may be the result of Notch1 signalling repression mediated by PTOV1 overexpression (Alaña *et al.*, 2014; Lai, 2004). Neuron specific enolase (NSE) is a glycolytic metalloenzyme (Rech *et al.*, 2006) and expression of NSE occurs late

into neuronal differentiation. It is therefore considered to be a marker of mature neurons (Isgro *et al.*, 2015). NSE is a clinical biomarker used to detect both primary NEPC and NED of PCa via immunohistochemistry and is considered to be one of the best and most studied biomarkers for this disease state (Komiya *et al.*, 2013). Expression and localisation of hASH1 and NSE following AD was assessed using immunocytochemistry and visualised via confocal microscopy (Fig. 3.13).

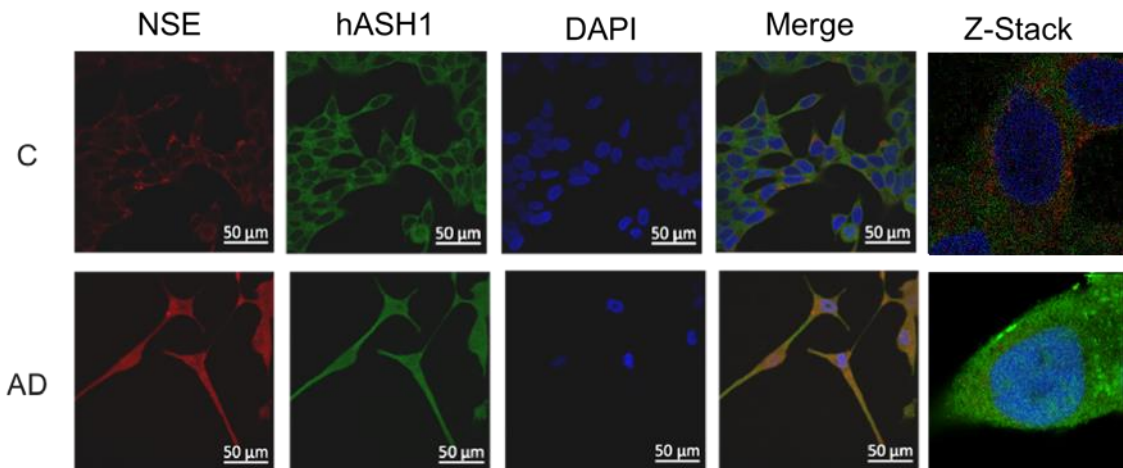


Figure 3.13. Androgen deprivation triggers neuronal-like changes in LNCaP morphology associated with hASH1 nuclear localisation. Representative confocal microscopy images (from n=3) of LNCaP cells stained with anti-hASH1 and anti-NSE antibodies and DAPI after 15 d of culture in androgen deprived (AD) or control (C) conditions (63 x magnification). Scale bar represents 50 μm . Z-stack images were taken at 63 x magnification with additional digital zoom to confirm the presence and absence of detected hASH1 in the nuclei of cells, a representative image taken from the centre of the z-stack is shown for control and AD conditions. For control condition z-stack, 22 vertical slice images with 6.685 μm spacing were captured and for AD conditions 26 vertical slice images with 8.173 μm spacing were captured, the spacing between images was determined using the optimal pre-set in Zen Blue software controlling a Confocal LSM 880 microscope (Zeiss, UK).

When cultured in control media, LNCaP cells showed almost undetectable expression of NSE and very low intensity hASH1 staining, which appeared to be exclusively cytoplasmic (Fig. 3.13, upper panel). NSE staining was intensely

upregulated in LNCaP cells after 15 d of culture in AD conditions with profuse staining throughout the cell body and neurite-like extensions (Fig. 3.13, lower panel). In addition, the staining intensity of hASH1 was markedly increased and showed abundant staining throughout the cell, including the nucleus (Fig. 3.13). Zoomed images and z-stack analyses taken of representative individual cells revealed that nuclear hASH1 was exclusive to cells which had been AD and had acquired neuronal-like morphological changes. This data demonstrates that the transcription factor hASH1 is excluded from the nucleus of LNCaP cells in the presence of androgen, but becomes localised to the nucleus in AD conditions. This data suggests that hASH1 nuclear localisation may be an important step in NED, as evidenced by markedly increased NSE staining alongside hASH1 nuclear localisation. Ideally, future experiments could be conducted to further the evidence that hASH1 is sequestered within the nucleus after AD and to confirm that hASH1 is bound to chromatin and transcriptionally active. This could be achieved using Chromatin immuno-precipitation (ChIP) and ChIP-Seq or ChIP-qPCR to identify potential hASH1 target genes.

3.2.5 Validation of AD mediated effects using synthetic androgen

Since charcoal-stripping of FBS does not exclusively remove androgens, experiments using synthetic androgen R1881 were performed to control for this and investigate whether the morphological and molecular changes observed thus far were specific to the presence or absence of androgens in the culture media. As AD has been shown to trigger NED (Fig. 3.8) (Shen *et al.*, 1997) the role of AR signalling in preventing NED was investigated and as a control for the limitations of using charcoal-stripped FBS. Concentrations of R1881 and DMSO vehicle were derived from the literature (Svensson *et al.*, 2014) and assessed empirically for their effect on cell viability using Alamar blue assay (Fig. 3.14).

3.2.5.1 Effect on cell viability of synthetic androgen R1881

Concentrations of R1881 synthetic androgen were derived from the literature focussing on the prevention and reversal of PCa NED (Svensson *et al.*, 2014). The effect of R1881 on cell viability was assessed using Alamar blue assay (Fig. 3.14) at 1 nM and 10 nM and DMSO at a concentration of 0.01% which was used as a vehicle for the R1881. Analysis of the data showed that neither R1881 or

DMSO significantly increased or decreased the percentage reduction of the Alamar blue reagent. Since the data demonstrated that 1 nM and 10 nM R1881 did not significantly alter LNCaP, DU-145 or PC-3 cell viability when using a 0.01% DMSO vehicle these concentrations were selected for use in further experiments.

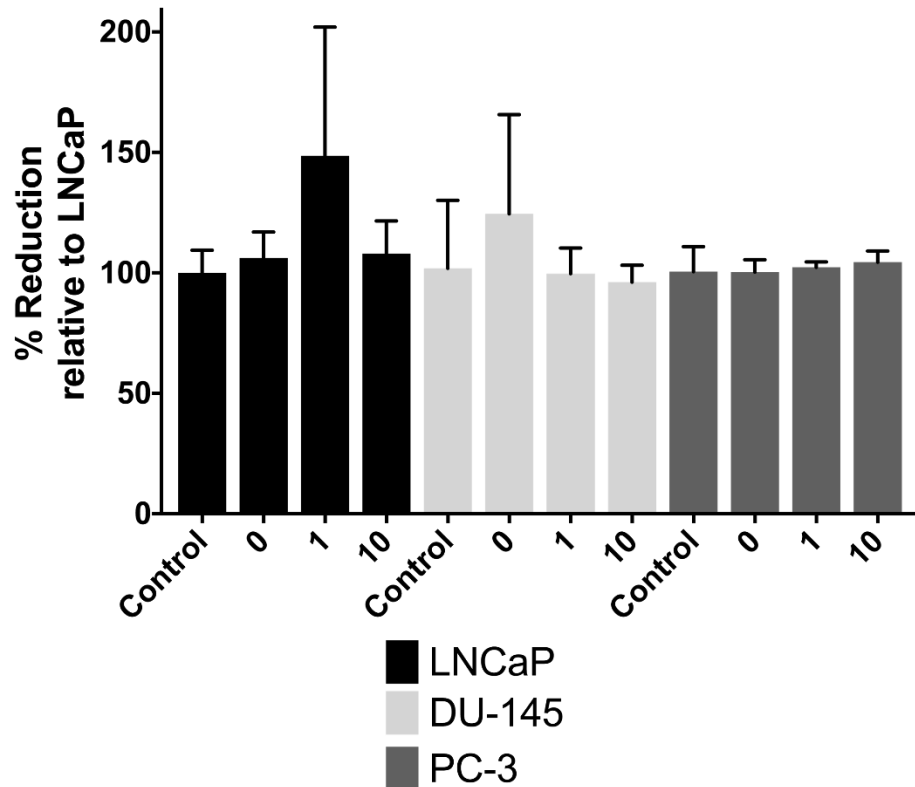


Figure 3.14. Assessment of synthetic androgen R1881 and DMSO vehicle on cell viability of prostate cancer cell lines. Prostate cancer cell lines LNCaP, DU-145 and PC-3 cells cultured in the presence of 0 (vehicle only), 1 and 10 nM R1881 or untreated control (media only). DMSO was used as a vehicle at a final concentration of 0.01%. Data is expressed as mean \pm SEM, (n=3) analysed using one-way ANOVA with Dunnett's correction.

3.2.5.2 Further refinement of AD experiment design

To investigate the effect of androgen signalling on NED, LNCaP cells were cultured in control media or, charcoal-stripped media \pm synthetic androgen (R1881) for 5, 10 and 15 days (Fig. 3.15).

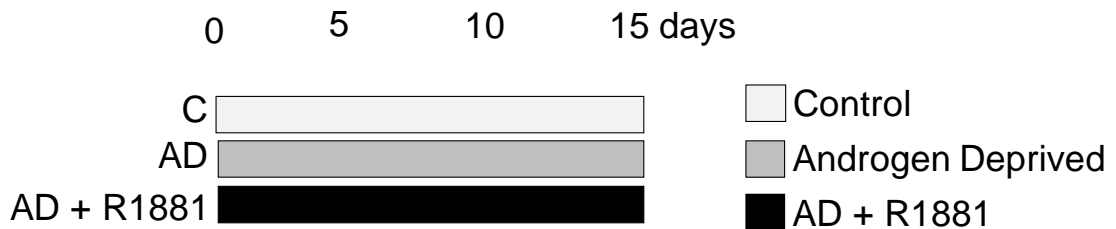


Figure 3.15, Visual representation of experiment design for androgen deprivation experiments. LNCaP cells were cultured in either control media (C), androgen deprived (AD) media which contained charcoal-stripped foetal bovine serum, or AD media with synthetic androgen R1881 (AD+R1881), for 5, 10 and 15-days. Protein lysates were collected at 5, 10 and 15 days, whilst RNA was extracted at 15 days with time matched controls cultured in complete media.

3.2.5.3 Androgen-sensitive LNCaP cells display altered morphology during androgen deprivation

LNCaP cells were cultured in control media and AD media \pm synthetic androgen R1881 and visualised using light microscopy at day 15 of culture (Fig. 3.16). As previously shown, 15 d AD induced development of long, neurite-like extensions. Correspondingly, this differentiation was inhibited by the synthetic androgen R881. AD + Vehicle treated cells continued to undergo differentiation, mirroring the morphology of the AD cells.

These findings demonstrate that the morphological changes of LNCaP cells cultured in charcoal-stripped media are likely to be predominantly mediated by a reduction in androgen concentration rather than any other FBS constituent removed through charcoal-stripping.

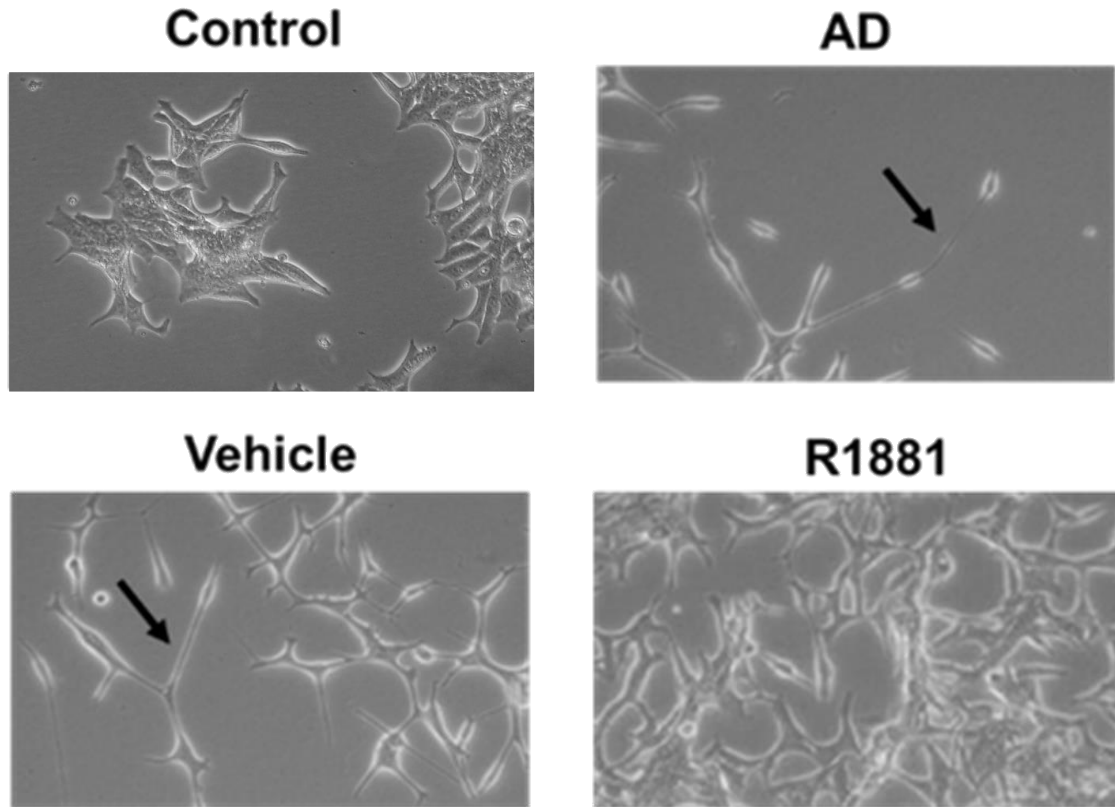


Figure 3.16. Presence of androgen prevents neuroendocrine differentiation. Representative bright field microscopy images of LNCaP cell morphology after 15 d of culture in either control, androgen deprived (AD) and androgen deprived \pm DMSO (vehicle) or 1 nM R1881 synthetic androgen (R1881) conditions (20 \times magnification). Representative images of an n=3. Arrows indicate neurite-like extensions.

3.2.5.4 Validating the effect of AD on NED related genes in LNCaP cells

Expression of a key panel of genes in LNCaP cells cultured in complete culture media with 10% FBS and AD conditions (10% charcoal-stripped FBS) \pm synthetic androgen was assessed using qRT-PCR analysis (Fig. 3.17). This panel of genes was selected through extensive literature searches and refining a shortlist of genes that appeared to be at ‘crux’ points of the proposed NED pathway, i.e. the initiators and preventers (PTOV1/REST), the hypothetical driving transcription factor hASH1 (previous implication of hASH1 in pan-cancer NED is discussed in chapter 1), a well-established biomarker (NSE) and the downstream potential effectors of the NED phenotype (GAD1 and MMP-9). Data revealed that PSA

expression was greatly downregulated by AD but was maintained at basal levels by 1 nM R1881 (Fig. 3.17). As previously stated, expression of NSE returns to basal levels after 15 d of AD (Fig. 3.12), however addition of 1nM R1881 to charcoal-stripped media resulted in significant downregulation of NSE (-3.12-fold; $p = 0.02$), becoming highly significant when cultured in the presence of 10 nM R1881 (-2.77-fold; $p = 0.0017$) (Fig. 3.17). PTOV1 expression was slightly elevated by 15 d of AD, whilst 1 nM R1881 was sufficient to prevent this increase and maintain PTOV1 expression below basal levels. Importantly, hASH1 was upregulated 3.41-fold after AD and was downregulated 3.8-fold in the presence of 1 nM R1881, becoming significantly downregulated in the presence of 10 nM R1881 (8.6-fold; $p = 0.044$) (Fig. 3.17). This data demonstrates that hASH1 expression can be modulated by the availability of androgen, a finding that robustly supports the proposed pathway of AD induced NED in prostate cancer cells.

Expression of REST is, perhaps surprisingly, robustly expressed under both control and AD conditions (Fig. 3.17). REST expression is also significantly downregulated by 1nM R1881 treatment ($p = 0.009$) but to a lesser extent by 10 nM R1881 ($p = 0.08$). Expression of GAD1 was assessed as a possible source of paracrine support potential in AD LNCaP cells. It was found that whilst GAD1 was upregulated by AD (2-fold), unlike other associated changes in gene expression, GAD1 was not downregulated by 1 nM or 10 nM R1881, suggesting modulation of GAD1 expression was not specifically androgen mediated.

MMP-9 is a tumour aggression marker that is potentially inducible by GABA receptor signalling (Azuma *et al.*, 2003). Due to discovery of GAD1 upregulation (Fig. 3.17), expression of MMP-9 was investigated. Expression of MMP-9 was not significantly upregulated by AD (1.85-fold), but was significantly downregulated when charcoal-stripped media contained 1 nM R1881 ($p = 0.04$) and more so with 10 nM R1881 (2-fold; $p = <0.001$). In all cases where gene expression responded to synthetic androgen, 1 nM R1881 was sufficient to reduce expression below basal levels. This data demonstrates that key components of the proposed NED pathway are specifically modulated by the availability of androgen.

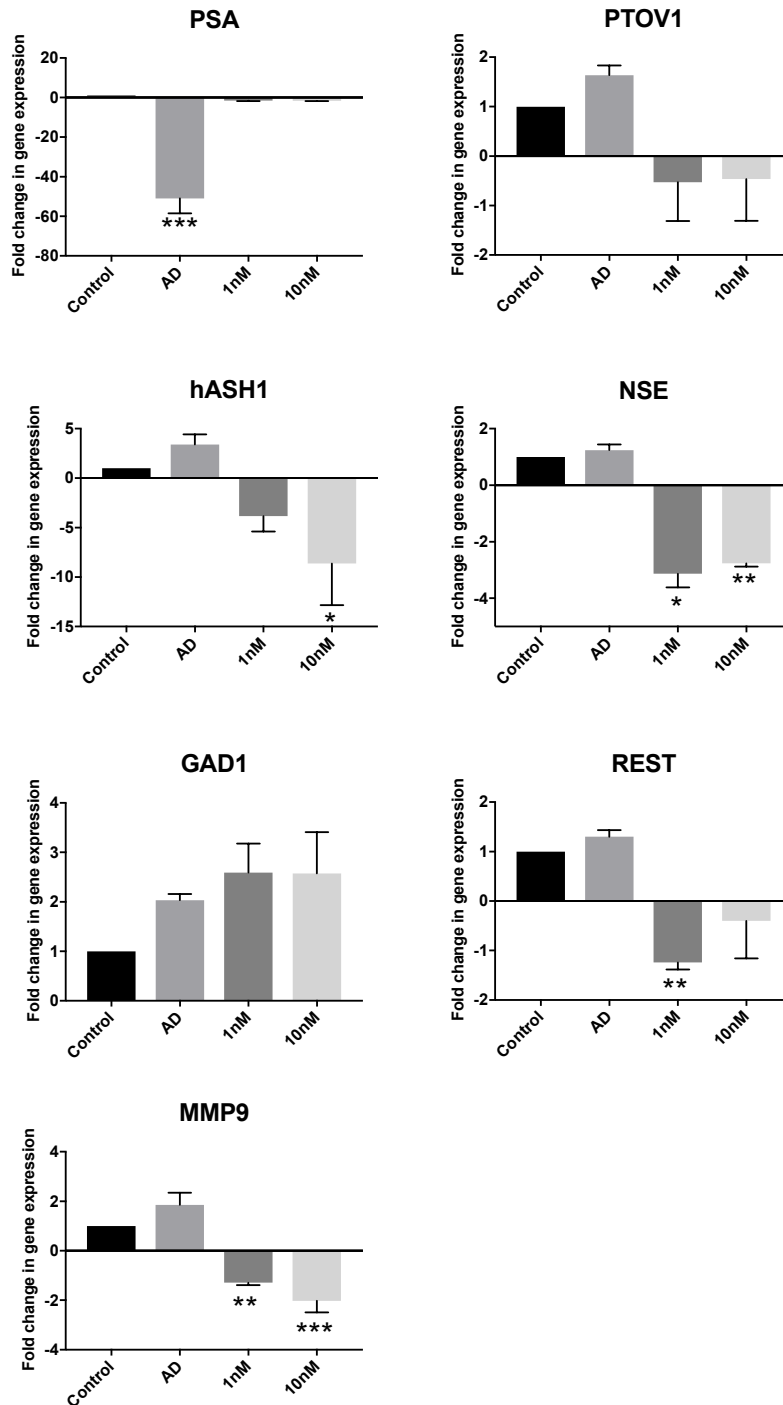


Figure 3.17. Androgen supplementation prevents activation of the canonical neurogenesis pathway. A. Relative expression of PSA, PTOV1, hASH1, NSE, REST, GAD1 and MMP-9 was analysed in LNCaP cells before and after 15 d of culture in control, androgen deprived or androgen deprived supplemented with 1nM or 10nM R1881 conditions via qRT-PCR. Data is expressed as mean \pm SEM where $n=3$ $p < 0.05$ (*), $p < 0.01$ (**) and $p < 0.001$ (***).

3.2.5.5 Protein expression in response to androgen deprivation

Expression analysis of key proteins was performed using immunoblot. Analysis determined that AR expression remained stable between untreated, AD, vehicle and 1 nM R1881 treatment at 15 d (Fig. 3.18B). However, PSA expression was undetectable after 15 d AD, whereas PSA expression was robustly maintained in LNCaP cells treated with 1 nM R1881. These results support the gene expression data generated via qRT-PCR analysis (Fig. 3.17) and further validate the model of AD used in this study and that PSA is a reliable indicator of androgen signalling activity.

Protein expression of hASH1 was elevated by 10 d of AD and increased further by 15 d (Fig. 3.18A). Supplementation of charcoal-stripped media with 1 nM R1881 was not sufficient to prevent increased hASH1 expression. This suggests that a higher concentration of androgen may need to be maintained in order to prevent upregulation of hASH1, this data strongly supports the qRT-PCR data which demonstrated that hASH1 was only significantly downregulated when in the presence of 10 nM R1881 synthetic androgen.

NSE expression was detected at a low level in untreated cells and did not become considerably upregulated until 10 d of AD, becoming substantially higher at 15 d of culture. Up to 10 d the presence of 1 nM R1881 did not appear to prevent NSE upregulation. However, by 15 d of culture with 1 nM R1881, expression of neuronal marker NSE was undetected. This data suggests that expression of NSE is regulated by androgen signalling, evidenced by the data showing that when PSA is robustly detected, NSE is only expressed at a very low level. Whereas when PSA expression is lost, there is a dramatic increase in NSE expression (Fig. 3.18B).

Interestingly, whilst the data suggests that 1 nM R1881 prevents increased NSE expression, it does not downregulate expression of hASH1. Confocal analysis (Fig. 3.13) demonstrated that during AD the localisation of hASH1 changes from excluded from the nucleus to prevalent in the nucleus. In the context of the localisation data (Fig. 3.13), the data presented in Fig. 3.18 would suggest that it is the localisation of hASH1 which is significantly more important in the NED

process than its overall level of expression. Expression of PCa stem cell marker CD44 was not detectable in LNCaP cells throughout the NED process, whilst CD44 was robustly expressed by castrate-resistant cell line DU-145 (Fig. 3.18A).

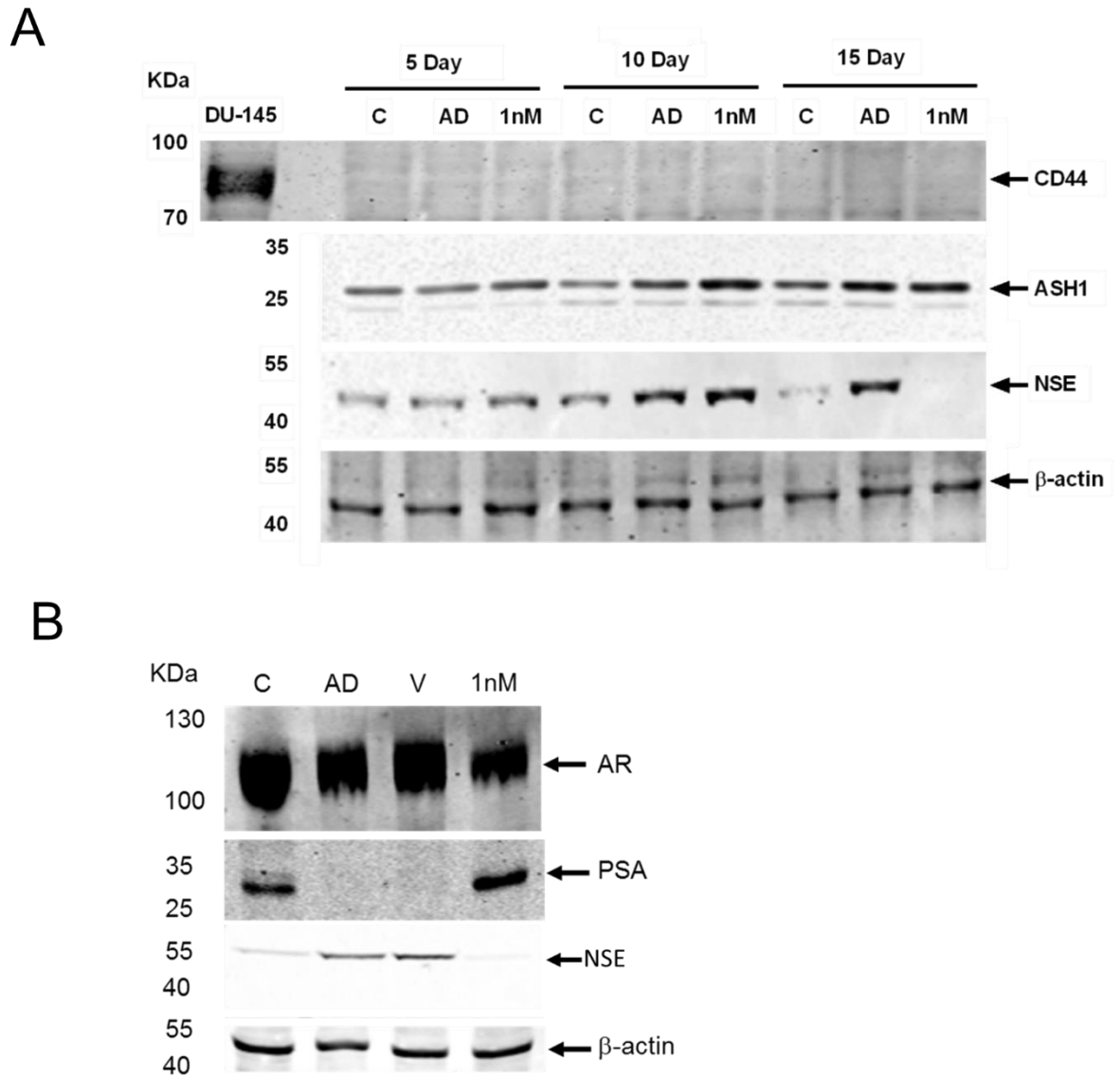


Figure 3.18. Androgen supplementation prevents activation of the canonical neurogenesis pathway. A. Representative immunoblot analysis of CD44, hASH1 and NSE in LNCaP cells at 5, 10 and 15 d of control, androgen deprived or androgen deprived supplemented with 1nM R1881 culture conditions. **B.** Representative immunoblot analysis of AR, PSA and NSE expression in LNCaP cells after 15 d of culture in control (C), androgen deprived (AD) or androgen deprived \pm 0.01% DMSO vehicle (V) or 1 nM R1881. Beta actin was used as a loading control.

3.2.6 Conclusions

A panel of the most frequently studied androgen-sensitive and castrate-resistant prostate cancer cell lines were thoroughly characterised at a molecular and cellular level (Figs. 3.2-3.7). The androgen-sensitive LNCaP cell line was used to establish a model of AD-induced NED (Fig. 3.8-3.10). This model was validated and used to investigate the hypothetical NED pathway proposed in this study (Fig. 3.11-3.18). In summary, AD induced NED in androgen-sensitive LNCaP cells. Addition of synthetic androgen to AD conditions confirmed that reduction of available androgen is a specific inducing stimulus of NED. AD-induced NED is associated with a neurite-like morphology, nuclear localisation of hASH1 and upregulation of NSE, alongside downregulation of PSA. All of these NED associated changes were prevented when AD conditions were supplemented with synthetic androgen. Therefore, this data shows that NED is specifically inducible by reduction of androgen and that canonical neurogenesis promoter hASH1 may be facilitating this phenotypic change (Figure 3.19).

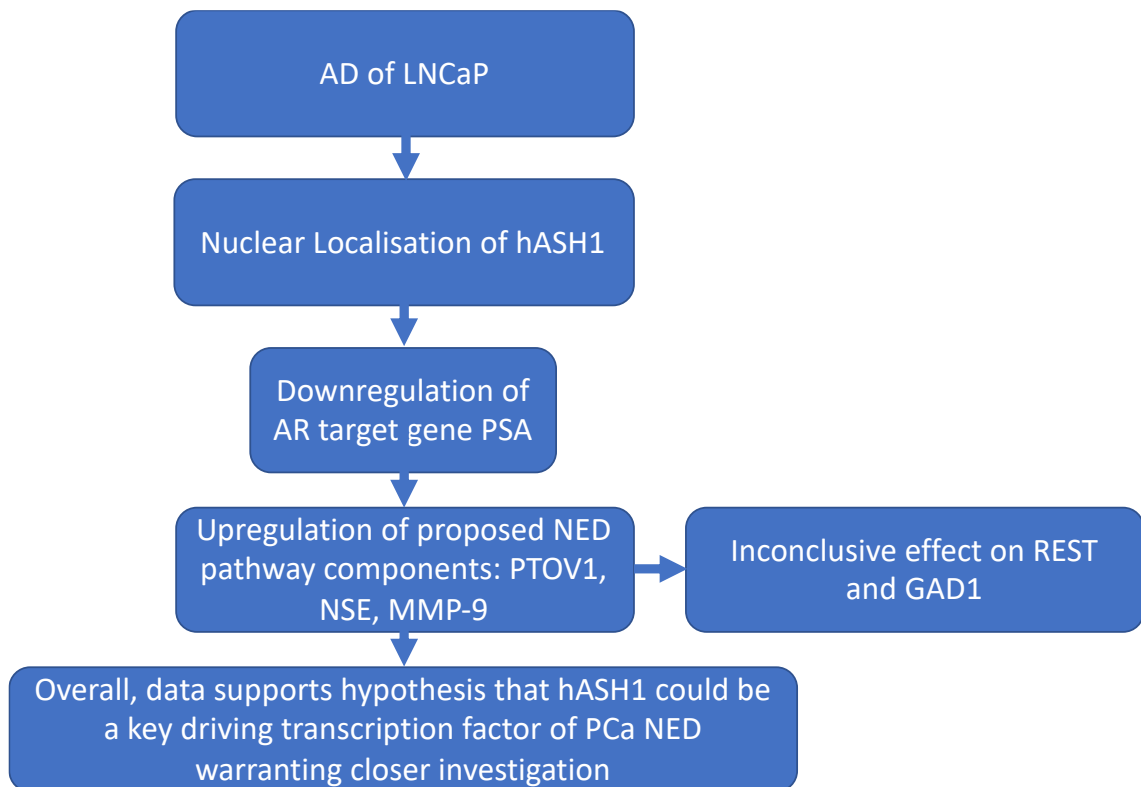


Figure 3.19. Schematic summary of chapter 3 results in relation to the proposed model of AD induced PCa NED.

These results, summarised in Figure 3.19, strongly support the proposed pathway of PCa NED initiation and maintenance and warrants further investigation, particularly whether the nuclear localisation of hASH1 and the concurrent development of the NED phenotype could be prevented or reversed.

3.3 Discussion

Escape from ADT and the progression of prostate cancer to CRPC remains one of the greatest challenges in the treatment and management of prostate cancer. Therefore, the development and study of models of ADT resistance are critical to illuminating the molecular drivers of the CRPC transition. Recent research has demonstrated that ADT resistance and NED not only remains a challenge, but that NED is becoming more frequent. A cohort study showed that the percentage of patients exhibiting NED more than doubled to 13.3% in the year 2012-2016, compared to 6.3% in 1998-2011 (Bluemn *et al.*, 2017). Critically, this increase in incidence of NED occurred after the implementation of current generation ADT drugs enzalutamide and abiraterone acetate, suggesting that the increased potency of androgen-blockade could be contributing to the development of NED (Bluemn *et al.*, 2017).

The aim of this study was to assess the basal characteristics of androgen-sensitive and castrate-resistant prostate cancer cell lines and to establish an *in vitro* model of AD induced NED. The first objectives using this model were to identify the molecular components of the NED pathway and to assess how neuronal-like these differentiated cells were. The next objective was to ascertain whether these molecular and phenotypic changes observed in the AD-induced NED model were specifically mediated by androgen availability.

3.3.1 Characterisation of prostate cancer cell lines

Validation of the prostate cancer cell lines used in this study was performed using morphological and molecular analysis to ensure that these cells were conforming to their known characteristics. The first step was to assess the expression of the AR and AR target gene PSA. As previously reported in the literature (Alimirah *et al.*, 2006), LNCaP cells displayed robust AR and PSA expression as assessed

by qRT-PCR and immunoblot, whilst CRPC cell lines DU-145 and PC-3 did not show detectable expression of AR or PSA (Fig. 3.2).

Quantitative scratch assays (Fig. 3.6) were used to assess the growth characteristics of LNCaP, DU-145 and PC-3 cells. Consistent with previous literature, CRPC cell lines DU-145 and PC-3 displayed faster growth and more rapid wound closure than LNCaP cells (Alimirah *et al.*, 2006; Valero *et al.*, 2012). Overall, this initial assessment of these cell lines confirmed that their major characteristics conformed to those reported in the literature (Horoszewicz *et al.*, 1983; Kaighn *et al.*, 1979; Stone *et al.*, 1978). Future experiments to further assess the proliferative rate of these cell lines could be performed using incuCyte (Essen Biosciences, Germany) imaging to quantify confluence and cell number over time, or the use of fluorometric assays such as MTT or Alamar blue which assess cellular respiration to indicate proliferation.

Availability of PCa cell lines faithful to the clinical presentation of the disease are widely regarded to be lacking in the field of PCa research. Although LNCaP cells were isolated from a patient after ADT relapse, LNCaP is androgen-sensitive and although AD does not result in mass LNCaP cell death, it greatly slows their growth rate compared to CRPC cell lines like DU-145 and PC-3 which are known to be unaffected and androgen-independent (Horoszewicz *et al.*, 1983; Kaighn *et al.*, 1979; Stone *et al.*, 1978).

For this study, DU-145 and PC-3 were gifts and funding was only available for one additional cell line. Given that LNCaP cells have been used previously as models of PCa NED (Rapa *et al.*, 2013; Farach *et al.*, 2016), LNCaP cells were the clear choice for this study. Criticisms of DU-145 and PC-3 are that they do not express AR or PSA, however these cell lines continue to be widely used in the field as androgen-independent models of CRPC.

Alternative options to DU-145 and PC-3 are CWR22Rv1 and VCaP cell lines. VCaP has been previously grown in mice and is contaminated with the Bxv-1 retrovirus. VCaP cells also have extremely slow growth rate making them less practical to work with than DU-145 and PC-3, they also grow in colonies which

makes them unsuitable for scratch assays (Korenchuk *et al.*, 2001; Knouf *et al.*, 2009; Sfanos *et al.*, 2011).

CWR22Rv1 is an increasingly popular cell line model of CRPC, however CWR22Rv1 is known to be castrate resistant through expression of AR-V7 which is not a mechanism that we wished to focus on in this study. This study aimed to investigate androgen receptor independent mechanisms of castrate-resistance, therefore DU-145 and PC-3 are appropriate models as they do not express AR or PSA and are unaffected by AD (Sramkoski *et al.*, 1999; Knouf *et al.*, 2009).

3.3.2 Androgen receptor signalling in androgen-sensitive and CRPC cell lines.

LNCaP cells are described as androgen-sensitive and express AR and PSA robustly (Wu *et al.*, 2014). When discussing the androgen receptor signalling status of CRPC cell lines DU-145 and PC-3, it must be considered that whilst these cells are AR negative, the majority of CRPC tumours are AR positive (Shukla *et al.*, 2017). This distinction is important because AR positive CRPC tumours do not rely on androgens but they do retain the AR signalling transcriptome through other mechanisms (Jones *et al.*, 2015; Kong *et al.*, 2015). Therefore, the majority of CRPC tumours are androgen-independent but certainly not AR-independent as they rely on mechanisms to reactivate AR signalling during ADT (Shukla *et al.*, 2017). Nonetheless, DU-145 and PC-3 remain the most frequently used *in vitro* models of CRPC. Androgen-pathway independent prostate cancers are known to exist and occur relatively frequently clinically, despite AR positive CRPC tumours comprising the majority of cases (Bluemn *et al.*, 2017). Another study found that DU-145 and PC-3 cells express AR but only at a very low level (Alimirah *et al.*, 2006), which is likely why it was not detected in this study or the vast majority of the published literature using these cell lines (Alimirah *et al.*, 2006; Yadav *et al.*, 2017). The PSA encoding gene, *KLK3*, contains androgen response elements and can therefore be a useful indicator of intact, canonical AR signalling (Luke and Coffey, 1994).

3.3.3 Advantages and disadvantages of different Androgen-deprivation simulation methods

Charles Huggins discovered that prostate cancer could be modulated by hormones as early as 1941 (Huggins, 1941). It is therefore unsurprising that there have been a wealth of studies utilising hormone modulation as a method of investigating the mechanistic biology of prostate cancer, both *in vivo* and *in vitro*. Despite a broad array of published literature, there remains several different approaches to simulating ADT, not least because approaches to ADT itself have changed drastically over the last 75 years, with new anti-androgens, combination therapies and treatment strategies continuing to be developed (Ryan *et al.*, 2015; Beltran *et al.*, 2011; Satoh *et al.*, 2014).

There are several models for inducing NED via AD in PCa, including serum reduction, charcoal stripping of serum and direct use of ADT therapeutics. The most commonly used model of AD (and the one used for this study) is to use charcoal-stripped FBS in cell culture media in order to reduce testosterone and dihydrotestosterone in the media (Rapa *et al.*, 2013; Shen *et al.*, 1997). Although charcoal-stripping FBS is not specific to removing only androgens, use of DHT or synthetic androgens such as R1881 can be used to confirm whether changes resulting from culture in CS-FBS are androgen mediated (Svensson *et al.*, 2014). The effects of charcoal-stripping on FBS has previously been investigated and found to effect hormones and vitamins; cortisol, oestradiol, folic acid, thyroxine, progesterone, triiodothyronine, vitamin B₁₂ and testosterone (Cao *et al.*, 2009). The reduction in androgen concentration from charcoal-stripping FBS was found to be 86% (Cao *et al.*, 2009).

An alternative approach that has not been reported in the literature, which could further enhance the charcoal-stripping method, would be to determine the depletion of non-androgen hormones via ELISA or mass-spectrometry approaches. The non-androgen components reduced by charcoal-stripping could then be manually replaced to match the concentration in non-charcoal stripped FBS of the same batch. This method could provide a refinement to the charcoal-stripping methodology widely used in the field of hormone-related cancer

research. However, it is also likely to be considerably more expensive than the standard charcoal-stripping approaches used in this study.

Clinically, successful application of ADT is regarded as a target serum androgen concentration <500 ng/L (173 pM) and after orchiectomy <200 ng/L (69 pM) (Bertaglia *et al.*, 2013; Mottet *et al.*, 2011). However, the latest ADT regimens utilising abiraterone acetate and/or enzalutamide are able to consistently achieve serum testosterone levels <50 ng/L (Breul *et al.*, 2017; Hashimoto *et al.*, 2017). The level of serum testosterone found in FBS and CS-FBS was previously determined as 22 ng/L and 5 ng/L respectively (76.3 pM and 17.3 pM) (Sedelaar & Isaacs, 2009) which is consistent with the 86% reduction reported in a separate study (Cao *et al.* 2009).

It is an important consideration that serum androgen concentration of prostate cancer patients is not likely to be representative of the level of androgen localised within the tumour mass or metastases. Due to variation in vascularisation, access to serum androgen is likely to differ within the tumour micro-environment. It is also of note that NED has also been demonstrated through hypoxia (Danza *et al.*, 2012) and serum starvation (Farach *et al.*, 2016). Therefore, it would be expected that areas of the tumour micro-environment that are poorly vascularised would produce a strong selective pressure towards the NE phenotype as these areas would have poorest access to oxygen and serum androgen.

An alternative AD simulation method is to reduce the amount of FBS used in the media to also reduce concentration of androgens. The problem with this serum starvation approach is that it is the most non-specific method for removing androgens from the media and is likely to induce an array of cell stress responses that are non-specific to AD. In some cases, partial serum starvation is used in combination with charcoal-stripped FBS (Belandia *et al.*, 2005; Svensson *et al.*, 2014), however this approach makes it difficult to delineate whether observed effects were due to specific AD or serum starvation. Finally, several studies have directly utilised pharmacological methods of AD using anti-androgens such as enzalutamide directly (Svensson *et al.*, 2014). Importantly, each of these models

has been reported to induce differentiation of LNCaP cells *in vitro*, despite the differences and limitations of each approach.

Although charcoal-stripping of FBS is non-specific to androgen, critically, it has a higher degree of specificity than the serum starvation technique utilised by (Farach *et al.*, 2016) and others. The rationale for not using ADT pharmaceuticals directly is as follows; **(1)** LHRH agonists and antagonists target T and DHT production, which is not a consideration *in vitro*. **(2)** antiandrogens such as enzalutamide, flutamide and bicalutamide target the AR, however, AR mutations and differing expression of AR splice variants can alter the efficacy of these compounds or lead to off-target effects (Bassetto *et al.*, 2016; Scher & Kelly, 1993). **(3)** Calculating suitable working concentrations of these drugs would likely be non-representative of that of the *in vivo* environment, mainly due to differences in bioavailability of both the compound and serum androgens. Using ADT drugs at too high concentration may have resulted in a greatly exaggerated effect on NED. **(4)** Using serum starvation would likely have activated autophagy pathways which would have dramatically altered the cellular metabolism and have had genome wide effects not directly associated with NED (Adachi, Koizumi, & Ohsumi, 2017). **(5)** Using the well-established CS-FBS model allows for this project to be taken in context of previous similar studies and aids elucidation of the NED process through consistency.

3.3.4 Neuroendocrine gene expression signatures of prostate cancer cells

As an initial investigation of the proposed NED pathway, the expression of REST, clinical NED biomarker NSE and GABA synthesis enzyme GAD1 was analysed. CRPC cell line DU-145 showed a significantly higher expression of NSE (38-fold), and REST (3-fold) and GAD1 was also upregulated although not significantly (10-fold) compared to LNCaP cells (Fig. 3.4). Although it would be expected that higher NSE expression should be concurrent with lower REST expression, the REST protein is known to be regulated post-transcriptionally via ubiquitin ligase beta-TrCP (Guardavaccaro *et al.*, 2008). PC-3 cells also displayed much higher NSE expression (14-fold) than LNCaP cells, whilst expression of GAD1 and REST were similar to LNCaP cells (0.75-fold and 1.13-fold respectively). These

findings demonstrate that CRPC cells may possess increased NED compared to androgen-sensitive PCa cell line LNCaP.

3.3.5 Androgen-deprivation triggers neuronal-like morphological changes in androgen-sensitive LNCaP prostate cancer cells

The phenomenon of AD inducing morphological changes in LNCaP cells has been observed previously (Shen *et al.*, 1997). However, the extent to which these cells mimic neurons or NE cells at a molecular level has not yet been fully elucidated. It has previously been demonstrated that in response to AD, LNCaP cells acquire neuronal-like morphology and increased expression of NSE, which was reversed when cultured in complete media (Shen *et al.*, 1997). Research on PCa NED has focussed upon four main areas; the origin of these differentiated cells and the molecular pathways of differentiation (Rapa *et al.*, 2008, 2013; Sauer *et al.*, 2006), the extent to which these cells are NE or neuronal in phenotype (Grigore *et al.*, 2015; Farach *et al.*, 2016), how these cells may be resistant to treatment (Hu *et al.*, 2015) and the advantages these cells may grant to surrounding cancer cells (Ippolito *et al.*, 2006; Ippolito & Piwnicka-Worms, 2014; Komiya *et al.*, 2009; Wu *et al.*, 2014).

In this study, AD LNCaP cells gained long neurite-like extensions (Fig. 3.8) similar to those previously reported in the literature (Shen *et al.*, 1997). At 5 d short projections were observed, at 10 d these projections became more pronounced and by 15 d neurites had become long and well-developed with many cells connected physically by these projections. Using confocal microscopy to image large regions of microscope slides containing untreated and AD LNCaP cells it was possible to visualise and quantify the length of these neuronal-like projections. The cells which appeared to differentiate most clearly under AD were on the edges of colonies of cells and those in lower density areas. Often, images showed that two or more distant cells had become interconnected by these neurite-like extensions. This suggests that there may be some mechanism of chemotaxis encouraging these projections to extend towards nearby cells, although this was not investigated in this study. Growth of neurites has previously been described as a non-random process with different neurite branching patterns observed uniquely between different neuron types within the central

nervous system (Wong & Ghosh, 2002). It is unclear what, if any, methods of intracellular communication these neurite-like projections might provide. Having established a model of AD-induced NED which produced a morphology similar to that previously reported in the literature (Hu, Choo, & Huang, 2015; Lin *et al.*, 2016; Rapa *et al.*, 2013), the next aim was to investigate the molecular pathways facilitating this phenotypic shift.

3.3.6 Molecular characterisation reveals neuronal-like signature of androgen deprived LNCaP cells.

To assess the underpinning pathway of NED of LNCaP cells in response to AD, the involvement of the androgen axis and the components of the proposed NED pathway were characterised. AR and PSA expression was assessed to validate that culture in CS-FBS conditions reduced AR signalling. PTOV1 is highly prevalent oncogene in prostate cancer development and has been previously demonstrated to be a powerful antagonist of Notch1 signalling (Alaña *et al.*, 2014) which in turn is known to upregulate hASH1 degradation (Sriuranpong *et al.*, 2002). Therefore, PTOV1 expression may be a core pre-requisite of the proposed pathway of NED.

Analysis of PSA expression at 5 d of AD showed a decrease in mRNA expression and continued to decline at 15 d (Fig. 3.12). Analysis of PSA by immunoblot demonstrated a similar trend in protein expression (Fig. 3.13). Given the stable AR expression demonstrated throughout the AD treatment, the sharp reduction in PSA expression indicates that there has been a reduction in AR signalling caused by a lack of available androgen in the cell culture media. Taken together, these data indicate that the CS-FBS culture conditions model for AD simulation are working as intended and in accordance with previous studies using this model.

In keeping with the proposed pathway of NED, PTOV1, hASH1 and NSE were significantly upregulated by AD (Fig. 3.11). This data supports the analysis performed on hASH1 and NSE expression by confocal microscopy (Fig. 3.13) where strong upregulation was observed in addition to hASH1 nuclear localisation. This is an indication that the canonical neurogenesis pathway may

have been activated by AD via disruption of Notch1 signalling by increased PTOV1 expression. This suggestion is supported by previous studies which have demonstrated PTOV1 inhibition of Notch1 signalling (Alaña *et al.*, 2014).

3.3.7 Morphological changes are associated with hASH1 nuclear localisation and activation of canonical neurogenesis pathway.

Previous studies have investigated Notch1 signalling not only in relation to neurogenesis, but in the wider context of cancer progression in multiple different cancer types (Axelson, 2004; Capaccione & Pine, 2013; Danza *et al.*, 2012; Orr *et al.*, 2009; Pedrosa *et al.*, 2015; Ristorcelli *et al.*, 2009). Notch1 signalling is a vital component in the determination and maintenance of cell fate (Lai, 2004), therefore, a reduction in Notch1 expression or signalling could lead to aberrant cell differentiation and transdifferentiation (Danza *et al.*, 2012). Notch1 signalling has been implicated in hypoxia-induced PCa NED (Danza *et al.*, 2012). In response to hypoxia, LNCaP cells showed decreased expression of Notch1 which resulted in lowered expression of Hes1 and Hey1 (Danza *et al.*, 2012). One previously discovered mechanism of Notch1 signalling disruption is transduction of protein prostate tumour overexpressed-1 (PTOV1), which was demonstrated to downregulate Notch1 targets Hes1 and Hey1 by occupying their promoter regions, thus blocking transcriptional activity of Notch1 (Alaña *et al.*, 2014).

Interestingly, Notch1 signalling is known to cause rapid degradation of hASH1 (Sriuranpong *et al.*, 2002). In addition, hASH1 has previously been demonstrated to be correlated with in PCa tumours with NED and tumours treated with ADT (Rapa *et al.*, 2008). Furthermore, transduction of hASH1 in LNCaP cells induced NED morphology and expression of NED markers chromogranin A and synaptophysin (Rapa *et al.*, 2013). The present study builds upon these findings and provides a more complete molecular analysis of involvement of hASH1 in the process of NED. The first step in achieving this was the assessment of hASH1 protein expression and localisation during the differentiation process via confocal microscopy.

The data shows, for the first time, that untreated LNCaP cells possess low-level basal expression of hASH1 protein that is rigorously excluded from the nucleus

(Fig. 3.13). After AD, expression of hASH1 increases and confocal microscopy demonstrated that hASH1 became localised to both the nucleus and cytoplasm of LNCaP cells. In addition, expression of neuronal marker NSE dramatically changed from low and punctate to robust and perfuse throughout the cell body and neurite-like extensions concurrent with hASH1 nuclear localisation (Fig. 3.13). These findings suggest that hASH1 nuclear localisation may be a key trigger of neuronal-like phenotype acquisition. Interestingly, hASH1 has previously been postulated as a potential therapeutic target in small cell lung cancer, which also possesses NE-like features (Castro *et al.*, 2011; Meder *et al.*, 2016; Osada *et al.*, 2005). Prompting further investigation into the role of hASH1 and the potential to for hASH1 nuclear localisation to be reversed.

3.3.8 Neuronal-like molecular profile is suppressed by androgen receptor signalling.

Having demonstrated the effects of AD in inducing neuronal differentiation of LNCaP cells *in vitro*, the next step was to demonstrate that this effect was indeed specific to AR signalling and not mediated by any other factor removed through the charcoal-stripping of FBS in the media. R1881 in AD media maintained expression of PSA at basal levels and PTOV1 expression was reduced to below basal level by treatment with R1881 (Fig. 3.17). Previously it has been reported that PTOV1 is androgen inducible in human aorta and is necessary for the androgen mediated proliferation of aorta tissue (Nakamura *et al.*, 2006). PTOV1 is also known to contain an androgen responsive element (Benedit *et al.*, 2001; Cánovas *et al.*, 2015). This study is the first to directly investigate PTOV1 expression in response to AD in LNCaP prostate cancer cells. This data demonstrates that PTOV1 expression is upregulated by AD and reduced below basal levels by R1881 (Fig. 3.17). PTOV1 is typically regarded as an androgen inducible gene (Nakamura *et al.*, 2006), the increase in PTOV1 expression in response to AD and the decrease in the presence of R1881 may indicate that mechanisms regulating PTOV1 expression have become distorted in the setting of prostate cancer.

This increase in expression of hASH1 by AD was prevented and reduced to below untreated levels by R1881 (Fig. 3.17). However, increased expression of hASH1

protein did not appear to be prevented by R1881 (Fig. 3.18). This data posed the question that if 1 nM R1881 was able to prevent morphological change but did not downregulate hASH1 expression, perhaps it is localisation of hASH1 to the cell nucleus which is the critical factor instigating morphological change and not expression level alone, since only nuclear hASH1 will be transcriptionally relevant. siRNA knockdown of hASH1 expression previously prevented expression of NE biomarkers synaptophysin and chromogranin A after 15 d of AD (Rapa *et al.*, 2013). Significant downregulation of NSE was observed in LNCaP cells cultured in the presence of R1881. Downregulation of PTOV1, hASH1 and NSE by R1881 treatment indicates that three critical components of the proposed pathway of neurogenesis and NED of prostate cancer are mediated by AD primarily, rather than any other serum component which may have been altered by charcoal-stripping the FBS.

Potential repressors of neurogenesis were also assessed in order to assess whether a reduction in their expression may be associated with AD and therefore facilitating increased neurogenesis and NED. Expression of REST was slightly increased by AD and was decreased in the presence of R1881. This data suggests that REST is constitutively expressed by LNCaP cells in order to prevent aberrant differentiation, yet is unable to prevent differentiation of LNCaP cells under AD conditions. It is possible that degradation of the REST protein, which is mediated via ubiquitin ligase beta-TrCP (Guardavaccaro *et al.*, 2008), may be increased under AD conditions. REST acts as a controller of neurogenesis by preventing transcription of neuronal genes such as synaptophysin in non-neuronal tissues (Lapuk *et al.*, 2012) and has been identified as a tumour suppressor (Westbrook *et al.*, 2005). In this study, LNCaP, and PC-3 cells showed similar expression of REST but DU-145 showed significantly higher levels (Fig. 3.4). NSE was significantly higher in CRPC cell lines and AD LNCaP cells. Mutation and silencing of REST is a common feature in colorectal cancer (Westbrook *et al.*, 2005). However, the data supports the finding of Lin *et al.*, (2016) who demonstrated that REST gene expression is unaffected during NED but that REST protein expression reduction is essential to the hypoxia induced NED process (Lin *et al.*, 2016). This is consistent between two very different methods of NED induction, AD and hypoxia.

Having established that hASH1 nuclear localisation is concurrent with acquisition of NED phenotype in AD LNCaP cells, alongside the prior knowledge that hASH1 is able to promote development of GABAergic neurons (Castro *et al.*, 2011), the GABA synthesis potential of these cells was investigated. Gene expression of GAD1 was found to be slightly upregulated by AD, however, expression was not downregulated in the presence of R1881. This finding suggests that GAD1 upregulation may not be mediated specifically by AD but by other factors associated with charcoal-stripping the FBS.

Expression of MMP-9 has previously been demonstrated to be induced by GABA signalling in prostate cancer (Azuma *et al.*, 2003) and so therefore MMP-9 expression was assessed in response to AD as a potential indicator of GABA signalling. The data shows that MMP-9 expression was upregulated by AD and significantly downregulated in the presence of R1881. LNCaP cells were also found to lack detectable expression of CD44, a PCa stem cell marker (Patrawala *et al.*, 2006; Tu & Lin, 2012; Zhang & Waxman, 2010). Although no conclusive statements can be made from this analysis, this data would appear to suggest that LNCaP cells are not particularly 'stem-like' and nor do they become 'stem-like' during differentiation to the neuronal phenotype. This is supported by data demonstrating that NED LNCaP cells arise from transdifferentiation from epithelial phenotype cells (Sauer *et al.*, 2006).

3.3.9 Neuronal-like morphological changes are prevented and reversed by androgen receptor signalling.

LNCaP cells which retained expression of PSA and therefore AR signalling, were prevented from undergoing morphological change and did not grow neurite-like extensions. This demonstrates that the AR is the critical mediator of morphological changes associated with culture in charcoal-stripped media. Acquisition of the neuronal-like phenotype can be avoided when a low level of androgen signalling is maintained. These findings are potentially of interest clinically, where the assumption that maximal androgen blockade as an optimal treatment goal may be significantly flawed and overly simplistic in approach.

3.3.10 Disruption of Notch1 signalling may promote aberrant cell fates

Notch1 is critical to regulation of prostate development and is also expressed in progenitor cells of the prostate basal membrane where it regulates cell differentiation (Belandia *et al.*, 2005). Notch signalling is a vital component of cell fate determination and its repression may result in differentiated prostate cells being more malleable and plastic in their phenotype and thus more responsive to changing conditions. Notch1 negatively regulates hASH1 via upregulation of bHLH transcriptional repressor genes *Hes1* (Paquette, Perez, & Anderson, 2000) and *Hey1* (Axelson, 2004; Ishibashi *et al.*, 1995). Prostate tumour over-expressed 1 (PTOV1) acts as a negative regulator of Notch1 signalling by interacting with the Notch repressor complex (Alaña *et al.*, 2014). It has previously been demonstrated that Notch1 signalling is downregulated in hypoxic conditions and associated with increased expression of NED markers (Danza *et al.*, 2012). Downregulation of Notch1 signalling could potentially allow for increased hASH1 expression (Danza *et al.*, 2012), which could promote NED. AD has been demonstrated to increase expression of hASH1 and is associated with NED in PCa (Rapa *et al.*, 2008). Overall, the data presented in this study would suggest that prostate cancer cells likely have multiple transcriptional profiles that are repressed by AR signalling. However, under the conditions of ADT the pressure of the AR on cell fate is greatly reduced, allowing for aberrant transcriptional signatures to become 'de-repressed' (Bishop *et al.*, 2017; Bishop *et al.*, 2015) and making the determination of cell-fate a more fluid and malleable dynamic that is better able to conform to the conditions of the microenvironment. Research has also demonstrated that activation of a gastrointestinal transcriptome gave rise to a castrate-resistant phenotype in prostate cancer cells (Shukla *et al.*, 2017), suggesting that utilisation of aberrant transcriptional profiles is an effective ADT resistance mechanism in PCa.

3.3.11 hASH1 as a therapeutic target

Whilst transcription factors are often considered to be intractable drug targets, their upstream interactors are often druggable and can provide the desired attenuation of the transcription factors activity (Johnston & Carroll, 2015). ADT has remained the first line treatment for advanced prostate cancer for over half a century, becoming increasingly more refined and potent with successive

generations of drugs, yet the problem of ADT escape through NED is increasing. Therefore, research which could lead to adjuvant therapeutics alongside ADT to prevent NED is vitally important, as this could greatly extend the period of time in which ADT is able to restrict tumour growth. The research undertaken in this study has helped to illuminate one mechanism of ADT induced NED (hASH1 nuclear localisation) in an *in vitro* LNCaP model. However, further research is greatly required to demonstrate that hASH1 could be a viable therapeutic target. Previously hASH1 has been touted as a therapeutic target for small cell lung cancer (Osada *et al.*, 2005) as well as maintenance of REST expression, which could obviate the activity of hASH1 in response to ADT (Chang *et al.*, 2017). IN order to further confirm that nuclear hASH1 in NED PCa is both bound to chromatin and transcriptionally active, it will be important to conduct further experiments. These would include chromatin fraction western blots, which would confirm the presence of hASH1 on chromatin. ChIP-Seq or ChIP-qPCR experiments to identify the likely target genes of hASH1 in AD conditions and ideally RNA-Seq, which could be integrated with ChIP-Seq data to support the hypothesis that hASH1 is transcriptionally active in NED PCa cells.

3.4 Conclusions

The aim to develop and characterise of a model of AD induced NED using the androgen-sensitive prostate cancer cell line LNCaP has been completed. Key molecular components of the AD induced NED pathway such as hASH1, PTOV1, and REST have also been investigated at a molecular level. Confocal microscopy analysis demonstrated that transcription factor hASH1 is excluded from the nucleus in untreated LNCaP cells but localises to the nucleus after AD. Bright-field microscopy demonstrated that alongside this change in hASH1 localisation, LNCaP cells also develop a neuronal-like morphology, the extent of which has been quantified using confocal microscopy to measure the length of neurite-like extensions.

Analysis of gene and protein expression during the course of AD induced NED also largely supported the hypothesis that PTOV1 and REST may be important facilitators and regulators of the activation of neuronal-like differentiation programs in LNCaP cells respectively. The ability of low concentrations of

synthetic androgen to prevent the NED process was also demonstrated, highlighting a key finding that hASH1 upregulation is insufficient to cause NSE upregulation without nuclear localisation of hASH1, potentially identifying hASH1 as a candidate protein for further investigation, either as a biomarker of early (pre-NSE upregulation) NED or as a therapeutic target.

3.5 Limitations, weaknesses and future experiments

As the majority of work in this chapter served to characterise the three PCa cell lines and the AD LNCaP based model of PCa NED, much of the results are not novel. However, this robust characterisation was necessary in order to study the proposed NED pathway and to provide a robust understanding of how these cell lines behaved in an untreated state. In terms of the scratch assays performed, it is important to consider that these assays are only a very simplistic method of assessing growth and the invasive and metastatic potential of cell lines. For example, as cells are confluent when the scratch is made, the speed at which they close the wound is likely to be different to when cells are still in the exponential phase of growth. Therefore, growth rate would have been better assessed by measuring cell number over time via methods such as IncuCyte. Secondly, scratch assays are only a basic indicator of invasive potential, to properly assess invasion, transwell culture plates coated with Matrigel or collagen could have been used as these assays more closely represent the process of invasion. Finally, when assessing migration via scratch assay it is important to consider that to properly delineate migration activity from growth, it would be ideal to employ a real time image capture system (such as Incucyte) and to track and quantify individual migrating cells via software analysis (Liang, Park & Guan, 2007). Furthermore, using the scratch assay, even when performing multiple careful washes after the scratch is made, it is inevitable that some free-floating cells will remain which could mistakenly be identified as migrating cells at early timepoints. Overall, migration as assessed by scratch assay is a qualitative measure, that could be adapted to a quantitative analysis (either via software, or using a GFP reporter tag on EMT related genes such as N-cadherin) (Liang, Park & Guan, 2007; Camand *et al.*, 2012). However, in most cases, a transwell assay

(without substrate) would be a preferable, yet more expensive, methodology for quantifying migration activity in vitro (Gianelli *et al.*, 1997; Justus *et al.*, 2014).

As discussed in section 3.3.3, the charcoal-stripped FBS method of AD has many inherent limitations, including the non-specificity to androgen and the fact that concentrations of androgen are likely to vary between lots of FBS and CS-FBS from suppliers. As the concentration of androgen in either the control or AD media were not empirically tested, i.e. via ELISA, the variability in androgen and other off-target effects of charcoal-stripping could not be assessed or accounted for. A potential improvement to the CS-FBS method would have been to individually re-supplement each component back to the concentrations found in standard FBS. In addition, only a small number of timepoints were assessed for gene and protein expression (5 and 15 d) in response to AD. This meant that perhaps the very early molecular changes associated with NED would not have been observed, further experiments to capture timepoints at 2, 4 and 6 h of AD treatment would likely add value and understanding to the molecular drivers of PCa NED.

4. Molecular reversibility of neuroendocrine differentiation in prostate cancer cells

4.1 Introduction

The role of NED cells within prostate tumours and metastases remains unclear and is an under-researched area of prostate cancer biology (Grigore *et al.*, 2015). However, NED has been shown to confer therapeutic resistance upon prostate cancer cells (Beltran *et al.*, 2016; Hu, Choo, & Huang, 2015; Karantanos, Corn, & Thompson, 2013; Zou *et al.*, 2017). A key aspect of NED prostate cancer cells is their very low proliferative capabilities compared to epithelial PCa cells (Danza *et al.*, 2012). This has led to speculation that forcing PCa cells towards NED could be a viable therapeutic option to slow the growth of tumours. However, a recent study showed that the pan-tyrosine kinase inhibitor Dovitinib induces NED in LNCaP cells and in PC-3 xenografts in mice (Yadav *et al.*, 2017). This study demonstrated that whilst dovitinib initially reduced tumour growth rate, after nine days PC-3 xenografts became dovitinib resistant. These resistant tumours displayed significantly increased growth rate and greatly upregulated expression of the NED biomarker NSE (Yadav *et al.*, 2017).

Usually in the cancer paradigm, the development of therapeutic resistance results in an increased growth rate, due to selection of cancer cells that proliferate best under the specific selection pressure of the therapeutics (Friedman, 2016). This poses the question as to why NED is associated with more advanced, more aggressive disease. One possible mechanism by which NED could support disease recurrence is if NED cells could act as a 'reservoir', similar to the cancer stem-cell reseeding paradigm, where resistant NED cells could transdifferentiate back into epithelial phenotype PCa cells (Shen *et al.*, 1997). Another possible mechanism could be that NED cells exert survival and growth promoting effects upon other cells within the tumour via paracrine signalling (Chang *et al.*, 2017). This chapter focuses on determining the effects of intermittent androgen deprivation (IAD) and discusses the potential clinical implications.

4.1.1 Clinical use of intermittent ADT

It is well established that PCa tumours treated with ADT often display increased NED (Shen *et al.*, 1997; Terry & Beltran, 2014). As such, intermittent (I)ADT has long been touted as a solution to delaying the development of CRPC in response to ADT (Feldman & Feldman, 2001). The intermittent use of radio and chemotherapeutics clinically is well accepted, primarily because poorly tolerated toxicity necessitates discontinuous use. Whereas, in the case of ADT, intermittent treatment is proposed to delay hormone therapy resistance, improve patient quality of life and reduce financial costs (Shore & Crawford, 2010). Indeed, Seruga *et al.* (2008) argue that IADT should be the standard of care for PCa (Seruga & Tannock, 2008). However, European Association of Urology guidelines continue to mandate that ADT be constant (i.e. no treatment holidays) and do not support the use of IADT clinically (Heidenreich *et al.*, 2014).

Early IADT trials focussed on the quality of life enhancements offered by IADT and were very favourable (Klotz *et al.*, 1986). Unfortunately, the small sample size (n=20) makes it impossible to draw accurate conclusions on overall survival or disease progression. Higher powered studies (n=3040 and n=1386) focussing on overall survival, found that IADT was at best non-inferior to constant ADT (cADT) or performed considerably worse than cADT (Crook *et al.*, 2012; Hussain *et al.*, 2013; Mottet *et al.*, 2012). One study used eight-month treatment cycles, with treatment holiday length determined by rising PSA level or disease progression (Crook *et al.*, 2012). Whereas, another study began with 6 months ADT, followed by 30 days on, then 30 days off therapy with PSA concentration 10 ng/mL or disease progression as a cut off to resume ADT (Mottet *et al.*, 2011). A lack of molecular stratification of tumours in these trials means that it is not possible to infer if IADT reduced NED or benefitted/harmed patients with high NED compared to cADT. This lack of stratification, to account for tumour heterogeneity, could also explain the inconclusive findings of IADT clinical trials to date (Hussain., 2017). Evidently, before more structured clinical trials can investigate the effects of IADT on NED, a greater understanding of the molecular drivers of NED is required.

4.1.2 Potential implications of NED reversibility

The implications of NED reversibility could be advantageous or detrimental to patient survival. NED is correlated with disease progression and poor prognosis (Hu *et al.*, 2015), therefore prevention of NED and mechanisms to target NED cells are considered desirable. In addition, NED can be induced by a variety of clinically used therapeutics, including ADT, radiotherapy and some chemotherapeutics such as docetaxel (Hu *et al.*, 2015). NED cells are also inherently resistant to these therapies (Hu *et al.*, 2015). The preferred chemotherapeutic option for NED PCa are platinum based therapeutics such as cisplatin (Vlachostergios & Papandreou, 2015). At first glance, if NED was a reversible process, these effects could be mitigated and potentially slow disease progression. However, considering the high therapeutic resistance of NED cells, reversibility to an epithelial phenotype could also become a method of tumour reseeding, similar to that of the cancer stem cell (CSC) niche paradigm (Fig. 4.1).

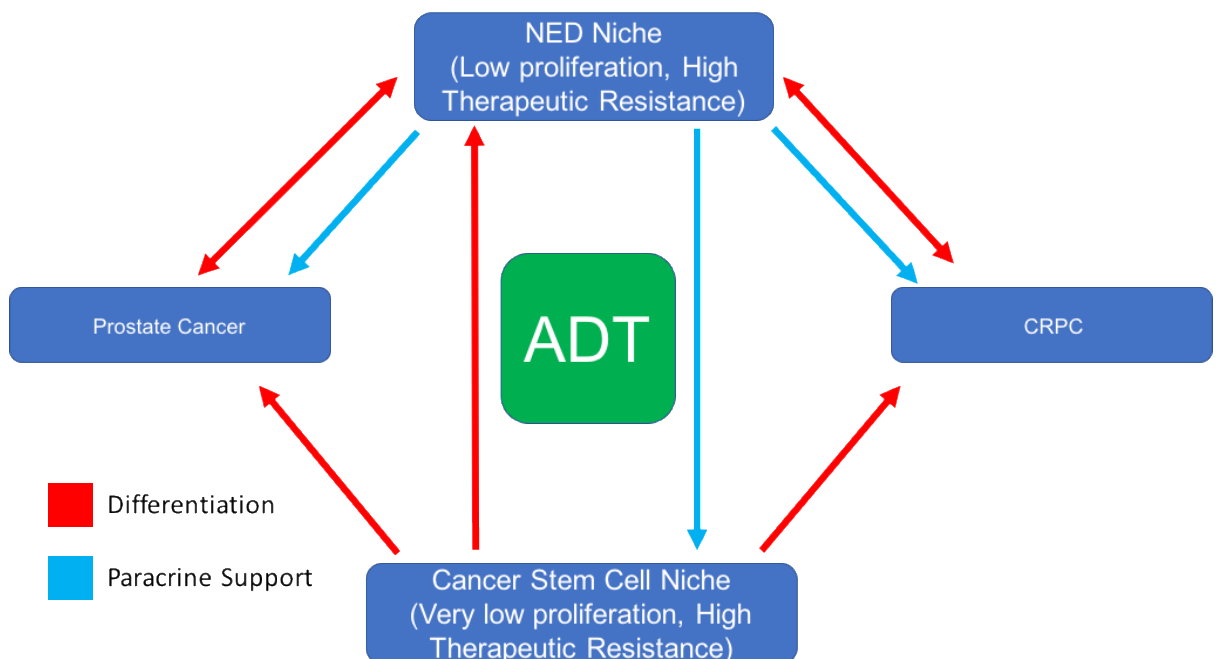


Figure 4.1 Schematic diagram depicting proposed interactions between neuroendocrine differentiation (NED) in prostate cancer cells and the tumour environment. ADT (androgen deprivation therapy), CRPC (castrate-resistant prostate cancer).

The CSC niche can contribute to disease recurrence and progression through classical tumour reseeding (Chang, 2016). The CSC niche has low proliferation and high therapeutic resistance, meaning that after the application of therapeutic regimens such as ADT, CSCs can remain (Lang *et al.*, 2009), these cells can then contribute to disease progression by repopulating the tumour with castrate-resistant or androgen-independent cells (Lang *et al.*, 2009). The less differentiated state of CSCs grants increased ability to adapt under the selective pressure of applied therapeutics (Chang, 2016; Lang *et al.*, 2009). It is a possibility that the NED niche may also be able to fulfil a similar role, by becoming treatment resistant (Hu *et al.*, 2015) and later transdifferentiating back into an epithelial PCa (Shen *et al.*, 1997) or castrate-resistant prostate cancer (CRPC) phenotype (Fig. 4.1). An example of a similar phenomenon would be breast cancer dormancy, where micro-metastases can remain hidden within the bone marrow niche, sometimes for decades, before disease recurrence (Price *et al.*, 2016). The NED niche may also influence the growth, survival and differentiation of surrounding tumour cells through paracrine support (Chang *et al.*, 2017). These paracrine secretions from the NED cell niche could also influence the differentiation of residual CSCs remaining after treatment along with NED cells, or provide mechanisms for PCa to become androgen-independent (Fig. 4.1).

4.1.3 Previous NED reversibility studies

The reversibility of the AD-induced NED phenotype was first investigated by Shen *et al.* (1997), who found that the NED morphology was reversed when NED LNCaP cells were returned to media containing 10% FBS. Interestingly, supplementation of AD culture conditions with 1 nM dihydrotestosterone (DHT) was insufficient to revert the NED morphology, but was sufficient to prevent its acquisition (Shen *et al.*, 1997). Remarkably, only two subsequent studies in the literature have since investigated the reversibility of the NED phenotype (Cox *et al.*, 1999; Deng *et al.*, 2008). An early study first identified that NED of LNCaP cells was inducible by cAMP and after withdrawal of the inducing cAMP, the NED phenotype was lost (Cox *et al.*, 1999). Interestingly, upon loss of the NED phenotype, activity of tyrosine kinase and MAPK proteins was increased and cells re-entered the cell cycle (Cox *et al.*, 1999). In addition, LNCaP growth was powerfully inhibited by cAMP and induced expression of NSE. Upon withdrawal

of cAMP, expression of NSE was reduced to basal levels. Thus, the NED phenotype induced by cAMP is reversible in terms of morphology and NSE expression (Cox *et al.*, 1999). The second NED reversibility study identified that the NED phenotype is also induced through irradiation (Deng *et al.*, 2008). Activation of cAMP response element-binding protein (CREB) and activating transcription factor 2 (ATF2) were sufficient to reverse radiation-induced NED (Deng *et al.*, 2008). This study aims to be the first investigation of the reversibility of the underpinning pathway facilitating AD induced NED, and to examine the effects of IADT on NED LNCaP cells.

4.1.4 Development of an IAD model

IADT was investigated using Charcoal stripped FCS to induce NED in LNCaP cells. In order to mimic treatment cessation periods, NED cells were supplemented with R1881 for 15 days before they were subjected to a second cycle of AD conditions via CS-FCS. For comparison, LNCaP cells were also maintained in complete media or AD media or AD media with DMSO vehicle for the entire 30 d period as a control (Fig. 4.2).

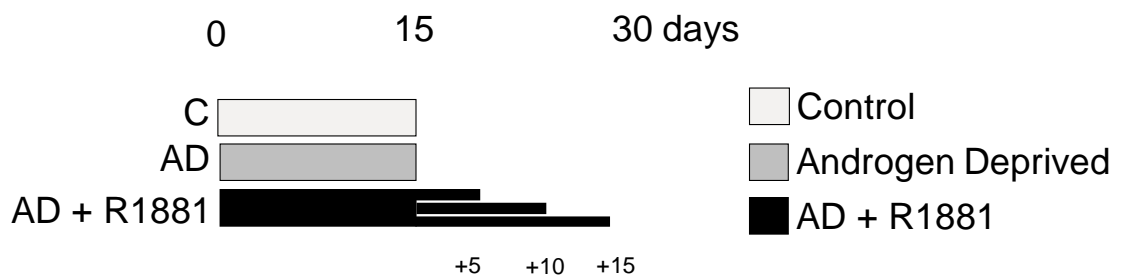


Figure 4.2, Schematic diagram detailing the experiment design for androgen deprivation cessation experiments. LNCaP cells were cultured in either control media (C) or androgen deprived media (AD) for 15 d. LNCaP cells were then either maintained for a further 5, 10 or 15 d in AD media supplemented with synthetic androgen (AD+R1881).

Importantly, this model uses treatment lengths which would be realistic to apply clinically (Mottet *et al.*, 2012) and also allows for substantial development of NED before AD cessation. A key difference between this model and any previously used model of NED reversibility is the use of synthetic androgen R1881. Whilst Shen *et al.*, 1997 supplemented cultures with DHT, R1881 is known to be more stable than DHT in cell culture media and is not metabolised (Bonne & Raynaud, 1976; Brown, Rothwell, & Migeon, 1981). Thus, the concentration of R1881 remains more consistent than when using endogenous DHT. Furthermore, this study aimed to specifically assess the effects of androgen re-introduction, which would not be possible using normal FBS as a source of androgens due to the many other hormones which would also be re-introduced.

4.1.5 Investigating the molecular and morphological reversibility of NED

Previous experiments demonstrated that a NED transcriptional profile and resulting phenotype can be specifically induced by AD (Chapter 3). This led to the investigation of whether reintroduction of androgen to NED cells could reverse the changes, at both a molecular and morphological level. This specific research question has high clinical relevance as the use of IADT has long been proposed by clinicians as a method of delaying the transition to CRPC (Oliver, *et al.*, 1997). Current European Association of Urology guidelines mandate that patients should continue to receive ADT even after the progression to CRPC (Heidenreich *et al.*, 2014). Therefore, studies providing data on the molecular response of androgen-sensitive PCa cells to successive cycles of ADT and the effects upon NED are of significant clinical relevance and interest. The reversibility of NED induced by AD has never been investigated in depth at a molecular level (Grigore, Ben-Jacob, & Farach-Carson, 2015; Hu, Choo, & Huang, 2015).

4.1.6 Study aim and research questions

Study aim: To establish an *in vitro* model of intermittent androgen deprivation and use this model to investigate the reversibility of NED and the phenotypic and molecular effects of a second cycle of AD on NED in LNCaP cells.

Research questions: **(1)** To what extent are the molecular (NSE expression and hASH1 nuclear localisation) and morphological (neurite-like extensions) changes associated with NED reversible? **(2)** How does intermittent AD effect the NED pathway?

4.2 Results

4.2.1 Reversibility of neuroendocrine morphology

The morphology of LNCaP cells was observed using light microscopy during AD and 5, 10 and 15 d after supplementation with R1881. During AD, LNCaP cells developed long neurite-like processes (Fig. 4.3 Panel ii). Interestingly, the majority of these neurite-like extensions appeared to have been lost after a further 15 d of culture in the presence of 1 nM R1881 synthetic androgen (Fig. 4.3 panel iii-v) and the cellular morphology closely resembled that of untreated LNCaP cells (Fig. 4.3 panel i).

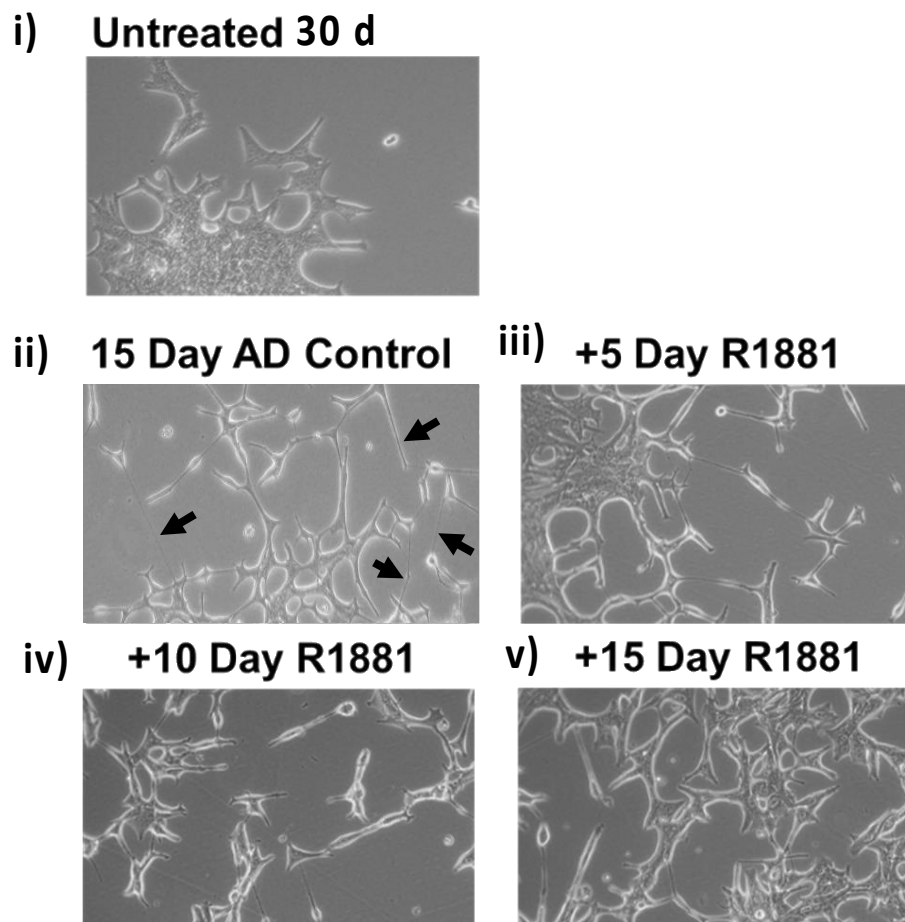


Figure 4.3. Reintroduction of androgen reverses neuroendocrine differentiation morphology. Representative bright field microscopy images of LNCaP cells which were untreated (i) for 30 d, androgen deprived (AD) for 15 d (ii) and then 15 d supplemented with 1 nM R1881 (iii, iv and v) (20 \times). Arrows indicate presence of neurite-like extensions.

The absence of neurite-like processes from NED LNCaP cells treated with synthetic androgen, suggests that NED is unlikely to be an immutable change and that these cells may retain androgen sensitivity. The implications of NED plasticity are multi-faceted; since NED cells have high therapeutic resistance, particularly to radiotherapy (Hu *et al.*, 2015), the reversal of NED could re-sensitise these cells to treatment. Conversely, the ability to revert from NED back to an epithelial phenotype could be a mechanism of post-treatment tumour reseeded (Shen *et al.*, 1997), a paradigm usually associated with the cancer stem-cell niche (Fig. 4.1). To better understand the nature and extent of NED reversibility, the molecular components underpinning NED were investigated.

4.2.2 Molecular reversibility of NED

Previous experiments demonstrated that AR expression remained stable throughout 15 d of AD (Chapter 3), by 30 d of AD, expression of AR was upregulated (Fig. 4.4). After reintroduction of synthetic androgen, AR expression was reduced compared to 30 d AD treated cells, but remained elevated compared to untreated LNCaP cells. Curiously, upon AD, an additional band with a MW of ~90 kDa was detected on the AR immunoblot, (Fig. 4.4) this could be an AR splice variant. Furthermore, upon reintroduction of R1881, the expression of this band was lost. Many AR splice variants are known to be ligand independent (see Appendix 1) (Dehm *et al.*, 2011; Jones *et al.*, 2015).

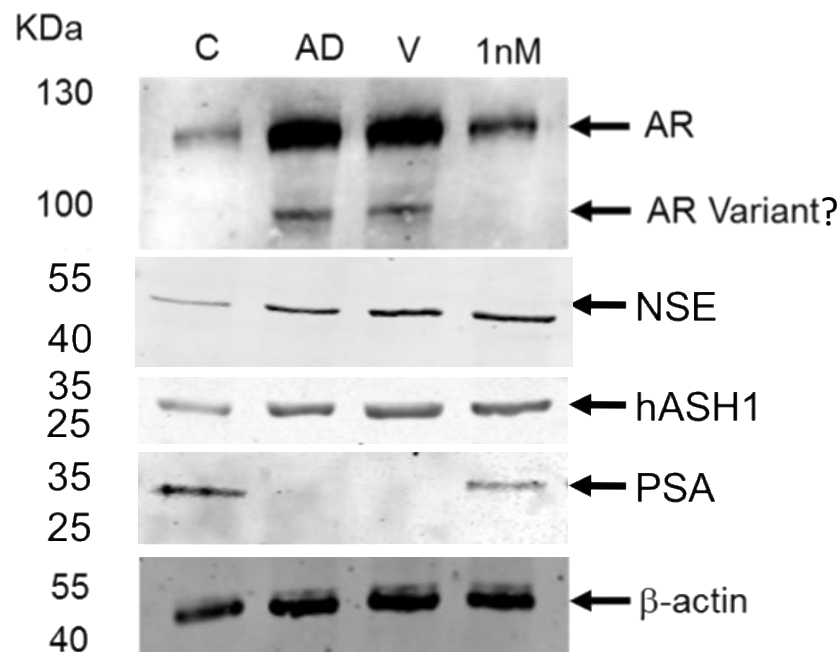


Figure 4.4. Molecular changes associated with reversal of neuroendocrine differentiation via androgen reintroduction. Representative immunoblot images of androgen receptor (AR), neuron-specific enolase (NSE), human Achaete-scute homolog 1 (hASH1) and prostate specific antigen (PSA) expression in LNCaP cells after 30 d of culture in control (C) or androgen deprived (AD) conditions or 15 d in androgen deprived media, followed by a further 15 days \pm DMSO vehicle (V) or 1nM R1881 (1 nM).

PSA is a marker of canonical AR transcriptional activity (Luke & Coffey, 1994), immunoblotting confirmed that PSA expression was robust under control culture conditions, undetected under AD conditions and in AD conditions with vehicle control (Fig. 4.4). This indicates that despite robust expression of AR, canonical AR signalling was effectively disrupted by AD. Expression of PSA in NED LNCaP cells was restored after 15 d of R1881 supplementation to the AD culture conditions (Fig. 4.4). Interestingly, the expression of PSA in AD and R1881 treated cells was considerably lower than in untreated LNCaP cells. This data revealed that NED LNCaP cells not only retain AR expression, but potentially the capacity for canonical prostatic AR-directed gene transcription.

The expression of NSE was also assessed as a marker of the NED phenotype (Fig. 4.4). In keeping with previous data, NSE is considerably upregulated by AD. Remarkably, after reintroduction of androgen, and restoration of PSA expression, NSE expression remains elevated. These findings demonstrated that 1 nM R1881 was sufficient to reverse NED morphology (Fig. 4.3), however transcription factor hASH1 and NED biomarker NSE remain elevated (Fig. 4.4), suggesting that AR and hASH1 transcriptional activity may not be mutually exclusive after cessation of AD.

Data in chapter 3 identified hASH1 nuclear localisation as a potential key driver of NED, hASH1 upregulation has previously been demonstrated to be associated with PCa NED (Rapa *et al.*, 2013), therefore the expression of hASH1 was assessed in response to the reintroduction of androgen to NED LNCaP cells. hASH1 expression after 30 d of AD was upregulated (Fig. 4.4). Of critical importance, expression of hASH1 remained elevated even after re-introduction of androgens (Fig. 4.4). The sustained elevation of hASH1 expression suggested that whilst the morphology and some molecular characteristics of NED may be reversible, these NED LNCaP cells treated with R1881 may retain some aspects of the NED phenotype.

4.2.3 hASH1 retains nuclear localisation upon reintroduction of androgen

Previous analysis of hASH1 localisation demonstrated that hASH1 is excluded from the nucleus of untreated LNCaP cells (Fig. 3.13). However, after AD and acquisition of the NED phenotype, hASH1 localises to the nucleus. Coupled with the evidence that upregulation of hASH1 was not reversed by cessation of AD, the localisation of hASH1 was investigated using confocal microscopy (Fig. 4.5).

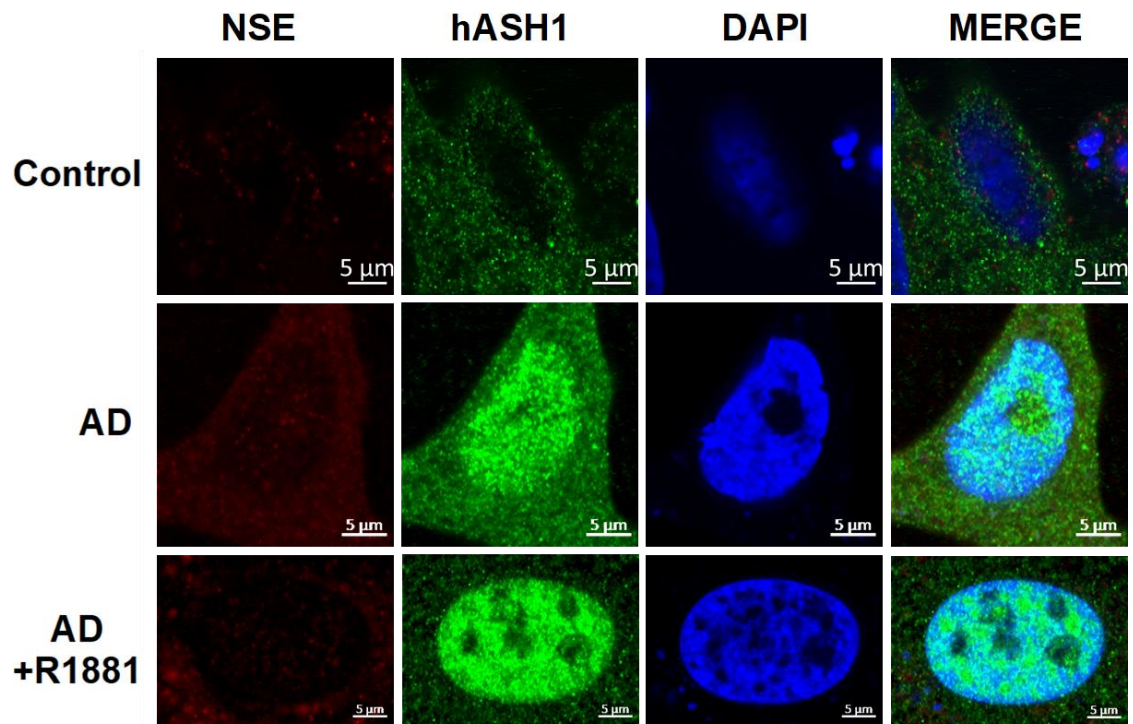


Figure 4.5. Neurogenesis promoter hASH1 retains nuclear localisation despite a reversal of neuroendocrine morphology. Representative confocal microscopy images of LNCaP cells stained with anti-hASH1 and anti-NSE antibodies after 30 d of culture in complete RPMI1640 media (control) or androgen deprived conditions (AD) or 15 d androgen deprivation followed by 15 d in the presence of 1 nM R1881 (AD+R1881) (63 x with digital zoom onto a single representative cell). Scale bar represents 5 μm.

Untreated LNCaP cells (control) displayed very low hASH1 expression which was exclusively cytoplasmic (Fig. 4.5), matching previous findings (Fig. 3.13). Correspondingly, expression of NSE was not detected when hASH1 was excluded from the nucleus (Fig. 4.5). After 15 d of AD, NSE expression is detected

in the cytoplasm, consistent with previous results (Fig. 3.13). hASH1 is also upregulated and was intensely localised to the nucleus. When R1881 synthetic androgen was added to NED LNCaP cells, NSE expression decreased, in line with the immunoblot analysis (Fig. 4.5, Panel AD+R1881 15 Day). However, whilst the cytoplasmic hASH1 returned to basal levels, these cells robustly retain hASH1 within their nucleus. This demonstrated that despite the high degree of reversibility of other molecular changes associated with NED, the localisation of hASH1 to the nucleus may be a more permanent adaption. Analysis of hASH1 localisation has never previously been performed in a model of IAD and represents an important finding of clinical interest, as hASH1 could be utilised as a biomarker of NED or as a therapeutic target.

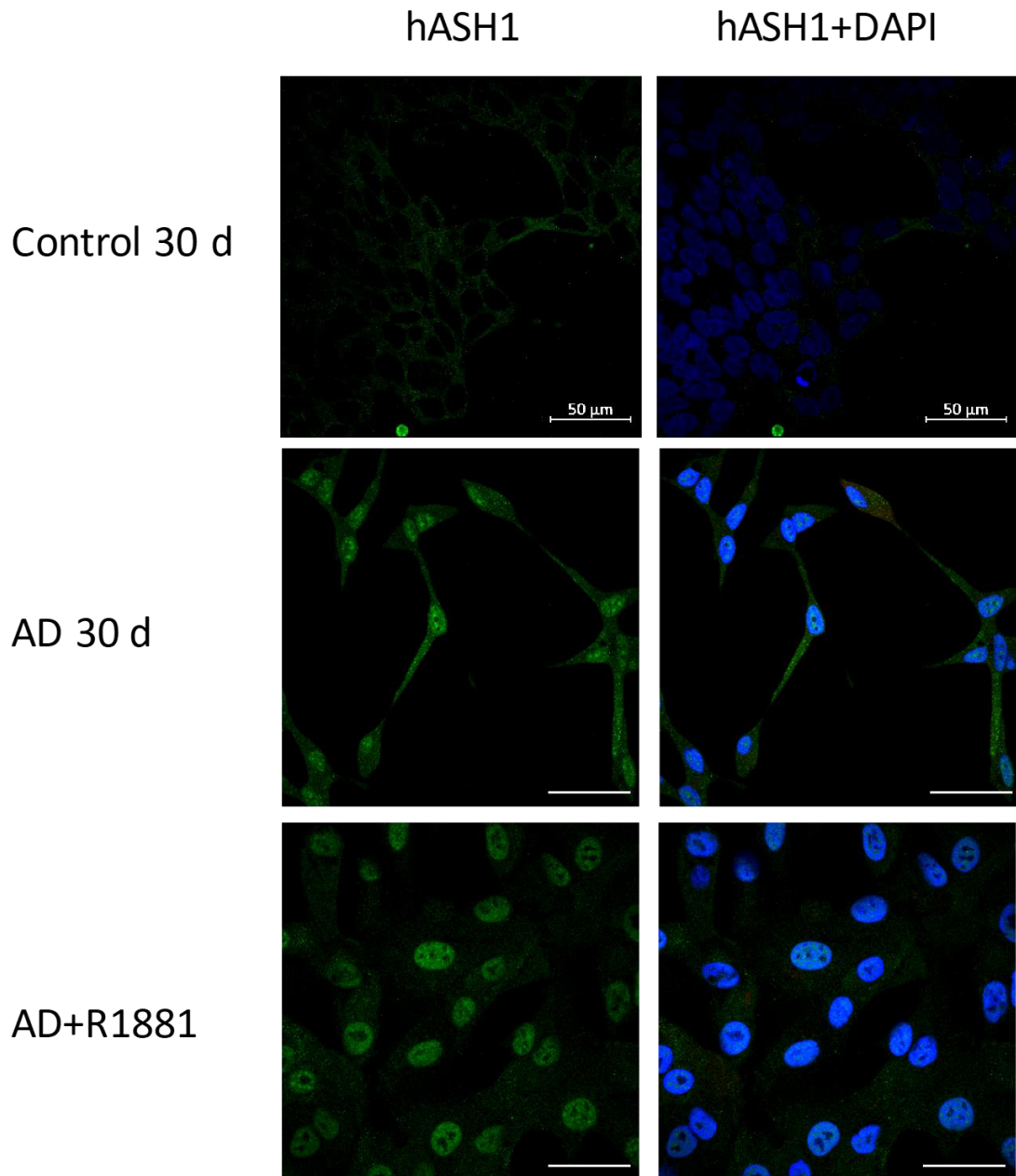


Figure 4.6. Retention of nuclear hASH1 is widespread and neurite-like processes containing hASH1 are lost. Representative confocal microscopy images of LNCaP cells stained with anti-hASH1 after 30 days of culture in complete RPMI1640 media (control), androgen deprived conditions for 30 d (AD) or 15 d AD followed by a further 15 d in the presence of 1 nM R1881 (AD+R1881) (63 x magnification), Scale bar represents 50 μm .

Using a wider field of view for confocal analysis demonstrated that hASH1 nuclear exclusion is ubiquitous in LNCaP cells maintained in control conditions, however a key limitation must be acknowledged that signal for hASH1 and DAPI in these images was low and not easily visible (Fig. 4.6). After 30 d of continuous AD (cAD) hASH1 was concentrated in the cell nucleus and prevalent in the cytoplasm, including throughout the neurite-like projections (Fig. 4.6). After culture in media containing 1 nM synthetic androgen, LNCaP cells reverted to a morphology similar to control untreated LNCaP cells, losing their neurite-like extensions. After AD cessation, where cells were AD for 15 d and were then supplemented with synthetic androgen for 15 d, hASH1 appears to be retained and enriched within the nucleus, whilst cytoplasmic hASH1 is diminished (Fig. 4.6). Interestingly, NED LNCaP cells not only display strong nuclear hASH1 localisation, but hASH1 expression was detected throughout the neurite-like extensions of these cells. This data supports the notion that hASH1 localisation is a durable change during AD-induced NED and is retained, despite the reversibility of other NED features.

4.2.4 Investigating the reversibility of NED and effects of IAD

After analysing the response of AD-induced NED LNCaP cells to reintroduction of androgen (AD cessation), the model was further extended to recapitulate IADT. Following reintroduction of androgen, NED LNCaP cells were then subjected to a second cycle of AD, by culturing NED LNCaP cells in media containing 10% charcoal-stripped FBS for a further 15 d. Thus, following 15 days AD, NED cells were then exposed to synthetic androgen for 15 days, followed by a second 15 day-period of AD. Details of experimental conditions are shown in figure 4.7.

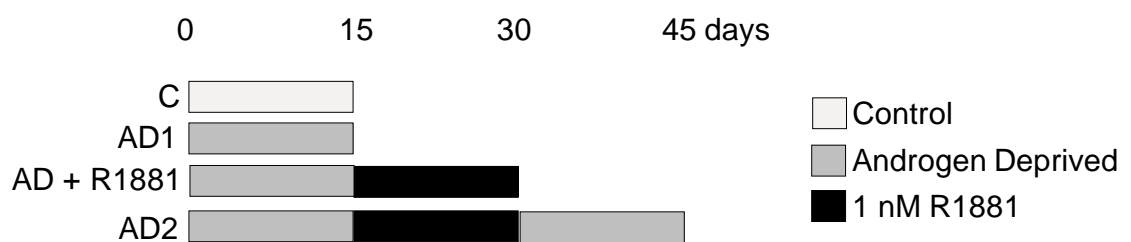


Figure 4.7. Schematic diagram showing the experimental design for investigation of IAD, including two 15-day cycles of AD separated by a 15-day intermediate period of androgen reintroduction. LNCaP cells were cultured in either control media (C), androgen deprived for 15 d (AD1), AD for 15 d then AD media with 1 nM R1881 for 15 d (AD+R1881) or AD media for 15 d then AD media with 1 nM R1881 for 15 d and finally AD media for a further 15 d (AD2).

4.2.5 Effect of IAD on LNCaP cellular morphology

The effects of IAD on the morphology of LNCaP cells was assessed using confocal microscopy using a membrane stain to visualise the cells (Fig 4.8).

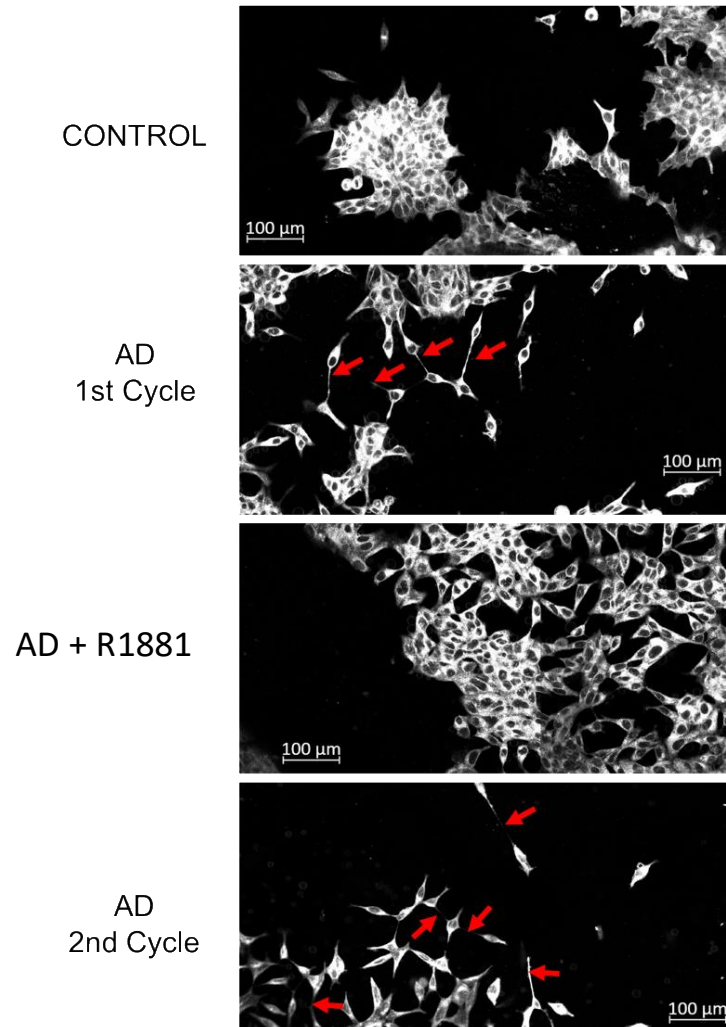


Figure 4.8 Morphological changes of LNCaP cells throughout intermittent AD. Representative confocal microscopy images of LNCaP cells stained with neurite outgrowth staining kit (non-specific membrane stain) maintained in complete media (Control), androgen deprived conditions for 15 days (AD 1st Cycle), intermittent AD consisting of 15 d AD and 15 d with 1 nM R1881 (AD+R1881) or a second 15 d androgen deprivation cycle (AD 2nd Cycle) (20 x magnification, 5x5 tile scan, digital zoom to representative field), Scale bar represents 100 μ m, red arrows indicate neurite-like projections.

Consistent with previous experiments, LNCaP cells acquired neurite-like projections after the first 15-day AD cycle which were lost after introduction of synthetic androgen. After a second 15 d period of AD, LNCaP cells re-acquired neurite-like projections, further highlighting the plasticity of LNCaP cell phenotypes (Fig. 4.8).

4.2.6 Molecular analysis of the effect of IAD on AR signalling

To investigate the effects of simulated IAD with two 15 d cycles of AD, expression of genes involved in the AR signalling axis and NED pathway were assessed using qRT-PCR. Consistent with previous results, AR and PSA were robustly expressed in LNCaP cells cultured in control media (Fig. 4.9). After 15 days of AD, AR expression was slightly elevated and remained similarly elevated after androgen reintroduction. As expected, PSA expression rapidly declined after 15 d AD ($p = <0.001$). After 15 d of reintroduction of androgen, PSA expression returned to basal levels but AR remained slightly increased. This further supports the immunoblot data and confirms that NED LNCaP cells may re-establish aspects of canonical AR signalling after androgen reintroduction (Figs. 4.4 and 4.15). Unexpectedly, after a second 15 d AD cycle, NED LNCaP cells lost detectable expression of AR (Fig. 4.9), with a concurrent loss of detectable PSA expression.

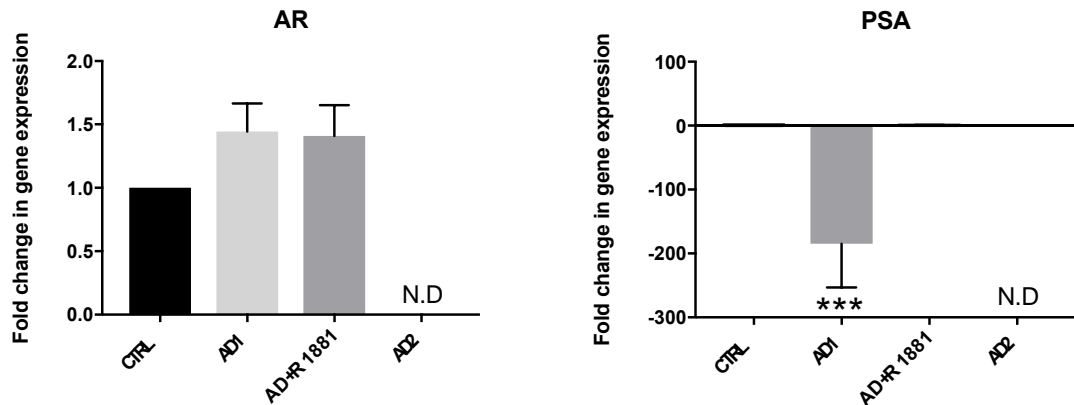


Figure 4.9 Expression of androgen receptor (AR) and prostate specific antigen (PSA) in LNCaP cells after two androgen deprivation cycles. Relative expression of AR and PSA in LNCaP cells that were either untreated (CTRL), subjected to constant AD (AD1), AD followed by cessation of AD (AD+R1881) (1.027-fold change) or a second cycle of AD (AD2) after the AD cessation period, analysed via qRT-PCR. Data is expressed as mean \pm SEM, (n=3) $p < 0.05$ (*), $p < 0.01$ (**) and $p < 0.001$ (***) as determined by one-way ANOVA with Dunnett's correction. N.D, not detected. In AD2 samples, robust expression of reference gene ACTB was detected at Ct 15.10 (\pm 0.26) which is consistent with other experiments, demonstrating that the cDNA generated was viable.

4.2.7 Molecular analysis of the effect of IAD on NED pathway

Following investigation of the androgen signalling axis, the changes in expression of key genes in the NED pathway were assessed in response to IAD.

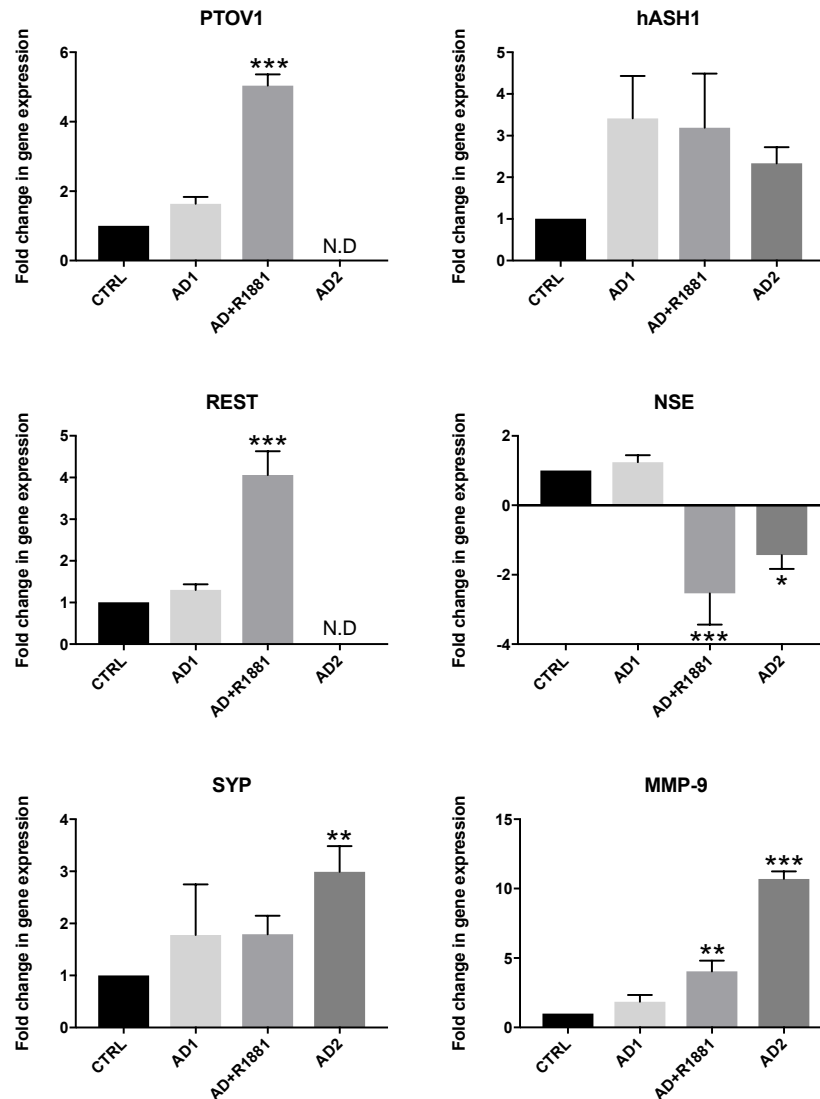


Figure 4.10 Expression of key NED associated genes during intermittent (I)AD. Relative expression of PTOV1, NSE, REST, hASH1, SYP and MMP-9 in LNCaP cells that were subjected to either one 15 d AD cycle (AD1), AD followed by cessation of AD for 15 d (AD+R1881) or a second 15 d AD cycle after AD cessation (AD2), compared to cells maintained in complete media (CTRL), analysed via qRT-PCR. Data is expressed as mean \pm SEM, (n=3) $p < 0.05$ (*), $p < 0.01$ (**) and $p < 0.001$ (***) as determined by one-way ANOVA with Dunnett's correction, N.D., not detected.

After the first AD cycle expression of PTOV1 was slightly upregulated (Fig. 4.10). Interestingly, PTOV1 expression was significantly upregulated (4.5-fold) ($p = <0.001$) by the reintroduction of androgen. Whilst this was surprising, it aligns with the hypothesis that PTOV1 may be involved in the disruption of cell fate (Alaña *et al.*, 2014; Meder *et al.*, 2016). An even more unexpected result was that expression of PTOV1 became undetectable after the second 15 d AD cycle.

NSE expression was not significantly upregulated by the first cycle of AD. Interestingly, NSE expression was significantly downregulated ($p = <0.001$) by the reintroduction of androgen to the NED LNCaP cells, supporting the hypothesis that reintroduction of androgen can ablate molecular and morphological features of NED (Fig. 4.8 and 4.9). Curiously, after the second 15 d cycle of AD, gene expression of NSE increased compared to the reversed NED LNCaP cells, but remained significantly below basal levels ($p = 0.01$).

The proposed pathway of NED implicates REST as a key inhibitor of NED under the pressure of canonical AR signalling. Previously, REST reduction has been demonstrated to be essential to hypoxia driven NED in PCa (Lin *et al.*, 2016). This data shows that REST gene expression is unchanged by one AD cycle but is significantly upregulated (4-fold; $p = <0.001$) when NED is reversed by the reintroduction of androgen (Fig. 4.10). This result, when paired with the REST immunoblot data (Fig. 4.11) strongly supports the hypothesis that REST can inhibit the NED pathway and even reverse it in an androgen signalling dependent manner. After the second cycle of AD, expression of REST was undetected (Fig. 4.10).

Consistent with the data produced by confocal microscopy hASH1 expression of was slightly upregulated by one AD cycle and this elevation was retained even after reintroduction of androgen. Following the second cycle of AD, hASH1 expression remained elevated above basal levels. SYP, is a clinically used biomarker of prostate cancer NED (Atree-Tacha *et al.*, 2017). Expression of SYP was slightly elevated after 1 cycle of AD and remained at this level during androgen reintroduction. Interestingly, synaptophysin expression was further elevated by a second cycle of AD, becoming statistically significant ($p = 0.002$).

MMP-9 expression is closely correlated with progression to CRPC and increased prostate cancer aggression (Azuma *et al.*, 2003). Interestingly, the expression of MMP-9 steadily increased throughout the treatments. MMP-9 was slightly upregulated after the first AD cycle, becoming significantly upregulated after AD cessation ($p = 0.001$) and increasing further to 10-fold above basal levels after a second cycle of AD ($p = <0.001$).

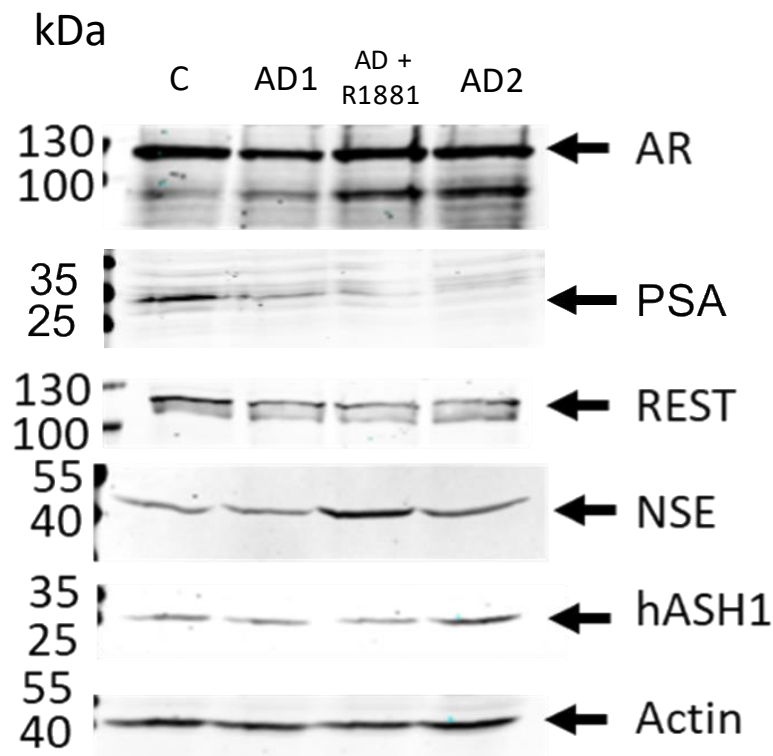


Figure 4.11 Expression of key neuroendocrine associated proteins during IAD. Representative immunoblot images of androgen receptor (AR), RE-1 silencing transcription factor (REST), prostate specific antigen (PSA), neuron specific enolase (NSE) and human achaete-scute homolog 1 (hASH1) in LNCaP cells which were either untreated (CTRL), subjected to one 15 d AD cycle (AD1), AD followed by cessation of AD (AD+R1881) or a second 15 d AD cycle after AD cessation (AD2). Beta actin was used as a loading control.

Expression of AR protein remained stable throughout IAD (Fig. 4.11), which is in contrast with the qPCR data (Fig. 4.9) where expression of AR was not detected in the AD2 sample. A possible explanation for this inconsistency between the gene and protein expression of AR in the AD2 samples is that in the long-term absence of androgen (2 AD cycles) the AR protein is not being activated and

therefore remains membrane bound and less able to be degraded in comparison to when it is translocating to the nucleus during AR-signalling. It is also possible that gene expression may be below detection whilst the AR protein remains present, thereby causing a discrepancy between the qPCR and immunoblot data. Another consideration is that the binding sites of the AR antibody and AR oligonucleotides used in qPCR are not the same. This could result in detection of other splice variants which retain that antibody binding site being detected via immunoblot, but not in qPCR experiments (see appendix 1; Fig. 8.1). However, in this case that difference is unlikely to be the main contributing factor to the discrepancy between the immunoblot and qPCR results, since the transcript variants with potential to be targeted by the AR antibody also have substantially different molecular weights and this was not apparent on the immunoblot analysis.

In addition, PSA protein expression is in consensus with the qPCR data for control and AD1 samples, but where the gene expression is restored to basal levels after re-introduction of R1881, this is not reflected at the protein level. This is potentially highlighting a 'lag time' between the restoration of PSA gene expression and the restoration of PSA protein concentrations to basal levels. In consensus with the qPCR data, PSA expression in the AD2 samples is extremely low when assessed via immunoblot and was undetected in the qPCR experiment. Interestingly, at the protein level, NSE expression appeared to peak at the end of the androgen reintroduction period and remain slightly higher than basal levels during the second AD period (Fig. 4.11). This discrepancy with the qRT-PCR data for NSE expression could be due to differences in the turnover of NSE mRNA and protein within the cells. Expression of hASH1 was notably upregulated at protein level after the second cycle of AD (Fig. 4.11). Expression of REST appeared to be moderately downregulated during the first AD cycle and remained this way throughout IAD, in future work this change could be quantified by employing additional methodologies such as densitometry or ELISA.

4.2.8 Analysis of hASH1 localisation throughout IAD

Previous analysis of hASH1 localisation during IAD (Fig. 4.5 and 4.6) showed that hASH1 nuclear localisation was enriched after cessation of AD. Therefore, the localisation of hASH1 was assessed after a second cycle of AD at 10 d (Fig. 4.12 and 4.13).

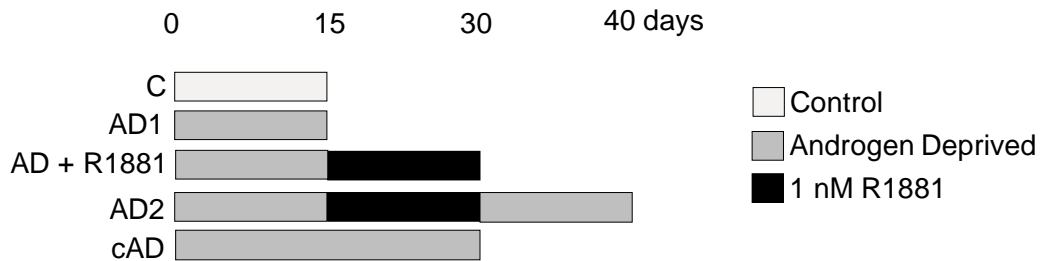


Figure 4.12 Schematic diagram detailing the experiment design for androgen deprivation cessation experiments assessing hASH1 localisation. LNCaP cells were cultured in either control media (C), androgen deprived for 15 d (AD1), AD for 15 d then AD media with 1 nM R1881 for 15 d (AD+R1881), AD media for 15 d then AD media with 1 nM R1881 for 15 d and finally AD media for a further 15 d (AD2) or continuous AD (cAD) for 30 days.

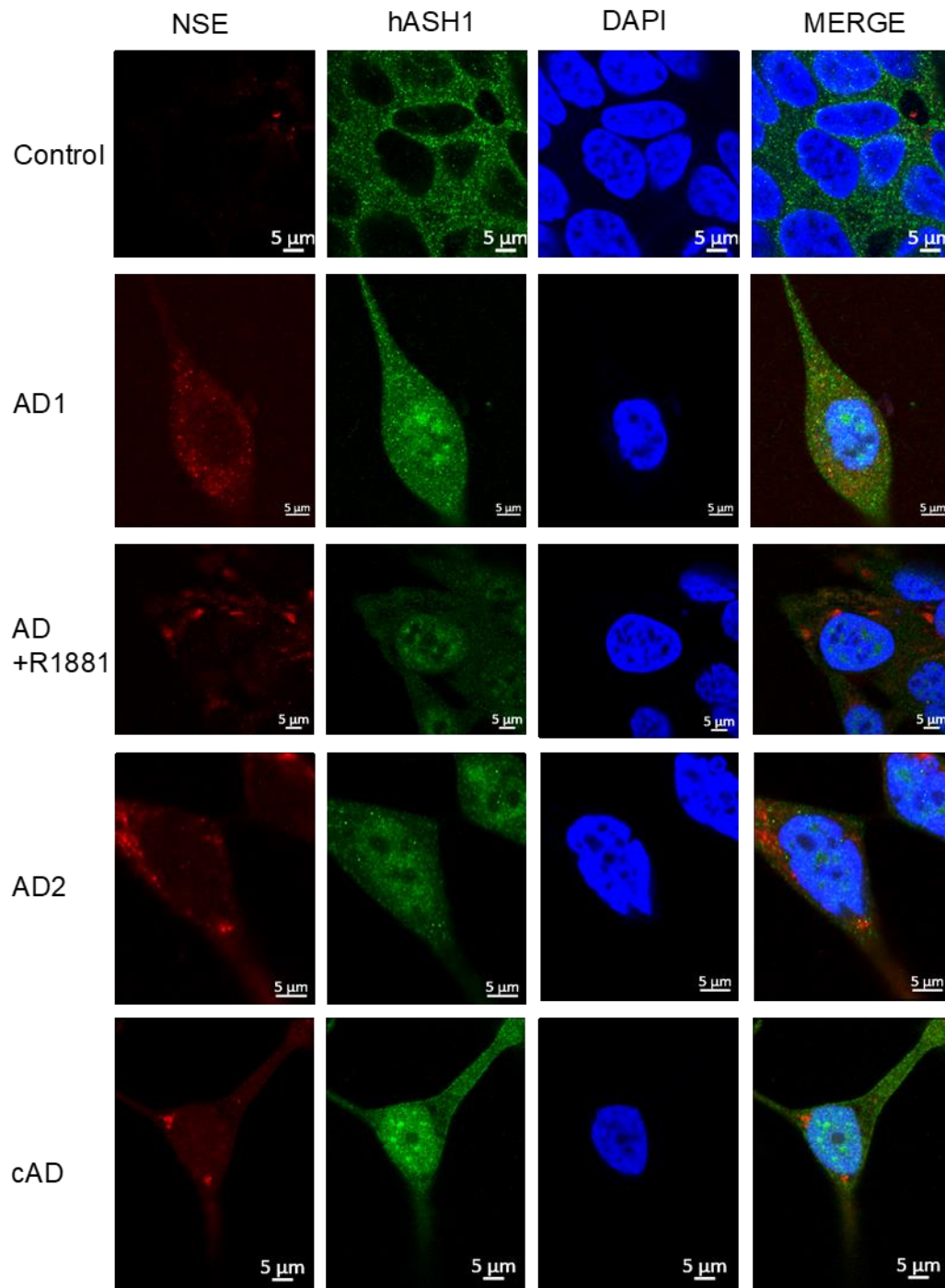


Figure 4.13 hASH1 localisation throughout IADT and 10 days into a second AD cycle. Representative confocal microscopy images of LNCaP cells stained with anti-hASH1 and anti-NSE after one 15 d androgen deprivation cycle (AD), intermittent ADT consisting of one 15 d AD cycle then 15 d AD cessation (AD+R1881), 10 d into a second androgen deprivation cycle after AD cessation (AD2) or continuous AD for 30 d (cAD) (63 x magnification, digital zoom into representative cells), Scale bar represents 5 μ m, n=3.

Consistent with previous data hASH1 was excluded from the nucleus of untreated LNCaP cells. After the first AD cycle hASH1 was profuse throughout the cell including the nucleus (Fig. 4.13). After reintroduction of androgen and loss of neurite-like projections, hASH1 became enriched within the nucleus, which was consistent with previous confocal analysis. After 10 days into the second AD cycle, hASH1 remains intensely localised to the nucleus, neurite-like projections are reacquired but expression of NSE remains low. In addition, cytoplasmic hASH1 is reduced whilst nuclear hASH1 remains high. These results establish, for the first time, the localisation of hASH1 during IAD and confirm that hASH1 is present within the nucleus throughout successive cycles of AD. This data would also suggest that the shift to nuclear localisation of hASH1 under AD is persistent. This is in alignment with hASH1 localisation during the commitment of neural stem cells to a neural cell fate, where chromatin-bound hASH1 is resistant to degradation compared to cytoplasmic hASH1 (Gillot, Davies, & Philpott, 2018), further supporting that hASH1 is likely to be chromatin bound in NED LNCaP cells.

4.3 Discussion

4.3.1 Research objectives and key findings

On the basis of previously published studies demonstrating AD induces NED of PCa, both *in vitro* (Shen *et al.*, 1997) and *in vivo* (Bluemn *et al.*, 2017; Rapa *et al.*, 2008), alongside the present studies characterised molecular pathway of AD-induced NED; the NED model was adapted to investigate the reversibility of NED. In addition, insight was sought into the molecular implications of Intermittent (I)ADT on the NED pathway and the effects of a 2nd successive AD cycle. Given the controversy that exists around the clinical use of IADT (Heidenreich *et al.*, 2014; Klotz *et al.*, 1986; Mottet *et al.*, 2012; Shore & Crawford, 2010) and the conflicting strategies on NED prevention, this study aimed to provide new evidence to facilitate a better-informed debate on these issues. The 15 day cycle length used for IADT experiments in this study is likely to be sufficiently long enough to be clinically relevant, because the change in androgen concentration from switching cells to CS-FBS media and back to full media is effectively instant. In patients, the half-life of enzalutamide is 5.8 days (USFDA, 2012), therefore a cycle time of 15 days using CS-FBS *in vitro* would be representative of longer

time frame clinically, which would give patients a longer window between cycles and be more realistic to implement. However, it must be considered that this is a limitation of this model and study.

Importantly, the model of NED reversibility used in this study is consistent with previous NED reversibility studies, which found NED morphology could be reverted to an epithelial phenotype after reintroduction of androgen (Shen *et al.*, 1997). For the first time, the underpinning molecular components underpinning the NED pathway were analysed during the reversal process and revealed that key molecular components of NED revert to basal states. This includes the restoration of AR signalling driving PSA expression and a significant upregulation of neurogenesis repressor REST. However, molecular investigation of NED reversibility also revealed unexpected complexity, namely the retention of hASH1 exclusively in the nucleus and elevated NSE expression. The retention of nuclear hASH1, when androgen was reintroduced, despite the loss of NED morphology and restoration of canonical AR signalling aspects, could suggest that hASH1 may retain transcriptional activity, which was previously mutually exclusive with androgen receptor signalling. This possibility of a hybrid phenotype was further evidenced by the data showing that NSE protein expression was highest after reversal of NED and remained elevated after the second AD cycle. In the context of the proposed NED model, this would suggest that some of the transcriptional activity induced by hASH1 is maintained when androgen is reintroduced which could mean that some of the resistance mechanisms of NED PCa persist.

Critically, these experiments demonstrated that reversal of NED could be a viable mechanism of disease recurrence and if hASH1 retains transcriptional activity, the resistance mechanisms of NED could also be retained. The ability for these cells to undergo a second NED would certainly support this notion. In addition, reversal of NED resulted in significant upregulation of MMP-9, which further increased after a second cycle of AD. Taken as a whole, this study demonstrates that the paradigm of complete NED reversibility is actually considerably more complex than previously thought. Furthermore, the evidence generated using this model suggests that reversal of NED may actually result in a more aggressive

phenotype, supported by the data showing increased MMP-9 gene expression and hASH1 nuclear localisation.

4.3.2 Morphological NED reversal and the relationship between form and function

Before investigating the molecular reversibility of NED, first a morphological assessment was made using light microscopy. The supplementation of synthetic androgen to NED LNCaP cells was sufficient to cause a loss of neurite-like projections, reacquisition of untreated morphology and restart cell proliferation evidenced by an observed increase in cell confluency compared to constant AD (Fig. 4.6), although this was not quantified. This return to a proliferative state was also observed in a cAMP induced model of NED (Cox *et al.*, 1999). The use of androgens to revert NED has previously been tested (Shen *et al.*, 1997), where 1 nM DHT prevented NED but was insufficient for NED reversal (assessed by morphology). However, replacing media containing CS-FBS to media containing unmodified 10% FBS was sufficient for loss of NED morphology (Shen *et al.*, 1997). Here, R1881 was used, the rationale for using R1881 is that it is not metabolised and has high affinity for the androgen receptor (Brinkmann *et al.*, 1986). Thus concentrations of R1881 remain stable throughout the cell culture period and the effects of metabolites is greatly minimised (Bonne & Raynaud, 1976; Brown *et al.*, 1981). The use of R1881 in PCa studies has become widespread and favoured over using endogenous ligands (Bishop *et al.*, 2017; Bluemn *et al.*, 2017; Foley & Mitsiades, 2016; Hu *et al.*, 2012; Reyes *et al.*, 2013).

Although morphological observation cannot reveal molecular mechanisms, the ultimate effects of many molecular actions depend upon the presence of specific morphology to facilitate their function. Previously, it has been suggested that NED PCa cells may facilitate the growth and survival of surrounding cancer cells via paracrine support (Bishop *et al.*, 2017; Bluemn *et al.*, 2017; Ippolito & Piwnicka-Worms, 2014; Mirosevich *et al.*, 2006). Considering the seemingly sophisticated and highly interconnected structures formed by the neurite-like extensions of NED LNCaP cells, it is possible that disruption of these formations could erode some of their potential functions. Certainly, under AD conditions distant LNCaP cells appear to extend neurites towards other cells, even over significant

distances of up to 257 μM , which is over 8.5 times greater than the average cell body width (Obin *et al.*, 1999). Although speculative, it would seem unlikely for such powerful chemotaxis of neurite outgrowth to be undirected, especially considering the large number of neurite-like projections (over 500) measured for this study.

4.3.3 Molecular reversibility of NED

Previously studies have demonstrated that NED induced by cAMP treatment was reversible upon withdrawal of cAMP (Cox *et al.*, 1999). Critically, the study investigating cAMP-induced NED did not analyse the molecular components of the NED pathway, merely the downstream biomarkers of NED (NSE expression and morphology) (Cox *et al.*, 1999). Tyrosine kinase and MAPK activity was elevated upon cAMP-induced NED reversal and re-entry to a proliferative state, suggesting perhaps that inhibitors of these kinases could block this mechanism (Cox *et al.*, 1999). Interestingly, the latest publications have demonstrated that pan tyrosine kinase inhibitor dovitinib also induces NED (Yadav *et al.*, 2017). Unfortunately, the reversibility of NED upon withdrawal of dovitinib was not investigated (Yadav *et al.*, 2017). Again, the wide variety of NED inducing agents would suggest an underlying NE transcriptional profile that, rather than being 'activated', is merely de-repressed when the transcriptional pressure of AR-signalling is lifted. In addition, the fact that even the most novel therapeutic strategies cannot escape NED (Wang *et al.*, 2018; Yadav *et al.*, 2017) is both concerning and a rationale to drive understanding of NED forward. Of particular interest, reintroduction of androgen caused a significant upregulation of REST mRNA expression. Taken in the context of a reduction in REST protein expression in NED LNCaP cells (Fig. 4.11), this further validates that REST expression is protective against NED.

PTOV1 is a known repressor of Notch1 signalling (Alaña *et al.*, 2014) and is upregulated by DHT LNCaP cells (Benedict *et al.*, 2001). Notch1 signalling is critical to the maintenance of cell fate in both developing and mature tissues as well as in cancer cells (Capaccione & Pine, 2013; Crabtree & Miele, 2016; Lai, 2004; Wang *et al.*, 2010). Therefore, it is perhaps unsurprising that PTOV1 was

upregulated after re-introduction of androgens. Furthermore, PTOV1 expression was undetected after a second AD cycle, which also resulted in the loss of AR and PSA signalling. This further supports the notion that NED cells retain androgen sensitivity and capacity for canonical AR signalling, whilst after two cycles of AD these cells lose androgen signalling. Of particular interest is that PTOV1 is upregulated during NED, but also upregulated to a higher level after NED reversal. This could support the notion that reversed NED cells would have increased potential to explore aberrant cell fates and strengthens the concept that PTOV1 is a potential key mediator of cell fate malleability (Alaña *et al.*, 2014; Cánovas *et al.*, 2015). The only previous mention of PTOV1 as associated with NED is a conference abstract from 2010, describing PTOV1 as a potential biomarker of NE tumours (de Torres *et al.*, 2010) from the same group that demonstrated PTOV1-mediated Notch signalling repression through repression of Notch1 target genes *Hes1* and *Hey1* (Alaña *et al.*, 2014).

4.3.4 Retention of nuclear hASH1 and the potential for hybrid phenotypes and heterogeneity

Interestingly, hASH1 mRNA and protein expression remained elevated after NED reversal. Analysis of hASH1 localisation revealed that after NED reversal, hASH1 is retained exclusively within the nucleus of LNCaP cells. This data, alongside the immunoblot data, points to an intense enrichment of nuclear hASH1. Functionally, if hASH1 is retained within the nucleus after NED reversal and restoration of AR signalling, these cells could possess a transcriptome influenced both by AR and hASH1, which were previously mutually exclusive in their activity. This hybrid phenotype could potentially utilise advantageous aspects of NED such as therapeutic resistance (Deng *et al.*, 2011; Farach *et al.*, 2016; Hu *et al.*, 2015), combined with the proliferative abilities of the epithelial phenotype (Wang *et al.*, 2010) (Fig. 4.14).

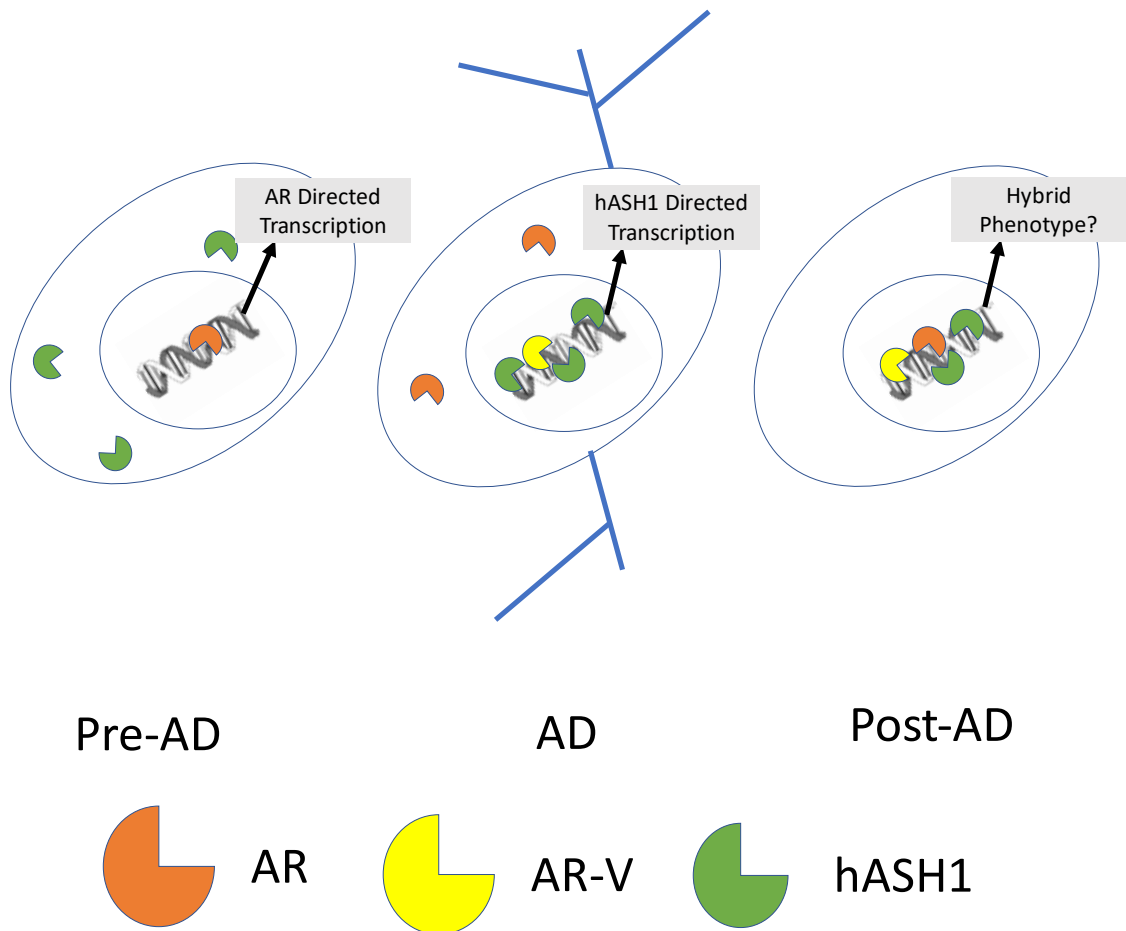


Figure 4.14 Schematic diagram illustrating the shift in transcription factor activity between LNCaP in the presence, absence and re-introduction of androgen. In untreated LNCaP, data demonstrated that expression of hASH1 is low and exclusively cytoplasmic and therefore hASH1 is unlikely to be transcriptionally active. Under AD conditions, in NED PCa cells, canonical AR signalling is greatly reduced, evidenced by PSA downregulation. Simultaneously, hASH1 becomes localised to the nucleus where it is potentially transcriptionally active, evidenced by expression of NSE. In addition, AR splice variants (see appendix; Figure 8.1) can be constitutively active even in the absence of androgen (Dehm *et al.*, 2011; Jones *et al.*, 2015). After re-introduction of androgen, aspects of canonical AR signalling are restored such as PSA expression, however hASH1 is retained in the nucleus of these cells, which could, speculatively, facilitate a hybrid phenotype.

It is important to note that whilst previous studies have implicated hASH1 as involved in NED in PCa (Rapa *et al.*, 2013) and small cell lung cancer (Borromeo *et al.*, 2016), an assessment of hASH1 localisation has never been performed in prostate cancer in response to androgen deprivation. Furthermore, the retention of nuclear hASH1 after NED reversal is entirely novel. To discuss the findings on hASH1 in prostate cancer NED it is necessary to compare studies which have analysed NED in the setting of small cell lung cancer, which shares NED properties (Ishii *et al.*, 2013; Meder *et al.*, 2016). A recent paper demonstrated that hASH1 is required for NED of lung cancer in a mouse model (Borromeo *et al.*, 2016). This study also analysed the target genes of hASH1 during NED using ChIP-Seq, something that has never been applied to hASH1 in the prostate cancer NED setting. In lung cancer NED, hASH1 target genes include a plethora of Notch signalling genes including *DLL1*, *DLL2*, *DLL3*, *JAG2* and *HES1* which were conserved between the mouse model and human tumour samples (Borromeo *et al.*, 2016). These findings corroborate the hypothesis that hASH1 can influence Notch signalling in a cancer setting to facilitate NED. In addition, GABA related genes *GAD2* (GABA synthesis) and *GABRB3* (GABA receptor beta 3 subunit) were found to be direct target genes of hASH1 in lung cancer NED (Borromeo *et al.*, 2016). Further strengthening the rationale to investigate the GABA receptor as a mechanism of paracrine support in prostate cancer NED, discussed in the following chapter.

Whilst the hASH1 transcriptional profile of NED lung cancer will likely differ to that of prostate cancer NED, the ability for hASH1 to target these genes, in a similar cancer NED setting, remains of interest. The next stage of hASH1 evaluation in prostate cancer NED will be to apply genomic approaches (ChIP-Seq, RNA-Seq) to validate target genes and proteomics to identify the protein-protein interactions of hASH1 and its effects as a pioneer factor on the chromatin landscape in untreated, AD and IAD treated LNCaP cells. Unfortunately, transcription factors such as hASH1 are often viewed as intractable drug targets (Johnston & Carroll, 2015), however, identification of the co-factors facilitating hASH1 transcriptional activity has the potential to reveal backdoor mechanisms of hASH1 therapeutic targeting (Johnston & Carroll, 2015).

4.3.5 Effect of IAD on the proposed NED pathway

The responsiveness of proposed key components of the NED pathway (PTOV1, hASH1, NSE, REST) to reintroduction of androgen served to further validate the hypothesis that these genes are in fact involved in NED. The finding that hASH1 was retained in the nucleus of cells that had been reverted from the NED phenotype back to a more epithelial phenotype led to speculation that this retention could facilitate increased sensitivity to successive periods of AD. Analysis of mRNA and protein expression after a second cycle of AD revealed significant complexity rather than the expected exaggerated expression of NED pathway components. It must be noted that the model of IAD takes place over 45-days, whereas the NED reversal model uses a 30-d end point. This considerably longer period of AD must be considered when comparing data between these two models. For example, LNCaP cells that had undergone two rounds of AD with a 15-d period of AD cessation in-between, displayed undetectable AR and PSA mRNA expression. However, analysis via immunoblot revealed that strong AR expression was maintained but confirmed that PSA protein expression was extremely low. This indicates that perhaps the rate of AR degradation has been reduced, causing AR protein to remain present in the absence of transcription. In addition, although AR protein is present, expression of PSA is still greatly reduced, indicated that AR activity remains depressed or that perhaps the AR acquires an altered transcriptional profile which no longer drives expression of PSA.

Importantly, the immunoblot data showing NSE expression highest in reversed NED cells suggests that the retention of hASH1 in the nucleus of these cells is likely to remain transcriptionally active. To confirm transcriptional activity, ChIP-Seq experiments to demonstrate the binding of hASH1 to promoter and enhancer regions and RNA-Seq or qRT-PCR to validate that these sites drove expression could be employed. The mRNA expression of hASH1 remains elevated throughout NED, reversal of NED and after a second period of NED. Whereas, hASH1 protein expression is markedly higher in cells that have undergone a second NED period. During simulated IADT, the localisation of hASH1 to the nucleus after the first cycle of AD is persistent and robustly supports the gene and protein expression data obtained through qRT-PCR and immunoblot. The

persistent nuclear localisation of hASH1 throughout IAD also contributes to the hypothesis that NED LNCaP cells may deploy a hybrid phenotype where AR and hASH1 signalling may become non-mutually exclusive.

Interestingly, NED biomarker synaptophysin becomes significantly upregulated after a second period of AD. In addition, MMP-9 expression is significantly elevated after NED reversal and rises considerably further after a second AD period. This data would suggest that IAD could actually be enriching the NED cell niche and that successive rounds of AD may contribute to the emergence of a phenotype with higher aggressive potential compared to constant AD. IAD may also promote increased prostate cancer aggression through the expression of MMP-9, which promotes invasive cell growth (Azuma *et al.*, 2003). Furthermore, this study heavily implicates transcription factor hASH1 in PCa NED, which is substantiated by many high profile studies showing that hASH1 is crucial to NED in lung cancer (Miyashita *et al.*, 2018; Borromeo *et al.*, 2016; Lenhart *et al.*, 2015; Augustyn *et al.*, 2014; Castro *et al.*, 2011). Canonically, hASH1 is responsible for the generation of GABAergic neurons (Mazurier *et al.*, 2014; Peltopuro *et al.*, 2010), which led to the investigation of GABA receptor activity in PCa NED in Chapter 5.

4.3.6 hASH1 as a potential therapeutic target

Transcription factor hASH1 has been strongly implicated in disease progression of neuroblastoma and is considered to be a potential therapeutic target (Wylie *et al.*, 2015). Furthermore, hASH1 has been tentatively described as a potential therapeutic target for small cell lung cancer (Demelash *et al.*, 2012; Nishikawa *et al.*, 2011; Osada *et al.*, 2008, 2005) and has been demonstrated to be absolutely required for lung cancer NED (Borromeo *et al.*, 2016). However, therapeutic targeting of transcription factors is often considered intractable due to the difficulty of direct drug inhibition (Johnston & Carroll, 2015). Therefore, identification of the co-factors and pioneer factors requisite for hASH1 DNA binding and transcriptional activity may elucidate novel mechanisms to target hASH1 indirectly for therapeutic effect. Most importantly, a novel approach to delaying or reducing NED in PCa would add value to most existing PCa therapeutics by targeting a shared resistance mechanism between ADT, radiotherapy and

tyrosine kinase inhibition. PCa NED is increasing in prevalence (Borromeo *et al.*, 2016), yet there is currently no approved therapeutic specifically targeting NED, therefore validation of potential therapeutic targets such as hASH1 is a crucial research area.

4.4 Conclusions

To conclude, the aims of this work were to establish an *in vitro* model of IAD and to use this model to investigate the extent of AD-induced NED reversibility and the effects of IAD on the components of the proposed NED pathway. This study has shed new light on the molecular reversibility of the AD induced NED pathway in LNCaP prostate cancer cells. The data challenges the established paradigm that NED is entirely reversible and instead identifies hASH1 as a key NED driver and its nuclear localisation as a persistent feature of NED that is not reverted by AD cessation. The responsiveness of key NED pathway genes to NED reversal, further strengthens the evidence that they are involved in the regulation and promotion of NED. Finally, an *in vitro* model of IADT was established for the first time and the NED pathway subjected to molecular investigation. This revealed that in this particular model, IAD induced a significant upregulation of MMP-9 and the data appeared to support the hypothesis that the retention of nuclear hASH1 promotes a hybrid phenotype which may be more aggressive. Therefore, this data would suggest that IADT may enrich NED and speed the acquisition of increased aggression compared to constant AD.

4.5 Limitations, weaknesses and future experiments

Although the key finding of this chapter is that hASH1 is a potential driving transcription factor in PCa NED, it must be acknowledged that this work has several limitations. Therefore, further experiments are necessary in order to robustly validate that hASH1 is a potential therapeutic target. First of all, the nuclear localisation of hASH1 after AD has only been demonstrated in the LNCaP cell line, which does not accurately represent the heterogeneity of patient tumours. Secondly, the present study did not assess hASH1 localisation in the presence of enzalutamide, which would have further validated that this is an AD specific effect and that direct inhibition of the AR could cause hASH1 nuclear localisation. Next, although the data presented in this chapter robustly

demonstrates the expression and localisation of hASH1 during intermittent AD, from these experiments it is not possible to conclude whether hASH1 is directly bound to chromatin or whether it is transcriptionally active. In order to assess the activity of hASH1 in these conditions, experiments such as CHIP-qPCR or CHIP-Seq could have been performed in order to identify the likely target genes of hASH1. In addition, in order to further demonstrate that hASH1 is driving the NED process, siRNA or shRNA experiments could have been performed to knock down expression of hASH1 and investigate whether this prevented the onset of NED morphology and expression of biomarkers such as NSE under AD conditions. Finally, using confocal microscopy to also study the location of AR and hASH1 in the same samples would have given more clarity to the hypothesis of a potential hybrid phenotype and whether AR and hASH1 nuclear localisation are mutually exclusive throughout intermittent AD.

5. Preliminary investigation of GABAergic signalling in Prostate Cancer

5.1 Introduction

Transcription factor hASH1 is a key driver of GABAergic neurogenesis during development (Gillotin, Davies, & Philpott, 2018; Mazurier *et al.*, 2014). Previous studies have demonstrated that GABA and other GABA receptor (GABAR) ligands can modulate the proliferation and aggression of many cancer types, including prostate cancer (PCa) (Abdul, Mccray, & Hoosein, 2013.; Azuma *et al.*, 2003; Wu *et al.*, 2014; Zhang *et al.*, 2013). Having confirmed the neurite-like phenotype of NED LNCaP cells (Chapter 3 & 4), and identification of nuclear localisation of hASH1 as a potentially key event in that process; the next step was to perform the first comprehensive assessment of GABA_AR and GABA_BR subunit expression in PCa and NED PCa cells.

5.1.1 Background and rationale for study

Fundamentally, the impetus to investigate GABAR presence, functionality and role in NED PCa stems from four well established principles. The first that hASH1 is a known key driver of GABAergic neuronal development (Castro *et al.*, 2006; Gillotin *et al.*, 2018; Mazurier *et al.*, 2014), the second that GABA has previously been shown to have tumour modulatory effects (Abdul, Mccray, & Hoosein, 2013.; Azuma *et al.*, 2003; Wu *et al.*, 2014; Zhang *et al.*, 2013), the third that GABAergic signalling is important to the formation of neural networks (Gao, Stricker, & Ziskind-Conhaim, 2001; Khozhai & Il'icheva, 2017b, 2017a; Mäkinen, Ylä-Outinen, & Narkilahti, 2018) and the fourth that elements underpinning GABAergic signalling are directly and indirectly regulated by androgen receptor signalling.

In addition, six GABA_AR subunit promoter regions are known to have AR consensus sites ($\alpha 3$, $\alpha 4$, $\beta 1$, $\gamma 1$, $\gamma 2$ and ϵ) (Steiger & Russek, 2004) although whether these sites are activated by AR in PCa cells has not been determined experimentally. Furthermore, GABAR activity in PCa has previously been linked to increased growth via GABA_AR activation (Wu *et al.*, 2014; Abdul, McCray & Hoosein, 2007) and increased invasive and metastatic potential via GABA_BR

activation as well as the effects of gabapentin (Azuma *et al.*, 2003; Bugan *et al.*, 2016). In addition to GABAergic activity mediated through GABARs, there is also substantial evidence for a metabolic role for GABA in PCa NED as a mechanism of androgen-independence by using GABA metabolites to input into the TCA cycle (Ippolito *et al.*, 2006; Ippolito *et al.* 2014; Nemans *et al.*, 2014; Olsen & DeLorey, 1999). The complex interdependencies between intermediates in the GABA metabolic and catabolic pathways and the TCA cycle result in several possibilities for GABA metabolism to be exploited for both growth or increased neurogenic potential (Ippolito *et al.*, 2006; Ippolito *et al.* 2014; Marmigere *et al.*, 2003). In addition to the ability to produce succinate from GABA to enter the TCA cycle, glutamate is also produced during this process. Glutamate has previously been demonstrated to increase expression of BDNF in hypothalamic neurons and contributes to the survival, differentiation and function of specific subpopulations of neuronal cells (Marmigere *et al.*, 2003). It is also known that BDNF can drive cell proliferation through the activation of AKT and inhibition of the PTEN tumour suppressor (Takeda *et al.* 2013; Temura *et al.* 1999), both of which are key PCa oncogenes (Gundem *et al.*, 2015).

5.1.2 Clinical use of Gabapentin in prostate cancer patients

A key challenge in the clinical treatment of metastatic (m)CRPC is the management of neuropathic pain, often caused by bone and particularly spinal metastases (occurring in 90% of mCRPC patients) which can be exceptionally painful for patients and often impossible to resect surgically (Bugan, *et al.*, 2016). Therefore, many mCRPC patients require long term, highly-potent analgesia. This presents the challenge of poorly tolerated side-effects and addictive properties of most opioid-based pain relief treatments. For these reasons, non-opioid-based analgesics such as gabapentin (GBP) (Fig. 5.1) have become increasingly popular and prescribed “off-label” to mCRPC patients (Caraceni *et al.*, 2004; Vedula, Li, & Dickersin, 2013).

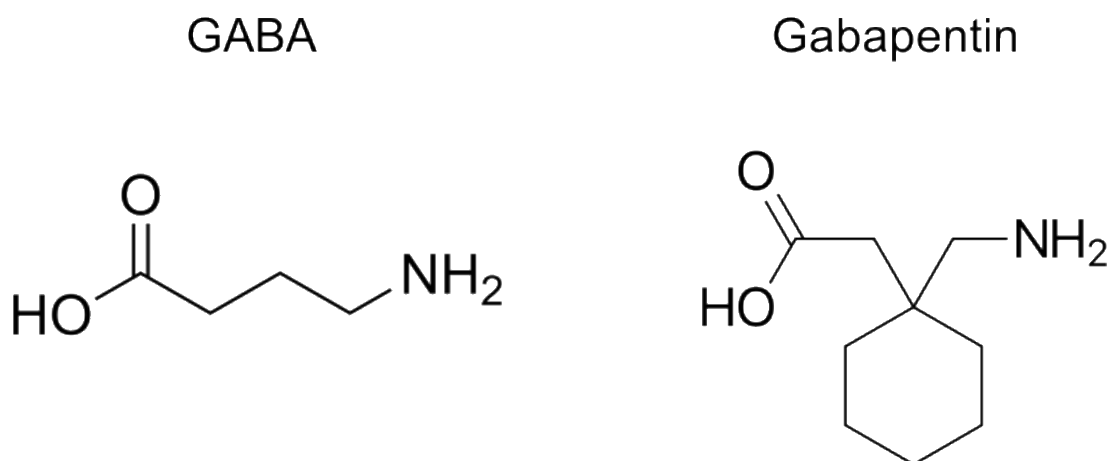


Figure 5.1 Chemical structures of GABA and Gabapentin. Gabapentin (GBP) was originally designed to be an analogue of GABA, despite this gabapentin is not thought to directly bind to GABARs, but instead binds to voltage-gated calcium channels (VGCCs) (Hendrich *et al.*, 2008). GBP closely resembles GABA structurally, but with the addition of a cyclohexane ring (Rose & Kam, 2002), which is thought to increase the molecules ability to cross the blood brain barrier (Yogeeswari, 2006). Distribution, metabolism and pharmacokinetic (DMPK) analyses of GBP show that the bioavailability of a 300mg oral dose in humans is around 60%, with peak plasma levels between 2.7-2.99 mg/L three hours post-ingestion (Rose & Kam, 2002). GBP concentrations in the cerebrospinal fluid are around 20% that of plasma concentration, whilst brain concentrations are 80% of serum concentration, highlighting the high capacity to cross the blood brain barrier. Furthermore, GBP cannot be metabolised by humans (Rose & Kam, 2002), meaning that no metabolites are produced, unlike GABA which can be metabolised into succinic semialdehyde which can be further metabolised into succinic acid by succinic semialdehyde dehydrogenase (SSADH) and enter the TCA cycle (Olsen & DeLorey, 1999).

Originally, GBP was developed and licensed to treat epilepsy in the late 1990's, later becoming a popular analgesic (Goa & Sorkin, 1993; Taylor, 1997). In addition to improved therapeutic index and lower addictive properties compared to opioid analgesics, GBP can also alleviate the neurotoxicity caused by chemotherapeutics and reduce hot flushes, nausea, and vomiting, all of which are suffered frequently by mCRPC patients (Bugan *et al.*, 2016). The impetus to

utilise GBP in mCRPC patients is clear, however, recent research has speculated that voltage-gated sodium channel blockers such as GBP could have the potential to modulate the tumour in addition to their analgesic effects (Lee *et al.*, 2014). GBP increases tumour growth of pancreatic cancers in Wistar rats (Dethloth *et al.*, 2000; Sigler *et al.*, 1995). More recently, GBP has been investigated in an *in vivo* rat model of PCa and found to modulate metastasis formation in a dose-dependent manner, whilst having no effect on primary tumour growth. At low doses (4.6 µg/kg), GBP had no effect on metastasis formation, at medium doses (9.1 µg/kg) GBP significantly decreased metastasis formation and at high doses (16.8 µg/kg) GBP increased metastasis formation and significantly reduced survival (Bugan *et al.*, 2016). In clinical trials analysing the effect of GBP on neuropathic pain, patients received 12-50 mg/kg daily depending on the amount of pain management required (Backonja & Glanzman, 2003). Previously, GBP (100 µM) was demonstrated to reduce proliferation of LNCaP cells by 35% *in vitro* and when added to drinking water of LNCaP xenograft bearing mice (400mg/L; 60 mg/kg daily) also reduced primary tumour size, the effect on metastases was not investigated as LNCaP cells have previously been shown to not form metastases *in vivo* (Warnier *et al.*, 2015). However, it should be noted that GBP is known to not be a direct GABA_A or GABA_B receptor agonist, but is postulated to exert effects indirectly through altered GABA secretion, uptake and metabolism (Lanneau *et al.*, 2001). GBP is a known ligand of the $\alpha 2\delta$ -2 subunit of voltage-gated calcium channels (VGCCs), as are other gabapentinoids such as pregabalin and phenibut (Warnier *et al.*, 2015; Zvejniece *et al.*, 2015). Despite widespread use of GBP, a recent double-blind randomised control study found no benefit of GBP for cancer induced bone pain compared to placebo (Fallon *et al.*, 2016). Therefore, the rationale to investigate potential cancer modulatory effects of GBP is clear.

5.1.3 Study aim and research questions

Study aim: To establish the expression profile of GABA_A and GABA_B receptor subunits in androgen-sensitive, castrate-resistant and NED PCa and to investigate the effects of GABAergic compounds on this study proposed PCa NED pathway.

Research questions: **(1)** Do PCa cells express the necessary GABA receptor subunits to form functional GABARs? **(2)** How does AD and intermittent (I)AD effect the expression of these subunits? **(3)** Does the gene expression of PCa and NED PCa cells change in response to stimulus by GABAergic compounds?

5.2 Results

5.2.1 Expression of GABAR subunits in PCa cell lines

As an initial, comprehensive assessment of GABARs in different PCa cell lines, qRT-PCR was employed to screen for GABA receptor subunit expression in LNCaP, DU-145 and PC-3 cells (Table 5.1).

Table 5.1 Assessment of GABA_AR and GABA_BR subunit expression in LNCaP, DU-145 and PC-3 PCa cells. Quantitative reverse transcription (qRT)RT-PCR was used to detect expression of 16 GABA_AR subunits and two GABA_BR subunits in PCa cell lines. cDNA from human brain was used as a positive control and presence (+) or absence (-) of expression was determined using melt-curve analysis. (n=3).

GABA Receptor Subunit	LNCaP	DU-145	PC-3
a1	+	-	-
a2	-	-	-
a3	+	-	-
a4	-	-	-
a5	+	-	-
a6	+	-	-
b1	-	+	+
b2	-	-	+
b3	+	-	+
g1	+	+	+
g2	-	-	-
g3	+	-	+
d	-	-	-
e	-	-	-
q	+	+	-
p	-	-	-
GABBR1	+	+	+
GABBR2	+	+	+

Interestingly, substantial differences in the presence and absence of GABA_A receptor subunit expression were identified between the androgen-sensitive LNCaP cells and the CRPC cell lines, DU-145 and PC-3 (Table 5.1). Most apparent was that expression of GABA_A α subunits were only evident in LNCaP cells, with no detected expression in DU-145 or PC-3. Furthermore, only the α 1, α 3, α 5, and α 6 subunits were detectable. Typically, formation of a functional GABA_AR requires two α subunits, two β subunits and one other subunit, which is usually a γ or δ subunit (Miller & Aricescu, 2014; Mulligan *et al.*, 2012). Thus, this initial analysis suggested that only androgen-sensitive LNCaP cells were likely to form functional GABA_ARs, although it should be considered that GABA_ARs can also be formed from five β 3 subunits in a homomeric structure (Miller & Aricescu, 2014), which could potentially grant PC-3 cells the ability to form GABA_ARs. However, homomeric β 3 GABA_ARs are unable to bind GABA, since the GABA binding site is at the interface of the α and β subunits (Sigel & Steinmann, 2012). Conversely, all three of the PCa cell lines expressed both subunits of the GABA_BR. The δ , ε and π subunits remained undetected in all samples, but were detected in brain positive controls, so were likely expressed below the detection threshold. Interestingly, π is reported to be found in the healthy prostate gland (Hedblom & Kirkness, 1997; Watanabe *et al.*, 2006), but was not detected in any of the tested PCa cell lines (Table 5.1). All three of the PCa cell lines expressed both subunits of the GABA_BR.

5.2.2 Quantification of GABA_AR and GABA_BR expression in prostate cancer cell lines

Having established which subunits were expressed in LNCaP, DU-145 and PC-3 cells, the relative abundance of GABAR subunit cDNAs in these cell lines was assessed (Fig 5.4).

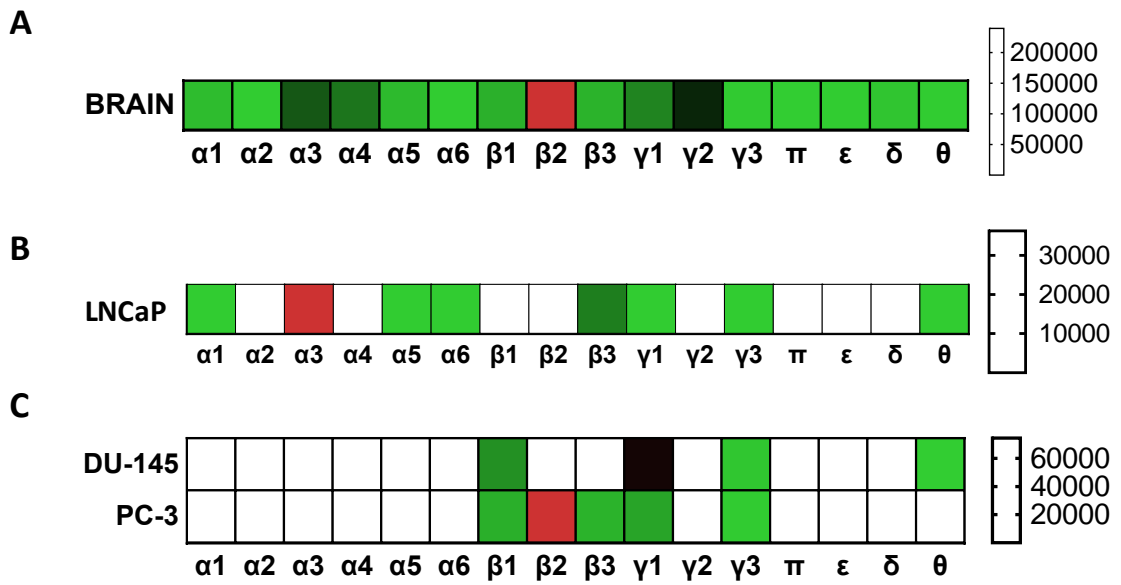


Figure 5.2 Quantitative relative expression of GABA_AR subunits in brain tissue and PCa cells. Heat map expression profile of GABA_AR subunits in **A.** Human whole brain tissue, **B.** CRPC cell lines DU-145 and PC-3 and **C.** LNCaP PCa cells. Higher expression is indicated in red; lower expression genes in green, white indicates not detected. Data is displayed as percentage increase or decrease relative to expression of $\gamma 1$ in untreated LNCaP cells n=3 (except brain where n=1).

Assessment of all GABAR subunit expression in PCa has only been undertaken previously in a presence/absence manner using end-point RT-PCR (Wu *et al.*, 2014). Although RNA-Seq experiments have also been performed and deposited into databases such as EMBL-EBI gene expression atlas and the cancer genome atlas (TCGA) and show expression of GABA_AR and GABA_BR subunits at 9 transcripts per kilobase million (TPM) and 7 TPM respectively, these datasets do not include NED LNCaP cells. Therefore, a quantitative assessment of GABAR

subunits in PCa cell lines and NED LNCaP cells via qRT-PCR is a useful contribution for researchers interested in the effects GABA and other GABAR ligands may exert on PCa cells as the response of the GABAR is highly influenced by its subunit composition.

The $\alpha 3$ subunit has previously been shown to be upregulated in non-small cell lung cancer and is implicated in protein kinase B (AKT) activation and metastasis in breast cancer (Gumireddy *et al.*, 2016) and was the most expressed subunit in LNCaP cells (Fig 5.5). Interestingly, in LNCaP cells, expression of subunit $\beta 3$ was the second most expressed and has previously been linked to decreased proliferation of hepatocellular carcinoma *in vivo* (Minuk *et al.*, 2007). In addition, the θ subunit was present in LNCaP and DU-145 cells and is known to facilitate GABA mediated growth of hepatocellular carcinoma both *in vitro* and *in vivo* (Li *et al.*, 2012). Overexpression of the π subunit increases proliferation of pancreatic cancer (Takehara *et al.*, 2007), and is also overexpressed in breast cancer where it is considered a viable biomarker (Symmans *et al.*, 2005). However, this subunit was not detected in any of the PCa cell lines tested.

5.2.3 Quantification of the effect of AD on GABA_A and GABA_B receptor subunit expression in LNCaP cells

The expression of GABAR subunits was also investigated in LNCaP cells in response to five days of culture in AD conditions (Fig. 5.3). The decision to study changes in GABAR subunit expression at the 5 d time point was taken because, of the time points assessed by qRT-PCR, this is the time point where NSE and hASH1 expression was observed to be highest. Early morphological indicators of NED phenotype are also present after 5 days AD, suggesting that this is a good time point to study GABA_AR subunits which are known to be involved in neurogenesis and synaptogenesis and their expression alters during development (Ben-Ari, 2002; Neelands *et al.*, 1999). Furthermore, the early molecular changes associated with NED could act as useful biomarkers that the NED process is beginning, which could have clinical utility where avoidance of full NED would be desirable, especially in the context of IADT. GABAR subunits

have previously been demonstrated to be viable biomarkers in multiple cancer types (Li *et al.*, 2012; Liu *et al.*, 2009; Symmans *et al.*, 2005).

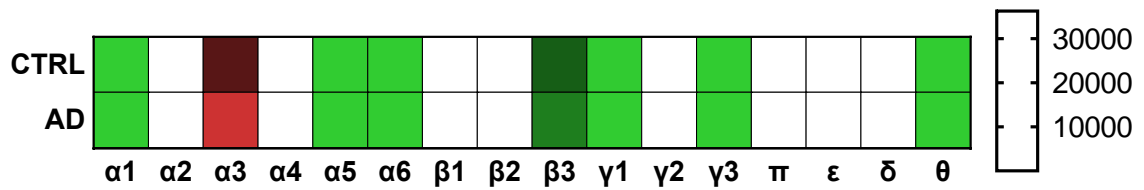


Figure 5.3 Relative expression of GABA_AR subunits in LNCaP cells subjected to androgen deprivation. Heat map expression profile of GABA_AR subunits in control (CTRL) and 5 d androgen deprived (AD) LNCaP PCa cells. Highest expressed genes are indicated in red; least expressed in green, not-detected in white. Data is displayed as percentage increase or decrease relative to expression of $\gamma 1$ in untreated LNCaP cells (n=3).

Overall the expression of most subunits did not appear to be responsive to 5 d AD treatment, however, small changes in $\alpha 3$ and $\beta 3$ were observed. Most importantly, there were no changes to presence and absence of different subunits. Displaying the GABA_AR subunit expression relative to the $\gamma 1$ subunit of LNCaP cells allowed for the identification of the most expressed subunits, which were $\alpha 3$ and $\beta 3$. It is perhaps surprising that there was no induction or complete repression of any GABA_AR subunits in response to AD, however this would not preclude changes in the predominant GABA_AR subtype.

Once it was established that there was expression of selected GABA_AR subunits in LNCaP cells and that expression of these subunit genes could be modified by AD – potentially in line with the onset of NED. The experiment was further refined by introduction of synthetic androgen to verify that the effects observed during AD were only attributable to lack of androgen, and not absence of other factors in the charcoal-stripped media.

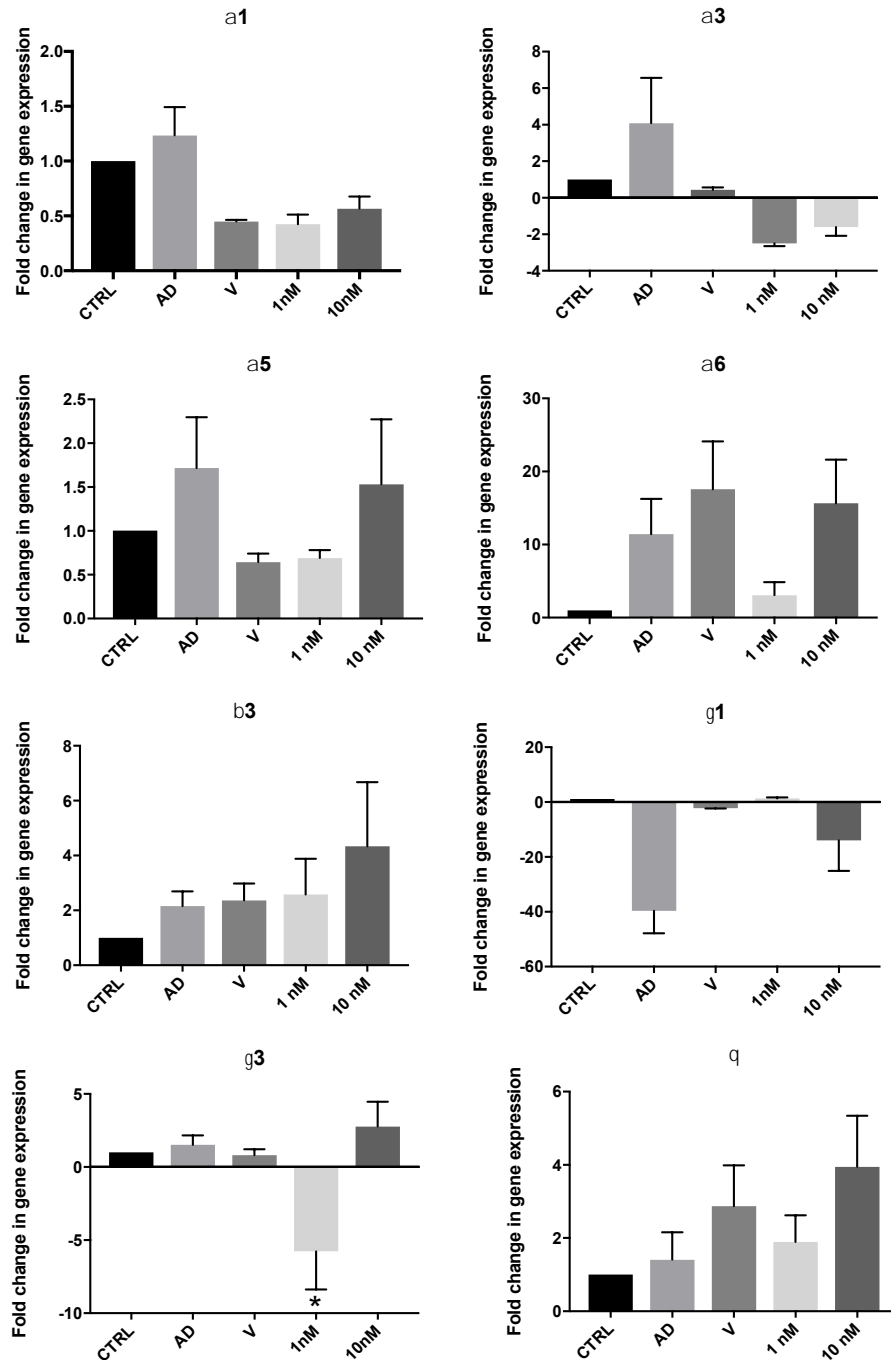


Figure 5.4 Expression of GABA_AR subunits in LNCaP cells cultured in androgen deprived (AD) conditions or in the presence of 1 nM or 10 nM synthetic androgen (R1881). Relative expression of GABA_AR subunits in LNCaP cells that were either untreated (CTRL), subjected to 5 d of AD (AD) or 5 d of AD conditions supplemented with either DMSO vehicle (V) or R1881 at 1 nM or 10 nM concentrations, were analysed via qRT-PCR, data was normalised to reference gene ACTB. Data is expressed as mean \pm SEM, (n=3) $p < 0.05$ (*) and $p < 0.01$ (**) as determined by one-way ANOVA with Dunnett's correction.

Of the subunits previously identified to be expressed by LNCaP and AD LNCaP cells, there were observed changes in expression caused by AD and androgen supplementation. The $\alpha 1$ subunit was not significantly altered in mRNA expression by AD and the effects of supplementing R1881 synthetic androgen had no effect beyond the vehicle control. Subunit $\alpha 3$ was upregulated by AD and downregulated below basal levels by 1 nM (2.4-fold) and 10 nM (1.6-fold) of R1881, however, the presence of the vehicle control also downregulated $\alpha 3$ subunit expression to basal levels, which would suggest that this effect is not androgen specific. Across the panel of GABA_AR subunits, it is apparent that for some subunits the expression in the vehicle sample does not replicate what is observed in the AD sample. The likely reason for this is that expression of many of these subunits as shown in Figures 5.4 and 5.5 is very low, meaning that small variances in expression will result in large fold changes, which is a clearly established limitation of using relative quantification methods in qPCR. Although it would seem unlikely, it is also possible that the 0.01% vehicle is having an effect on the GABA_AR subunit gene expression not previously observed with other transcripts, again an effect that would be amplified by the low expression of these targets. An ideal improvement to this analysis would have been to use absolute quantification method qPCR and to use TaqMan qPCR probes. The $\alpha 5$ subunit was slightly upregulated by AD (1.7-fold), downregulated by presence of the vehicle control (0.6-fold) and 1 nM R1881 (0.6-fold), but was upregulated compared to the untreated control in the presence of 10 nM R1881 (1.5-fold). Subunit $\alpha 6$ was upregulated by AD (11-fold) and in the presence of vehicle control (17-fold; $p = 0.09$), whilst 1 nM R1881 supplementation maintained expression closer to basal levels (3-fold) and 10 nM R1881 resulted in an upregulation similar to that of AD (15.6-fold; $p = 0.14$) which suggest that $\alpha 6$ subunit expression can be modulated by androgen. Interestingly, the $\alpha 6$ subunit, along with the $\alpha 1$ subunit have been demonstrated to be important to the anchoring of the complete GABA_AR to the cell surface (Peran, *et al.*, 2004), this increase in $\alpha 6$ subunit expression in response to AD could be an indicator of increased GABA_AR presentation on the surface of early NED PCa cells (Peran *et al.*, 2004). $\beta 3$ subunit expression was slightly elevated by both AD (2.1-fold) and AD with vehicle control (2.3-fold) and was not suppressed by either 1nM (2.5-fold) or 10

nM (4.3-fold) R1881 supplementation, suggesting that the $\beta 3$ subunit is unlikely to be regulated by AR signalling.

The $\gamma 1$ subunit was the only transcript to be significantly downregulated by AD ($p = 0.009$), however, androgen supplementation (1 nM, 10 nM) did not affect $\gamma 1$ subunit expression beyond that of the vehicle control (39.7-fold; $p > 0.99$). Finally, $\gamma 3$ subunit expression was not significantly influenced by AD or vehicle treatment but, interestingly, was significantly downregulated (5.7-fold) by addition of 1 nM of androgen ($p = 0.02$), however, at a higher concentration of R1881, the $\gamma 3$ subunit expression was upregulated 2.7-fold, although not significantly. Overall, these results would indicate that the majority of GABA_AR subunit expression is not specifically altered by 5 days of AD, with the exception of the $\alpha 6$ and $\gamma 3$ subunits.

5.2.4 Assessment of the effect of intermittent (I)AD on GABA_AR subunit expression in LNCaP cells

Having established that expression of some GABA_AR subunits were responsive to AD, the effects of IAD on expression in LNCaP cells was then investigated (Table 5.2).

Table 5.2 Presence and absence assessment of GABAR subunits during intermittent (I)AD. Using qRT-PCR, the expression of GABA_AR and GABA_BR subunits in LNCaP cells subjected to IAD was assessed. Presence or absence of expression was investigated in untreated cells (LNCaP), after 5 d of AD (AD1), after 15 d in AD conditions supplemented with synthetic androgen (AD+R1881) and after a further 15 d period of AD (AD2). Detection was determined using melt curve analysis of PCa samples compared to human brain cDNA n=3.

GABA Receptor Subunit	LNCaP	AD1	AD + R1881	AD2
a1	+	+	+	+
a2	-	-	-	-
a3	+	+	+	+
a4	-	-	-	-
a5	+	+	+	+
a6	+	+	+	-
b1	-	-	-	-
b2	-	-	-	-
b3	+	+	+	+
g1	+	+	+	+
g2	-	-	-	-
g3	+	+	+	+
d	-	-	-	-
e	-	-	-	-
q	+	+	+	+
p	-	-	-	-
GABBR1	+	+	+	+
GABBR2	+	+	+	+

Interestingly, throughout IAD treatment, the same GABA_AR subunit transcripts were expressed, with the exception of the α 6 subunit, which became undetectable by the end of the second period of AD (Table 5.2). The loss of α 6 subunit expression is interesting because this subunit helps to anchor GABA_ARs to the cell surface (Peran *et al.*, 2004). Both GABA_BR were also detected throughout IAD. This data suggests that LNCaP PCa cells retain the potential capacity to form GABA_A and GABA_B receptors at each stage of IAD during two

successive AD periods. Next, the changes in expression level were quantitatively assessed using qRT-PCR (Figure 5.7).

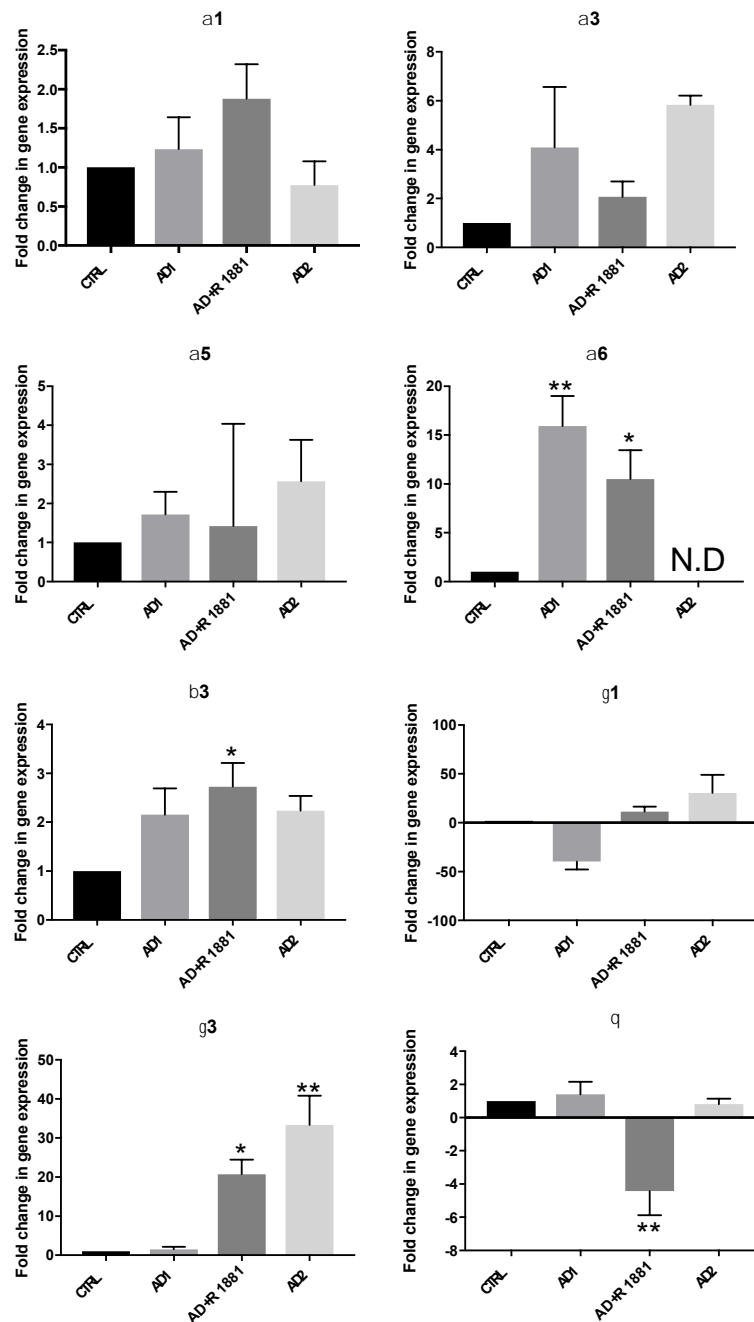


Figure 5.5 Expression of GABA_AR subunits in LNCaP cells subjected to IAD.

Relative expression of GABA_AR subunits in LNCaP cells that were either untreated (CTRL), subjected to 5 d AD (AD1), AD followed by cessation of AD (AD+R1881) or a second cycle of AD (AD2) after the AD cessation period, analysed via qRT-PCR normalised to ACTB. Data is expressed as mean ± SEM, (n=3) $p < 0.05$ (*) and $p < 0.01$ (**) as determined by one-way ANOVA with Dunnett's correction, N.D – not detected.

Analysis of GABA_AR subunit expression throughout IAD identified that subunit α 1 expression did not significantly change throughout IAD. The α 3 subunit was upregulated by the first (4-fold) and second (5.8-fold; $p = 0.07$) round of AD and was downregulated closer to basal levels by the intermediate period of cessation of AD (2-fold), rising again at the end of a second AD period. This would suggest that the α 3 subunit, which is known to be upregulated in non-small cell lung cancer and contribute to metastasis in breast cancer (Gumireddy *et al.*, 2016), is modulated by IAD. The α 5 subunit expression was slightly upregulated by the first round of AD (1.7-fold), appeared unchanged by AD cessation and was further upregulated after the second AD period (2.5-fold), although expression failed to become statistically significant compared to untreated cells. The α 6 subunit was significantly upregulated by AD (11-fold; $p = 0.003$), remained significantly upregulated during AD cessation ($p = 0.02$; 10.5-fold) and after the second round of AD, expression could not be detected.

The β 3 subunit was upregulated by AD (2.1-fold) and became significantly upregulated during AD cessation ($p = 0.03$; 2.7-fold), before returning to the same level as the first AD cycle by the end of the second cycle of AD (2.2-fold). This is particularly interesting because the β 3 subunit is thought to decrease the proliferation of hepatocellular carcinoma cells, considering the β 3 subunit is upregulated throughout IAD, this would fit with what would be expected during the application of AD to androgen-sensitive LNCaP cells and this upregulation is maintained even during AD cessation.

Expression of the γ 1 subunit was downregulated by 39.6-fold during AD and subsequently upregulated, 11.4-fold by AD cessation, expression continued to increase, reaching 30.6-fold by the second cycle of AD. The γ 3 subunit expression was unaffected by the first round of AD (1.5 fold; $p > 0.99$) but was significantly upregulated during AD cessation (20-fold; $p = 0.03$), continuing to rise dramatically to a 30-fold upregulation after the second cycle of AD ($p = 0.002$).

Overall, these experiments demonstrate that expression of GABAR subunits is differential between androgen-sensitive PCa cells and CRPC cells and that these cells could potentially possess functional GABARs. In addition, for the first time the differences in expression level have been quantified and the modulatory effect of androgen availability upon their expression has also been assessed. Finally, IAD appears to induce significant changes in GABA_AR subunit expression, in particular, a loss of $\alpha 6$ expression after a second period of AD after AD cessation.

5.2.5 Expression of CCCs during IAD

The effects of the GABA_AR can be both inhibitory and excitatory depending upon the polarity of the cell. Therefore, in order to gain a greater understanding of the potential involvement of the GABA_AR in a PCa setting, the expression of selected NKCC and KCC transporters was assessed using qRT-PCR. Although all KCC and NKCC were initially assessed for expression, only NKCC1, KCC1, KCC3 and KCC4 were detected. Interestingly, KCC2 which is a *de facto* biomarker of mature neurons (Ben-Ari, 2002), was not detected in any of the experimental conditions, including NED LNCaP cells. This would support the notion that NED PCa cells are utilising a hybrid phenotype and are not truly committed to a neuronal cell fate, but perhaps utilise certain advantageous aspects of the neuronal phenotype only.

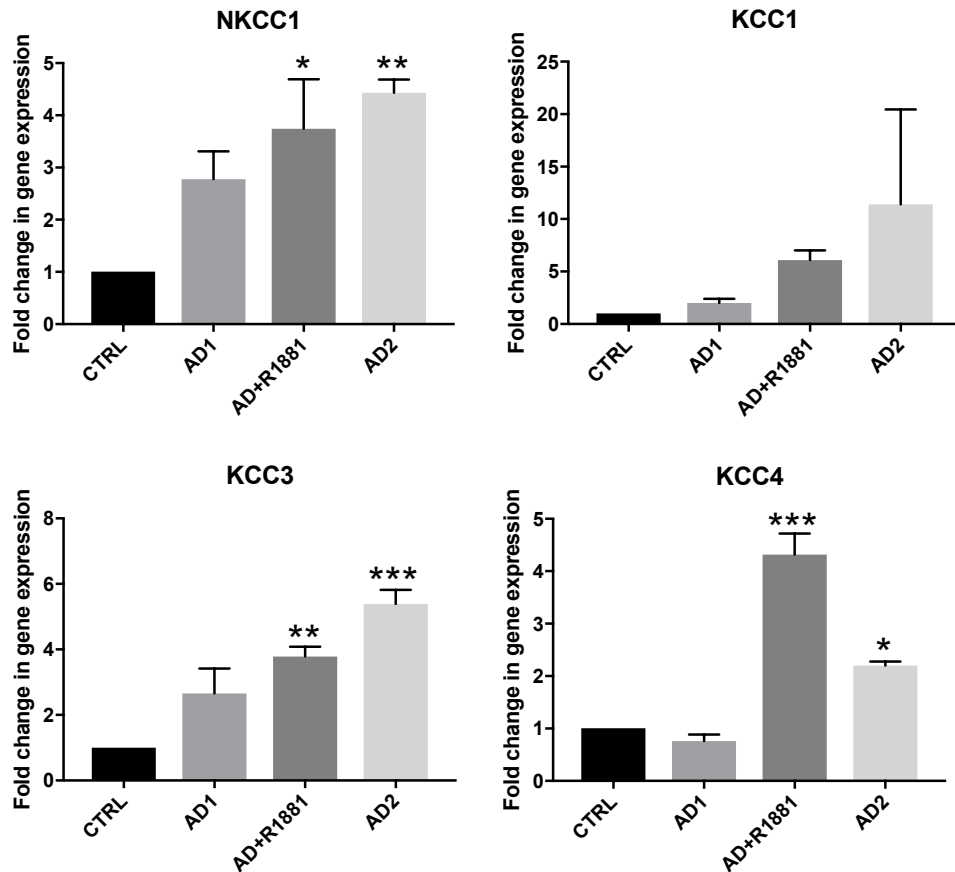


Figure 5.6 Expression of KCCs and NKCCs in LNCaP cells subjected to IAD.

Relative expression of NKCC1 and KCC1, 3 and 4 in LNCaP cells that were either untreated (CTRL), subjected to 5 d AD (AD1), AD followed by cessation of AD (AD+R1881) for 15 d or a second 15 d cycle of AD (AD2) after the AD cessation period, analysed via qRT-PCR, normalised to reference gene ACTB. Data is expressed as mean \pm SEM, (n=3) $p < 0.05$ (*), $p < 0.01$ (**) and $p < 0.001$ (***) as determined by one-way ANOVA with Dunnett's correction.

Overall, the expression of NKCC and KCC genes was significantly modified depending on the androgen availability in LNCaP cells (Fig. 5.6). NKCC1, responsible for chloride influx, was upregulated by AD (2.7-fold) and then, interestingly, became significantly upregulated (3.7-fold) during AD cessation ($p = 0.02$). Expression increased further (4.4-fold) following a second cycle of AD ($p = 0.006$). A similar trend was also observed with KCC1, which increased 2-fold after the first AD cycle, 6-fold during AD cessation and 11.4-fold after the second AD cycle, but failed to become statistically significant from untreated cells. KCC3 gene expression also showed a steady increase throughout IAD, being

upregulated by 2.6-fold the first cycle ($p = 0.08$) becoming significantly upregulated by 3.7-fold during AD cessation ($p = 0.007$) and increasing to 5.3-fold higher levels after a second AD cycle ($p = < 0.001$). Expression of KCC4 was slightly lower under AD conditions compared to untreated cells, was significantly upregulated by 4.3-fold during AD cessation ($p = < 0.001$), and remained elevated at the end of a second round of AD (2.2-fold; $p = 0.03$).

5.2.6 The effect of AD and IAD on GABA_BR expression

Following assessment of GABA_AR subunit expression, the expression of GABA_BR subunits in response to AD and IAD was assessed. Importantly, GABA_BRs are G-protein coupled receptors which are not influenced by the chloride gradient of cells and therefore function independently of NKCC and KCC activity.

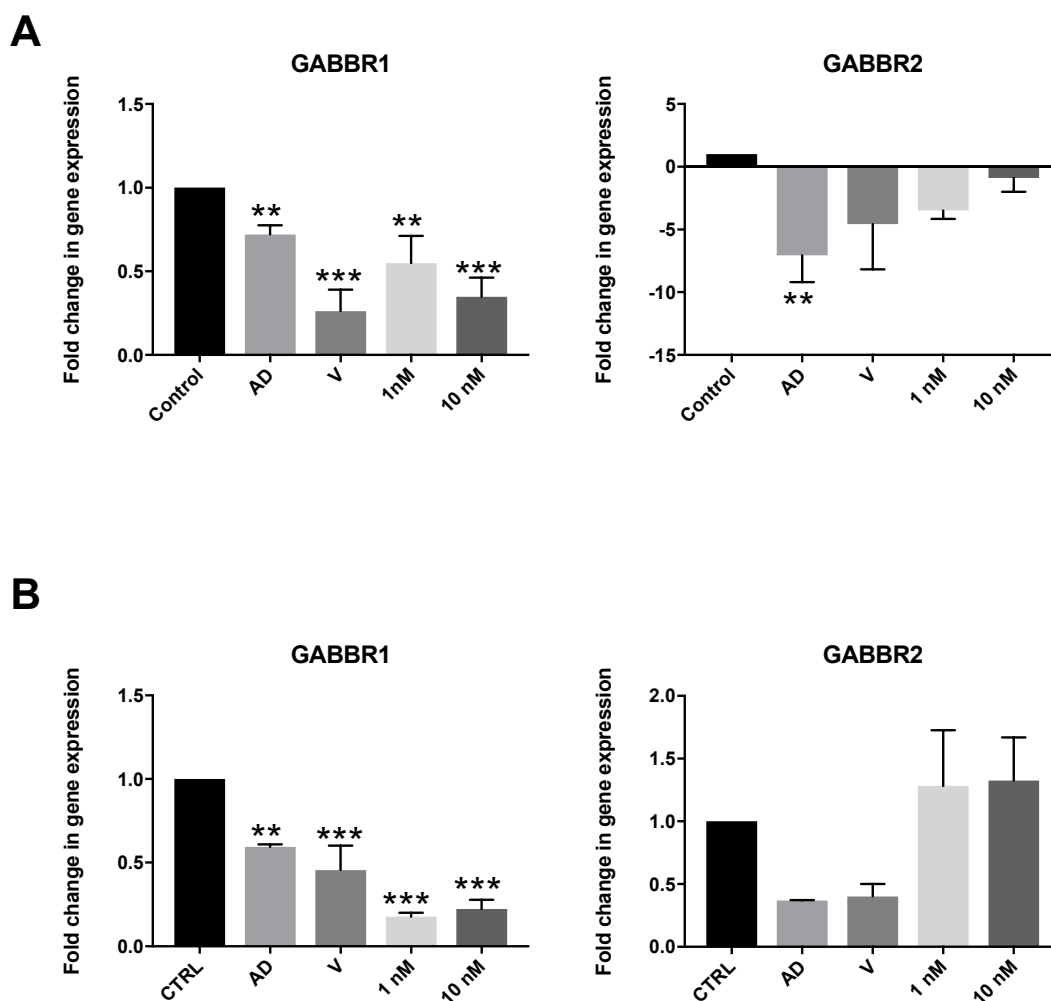


Figure 5.7 Expression of GABA_BR subunits in LNCaP cells subjected to AD. Relative expression of GABA_BR subunits in LNCaP cells analysed via qRT-PCR that were (A) either untreated (CTRL), subjected to 5 d of AD (AD) or 5 d of AD conditions supplemented with either DMSO vehicle (V) or R1881 at 1 nM or 10 nM concentrations. (B) Shows data for LNCaP cells that exposed to a longer, 15 d AD. Data is expressed as mean ± SEM, (n=3) $p < 0.05$ (*), $p < 0.01$ (**) and $p < 0.001$ (***) as determined by one-way ANOVA with Dunnett's correction.

After 5 days of AD, expression of GABBR1 and GABBR2 was significantly downregulated in LNCaP cells (0.72-fold $p = 0.004$ and 2.7-fold $p = 0.0026$ respectively). Expression of GABBR1 remained significantly downregulated when 1 nM (0.5-fold; $p = 0.001$) and 10 nM (0.34-fold; $p < 0.001$) of R1881 was present in AD media (Fig 5.11), which suggests that changes in GABBR1 expression during AD were not mediated by androgen availability. Following 15 days AD, GABBR1 was significantly downregulated (0.5-fold; $p = 0.004$).

Interestingly, supplementation to AD condition with 1 nM ($p < 0.001$) and 10nM ($p < 0.001$) R1881 further depressed GABBR1 expression, suggesting that GABBR1 expression is not specifically modulated by AD. GABBR2 expression was significantly downregulated (7-fold-fold, $p = 0.0026$) after five days AD and this downregulation was somewhat ameliorated by the presence of 1 nM (3.4-fold) and 10 nM (0.8-fold) R1881 in culture media, suggesting that GABBR2 expression is at least partly influenced by androgen availability. This effect was also observed when LNCaP cells were treated for a longer 15 d period. This data further supports that expression of GABBR2 may be changeable in relation to androgen availability in LNCaP cells. The GABA_BR is an obligate heterodimer (Gassmann & Bettler, 2012), so effects on GABBR2 would also mediate effects on the entire GABA_B receptor since GABBR2 subunit is needed to allow the GABBR1 subunit to leave the endoplasmic reticulum (Benarroch, 2012).

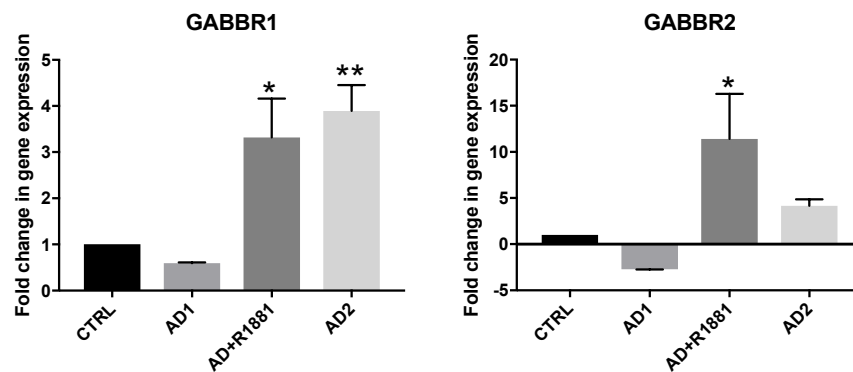


Figure 5.8 Expression of GABA_BR subunits in LNCaP cells subjected to IAD.

Relative expression of the two GABA_BR subunits in LNCaP cells that were either untreated (CTRL), subjected to 15 d AD (AD1), AD followed by cessation of AD (AD+R1881) or a second cycle of AD (AD2) after the AD cessation period, analysed via qRT-PCR, normalised to reference gene ACTB. Data is expressed as mean \pm SEM, (n=3) $p < 0.05$ (*), $p < 0.01$ (**) and $p < 0.001$ (***) as determined by one-way ANOVA with Dunnett's correction.

The expression of GABBR1 and GABBR2 was also assessed throughout IAD. As seen previously, expression of GABBR1 was downregulated by the first AD period but surprisingly was significantly upregulated (3.3-fold; $p = 0.02$) after 15 d of AD cessation and remained significantly upregulated (3.8-fold; $p = 0.005$) after the second AD period. Although unexpected, a possible explanation is that over this longer experimental time course, the level of GABBR1 is adjusting to the availability of GABBR2, which is supported by the data showing that the trend in GABBR1 and GABBR2 expression are in sync. During IAD GABBR2 expression decreased 2.7-fold after the first AD period, was significantly upregulated by AD cessation (11.4-fold; $p = 0.04$) and remained elevated above basal levels (although not significantly) by the end of the second AD period (4.1-fold).

5.2.7 GABA synthesis and metabolism pathways during IAD

Having established the presence of GABAR subunits in PCa cell lines and that expression of some of these subunits appeared to be responsive to AD, GABA signalling related gene expression was investigated (Fig 5.11).

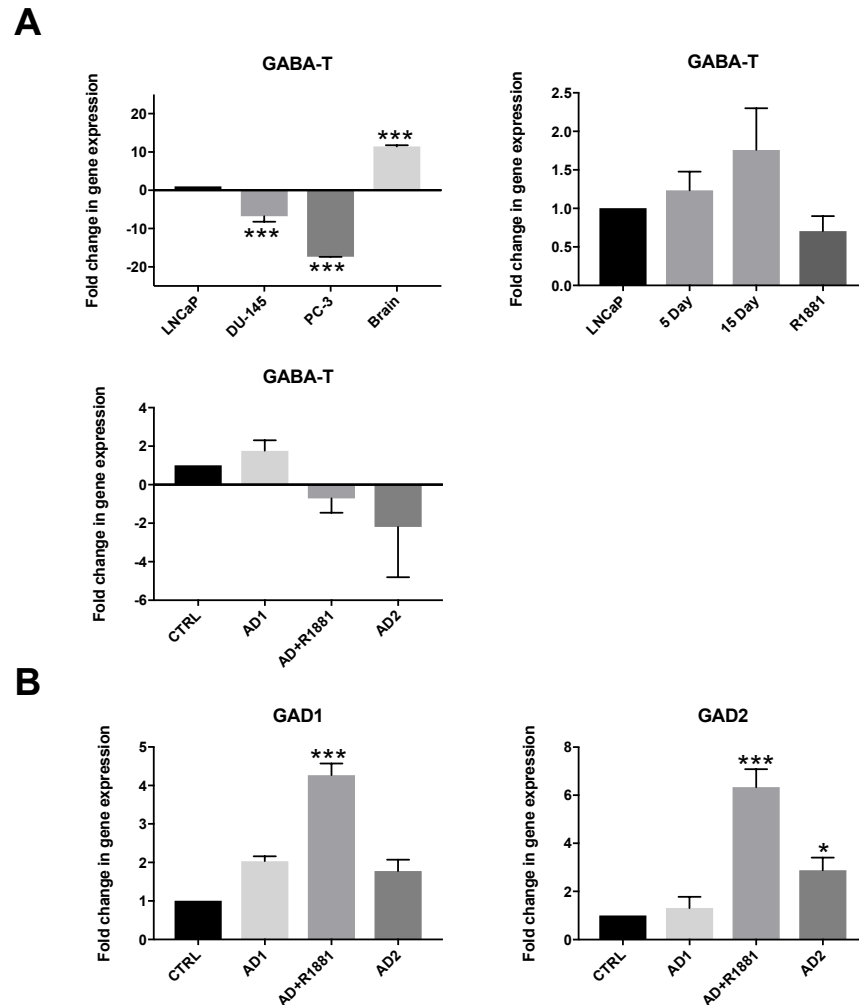


Figure 5.9. Expression of GABA synthesis and metabolism genes GAD1, GAD2 and GABA-T in PCa cells subjected to AD or IAD. (A) Relative expression of GABA transaminase (GABA-T) in LNCaP, DU-145 and PC-3 cells, or in LNCaP cells at five and fifteen days of AD and during IAD. **(B)** Relative expression of glutamate decarboxylase 1 and 2 (GAD1 and GAD2) in LNCaP cells subjected to IAD as follows, cells that were either untreated (CTRL), subjected to 15 d AD (AD1), AD followed by cessation of AD (AD+R1881) or a second cycle of AD (AD2) after the AD cessation period, analysed via qRT-PCR normalised to reference gene ACTB. Data is expressed as mean \pm SEM, (n=3) $p < 0.05$ (*), $p < 0.01$ (**), and $p < 0.001$ (***) as determined by one-way ANOVA with Dunnett's correction.

The metabolism of GABA has previously been proposed as a mechanism of survival in PCa cells in response to stress by providing alternative inputs to the TCA cycle and overexpression of GABA synthesis enzyme GAD1 is correlated with decreased patient survival (Ippolito & Piwnica-Worms, 2014). GABA transaminase (GABA-T) was assessed across a range of PCa cells and brain tissue. CRPC cells had significantly lower ($p = < 0.001$) expression (up to 15-fold) expression of GABA-T when compared to untreated LNCaP cells. Subjecting LNCaP cells to AD showed a small increase (1.2-fold) in GABA-T expression at 5 d of AD, rising slightly further (1.7-fold) by 15 days of AD. maintenance of androgen in the AD media via R1881 supplementation lowered the expression of GABA-T (0.7-fold). During IAD, GABA-T expression was downregulated to 0.7-fold during AD cessation, and further downregulated (2.19-fold) after the second period of AD, although not significantly. Of interest is that CRPC cell lines DU-145 and PC-3 displayed significantly lower GABA-T expression than LNCaP cells (6.7-fold; $p = < 0.001$ and 17.3-fold; $p = < 0.001$, respectively). This could suggest that CRPC cells may have less GABA catabolic activity, perhaps because they favour an environment richer in GABA, or potentially that LNCaP cells are preferentially utilising GABA to facilitate growth and survival.

Expression of GAD1 was upregulated by 2-fold ($p = 0.09$) during AD (Fig 5.11 panel B) and significantly upregulated, by 4.2-fold, during AD cessation ($p = < 0.001$), returning back to similar levels (1.7-fold) seen during the initial AD by the end of the second AD cycle (Fig. 5.9). Similarly, GAD2 was significantly upregulated (6.3-fold) during NED reversal ($p = < 0.001$) and remained significantly above basal levels (2.8-fold) after the second cycle of AD ($p = 0.04$). Interestingly, previous investigations into GAD1 expression in PCa did not detect GAD1 in LNCaP cells, but did in CRPC cell lines (Ippolito & Piwnica-Worms, 2014). The increased expression of both GAD1 and GAD2 would suggest that successive rounds of AD are selecting for LNCaP cells with higher potential to produce GABA, which would coincide with the hypothesis that NED PCa cells may exert effects through GABAergic signalling. Furthermore, GAD2 is preferentially expressed during development and is significantly upregulated by AD cessation, which coincides with the loss of NED morphology, perhaps

supporting the idea that early developmental transcriptional profiles are utilised to facilitate the change in LNCaP cell fate (e.g. the Notch1 pathway).

5.2.8 Effect on cell viability of GABA_AR and GABA_BR agonists

GABA_AR agonist muscimol and GABA_BR agonist baclofen were used to investigate the effect of GABA_AR and GABA_BR agonism on LNCaP and NED LNCaP gene expression. Concentrations of muscimol and baclofen were derived from the literature (Abdul *et al.*, 2008.; Azuma *et al.*, 2003). The effect of muscimol and baclofen on cell viability was first assessed using Alamar blue assay (Fig. 5.10). A range of concentrations between 1-500 μ M and ethanol vehicle at a concentration of 0.01% were assessed. Analysis of the data showed that neither muscimol, baclofen or the vehicle ethanol impacted cell viability. Therefore, this range of concentrations was used to investigate the effect of GABA_AR and GABA_BR agonism on LNCaP and NED LNCaP cells (Fig. 5.11) and this dose range and treatment length has been previously used in the literature (Abdul *et al.*, 2008.; Azuma *et al.*, 2003).

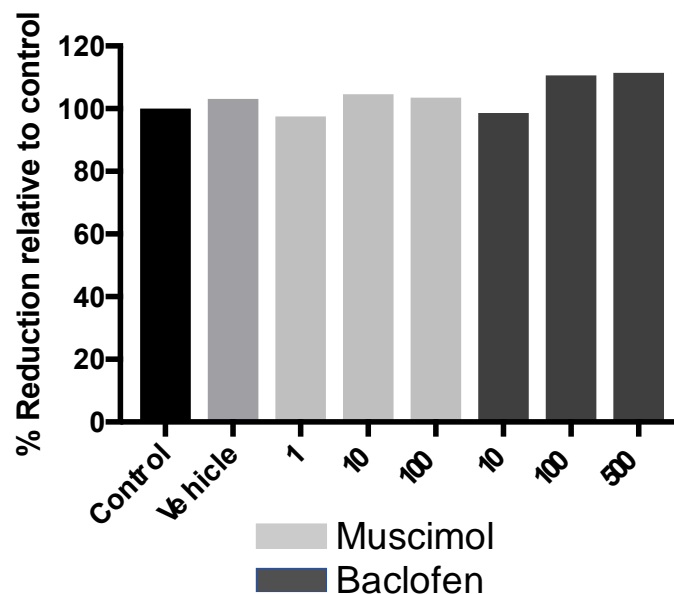


Figure 5.10 Assessment of muscimol, baclofen and ethanol vehicle on LNCaP cell viability. LNCaP cells were cultured in the presence of 1, 10 and 100 μ M muscimol, 10, 100 and 500 μ M baclofen or vehicle only with the reduction of Alamar blue reagent shown relative to untreated LNCaP cells. Ethanol was used as a vehicle at a final concentration of 0.1% (n=1).

5.2.9 Effects of muscimol and baclofen on NED LNCaP gene expression

Having established the presence of GABAR subunits in PCa cells, the next aim was to investigate if these subunits might form functional receptors and to delineate whether these receptors exerted changes upon NED pathway associated gene expression and whether these were likely mediated by GABA_A or GABA_B receptor populations.

Muscimol is a highly specific agonist of the GABA_AR, whilst baclofen is a highly specific agonist of the GABA_BR (Napoleone, 1990). To investigate the potential effects on the NED pathway of GABA_A or GABA_B receptor agonism in LNCaP cells, drugs were added to normal cell culture media (10% FBS) for 48 h, LNCaP cells treated with vehicle in full media and AD LNCaP cells were included for comparison. Analysis of AR expression revealed a slight increase when LNCaP cells were treated with 1 μ M of muscimol but not at 10 μ M or 100 μ M whereas, the GABA_BR agonist baclofen appeared to have little effect upon AR expression (Fig. 5.11). Expression of PSA was also largely unaffected by treatment with either muscimol or baclofen compared to the vehicle control. Expression of NED related genes PTOV1, REST and NSE also remained stable during muscimol and baclofen treatments, with a slight decrease in NSE expression at 10 and 500 μ M baclofen. MMP-9 expression has previously been demonstrated to be upregulated by baclofen in the rat hippocampus (Car & Michaluk, 2012) and this mechanism has been demonstrated to be conserved in the setting of PCa (Azuma *et al.*, 2003). In this study, the increase in MMP-9 expression in response to baclofen was not observed, with MMP-9 expression significantly decreased in the presence of 500 μ M baclofen. This is likely because in this study baclofen was applied to NED PCa cells and not to previously untreated PCa cells, in addition the present study utilised LNCaP cells, whereas Azuma *et al.* (2003) used the C4-2 CRPC sub-line of LNCaP (Azuma *et al.*, 2003). This could suggest that whilst NED PCa cells possess greater potential for GABA production, perhaps it is other subtypes of CRPC cells which are GABA sensitive. Overall, it would appear that varying concentrations of muscimol and baclofen had no effect upon gene expression in the panel of genes associated with NED LNCaP cells.

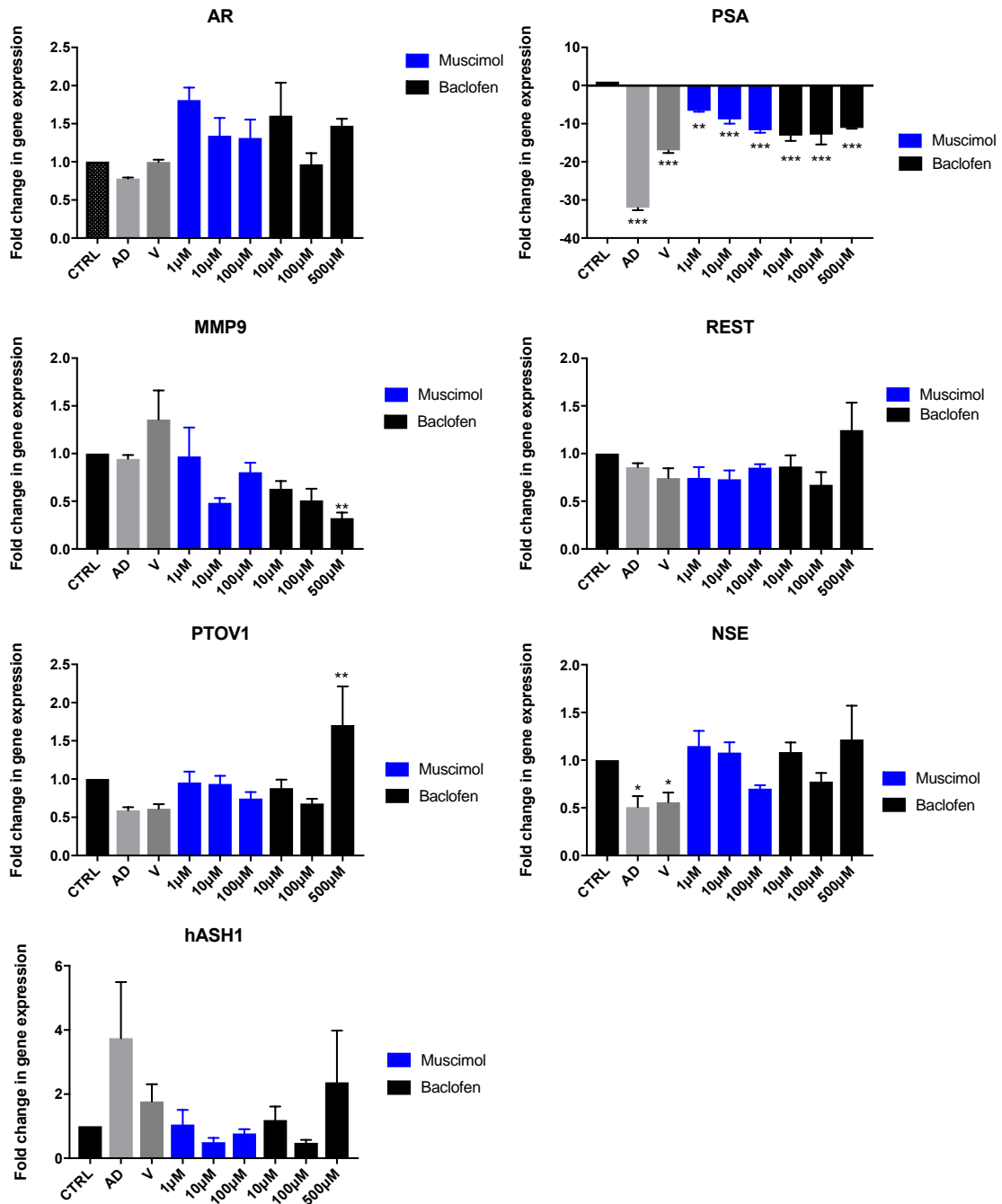


Figure 5.11 Effect of muscimol and baclofen on LNCaP gene expression.

Relative expression of a key panel of genes involved in NED in LNCaP cells that were either untreated (CTRL), subjected to 15 d androgen deprivation (AD), for the final 48 hours of AD, cells were treated with ethanol vehicle control (V) or muscimol (1-100 µM) or baclofen (10-500 µM) and analysed via qRT-PCR, normalised to reference gene ACTB. Data is expressed as mean ± SEM, (n=3) $p < 0.05$ (*), $p < 0.01$ (**) and $p < 0.001$ (***) as determined by one-way ANOVA with Dunnett's correction.

5.2.10 Effect of Gabapentin on NED pathway associated genes in LNCaP cells

Gabapentin (GBP) is a painkiller that is frequently prescribed to manage the pain of PCa patients, particularly when painful bone metastases have occurred or spinal cord compression (Costigan, 2009). GBP is also used to treat hot flushes in patients treated with ADT (Moraska *et al.*, 2010). A recent study demonstrated that in an *in vivo* rat model of PCa, administration of GBP significantly increased metastasis and reduced survival time (Bugan *et al.*, 2016). Importantly, although GBP mimics the chemical structure of GABA (Honarmand, Safavi, & Zare, 2011), it is not active at GABA_A or GABA_BRs (Goa & Sorkin, 1993; Kammerer *et al.*, 2011; Taylor *et al.*, 1992). Instead, the mechanism of action for GBP is thought to be as a ligand for the voltage-activated calcium channel (VACC), of which the $\alpha 2\delta$ calcium ion channel protein, which is expressed in prostate tissue (Chen *et al.*, 2014; Rao *et al.*, 2015; Scholl *et al.*, 2013), and acts as an inhibitor. It is this action on calcium ion channels that is thought to block synaptic transmission and alleviate neuropathic pain (Calandre *et al.*, 2008). Up-regulation of CACNA1D, a gene encoding one of the $\alpha 2\delta$ subunits, is implicated in PCa progression (Scholl *et al.*, 2013), suggesting that potential sensitivity to GBP would also increase during PCa progression. In addition, GBP is known to increase the availability of GABA in brain tissue (Cai *et al.*, 2012), an effect which could potentially also occur within a PCa tumour. Furthermore, GBP has been demonstrated to increase GABA synthesis and non-synaptic GABA neurotransmission via its effects on GAD1 and GAD2 (Taylor, 1997). Given the widespread use of GBP by PCa patients, and the previous evidence of cancer modulatory activity of both GABA (which can be enriched during GBP treatment) (Cai *et al.*, 2012; Taylor *et al.*, 1997; Taylor *et al.*, 1998) and GBP itself (Bugan *et al.*, 2016) the gene expression changes of LNCaP cells treated with GBP was investigated. Concentrations and treatment times of GBP were derived from the literature (Bugan *et al.*, 2016).

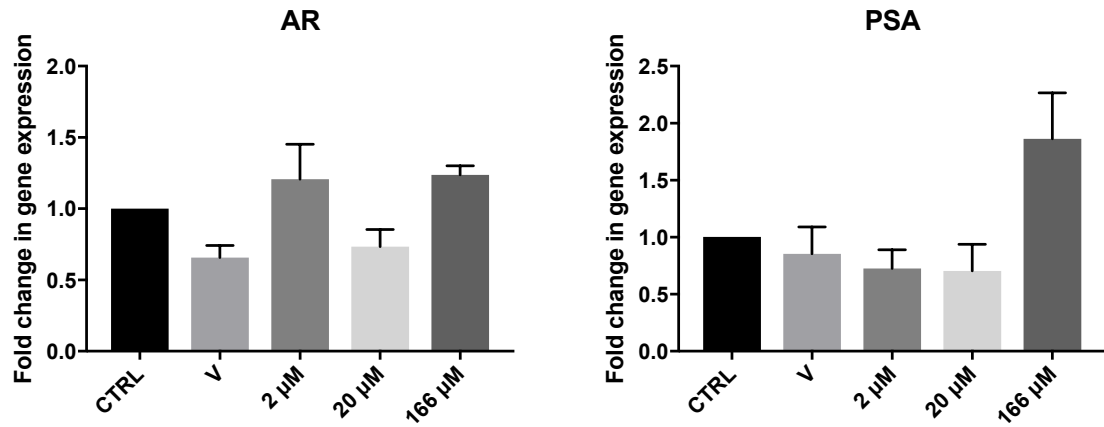


Figure 5.12 Effect of gabapentin on LNCaP cell AR and PSA expression in LNCaP cells not subjected to AD. Relative expression of AR and PSA in LNCaP cells that were either treated with ethanol vehicle control or Gabapentin (2-166 μ M), analysed via qRT-PCR, normalised to reference gene ACTB. Data is expressed as mean \pm SEM, (n=3), statistical analysis was performed using one-way ANOVA with Dunnett's correction.

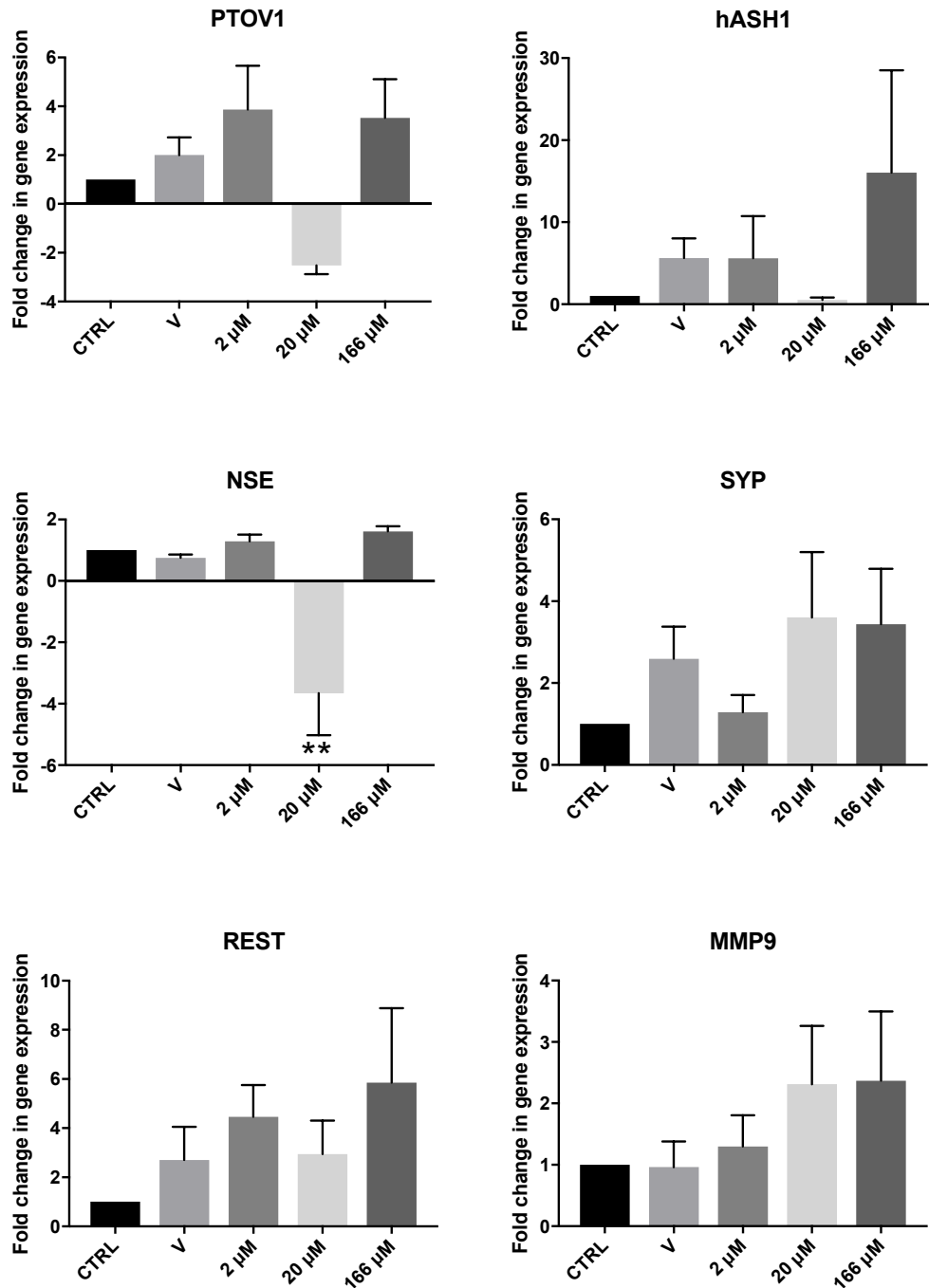


Figure 5.13 Effect of gabapentin on key NED related genes in LNCaP cells not subjected to AD. Relative expression of a key panel of genes relating to NED in LNCaP cells treated with ethanol vehicle control or Gabapentin (2-166 μ M), analysed via qRT-PCR, normalised to reference gene ACTB. Data is expressed as mean \pm SEM, (n=3) $p < 0.01$ (**) as determined by one-way ANOVA with Dunnett's correction.

Expression of AR and PSA did not appear to be affected by GBP treatment. Similarly to the previous investigation of drugs influencing the GABA receptor and the findings of (Bugan *et al.*, 2016), it was found that the response to GBP was dependent on the concentration. PTOV1 expression was elevated by 2 and 166 μM of GBP (3.8-fold and 3.5-fold), but downregulated by 20 μM (2.5-fold). The same effect was seen on the expression of hASH1 with 20 μM reducing expression to below basal (0.5-fold). In contrast, 166 μM caused upregulation (16-fold) but variability in this experiment was very high. Consistent with these findings, NSE was significantly downregulated by 166 μM of GBP (3.6-fold; $p = 0.001$) but remained close to untreated levels when treated with 2 and 166 μM GBP. This trend was also observed in REST expression which was higher with 2 μM and 166 μM than with 20 μM GBP treatment. Interestingly, under GBP treatment the expression profile of hASH1 and NSE were closely related, with NSE at lowest expression when hASH1 was also at lowest expression when treated with 20 μM GBP. MMP-9 expression has previously been demonstrated to be inducible by GABA (Azuma *et al.*, 2003) and GBP is known to increase the levels of GABA (Cai *et al.*, 2012), leading to speculation that GBP might indirectly induce MMP-9 expression, although this did not occur in this dataset, this could be because expression was only assessed at one timepoint (48 h).

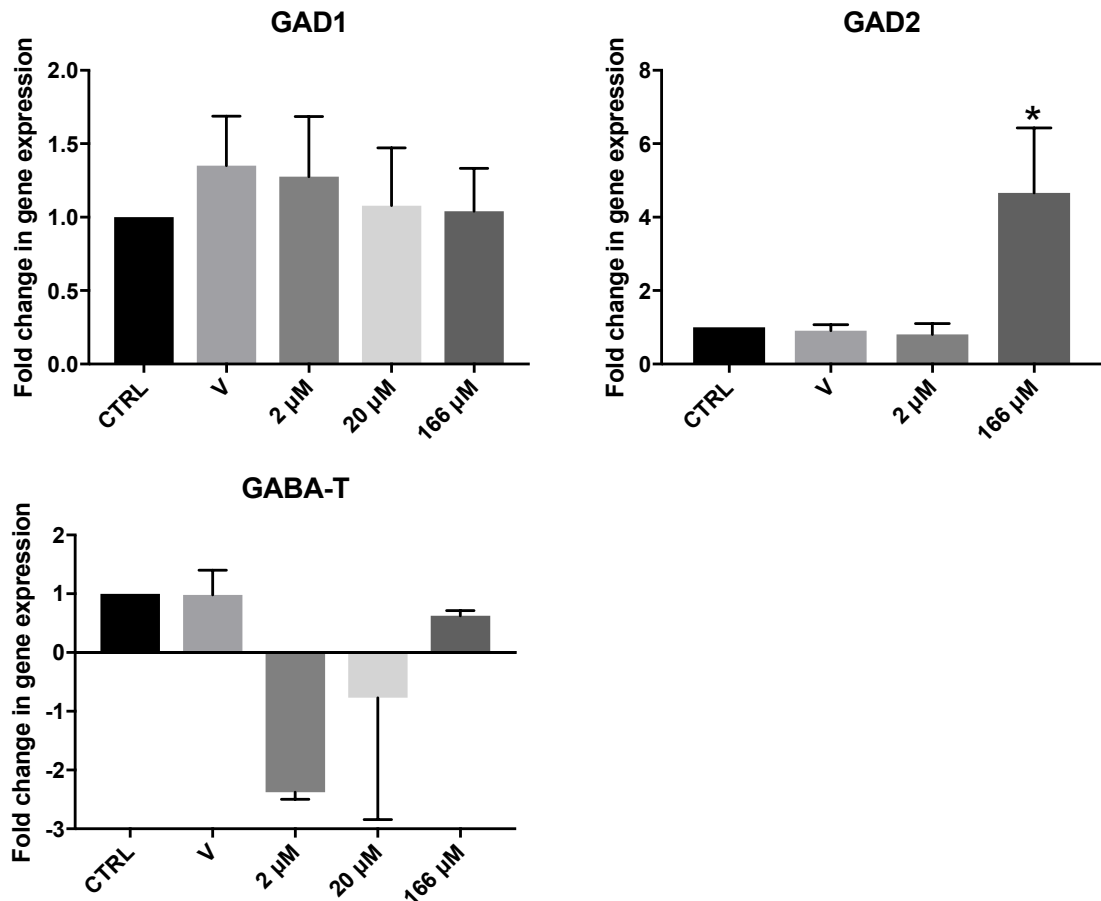


Figure 5.14 Effect of gabapentin on key GABA synthesis and metabolism related genes in LNCaP cells not subjected to AD. Relative expression of the two isoforms of glutamate decarboxylase (GAD1 and 2) and GABA transaminase (GABA-T) in LNCaP cells treated with ethanol vehicle control (V) or Gabapentin (2-166 μM), analysed via qRT-PCR, normalised to reference gene ACTB. Data is expressed as mean ± SEM, (n=3) $p < 0.05$ (*) as determined by one-way ANOVA with Dunnett's correction.

Interestingly, expression of GAD1, which encodes GAD67, was unchanged by GBP treatment, however at 166 μM the expression of GAD2, encoding GAD65, was significantly upregulated (4.6-fold; $p = 0.02$) (Fig. 3.16), which is consistent with a previous publication asserting that GBP increases GABA synthesis in rat brain tissue (Taylor, 1997). Interestingly, consistent with the upregulation of GABA synthesis enzyme GAD2, GABA-T a GABA metabolic enzyme was downregulated by 2 and 20 μM of GBP (2.3-fold; $p = 0.09$ and 0.7-fold, respectively). This is consistent with previous studies showing that GBP

increases the level of GABA in the brain tissue (Cai *et al.*, 2012) and would support the suggestion that a similar effect could manifest in PCa cells or potentially tumours.

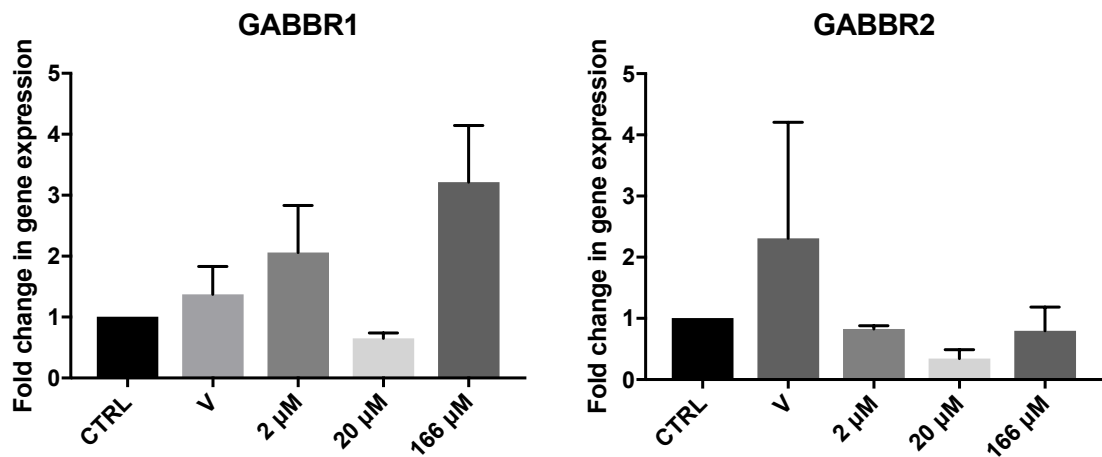


Figure 5.15 Effect of gabapentin GABA_BR subunit gene expression in LNCaP cells not subjected to AD. Relative expression of GABA_BR subunits in LNCaP cells treated with ethanol vehicle control (V) or gabapentin (2-166 µM), analysed via qRT-PCR, normalised to ACTB. Data is expressed as mean ± SEM, (n=3), statistical significance was determined by one-way ANOVA with Dunnett's correction.

Although GBP is not thought to directly interact with GABARs, the expression of GABBR1 and GABBR2 was slightly suppressed by 20 µM GBP treatment, although not significantly. Given that GAD1 and GAD2 both synthesise GABA, it is possible that GABA synthesis feedback mechanisms are being stimulated by the presence of GBP at specific concentrations. Interestingly, higher concentrations of GBP actually increased the expression of GABBR1 3.2-fold, but failed to reach statistical significance. For both GABBR1 and GABBR2, 20 µM of GBP caused the strongest downregulation of expression. Higher than expected variability was observed in GABBR2 expression when treated with vehicle, most likely due to technical error which is accentuated by the overall low expression of GABAR subunits in PCa cells.

Overall, the investigation into the effects of GBP on LNCaP gene expression demonstrated that GBP can have dose dependent effects upon the expression of genes proposed to be key to PCa NED including PTOV1, hASH1 and NSE. Furthermore, the analysis of genes involved in GABA synthesis and metabolism revealed that GBP may be able to increase GABA levels in prostate, a mechanism which has previously been described in brain tissue (Cai *et al.*, 2012). Although this initial assessment of GBP effects on LNCaP cells, future experiments will seek to identify if NED LNCaP cells may respond differently or if the expression of GABA_AR subunits is influenced by GBP. In a broader outlook, these experiments highlight the potential for non-oncological pharmaceuticals that are frequently prescribed to cancer patients to have unexpected modulatory effects upon cancer cells.

5.3 Discussion

Previous experiments implicated hASH1 as a driver of PCa NED (Chapter 3 & 4). hASH1 is known to promote the development of GABAergic neurons (Mazurier *et al.*, 2014; Peltopuro *et al.*, 2010). Therefore, the overall aims of this chapter were to establish whether prostate cancer (PCa) cells express the necessary GABAR subunits to form functional GABARs and assess how AD, IAD and NED effect their expression. Next, it was assessed whether PCa cells and NED PCa cells were sensitive to GABAergic compounds. The key contribution of this body of work has been to robustly map the expression of GABA_A and GABA_BR subunits in the classical PCa cell lines and during NED in response to IAD. This is a useful tool for those researching the GABAergic effects and sensitivity of this disease, something which is a growing area of research (Ippolito & Piwnica-Worms, 2014; Wu *et al.*, 2014; Xia *et al.*, 2017) and is currently operating without a good knowledge of GABAR status under these conditions. Previously, quantitative assessment of GABAR subunit expression has never been performed in these cell lines or under IAD conditions.

5.3.1 Presence of GABA_A and GABA_BR subunits in PCa cell lines

As an initial exploratory assessment of the potential for PCa cells to form GABARs, the expression of GABA_AR and GABA_BR subunits was assessed in the

classical PCa cell lines LNCaP, DU-145 and PC-3. Interestingly, expression of GABA_AR α subunits was exclusive to the androgen-sensitive LNCaP cells (Fig 5.3). The α 3 subunit is known to contain an AR consensus site within its promoter region (Steiger & Russek, 2004) and was only expressed in androgen-sensitive LNCaP cells, however, expression of the α 3 subunit was actually slightly upregulated during AD. This would suggest that the α 3 subunit expression is being modulated by other transcription factors independent of the AR. In contrast, the only other GABA_AR subunit with an AR consensus site (the γ 1 subunit) did appear to be modulated by androgen availability in LNCaP cells (Fig. 5.4). Whilst all PCa cell lines tested expressed at least one β and γ subunit. This would suggest that both CRPC cell lines used in this study (DU-145 and PC-3) are likely to lack the ability to form functional GABA_ARs, which typically require two α , two β and one γ subunit to form a functional heteropentamer (Akinci & Schofield, 1999). However, expression of both the prerequisite GABA_BR subunits was detected in androgen-sensitive LNCaP cells and both CRPC cell lines.

A previous study has detected expression of the α 6 subunit via immunoblot analysis in LNCaP, DU-145 and PC-3 cells (Abdul *et al.*, 2008). Expression of the α 6 subunit is associated with anchoring the completed GABA_AR to the cell surface (Abdul *et al.*, 2008). As such, the α 6 subunit has previously been used as a biomarker for functional GABA_ARs (Abdul *et al.*, 2008), the data herein supports that LNCaP cells express α 6 subunit, although expression of α 6 was not detected in DU-145 and PC-3 via qRT-PCR.

Another difference in GABA_AR subunit expression between LNCaP and CRPC cell lines was that LNCaP cells did not express the β 1 subunit, whilst both CRPC cell lines had β 1-subunit expression (Table 5.1). Furthermore, none of the PCa cell lines investigated co-express more than one of the components of the major mammalian heteropentamer (α 1, β 2, γ 2) (Olsen & Sieghart, 2008). Interestingly both LNCaP and PC-3 cells express the β 3 subunit, which is the only subunit capable of forming functional homomeric GABA_ARs (Miller & Aricescu, 2014). This could potentially allow PC-3 cells to form GABA_ARs despite lacking

expression of any α subunits, however, a GABA_AR of that composition would lack the GABA binding site (Jacob *et al.*, 2008). Previously, it has been reported that high GABBR2 alongside low $\alpha 3$ expression results in better prognosis for non-small cell lung cancer patients (Zhang *et al.*, 2013) and $\alpha 3$ is typically overexpressed in this cancer type (Gumireddy *et al.*, 2016), considering that this data shows that LNCaP express the $\alpha 3$ subunit, whilst CRPC cell lines do not, this would suggest that a similar relationship is not present in the PCa setting, or may indeed be inverse.

The θ subunit of the GABA_AR has previously been shown to specifically facilitate GABA mediated growth of hepatocellular carcinoma (Li *et al.*, 2012) and in the present study was detected in LNCaP and DU-145 cells but not PC-3. What is particularly interesting is that the θ subunit grants additional pharmacological properties to $\alpha 3\beta 1$ containing GABA_ARs that would normally require the presence of a $\beta 1$ or $\beta 2$ subunit (Ranna *et al.*, 2006). This is especially interesting, because LNCaP cells do not express the $\beta 1$ or $\beta 2$ subunits, whilst these are two of the most expressed subunits in CRPC cell lines PC-3 and DU-145. Furthermore, PC-3 cells were the only PCa cell line tested found to express both $\beta 1$ and $\beta 2$ subunit but does not express the θ subunit (Fig. 5.2). This data supports the notion that the θ subunit is substituting the lack of $\beta 1$ and $\beta 2$ subunit expression in LNCaP cells.

The only other presence and absence study conducted for GABA_AR subunit expression in PCa LNCaP and PC-3 cells used semi-quantitative RT-PCR (Wu *et al.*, 2014). In comparison to the findings in this study, there are many results in agreement and many which are differential. For example, in LNCaP cells, both the present study and the previous study assert that the $\alpha 1$, $\alpha 3$, $\alpha 5$, $\alpha 6$, $\beta 3$ and θ subunits are expressed and that $\alpha 2$, $\beta 1$ and $\beta 2$ were not detected. In conflict with a previous study, the $\gamma 1$ and $\gamma 3$ subunits were detected and the $\alpha 4$, $\gamma 2$, δ , ϵ and π subunits were not (Wu *et al.*, 2014). In PC-3 cells, the majority of these findings conflicts with the Wu *et al.* (2014) study, only the $\beta 3$ and $\gamma 1$ subunits were detected in both studies. Interestingly, Wu *et al.* (2014) detected expression of

four out of six α subunits, whilst this study did not detect any α subunits in PC-3 (Fig. 5.2). The overall low level of expression of GABAR subunits is consistent with the low TPM values reported in online databases such as EMBL-EBI gene expression atlas for prostate tissue.

5.3.2 Expression of GABA_ARs and GABA_BRs subunits in PCa cell lines

Data in this study suggests that LNCaP cells preferentially expressed the α 3 and β 3 subunits, whilst the most prominent subunit in PC-3 cells was β 2 (also observed in brain) and in DU-145 it was the γ 1 and β 1 subunits that showed strongest expression. Interestingly, the α 3 subunit, which is usually well expressed at birth in the mammalian brain, before receding in adulthood (Laurie, Wisden, & Seeburg, 1992; Ohlson *et al.*, 2007) was the most expressed subunit in LNCaP cells. Furthermore, RNA editing of the α 3 subunit is thought to be a key mediator of the shift from excitatory to inhibitory function of the activated GABA_AR (Ohlson *et al.*, 2007), as the RNA editing of this subunit can affect its properties (Nimmich, Heidelberg, & Fisher, 2009). RNA editing generally has also been implicated in the growth, progression and metastasis of cancer (Peng *et al.*, 2018). This could be an indicator that the expression profile of GABAR subunits in undifferentiated LNCaP cells more closely resembles that of the developing brain, rather than mature, which would be supported by the lack of detected KCC2 expression via qRT-PCR or immunoblot (Li & Xu, 2008). Although definite conclusions cannot be formed from expression data alone, this data would suggest that if GABA_ARs are functional within LNCaP cells, they are more likely to be excitatory rather than inhibitory (Ben-Ari, 2002), although this is dependent upon CCC expression profiles (Li & Xu, 2008). Although only mRNA expression of GABAR subunits was assessed, functional GABARs have previously been identified in the prostate and seminal vesicles of the rat, suggesting that GABARs could possibly be present in human prostate (Napoleone *et al.*, 1990).

5.3.3 Effect of AD on GABA_AR and GABA_BR subunit expression

Following discovery of GABA_AR subunit expression in LNCaP cells, the effects of androgen deprivation (AD) induced NED on the expression of GABA_AR subunits in LNCaP cells was investigated. Using heat maps to show relative expression suggested little change in subunit expression, except the α 3 subunit which was more prominently expressed after androgen deprivation and is known to be important to neuronal development, where α 3 subunits are gradually replaced with α 1 subunits during the switch from excitatory to inhibitory GABA_AR activity (Succol et al., 2012). The expression of GABA_AR subunit expression and GABA_AR composition is known to change during the development of canonical neurons (Neelands *et al.*, 1999). Expression of the α 3 subunit was suppressed when 1 nM and 10 nM of R1881 were supplemented to AD conditions, which would appear to suggest that the observed increase after AD may be genuine. Meanwhile, expression of the α 1 subunit, which is important for the anchoring of GABA_ARs to the cell surface (Peran *et al.*, 2004), did not appear to be altered by androgen availability.

The α 5 subunit was slightly upregulated by both AD and 10 nM of R1881, suggesting that α 5 expression was not altered by AD. The α 6 subunit was the most upregulated subunit by AD (15-fold), however was only statistically significant in the presence of vehicle in AD conditions, R1881 supplementation prevented this upregulation, supporting the notion that α 6 expression might be modulated by androgen availability. This is particularly interesting because the α 6 subunit, along with the α 1 subunit, helps to anchor GABA_ARs to the cell surface (Peran *et al.*, 2004) and have previously been used a biomarker for GABA_ARs (Abdul *et al.*, 2008). The β 3 subunit was slightly upregulated by AD but not significantly and was also slightly upregulated during R1881 supplementation, indicating that the β 3 subunit is unlikely to be androgen responsive. The γ 1 subunit was the most downregulated under AD (38-fold) but in the presence of the vehicle this effect was not replicated, suggesting that γ 1 subunit expression is not modulated by androgen availability either. Interestingly, the γ 3 subunit was significantly downregulated by maintenance of 1 nM R1881 to AD conditions, but was slightly elevated in the presence of 10 nM R1881.

5.3.4 The effect of IAD on expression of GABA_AR

LNCaP cells were subjected to IAD consisting of 5 days AD, 15 days with R1881 and a further 15 days in AD. GABA_AR subunits were initially assessed at the 5 d time point because the interest was in seeing the changes during onset of NED and this time point matches the peak mRNA expression of both NSE and hASH1 from previous experiments (Chapter 3). Assessing presence and absence, reveals that no previously undetected subunits were detected throughout IAD, however after the second period of AD, expression of $\alpha 6$ became undetected (Fig. 5.7). Considering that the $\alpha 6$ subunit helps to anchor GABA_ARs to the cell surface, a loss of $\alpha 6$ subunit expression after a second cycle of AD would suggest these cells would possess lessened GABA_AR activity. Analysing fold change in expression, the $\alpha 1$ subunit was unaffected by IAD, whilst $\alpha 3$ was upregulated by AD, slightly downregulated during R1881 reintroduction and then upregulated once more under a second AD period. This finding supports the previous experiment which suggested that the $\alpha 3$ subunit could be modulated by androgen signalling (Fig. 5.7). Particularly exciting is that the $\alpha 3$ subunit is upregulated in non-small cell lung cancer and is implicated in AKT and metastasis in breast cancer (Gumireddy *et al.*, 2016). This data would suggest that the $\alpha 3$ subunit could be important in hormone-sensitive cancer types. In addition, the $\alpha 3$ subunit was the most expressed subunit in untreated LNCaP, meaning that perhaps successive cycle of IAD are enriching LNCaP cells expressing the $\alpha 3$ subunit.

The $\alpha 5$ subunit expression was unresponsive to IAD. The expression of the $\beta 3$ subunit, which has previously been shown to decrease the proliferation of hepatocellular carcinoma, was slightly upregulated by AD, became significantly upregulated during the reintroduction of androgen and remained slightly elevated by the end of a second period of AD. It is well established that the slower growth rate of NED PCa cells can inherently provide greater resistance to radiotherapy and some chemotherapeutics (Grigore, *et al.*, 2015; Hu, *et al.*, 2015). Interestingly, $\gamma 1$ subunit expression was downregulated by AD and was slightly upregulated during the reintroduction of androgen, increasing further by the end of a second period of AD. This would suggest that the successive cycles of AD

resulted in LNCaP cells becoming resistant to the lack of androgen causing a downregulation of $\gamma 1$ subunit and could indicate that the $\gamma 1$ subunit is particularly important to the partial loss of NED phenotype. The expression pattern of the $\gamma 3$ subunit was similar to that of the $\gamma 1$ subunit during IAD, becoming significantly increased during AD cessation and upregulated further after a second cycle of AD. A previous study has shown that neurons with the highest expression of the $\gamma 1$ and $\gamma 3$ subunits are the most resistance to neurodegeneration during the pathology of Alzheimer's disease (Iwakiri *et al.*, 2009). This data is particularly exciting as it could indicate that in response to IAD, NED LNCaP cells are increasing expression of the $\gamma 1$ and $\gamma 3$ subunits to increase their resilience. Further studies would be required to investigate this further, but could lead to the establishment of the $\gamma 1$ and $\gamma 3$ subunits either as a useful biomarker of increasing NED resilience or interesting therapeutic targets for degradation in the prostate, for example utilising a benzodiazepine-like structure (which binds at the interface of an α subunit and a γ subunit) conjugated to an anti-cancer agent for targeted delivery, especially considering two α subunits are also enriched in expression by IAD ($\alpha 3$ and $\alpha 6$).

5.3.5 Expression of selected CCCs during IAD

Expression of CCCs during IAD was investigated primarily due to their influence on GABA_AR activity (Li & Xu, 2008; Succol *et al.*, 2012). However, there is also mounting evidence that CCCs are interesting modulators of cancer proliferation and metastasis in their own right, especially in cancers that are hormone sensitive such as breast (Hsu *et al.*, 2007), ovarian (Chen *et al.*, 2009) and cervical cancer (Chiu *et al.*, 2014). Expression of NKCC1 was elevated (2.7-fold), although not significantly, following five days of AD, becoming significantly upregulated (3.7-fold; $p = 0.02$) after a 15 d of androgen reintroduction and increasing further after a 15 d second period of AD (4.4-fold; $p = 0.006$). NKCC1 is typically expressed during early neuronal development, therefore it is interesting that NKCC1 is increasingly upregulated throughout IAD treatment and would be consistent with what would be expected if hASH1 nuclear localisation is driving neurogenesis (Mazurier *et al.*, 2014; Peltopuro *et al.*, 2010). NKCC2 is reported to be specific to kidney tissue, therefore it was expected that expression was not detected in

LNCaP PCa cells (Simon *et al.*, 1996). KCC2 expression was not detected throughout IAD, which is a further indicator that the neuronal-like morphology of NED PCa cells is more akin to developing neurons than mature neurons (Li & Xu, 2008). Expression of KCC1 steadily increased throughout IAD but did not become significant. Expression of KCC3 also steadily increased throughout IAD and did become significant by the end of 15 days reintroduction of androgen, increasing further after a 2nd period of AD. KCC4 expression was unaffected by 5 days AD but was significantly upregulated after 15 days of reintroduction of androgen, expression then fell slightly at the end of the second AD period, but remained significantly above untreated control LNCaP cells.

CCCs operate as heterodimers, KCC1 with KCC3, KCC2 with KCC4 and NKCC1 with KCC4 (Kahle *et al.*, 2015). The data presented herein would suggest that of these pairs, only KCC1 with KCC3 and NKCC1 with KCC4 would be applicable to LNCaP cells. Interestingly, KCC4 has been implicated in promoting invasion of cervical and ovarian cancer and is upregulated in metastases (Chen *et al.*, 2009). The mechanism by which KCC4 is able to promote invasion is thought to be through interaction with insulin-like growth factor 1 (IGF-1) and epidermal growth factor (EGF) (Chen *et al.*, 2009). KCC3 has also been demonstrated to be involved in cellular proliferation and significantly upregulated in ovarian cancer tissue, but not significantly upregulated in metastases (Chen *et al.*, 2009), instead KCC3 is thought to be more involved in the tumourigenesis of cervical cancer rather than metastasis (Chiu *et al.*, 2014). However, in oesophageal squamous cell carcinoma (OSCC) depletion of KCC3 via siRNA significantly reduced invasion and KCC3 was predominantly expressed on the invading front of the tumour (Shiozaki, *et al.*, 2014). KCC3 and KCC4 upregulation have also been investigated *in vivo* using breast cancer xenografts, where depletion of KCC3 and KCC4 inhibited proliferation and invasion (Hsu *et al.*, 2007). Furthermore, depletion of NKCC1 in OSCC cells reduced proliferation via G2/M cell cycle phase arrest (Shiozaki, *et al.*, 2014). In addition, KCC1 expression is also significantly higher in cervical cancer and was most expressed in the most poorly differentiated cells (Lu *et al.*, 2007). Similarly, the mechanism of KCC1 upregulation in cervical cancer is thought to be induced by IGF-II, acting through the ERK1/2MAPK and PI3K/AKT pathways (Zhang *et al.*, 2009).

The importance of NKCC1 and KCC1, KCC3 and KCC4 upregulation in the progression of several cancer types, including hormone-sensitive cancers such as breast, ovarian and cervical cancer (Chen *et al.*, 2009; Chiu *et al.*, 2014; Hsu *et al.*, 2007; Lu *et al.*, 2007; Zhang *et al.*, 2009) lends great context to the data discussed herein relating to prostate cancer and NED. The data in this investigation shows a stepwise increase in expression of CCCs after each stage of the IAD simulation, which not only fits with the role of CCCs in cellular differentiation, but also would suggest that IAD is selecting for a potentially more aggressive phenotype with significantly increased CCC expression. It would appear that the involvement of CCCs in estrogen driven cancer types is becoming well established. Considering that both the estrogen receptor (ER) and AR can both bind to chromatin at forkhead motifs, facilitated by pioneer factor FOXA1, 70% of AR binding and 50% of ER binding occurs at sites co-occupied by FOXA1 in prostate and breast cancer (Robinson & Carroll, 2012). Further investigation of the ability of AR or ER to modulate CCC expression in prostate cancer is clearly needed. Finally, the lack of KCC2 expression in LNCaP cells at any stage of IAD would support the theory that NED LNCaP cells are not mature neurons (Li & Xu, 2008) and are instead utilising components of the canonical neurogenesis pathway to promote survival, AD resistance and acquire a hybrid phenotype after a second cycle of AD.

5.3.6 Expression of GABA_BR subunits during AD and IAD

GABA_BR activation has previously been linked to activation of EGR and increased migration of PCa cells (Xia *et al.*, 2007), making it an interesting candidate as a mechanism of PCa NED mediated ADT resistance. After 5 days of AD, expression of GABBR1 was significantly downregulated, an effect which was also observed in the presence of the vehicle in AD conditions. The addition of R1881 to AD media did not ameliorate this downregulation, suggesting that GABBR1 expression is unlikely to be specifically modulated by androgen signalling. In contrast, GABBR2 expression was significantly downregulated by AD and this effect was lessened when R1881 was present in the AD media, suggesting that GABBR2 may be somewhat modulated by androgen expression. These results were recapitulated when assessing after an initial 15 days of AD

instead of 5 days. GABBR1 expression was significantly downregulated after 15 days of AD and the addition of R1881 actually suppressed the expression further, supporting the notion that GABBR1 is not mediated by androgen signalling. However, GABBR2 was downregulated by AD and vehicle in AD conditions, whilst addition of R1881 to AD conditions maintained GABBR2 at basal levels.

During IAD, the expression of GABBR1 was slightly downregulated after 15 days of AD, but was significantly upregulated by the reintroduction of androgen to AD conditions, remaining at this level after a second period of AD. This result is contrary to the findings of the studies where R1881 was added at the start of AD, which appeared to show that GABBR1 was not modulated by androgen signalling. In the context of IAD, it would appear that AD cessation causes an upregulation in GABBR1 that is maintained through the second period of AD. GABBR2 expression also appeared to be androgen mediated during IAD, where it was downregulated by AD but significantly upregulated after reintroduction of androgen to AD conditions. After a second period of AD, the expression of GABBR2 was slightly suppressed compared to AD+R1881 but remained non-significantly upregulated compared to control LNCaP cells. In the context of the present study, it is important to consider that the oligonucleotides used to detect GABBR1 and GABBR2 expression were designed to target transcript variant 1 of both genes and would not have detected additional splice variants. For GABBR1 the GABBR1_a splice variant is predominantly expressed in the developing brain, whereas GABBR1_b becomes the more expressed variant in adulthood (Fritschy *et al.*, 1999). Utilising additional primer sets to investigate GABA_BR splice variant expression could have facilitated increased characterisation of the NED PCa cells and given deeper insights into the potential GABA response of these cells. Having determined that GABA_BRs are present in PCa and NED PCa cells, investigating the splice variant expression would be an ideal future experiment.

5.3.7 Expression of genes involved in GABA synthesis and metabolism during IAD

The expression of GABA transaminase (GABA-T), an enzyme, which metabolises GABA, was significantly lower in CRPC cell lines DU-145 and PC-3 compared to LNCaP cells (Fig. 5.9). During AD, the expression of GABA-T was slightly increased at 5 and 15 days in LNCaP cells but not to a significant level. When R1881 was present in AD conditions, the expression of GABA-T was slightly suppressed compared to untreated LNCaP cells, suggesting that GABA-T expression might be weakly modulated by androgen signalling. During IAD, GABA-T was slightly elevated after 15 days of AD and was downregulated during the reintroduction of androgen to AD conditions, becoming further suppressed after a second period of AD. This would suggest that successive cycles of AD causes a fundamental change in GABA metabolism in NED LNCaP cells (Ippolito *et al.*, 2014). Expression of GAD1 during IAD was slightly elevated after the first AD period, became significantly upregulated by the reintroduction of androgen to AD conditions and returned to the same levels as was observed after 1 AD cycle by the end of the second AD cycle. GAD2 expression was not affected by the 1st period of AD, was also significantly upregulated by the reintroduction of androgen to AD conditions and remained significantly elevated, but to a lesser degree, by the end of the second AD period. Not only would this suggest an increase in GABA synthesis, but coupled with the downregulation of GABA-T by the second AD cycle would also suggest that GABA levels within these cells is likely to be increasing. Furthermore, the GAD2 gene encodes isoform GAD65 which is predominantly found in nerve terminals and preferentially synthesises GABA for vesicular release, whereas GAD1 encodes GAD67 which is distributed throughout cells and synthesises mainly cytoplasmic GABA. This would strongly hint at the possibility that NED LNCaP cells have the potential to secrete GABA in a paracrine manner, or more conservatively, are becoming more specialised towards that function (Soghomonian & Martin, 1998).

5.3.8 The effect of muscimol and baclofen on a key panel of genes in AD LNCaP cells.

Using selective GABA_AR and GABA_BR agonists (muscimol and baclofen respectively) (Benarroch, 2012; Napoleone *et al.*, 1990) allowed for the investigation of GABAergic signalling upon a key set of genes in NED LNCaP cells. Interestingly, although AR expression was not affected by either muscimol or baclofen, there were significant effects of GABA_AR and GABA_BR agonism on the expression of PSA when compared to the vehicle control. All concentrations of muscimol significantly increased PSA expression compared to vehicle control, the lowest tested concentration (1 µM) of muscimol increased PSA expression the most, an effect which was reduced in a stepwise manner at increasing concentrations. Conversely, only the highest concentration of baclofen (500 µM) produced a statistically significant increase in PSA expression.

A possible explanation for GABAergic signalling to increase PSA expression is that GABA has previously been shown to increase androgen production in rat testicular tissue (Ritta, Campos, & Calandra, 1987), which could potentially stimulate an increase in PSA expression under AD conditions. It is already established that prostate cancer tumours are capable of producing DHT under AD conditions from androgen precursors (Chang, Ercole, & Sharifi, 2014; Chang *et al.*, 2011). The fact that this effect was observed through both GABA_AR and GABA_BR signalling is particularly interesting and increased androgen synthesis in response to GABAergic signalling could be a potential mechanism of NED facilitating ADT resistance clinically. However, it is likely that this relationship would be best studied using *in vivo* xenografts, as it is unclear whether cell culture media with charcoal-stripped serum would contain representative levels of these androgen precursors.

Furthermore, interesting links have previously been discovered between androgen availability and the excitatory nature of GABA_ARs. In neurons derived from female rats, multiple applications of muscimol result in an attenuated response in intracellular [Ca²⁺] compared to the first application, whereas male derived neurons (and female derived neurons pre-treated with androgen) showed

no attenuation with multiple applications of muscimol (Nuñez & McCarthy, 2008). In the context of the present study, this would appear to suggest that GABA_AR activity could be significantly altered by AD. Excitingly, this effect was also found to be inversely correlated to expression of the γ 2 subunit (Nuñez & McCarthy, 2008) which was not detected in any of the PCa cells tested, including NED LNCaP cells throughout simulated IADT, suggesting that if this mechanism is present in PCa cells, it would be operating under optimal conditions. Expression of PTOV1, REST and NSE were not modulated by muscimol or baclofen treatments. However, expression of hASH1, which is a key driver of GABAergic neuronal development (Mazurier *et al.*, 2014; Peltopuro *et al.*, 2010; Yang *et al.*, 2017), was inhibited both by GABA_AR and GABA_BR stimulation during AD. This would align with research demonstrating that GABA mediated activation of both GABA_ARs and GABA_BRs can inhibit neurogenesis in the developed brain (Giachino *et al.*, 2014; Pallotto & Deprez, 2014).

5.3.9 The effect of gabapentin on LNCaP cells

An initial assessment of potential effects of gabapentin (GBP) on PCa cells was conducted on LNCaP cells which had not been subjected to AD. The most interesting finding of these experiments were that at concentrations of 20 μ M GBP key genes implicated in the NED pathway (PTOV1, hASH1 and NSE) were downregulated, although only NSE was significantly downregulated. In addition, GABA-T was downregulated in the presence of 2 and 20 μ M GBP and GAD2 was upregulated by 166 μ M GBP, indicating that GBP can potentially reduce GABA metabolism and increase GABA synthesis. Interestingly, this aligns with the proposed mechanism of action of gabapentin, where it is thought to increase concentrations GABA by increasing GABA synthesis (Cai *et al.*, 2012). If this mechanism is active in these epithelial PCa cells, it could mean that increasing availability of GABA reinforces the epithelial phenotype and inhibits the proposed NED pathway. Interestingly, NED LNCaP cells treated with muscimol and baclofen did not exhibit this inhibitory effect of PTOV1, hASH1 and NSE expression, which could suggest that increasing GABA levels only inhibit the proposed NED pathway in epithelial phenotype LNCaP cells.

5.3.10 Future Functional GABAR experiments

The results of muscimol and baclofen treatment experiments demonstrated that, within the scope of this study, agonism of the GABA_AR and GABA_BR appeared to have very minimal effect upon the investigated NED pathway components in the AD LNCaP model. These results help to confirm and support a previous pharmacological and functional study, which also reported no effect in the LNCaP model and concluded that the effects of inhibiting GABA production were unlikely to be a direct consequence of inhibiting GABARs (Ippolito *et al.*, 2006). A later paper from the same group proposes, after analysis using a novel fluorescence based functional assay, that it may be the metabolism of GABA that is responsible for increased PCa NED cell survival and growth via ALDH5A1 activity to supply the TCA cycle in these cells (Ippolito *et al.*, 2014).

Clearly, to further elucidate the activity of GABA in PCa NED cells, the next steps would be to employ more complex functional assays in order to properly assess and delineate the effects of GABA and GABA antagonist supplementation on GABAR dependent and GABAR independent pathways. In order to investigate the activity of GABA_ARs and CCCs, it is possible to visualise and measure the cellular chloride concentration using synthetic dyes such as SPQ, MQAE or MEQ. These dyes are fluorescent and are quenched when they come into contact with chloride ions, therefore cells with highest chloride concentrations will display the lowest fluorescence (Arosio & Ratto, 2014; Inglefield & Schwartz-Bloom, 1999). Using live cell confocal microscopy, it would likely be possible to visualise the effect of GABA_AR agonists and antagonists on intracellular chloride ion concentrations, allowing for determination of likely GABA_AR activity in AD LNCaP cells in real time. A second approach to a functional assay to assess GABA_AR activity would be to take an electrophysiology approach and to measure directly the polarisation of AD LNCaP cells in response to GABA_AR ligands (Ippolito *et al.*, 2006).

To investigate the presence of assembled GABA_BRs in the AD LNCaP model, a first step could be to use radio-labelled baclofen (Hill & Bowery, 1981), however additional assays would need to be performed to investigate whether agonism or antagonization of the GABA_BR had a functional effect upon the cell. A long

standing and well utilised method of measuring GABA_B-specific activity in response to a specific agonist is measuring increases in inositol triphosphate using ion exchange chromatography (Komatsu, 1996; Brauner-Osborne & Krosgaard-Larsen, 1999). This functional assay could be applied as a functional assay to investigate the activity of GABA_BRs in the AD LNCaP model.

5.3.11 GABA results in relation to previous studies

It is important to consider that in-depth characterisation of GABAR presence and functionality in non-neuronal tissues remains an emerging field and one where there are often conflicting reports. This is primarily due to the complexity of GABARs both in terms of multitude of different conformations of the GABAAR and the interdependence of both GABARs on CCCs for their functionality. Furthermore, when assessing whether present GABARs are functional, it is difficult to delineate whether effects of agonists and antagonists are directly mediated by the target GABAR or instead results of indirect activity such as increasing GABA concentrations.

Although some studies have investigated the role of GABA and GABARs in NE cells of the prostate, it is already well established that PCa NED cells are more closely aligned to PCa epithelial cells, rather than direct expansion of the NE cell niche (Sauer et al., 2006). Therefore, studies investigating GABA activity in prostate NE cells are unlikely to be applicable to PCa NED cells (Solorzano *et al.*, 2018).

Furthermore, even fundamental questions such as the presence of functional GABA_ARs in LNCaP cells remains controversial. For example, a previous study concluded that LNCaP GABA_ARs were non-functional as they did not respond to GABA (Ippolito *et al.*, 2006), however this has been refuted by several more recent publications which have shown growth modulatory effects of GABA_AR specific agonists in LNCaP cells both in vitro, where isoguvacine increases proliferation of LNCaP cells and dihydroergotoxine decreased proliferation

(Abdul, McCray & Hoosein, 2009). These findings have been confirmed by other investigators showing proliferation increases in LNCaP cells treated with isoguvacine can be blocked using picrotoxin (Wu *et al.*, 2014).

In relation to the previous literature, it is important to consider that characterisation of changes in cell proliferation were not conducted, instead this study focused on whether activation of the GABA_AR or GABA_BR influenced the expression of genes thought to drive PCa NED. In the present study, there is little evidence to support that GABA_AR agonism has any effect on the NED related genes that were assessed. Although a negative result, the effect of GABA_AR agonism on the drivers of the NED process has not previously been assessed. In comparison, investigations into agonism of the GABA_BR revealed some changes in the proposed NED pathway, with PTOV1 being significantly upregulated by baclofen treatment, whilst MMP-9 was significantly downregulated by 500 μ M baclofen. In comparison to previous literature, the downregulation of MMP-9 is contrary to what has previously reported, with multiple studies linking GABA_BR agonism with increased MMP-9 expression in both rat hippocampal neurons (Car & Michaluk, 2012) and PCa NED (Azuma *et al.*, 2003). In order to further assess whether GABARs are functional in the LNCaP NED model, more bespoke experiments and assays would need to be performed as described in section 5.3.10.

5.4 Conclusions of GABAR studies

One of the fundamental findings of this comprehensive investigation of GABAR subunit expression in PCa cell lines, was that only LNCaP cells express α subunits of the GABA_AR. Therefore, although it is possible for functional GABA receptors to be present in DU-145 and PC-3 cells, they would be unable to bind the endogenous ligand GABA. This is an important discovery that illuminates a principle difference between androgen-sensitive PCa and CRPC.

This initial assessment of GABAR subunit expression across LNCaP, PC-3 and DU-145 cells also facilitated the deduction that, as seen in a xenopus model (Ranaa *et al.*, 2006), the θ subunit is likely to be substituting for a lack of β 2 and

β 3 subunit expression. Considering that the β 1 and β 2 subunits are the most expressed subunits in PC-3 CRPC cells, this could be an important finding with clinical relevance both as a drug target and as a biomarker.

Overall this chapter presents evidence that NED LNCaP cells possess a phenotype more akin to developing neurons than mature neurons. This is evidenced by an absence of KCC2 expression (Li & Xu, 2008), high expression of the α 3 subunit (Laurie *et al.*, 1992; Liu *et al.*, 2009), which increases further under AD conditions and significantly upregulated NKCC1 expression during the NED process (Li & Xu, 2008). Analysis of GAD2 revealed upregulation during IAD and suggests that increased GABA synthesis is likely to be for vesicular release (Montori *et al.*, 2012; Soghomonian & Martin, 1998), hinting at the possibility of paracrine signalling. However, the expression of GAD2 is at odds with the lack of KCC2 expression, as both are associated with well differentiated neurons, rather than during development. This could be further evidence of a hybrid/aberrant phenotype that does not conform to the stereotypes of canonical neurons. The majority of the data would support that NED LNCaP neuronal-like cells are closer to developmental neurons than to mature neurons.

Investigating the effects of AD and IAD on GABAR subunit expression also highlighted that during AD, expression of the α 6 subunit increases significantly suggesting increased trafficking and anchoring of GABA_ARs to the cell surface after the NED process. Furthermore, the α 3 subunit was progressively upregulated at each AD cycle and was downregulated during the intermediate AD cessation period is closely linked to the invasion and metastasis of breast cancer (Gumireddy *et al.*, 2016). Whilst the interactions of estrogen signalling and GABAR activity and subunit expression are becoming well documented, there is a lack of research into the possibility that these mechanisms may also be present in androgen driven cancers such as PCa. After IAD expression of γ 1 and γ 3 was enriched. These two subunits are known to be neuroprotective and could potentially be a facilitator of enhanced survival for NED LNCaP cells (Iwakiri *et al.*, 2009). Considering that the α 3, γ 1 and γ 3 subunits were significantly

upregulated by IAD, this could implicate the $\alpha\gamma$ subunit interface as a potentially interesting drug delivery target in NED PCa for anticancer drug conjugates.

Also discovered was an enrichment of CCC expression progressively throughout IAD. CCC upregulation is well documented in cervical and ovarian cancer (Chen *et al.*, 2009; Chiu *et al.*, 2014; Zhang *et al.*, 2009) and the data presented herein gives clear rationale to study CCC upregulation in androgen driven cancers such as PCa. Finally, the assessment of GABA_BR subunits revealed that the GABA_{B2} subunit expression is modulated by the availability of androgen in the LNCaP cells, whereas GABA_{B1} appears to be expressed independent of androgen availability. Research in this chapter has helped to significantly elucidate the GABAR subunit expression profile across a range of PCa cell lines for the first time quantitatively and in the context of IAD. These findings have identified several intrinsic connections between androgen availability and GABAR subunits, CCCs and the proposed pathway of AD-induced NED in LNCaP cells which warrants further investigation.

5.5 Limitations, weaknesses and future experiments

Research in this chapter represents the first time that all subunits of the GABA_AR and GABA_BR have been quantitatively assessed in a model of PCa NED. However, there are still substantial limitations of this studies and areas which could be greatly strengthened by additional experiments or the use of different methodology. For the assessment of GABAR subunits, it would have been preferable to use TaqMan probes for qPCR, which are much better suited to presence and absence studies, instead of SYBR-green detection chemistry (Bustin, 2000; Gangisetty & Reddy., 2009). Secondly, although the effects of GABAR agonists on the NED pathway were investigated, the effects upon proliferation or migration were not assessed. Since these have previously been reported as downstream effects of GABAR activation in PCa NED, not assessing these variables is a major weakness of this study and a clear opportunity for future experiments. In addition, functional assays could have been utilised, such as using radiolabelled baclofen (Hill & Bowery, 1981), measuring increases in inositol triphosphate using ion exchange chromatography (Komatsu, 1996;

Brauner-Osborne & Krogsgaard-Larsen, 1999) or electrophysiology experiments to determine whether GABA_AR or GABA_BR agonists were affecting the cellular ion concentrations of these cells. Another weakness and limitation is that the expression of GABAR subunits were only assessed via qPCR and there was no investigation of whether there was detectable protein expression. As it is known that gene expression does not necessarily indicate expression at protein level, obtaining high quality antibodies targeting each subunit is clear and necessary next step in the process of characterising the GABARs in AD LNCaP cells. Finally, another clear limitation was that the effects of gabapentin were only assessed in normal LNCaP cells and not in AD LNCaP cells that possess the NED phenotype, this would be an important next step to determine if gabapentin could modulate PCa NED cells.

6. General Discussion and future directions

6.1 Summary of findings

The main findings of this investigation can be summarised as follows:

6.1.1 hASH1 is a likely key driver of AD-induced NED in PCa

Androgen deprivation (AD) of LNCaP induces a neuronal-like phenotype that is concomitant with a shift in localisation of transcription factor hASH1 into the nuclei of these cells. Although hASH1 has previously been suggested as a driver of AD-induced neuroendocrine differentiation (NED) in PCa, this study is the first to assess hASH1 localisation during IAD and the first to propose a pathway that could facilitate hASH1 mediated NED. Recent investigations of small cell lung cancer (SCLC) have conclusively linked hASH1 as being essential to NED in SCLC (Borromeo *et al.*, 2016; Meder *et al.*, 2016). In this study, hASH1 expression was found to be specifically modulated by AD, as were the proposed upstream components of this NED pathway (PTOV1 and REST). These findings suggest that hASH1 could be an interesting therapeutic target that warrants further validation. Although transcription factors like hASH1 are often considered intractable drug targets (Johnston & Carroll, 2015), gaining a better understanding of the potential upstream components of this pathway and direct interactors of hASH1 could identify mechanisms of indirect hASH1 targeting. Currently, there are no approved therapeutics which specifically target the process of PCa NED despite NED being a common mechanism of therapeutic resistance in patients (Borromeo *et al.*, 2016). Very interestingly, Rovalpituzumab, one of the only NED targeting drugs currently in clinical trials for SCLC is a DLL3 targeted antibody-drug conjugate. Critically, DLL3 is both a known target gene of hASH1 and a key ligand of Notch (Rudin *et al.*, 2017; Zhang *et al.*, 2018), therefore the efficacy demonstrated thus far of rovalpituzumab in SCLC would strongly support the hypothesis presented herein that Notch signalling is an important component of the hASH1 driven NED pathway. As of June 2018, rovalpituzumab is currently under appraisal by the National Institute for Health and Care Excellence (NICE).

6.1.2 The molecular reversibility of AD-induced NED is established for the first time

For the first time, the effects of intermittent AD on NED were investigated using an in vitro model, particularly in regard to the extent that NED could be reversed on a morphological and molecular level by cessation of AD. As previously reported using a cAMP induced NED model (Cox *et al.*, 1999), the morphological changes associated with NED, including neurite-like extensions, were lost upon AD arrest, the first time that this has been assessed in an AD-induced NED model. However, most interesting were the molecular implications of AD cessation, which demonstrated that although NSE expression was downregulated and REST and PTOV1 expression were upregulated alongside restoration of PSA expression to basal levels, the expression of hASH1 remained elevated and was intensely retained within the nuclei of LNCaP cells. This is a fundamental finding that demonstrates for the first time that whilst the morphological aspects of NED appear to be reversible, the nuclear localisation of hASH1 is persistent and robust, which hints that these cells may be employing aspects of a neuronal-like transcriptional profile as part of a hybrid phenotype. An important consideration for this hybrid phenotype hypothesis is whether ADT could induce the expression of AR splice variants and whether these variants could be active under AD conditions. A limitation of this study is that an assessment of AR splice variant activity was not performed, thus it is not possible to ascertain whether aberrant AR signalling may play a role in the maintenance of the NED phenotype. The ability of LNCaP cells to differentiate into neuronal-like cells which are highly therapeutic resistant (Deng *et al.*, 2011; Hu *et al.*, 2015; Yadav *et al.*, 2017) and then back into an epithelial phenotype could also be a sophisticated mechanism of disease recurrence with high clinical relevance.

6.1.3 The effects of intermittent AD on PCa NED were investigated for the first time

Investigating the effects of a second AD period after AD cessation revealed that LNCaP cells can undergo NED a second time and that hASH1 remains enriched within the nucleus, further supporting the evidence that hASH1 is a likely key driver of AD-induced NED in PCa. Studying hASH1 localisation throughout IAD indicates that the robust exclusion of hASH1 from the nucleus is permanently

lost. This raises the question how what mechanisms are in place to exclude hASH1 from the nucleus and could there be a way to stabilise this effect under AD conditions. One such viable strategy to prevent hASH1 access to the chromatin is the application of bromodomain and extra-terminal motif inhibitors (iBETs) which can block the binding of transcription factors to acetylated histones (Garnier, Sharp, & Burns, 2014; Shi & Vakoc, 2014) and is discussed further in section 6.5.1. What is already known is that only cytoplasmic hASH1 is targeted by ubiquitin for degradation, a process which is reliant on Huwe1 E3 ligase (Gillotin *et al.*, 2018). This would also support the findings within this study, that nuclear localisation of hASH1 is persistent and that clinically, this process is something which would be better avoided than attempted to reverse, the precise mechanism of how hASH1 is shuttled into the nucleus remains unknown at this stage (Gillotin *et al.*, 2018).

6.1.4 The first comprehensive assessment of GABAR subunit expression in PCa cell lines and the effect of IAD and GABAR agonists on their expression

A comprehensive and quantitative assessment of GABAR subunit expression across LNCaP, DU-145 and PC-3 PCa cell lines was performed for the first time. This analysis revealed interesting differences between androgen-sensitive LNCaP cells and the CRPC cell lines, primarily that only LNCaP cells with the potential to produce GABA_ARs able to bind GABA. Furthermore, throughout IAD this study identified for the first time that the $\alpha 3$ subunit, which is associated with increased aggression of breast cancer, is also upregulated in LNCaP cells after IAD (Gumireddy *et al.*, 2016). This studies analysis of GABA_AR subunit expression also suggested, with the context of other studies (Ranna *et al.*, 2006), that the θ subunit is likely to be substituting for a lack of $\beta 2$ or $\beta 3$ expression in LNCaP and DU-145 cells. This is particularly relevant considering that the $\beta 2$ subunit is the most expressed subunit in the PC-3 CRPC cell line and one of the most prevalent subunits expressed in brain tissue. Analysis of CCCs revealed two particularly interesting findings, the first being that after AD-induced NED in LNCaP cells, there is no detected expression of KCC2, which is a specific biomarker of mature neurons. This supports the hypothesis that NED LNCaP

cells are only partially differentiated and could be simply exploiting selected aspects of the neurogenesis transcriptional profile to confer a survival and AD resistance advantage. Secondly, the upregulation of NKCC1, KCC1, KCC3 and KCC4 have previously been associated with tumorigenesis, increased proliferation, invasion and metastasis in cervical, ovarian and oesophageal cancers (Chen *et al.*, 2009; Chiu *et al.*, 2014; Hsu *et al.*, 2007; Lu *et al.*, 2007; Shiozaki *et al.*, 2014; Shiozaki *et al.*, 2014; Zhang *et al.*, 2009). The data presented herein demonstrated that NKCC1, KCC1, KCC3 and KCC4 were progressively upregulated at each stage of IAD, with NKCC1, KCC3 and KCC4 being significantly upregulated by the end of the AD cessation period and remained so by the end of the second AD period (Fig. 5.6). These findings suggest that CCC upregulation, as established in cervical and ovarian cancer progression, may also be a feature of PCa.

Overall the findings of this investigation identify hASH1 as an interesting therapeutic target in NED PCa, provide the first molecular analysis of androgen-sensitive PCa cells treated with simulated IADT and the first quantitative assessment of GABA_AR and GABA_BR subunit expression, along with analysis of CCCs, across androgen-sensitive, CRPC and NED PCa in response to IAD. This study also required the development of a novel model of IAD, which is a useful contribution to the field and could facilitate further *in vitro* studies investigating IADT which is increasing in clinical interest. These findings have high translational relevance and provide a powerful rationale to further delineate the role of hASH1 on NED and validate this transcription factor as a therapeutic target. This could be achieved using additional genomic and proteomic approaches such as ChIP-Seq, RNA-Seq and RIME to identify both the target genes of hASH1 in the specific NED PCa context, it's abilities to act as a pioneer factor (Iwafuchi-Doi & Zaret, 2014; Park *et al.*, 2017; Wapinski *et al.*, 2013, 2017) during IAD and NED as well as mapping the hASH1 interactome which could identify additional routes to hASH1 therapeutic targeting (Mohammed *et al.*, 2016; Papachristou *et al.*, 2018). Furthermore, applying knowledge gained from the AD and IAD *in vitro* models to develop *in vivo* models, utilising LNCaP and patient derived xenografts will be critical to better understanding the role of hASH1, the impact of NED on

PCa tumours and to investigating whether IAD and methods of inhibiting hASH1 activity increase survival or reduce metastasis and therapeutic resistance.

6.2 hASH1 as a potential therapeutic target in NED PCa

Although transcription and pioneer factors are notoriously difficult drug targets (Johnston & Carroll, 2015), previous evidence has shown that the BET inhibitor JQ1 can downregulate hASH1 expression by disrupting the binding of BRD4 to the hASH1 promoter in SCLC cells (Lenhart *et al.*, 2015). This would provide a clear rationale to investigate the effects of JQ1 on hASH1 expression in NED PCa cells. Although JQ1 is not being pursued in clinical trials due to its short half-life (Wadhwa & Nicolaidis, 2016), next generation BET inhibitors such as I-BET762 from GlaxoSmithKline is currently in Phase I clinical trials for NUT midline carcinoma which is due to complete in December 2018 (<https://clinicaltrials.gov/ct2/show/NCT01587703>). Interestingly, the inhibition of proliferation seen in SCLC cells treated with JQ1 was conserved when treated with I-BET762 (Lenhart *et al.*, 2015). This next generation of BET inhibitors (iBETs) could potentially be applied in an adjuvant setting alongside ADT to alleviate or delay AD-induced NED. The most recent studies of BET inhibition in PCa have demonstrated that PCa can develop resistance to BET inhibition (Pawar *et al.*, 2018), which would seem to advocate for a select and precise use of iBETs alongside existing treatments to specifically mitigate NED. Overall, it must be considered that NED is only one of many resistance mechanisms of PCa, in effect novel treatment strategies for PCa could effectively aim to close off these avenues of adaption, effectively forcing the tumour evolution into a 'blind alley', facilitating new options for synthetic lethality, a concept recently demonstrated by combining ADT with PARP inhibition *in vivo* (Asim *et al.*, 2017). In the eventuality that direct or upstream targeting of hASH1 is not possible in PCa, a study of hASH1 activity in SCLC identified 24 hASH1 target genes that have existing targeted compounds (Augustyn *et al.*, 2014).

6.3 Clinical implications of the effects of IAD on PCa NED

Overall, the data presented herein would strongly support the EAU guidelines stating that ADT should be constant and not intermittent (Heidenreich *et al.*, 2014; Mottet *et al.*, 2011). Certainly, the future aims of PCa NED amelioration must be the initial prevention of NED and the prevailing dogma that NED is a completely reversible process (Cox *et al.*, 1999) is made obsolete by our findings and the knowledge that nuclear, chromatin bound, hASH1 is many times more stable and degradation resistant than when in the cytoplasm.

Our findings also support the hypothesis that NED PCa could function in tumour recurrence in a similar way to the cancer stem cell niche, i.e. utilising inherent radioresistance, chemoresistance and ADT-resistance to survive successive treatments whilst retaining the ability to transdifferentiate back into an epithelial phenotype and reseed the tumour or metastatic sites, for example 30-50% of high risk localised prostate cancer patients suffer disease recurrence within 5-years of receiving radiotherapy (Hu *et al.*, 2015).

6.4 Limitations and weaknesses of this study

Before considering future experiments, it is important to acknowledge the weaknesses and limitations of the present study. These limitations can be broadly categorised as either limitations in scale and scope, limitations of the LNCaP and CS-FBS model of PCa NED and the limitations of the methodology employed to investigate said model. Perhaps the chief limitation of this study is that a hypothesis driven approach was taken, i.e. a proposed NED pathway synthesised from previous literature and the use of informatics tools such as the STRING database (Skzclarczyk *et al.*, 2019; www.string-db.org) to guide this hypothesis. In comparison, an unbiased discovery-based approach would have been preferable, but would also have required the use of a much higher throughput 'screening' technique such as RNA-Seq or microarray to identify pathways activated and repressed by AD through a gene ontology approach in an unbiased manner. Clearly, the selection of a small panel of hypothesis driven genes has a high likelihood of not including genes that could be key to PCa NED, especially if those genes have not been widely studied or reported in the literature. However, there were some advantages to restricting the number of

targets assessed, for example this allowed for many different treatments and timepoints to be studied relatively inexpensively compared to using a large number of targets and a more restricted set of treatments and timepoints. Despite this, the number and frequency of time points assessed in this study were limited. It would perhaps have been valuable to include some much earlier timepoints such as 2, 4 and 6 h after AD or drug treatment to assess which molecular changes associated with NED are the first to occur.

In terms of the AD LNCaP model used to study PCa NED, a key limitation is that these experiments were only performed in one cell line and only *in vitro*, which does not represent the high heterogeneity of patient tumours or the complexities of the tumour microenvironment. It is certainly possible that the neuronal-like phenotype observed in LNCaP cells after AD could simply be an artefact of this particular cell line and not applicable to clinical disease. Previous studies which have shown hASH1 expression to be enriched in patients treated with ADT would appear to support the observations made in the present study. However, a weakness of this study is that hASH1 activity and localisation was not assessed in patient material or in LNCaP xenografts which could have added greater credibility to the assertion that hASH1 is a potential therapeutic target. It must also be considered that whilst the use of CS-FBS to mimic ADT is widespread and a justified approach, there are inherent limitations of this approach. For example, the concentrations of androgens and other components in the FBS and CS-FBS are likely to fluctuate between lots and the hormone concentrations and GABA were not empirically determined by ELISA. In addition, the process of charcoal-stripping, as mentioned previously, is not androgen specific, which in addition to the lot to lot variability of supplied FBS and CS-FBS could contribute to increased variability between experiments. Although the specificity of changes observed in AD conditions was verified by using R1881 synthetic androgen as a control, it would have also been of great benefit to use enzalutamide (in non-charcoal-stripped media) alongside the R1881 control to prove that changes in gene and protein expression were specifically mediated by changes in AR signalling.

Aside from the limitations of the model used, there are also substantial limitations arising from the methodologies employed to study the model. For example, the AR antibody and qPCR oligonucleotides used in this study did not target the regions of the protein or gene conserved between the majority of AR splice variants. This severely limited the ability to consider the effects that AR splice variants might have on the NED process or their activity during AD. In addition, since this study focused on a relatively concise panel of NED related genes, it would likely have been preferable to use TaqMan probes for qPCR instead of SYBR-green detection chemistry. This would have allowed for increased sensitivity for targets with low expression and would have been better suited to determining presence and absence of the GABAR subunits. In addition, to robustly determine whether GABARs were functional in NED LNCaP cells, functional assays could have been utilised, such as using radiolabelled baclofen (Hill & Bowery, 1981), measuring increases in inositol triphosphate using ion exchange chromatography (Komatsu, 1996; Brauner-Osborne & Krogsgaard-Larsen, 1999) or electrophysiology experiments to determine whether GABA_AR or GABA_BR agonists were effecting the cellular ion concentrations of these cells. Another clear limitation was that the effects of gabapentin were only assessed in normal LNCaP cells and not in AD LNCaP cells that possess the NED phenotype, this would be an important next step to determine if gabapentin could modulate PCa NED cells.

Finally, despite the evidence linking hASH1 nuclear localisation to the NED process, this study did not determine whether hASH1 was definitely mechanistically involved in PCa NED. On the strength of the data presented it is only possible to determine that hASH1 nuclear localisation is concomitant with NED. To more robustly evaluate hASH1 as a therapeutic target it would be necessary to determine whether overexpression or knock down of hASH1 was able to induce and prevent NED respectively. Furthermore, if hASH1 was determined to be an essential driver of NED, the use of ChIP-Seq or ChIP-qPCR experiments would reveal the target genes of hASH1 which could in itself highlight a more tractable drug target.

6.5 Future investigations

The future work facilitated by this thesis is likely to follow three core strands, the first being the validation of hASH1 as a therapeutic target, the second being a deeper investigation of GABAR pharmacology, influence of CCCs and GABA metabolism in NED PCa, with the third being to assess the mechanisms by which NED PCa cells can support the survival, growth and metastasis of surrounding cells. It is likely that all three of these research niches will investigate these questions in the context of IAD and in the presence of adjuvant and neo-adjuvant treatments with docetaxel, which is becoming an increasingly popular clinical option (James *et al.*, 2016; Vale *et al.*, 2016). These important future investigations will utilise the data presented in this thesis to strive towards translational research outputs.

6.4.1 Further investigations of hASH1 activity in PCa and validation as a therapeutic target

In order to truly validate hASH1 as a therapeutic target, additional genomic and proteomic techniques must be applied, alongside the developments of *in vivo* models to study NED PCa in a more representative microenvironment. As already performed in SCLC samples (Borromeo *et al.*, 2016), ChIP-Seq will be employed to both identify the direct target genes of hASH1 and to elucidate its ability to act as a pioneer factor. By mapping the location of histone marks that designate active regulatory sequences such as H3K27ac and active and poised enhancers such as H3Kme1 it will be possible (alongside hASH1 silencing experiments) to identify both the 'when' and 'where' that hASH1 acts as a pioneer factor (Activation *et al.*, 2016; Creighton *et al.*, 2010; Rada-Iglesias *et al.*, 2011).

The next goal of this investigation will be to discover how and why hASH1 is able to directly drive PCa NED and function as a pioneer factor. This will be achieved using the mass spectrometry technique RIME (Mohammed *et al.*, 2016) which will allow for the identification of the hASH1 interactome when bound to the chromatin. Gaining knowledge of the cofactors that either facilitate hASH1 chromatin binding, or the factors recruited to the chromatin by hASH1, could elucidate alternative mechanisms by which hASH1 activity could be disrupted, for example by identifying highly prostate-specific interactors or interactors for which

existing drugs could be repurposed. Finally, by integrating the data from the aforementioned experiments, RNA-Seq can be applied to validate and quantify which genes are likely to be specifically modulated in expression by hASH1 activity. This will provide substantial increases in the understanding of the minutiae of hASH1 activity and is likely to identify novel therapeutic targets for PCa NED, for which there is currently no specific targeted therapeutic.

In addition to these *in vitro* experiments, LNCaP and androgen-sensitive patient derived xenografts (PDX) will be implanted into NSG mice (treated with enzalutamide, castrated or untreated). These *in vivo* experiments will be crucial to discovering the true impact of hASH1 activity upon the growth, invasion and metastasis of tumours, as well as allowing for the study of hASH1 in a more representative microenvironment (LNCaP and PDX) as well as studying NED PCa cells in their context as a subpopulation of cells in a PDX model with preserved tumour heterogeneity (Cassidy, Caldas, & Bruna, 2015). Recent advances have allowed for this tumour tissue grown *in vivo* to also be subjected to the same CHIP-Seq and RIME analysis pipeline as *in vitro* experiments (Goetz *et al.*, 2017; Papachristou *et al.*, 2018) Critically, this analysis will also be performed on primary tumours and on the matched metastases grown *in vivo* after resection of the primary tumour.

6.4.2 Investigating the paracrine signalling potential of NED PCa cells

To investigate the intracellular and paracrine signalling potential of NED PCa cells within tumours, *in vitro* experiments will be used to identify the active signalling pathways and the effects of these will be validated *in vivo*. The first series of experiments will be to apply the conditioned culture media from long term AD-induced NED LNCaP cells to untreated LNCaP, DU-145 and PC-3 cells and using RNA-Seq to identify changes in gene expression when in the presence of any paracrine signalling molecules produced by NED LNCaP cells. ELISA assays will also be used to quantify the concentration of molecules thought to have paracrine signalling potential in PCa and NED PCa, including GABA, cAMP and IL-6 (Deeble *et al.*, 2001; Deng *et al.*, 2011; Ippolito *et al.*, 2014; Shen *et al.*, 1997a; Tawadros *et al.*, 2013; Wang *et al.*, 2018; Wu *et al.*, 2014b; Zhu *et al.*, 2014).

Next, transwell invasion assays will be used to investigate whether co-culture with NED LNCaP cells increases the invasive potential of LNCaP, DU-145 and PC-3 cells. Harvesting the non-invading cells from the top layer and the invasive cells in the bottom layer of the transwell plate will allow RNA-Seq analysis to compare the gene expression enrichment and depletion of both populations of cells and will allow for the identification of genes specifically upregulated by co-culture with NED LNCaP cells. Furthermore, identifying these genes will allow for bioinformatics analysis to infer which signalling pathways may be implicated. It may also be possible to employ a whole genome CRISPR screen approach, which combined with the co-culture invasion assays would identify which genes are likely to be essential for producing pro-invasive signalling molecules and which are essential for responding to them, which can be ascertained through sequencing and identifying which gRNAs are enriched or depleted in the invading and non-invading population (Prolo *et al.*, 2017).

Finally, the knowledge gained from the *in vitro* experiments will be used to investigate paracrine signalling potential *in vivo*. This will be achieved by implanting NED LNCaP and either prostate cancer cell lines or dissociated PDX material in co-cultures into NSG mice treated with ADT. By transfecting these cells with imaging markers such as RFP or luciferase it will be possible to track the invasion and metastasis of tumours (Sflomos *et al.*, 2016) in the presence or

absence of NED LNCaP cells. If this *in vivo* model can be established and well characterised, it will be used as a test bed for potential hASH1 and NED PCa targeted therapeutics.

6.4.3 Investigating the role of GABARs and CCCs in NED PCa

Data presented in chapter 5 demonstrated that IAD triggers an upregulation in CCCs, a phenomenon that has previously been seen during the progression of many cancer types, particularly estrogen driven cancers such as breast and cervical cancer (Chiu *et al.*, 2014; Hsu *et al.*, 2007; Shiozaki *et al.*, 2014; Zhang *et al.*, 2009). The first steps in future work would be to comprehensively validate the qRT-PCR data obtained thus far using a complete panel of NKCC and KCC antibodies and assess expression throughout IAD via immunoblot. Next, the same validation could be performed for the GABA_AR and GABA_BR subunits. In order to begin to determine the GABA_AR subunit composition, co-immunoprecipitation could be used to identify which subunits are assembled with each other (Klausberger *et al.*, 2001). A particularly interesting future experiment would be to use siRNA to knock down expression of the θ subunit, which is thought to substitute for a lack of β 2 and β 3 subunit expression. The expression of the θ subunit exclusively in PCa cells that did not express either or both of the β 2 and β 3 subunits would suggest that the properties of the β 2 and β 3 subunits are important to PCa cells and that disrupting expression of the θ subunit could potentially have an anti-cancer effect.

References

- Abdul, M., Mccray, S. D., & Hoosein, N. M. (2008). Expression of gamma-aminobutyric acid receptor (subtype A) in prostate cancer. *Acta Oncologica*, 47(8), 1546-1550.
- Adachi, A., Koizumi, M., & Ohsumi, Y. (2017). Autophagy induction under carbon starvation conditions is negatively regulated by carbon catabolite repression. *The Journal of Biological Chemistry*, 292(48), 19905–19918.
- Akinci, M. K., & Schofield, P. R. (1999). Widespread expression of GABAA receptor subunits in peripheral tissues. *Neuroscience Research*, 35(2), 145–153.
- Alaña, L., Sesé, M., Cánovas, V., Punyal, Y., Fernández, Y., Abasolo, I., ... Paciucci, R. (2014). Prostate tumor OVerexpressed-1 (PTOV1) down-regulates HES1 and HEY1 notch targets genes and promotes prostate cancer progression. *Molecular Cancer*, 13, 74.
- Alimirah, F., Chen, J., Basrawala, Z., Xin, H., & Choubey, D. (2006). DU-145 and PC-3 human prostate cancer cell lines express androgen receptor: implications for the androgen receptor functions and regulation. *FEBS Letters*, 580(9), 2294–300.
- Altree-Tacha, D., Tyrrell, J., & Li, F. (2017). mASH1 is Highly Specific for Neuroendocrine Carcinomas: An Immunohistochemical Evaluation on Normal and Various Neoplastic Tissues. *Archives of Pathology & Laboratory Medicine*, 141(2), 288–292.
- Altschul, S. F., Gish, W., Miller, W., Myers, E. W., & Lipman, D. J. (1990). Basic local alignment search tool. *Journal of Molecular Biology*, 215(3), 403–410.
- Aparicio, A. M., Harzstark, A. L., Corn, P. G., Wen, S., Araujo, J. C., Tu, S.-M., ... Logothetis, C. J. (2013). Platinum-based chemotherapy for variant castrate-resistant prostate cancer. *Clinical Cancer Research: An Official Journal of the American Association for Cancer Research*, 19(13), 3621–30.
- Arora, V. K., Schenkein, E., Murali, R., Subudhi, S. K., Wongvipat, J., Balbas, M. D., ... Sawyers, C. L. (2013). Glucocorticoid Receptor Confers Resistance to Antiandrogens by Bypassing Androgen Receptor Blockade. *Cell*, 155(6), 1309–1322.
- Arosio, D., & Ratto, G. M. (2014). Twenty years of fluorescence imaging of intracellular chloride. *Frontiers in Cellular Neuroscience*, 8, 258.
- Asim, M., Tarish, F., Zecchini, H. I., Sanjiv, K., Gelali, E., Massie, C. E., ... Helleday, T. (2017). Synthetic lethality between androgen receptor signalling and the PARP pathway in prostate cancer. *Nature Communications*, 8(1), 374.
- Ather, M. H., & Abbas, F. (2000). Prognostic Significance of Neuroendocrine Differentiation in Prostate Cancer. *European Urology*, 38(5), 535–542.

Attard, G., Sydes, M. R., Mason, M. D., Clarke, N. W., Aebbersold, D., De Bono, J. S., ... James, N. D. (2014). Platinum Opinion Combining Enzalutamide with Abiraterone, Prednisone, and Androgen Deprivation Therapy in the STAMPEDE Trial.

Augustyn, A., Borromeo, M., Wang, T., Fujimoto, J., Shao, C., Dospoy, P. D., ... Minna, J. D. (2014). ASCL1 is a lineage oncogene providing therapeutic targets for high-grade neuroendocrine lung cancers. *Proceedings of the National Academy of Sciences of the United States of America*, 111(41), 14788–93.

Axelsson, H. (2004). The Notch signaling cascade in neuroblastoma: role of the basic helix-loop-helix proteins HASH-1 and HES-1. *Cancer Letters*, 204(2), 171–8.

Azuma, H., Inamoto, T., Sakamoto, T., Kiyama, S., Ubai, T., Shinohara, Y., ... Watanabe, M. (2003). Gamma-aminobutyric acid as a promoting factor of cancer metastasis; induction of matrix metalloproteinase production is potentially its underlying mechanism. *Cancer Research*, 63(23), 8090–6.

Backonja, M., & Glanzman, R. L. (2003). Gabapentin dosing for neuropathic pain: evidence from randomized, placebo-controlled clinical trials. *Clinical Therapeutics*, 25(1), 81–104.

Barnard, E. A., Skolnick, P., Olsen, R. W., Mohler, H., Sieghart, W., Biggio, G., ... Langer, S. Z. (1998). International Union of Pharmacology. XV. Subtypes of γ -Aminobutyric Acid A Receptors: Classification on the Basis of Subunit Structure and Receptor Function.

Bassetto, M., Ferla, S., Pertusati, F., Kandil, S., Westwell, A. D., Brancale, A., & McGuigan, C. (2016). Design and synthesis of novel bicalutamide and enzalutamide derivatives as antiproliferative agents for the treatment of prostate cancer. *European Journal of Medicinal Chemistry*, 118, 230–243.

Baumann, S. W., Baur, R., & Sigel, E. (2002). Forced subunit assembly in $\alpha 1\beta 2\gamma 2$ GABAA receptors. Insight into the absolute arrangement. *The Journal of Biological Chemistry*, 277(48), 46020–5.

Baur, R., Minier, F., & Sigel, E. (2006). A GABA_A receptor of defined subunit composition and positioning: Concatenation of five subunits. *FEBS Letters*, 580(6), 1616–1620.

Belandia, B., Powell, S. M., García-Pedrero, J. M., Walker, M. M., Bevan, C. L., & Parker, M. G. (2005). Hey1, a mediator of notch signaling, is an androgen receptor corepressor. *Molecular and Cellular Biology*, 25(4), 1425–36.

Beltran, H., Beer, T. M., Carducci, M. A., de Bono, J., Gleave, M., Hussain, M., ... Tannock, I. F. (2011). New therapies for castration-resistant prostate cancer: efficacy and safety. *European Urology*, 60(2), 279–90.

Beltran, H., Prandi, D., Mosquera, J. M., Benelli, M., Puca, L., Cyrta, J., ... Demichelis, F. (2016). Divergent clonal evolution of castration-resistant

neuroendocrine prostate cancer. *Nature Medicine*, 22(3), 298–305.

Beltran, H., Rickman, D. S., Park, K., Chae, S. S., Sboner, A., MacDonald, T. Y., ... Rubin, M. A. (2011). Molecular Characterization of Neuroendocrine Prostate Cancer and Identification of New Drug Targets. *Cancer Discovery*, 1(6), 487–495.

Ben-Ari, Y. (2002). Excitatory actions of gaba during development: the nature of the nurture. *Nature Reviews Neuroscience*, 3(9), 728–739.

Benarroch, E. E. (2012). GABA_B receptors: structure, functions, and clinical implications. *Neurology*, 78(8), 578–84.

Benedict, P., Paciucci, R., Thomson, T. M., Valeri, M., Nadal, M., Càceres, C., ... Reventós, J. (2001). PTOV1, a novel protein overexpressed in prostate cancer containing a new class of protein homology blocks. *Oncogene*, 20(12), 1455–1464.

Berney, D. M., Beltran, L., Fisher, G., North, B. V., Greenberg, D., Møller, H., ... Cuzick, J. (2016). Validation of a contemporary prostate cancer grading system using prostate cancer death as outcome. *British Journal of Cancer*, 114(10), 1078–1083.

Bertaglia, V., Tucci, M., Fiori, C., Aroasio, E., Poggio, M., Buttigliero, C., ... Berruti, A. (2013). Effects of Serum Testosterone Levels After 6 Months of Androgen Deprivation Therapy on the Outcome of Patients With Prostate Cancer. *Clinical Genitourinary Cancer*, 11(3), 325–330.e1.

Bertrand, N., Castro, D. S., & Guillemot, F. (2002). Proneural genes and the specification of neural cell types. *Nature Reviews Neuroscience*, 3(7), 517–530.

Bill-Axelson, A., Holmberg, L., Garmo, H., Rider, J. R., Taari, K., Busch, C., ... Johansson, J.-E. (2014). Radical Prostatectomy or Watchful Waiting in Early Prostate Cancer. *New England Journal of Medicine*, 370(10), 932–942.

Bishop, J. L., Davies, A., Ketola, K., & Zoubeidi, A. (2015). Regulation of tumor cell plasticity by the androgen receptor in prostate cancer. *Endocrine-Related Cancer*, 22(3), 165–182.

Bishop, J. L., Thaper, D., Vahid, S., Davies, A., Ketola, K., Kuruma, H., ... Zoubeidi, A. (2017). The Master Neural Transcription Factor BRN2 Is an Androgen Receptor–Suppressed Driver of Neuroendocrine Differentiation in Prostate Cancer. *CANCER DISCOVERY*, 54.

Bluemn, E. G., Coleman, I. M., Lucas, J. M., Coleman, R. T., Hernandez-Lopez, S., Tharakan, R., ... Nelson, P. S. (2017). Androgen Receptor Pathway-Independent Prostate Cancer Is Sustained through FGF Signaling. *Cancer Cell*, 32(4), 474–489.

Bok, R. A., & Small, E. J. (2002). Bloodborne biomolecular markers in prostate cancer development and progression. *Nature Reviews Cancer*, 2(12), 918–926.

Bonkhoff, H. (2001). Neuroendocrine differentiation in human prostate cancer.

Morphogenesis, proliferation and androgen receptor status. *Annals of Oncology : Official Journal of the European Society for Medical Oncology*, 12 Suppl 2, S141-4.

Bonne, C., & Raynaud, J. P. (1976). Assay of androgen binding sites by exchange with methyltrienolone (R 1881). *Steroids*, 27(4), 497–507.

Bormann, J. (2000). The “ABC” of GABA receptors. *Trends in Pharmacological Sciences*, 21(1), 16–19.

Borromeo, M. D., Savage, T. K., Kollipara, R. K., He, M., Augustyn, A., Osborne, J. K., ... Johnson, J. E. (2016). ASCL1 and NEUROD1 Reveal Heterogeneity in Pulmonary Neuroendocrine Tumors and Regulate Distinct Genetic Programs. *Cell Reports*, 16(5), 1259–1272.

Bowery, N. G., Bettler, B., Froestl, W., Gallagher, J. P., Marshall, F., Raiteri, M., ... Enna, S. J. (2002). International Union of Pharmacology. XXXIII. Mammalian gamma-aminobutyric acid(B) receptors: structure and function. *Pharmacological Reviews*, 54(2), 247–64.

Bradford, M. M. (1976). A rapid and sensitive method for the quantitation of microgram quantities of protein utilizing the principle of protein-dye binding. *Analytical Biochemistry*, 72, 248–54.

Bräuner-Osborne, H., & Krosgaard-Larsen, P. (1999). Functional pharmacology of cloned heterodimeric GABAB receptors expressed in mammalian cells. *British Journal of Pharmacology*, 128(7), 1370–4.

Breul, J., Lundström, E., Purcea, D., Venetz, W. P., Cabri, P., Dutailly, P., & Goldfischer, E. R. (2017). Efficacy of Testosterone Suppression with Sustained-Release Triptorelin in Advanced Prostate Cancer. *Advances in Therapy*, 34(2), 513–523.

Brinkmann, A. O., Kuiper, G. G. J. M., de Boer, W., Mulder, E., Bolt, J., Van Steenbrugge, G. J., & Van Der Molen, H. J. (1986). Characterization of androgen receptors after photoaffinity labelling with [3H]methyltrienolone (R1881). *Journal of Steroid Biochemistry*, 24(1), 245–249.

Brown, T. R., Rothwell, S. W., & Migeon, C. J. (1981). Comparison of methyltrienolone and dihydrotestosterone binding and metabolism in human genital skin fibroblasts. *Journal of Steroid Biochemistry*, 14(10), 1013–1022.

Bruchovsky, N., Klotz, L. H., Sadar, M., Crook, J. M., Hoffart, D., Godwin, L., ... Goldenberg, S. L. (2000). Intermittent androgen suppression for prostate cancer: Canadian Prospective Trial and related observations. *Molecular Urology*, 4(3), 191–9.

Bugan, I., Karagoz, Z., Altun, S., & Djamgoz, M. B. A. (2016). Gabapentin, an Analgesic Used Against Cancer-Associated Neuropathic Pain: Effects on Prostate Cancer Progression in an In Vivo Rat Model. *Basic and Clinical Pharmacology and Toxicology*, 118(3), 200–207.

Bustin, S. A., Benes, V., Garson, J. A., Hellemans, J., Huggett, J., Kubista, M., ... Wittwer, C. T. (2009). The MIQE guidelines: minimum information for publication of quantitative real-time PCR experiments. *Clinical Chemistry*, 55(4), 611–22.

Bustin, S. A. (2000). Absolute quantification of mRNA using real-time reverse transcription polymerase chain reaction assays. *Journal of Molecular Endocrinology*, (25), 169-193.

Cai, K., Nanga, R. P., Lamprou, L., Schinstine, C., Elliott, M., Hariharan, H., ... Epperson, C. N. (2012). The impact of gabapentin administration on brain GABA and glutamate concentrations: a 7T ¹H-MRS study. *Neuropsychopharmacology: Official Publication of the American College of Neuropsychopharmacology*, 37(13), 2764–71.

Calandre, E. P., Rico-Villademoros, F., & Slim, M. (2016). Alpha 2 delta ligands, gabapentin, pregabalin and mirogabalin: a review of their clinical pharmacology and therapeutic use. *Expert Review of Neurotherapeutics*, 16(11), 1263–1277.

Canil, C. M., & Tannock, I. F. (2004). Is there a role for chemotherapy in prostate cancer? *British Journal of Cancer*, 91(6), 1005–11.

Cánovas, V., Lleonart, M., Morote, J., Paciucci, R., Cánovas, V., Lleonart, M., ... Paciucci, R. (2015). The role of prostate tumor overexpressed 1 in cancer progression. *Oncotarget*, 8(7), 12451–12471.

Camand, E., Peglion, N., Osmani, N., Sanson, M., Etienne-Manneville, S. (2012) N-cadherin expression level modulates integrin-mediated polarity and strongly impacts on the speed and directionality of glial cell migration. *Journal of Cell Science*, 125, 844-857.

Cao, Z., West, C., Norton-Wenzel, C. S., Rej, R., Davis, F. B., Davis, P. J., & Rej, R. (2009). Effects of resin or charcoal treatment on fetal bovine serum and bovine calf serum. *Endocrine Research*, 34(4), 101–8.

Capaccione, K. M., & Pine, S. R. (2013). The Notch signaling pathway as a mediator of tumor survival. *Carcinogenesis*, 34(7), 1420–1430.

Car, H., & Michaluk, P. (2012). Baclofen influences acquisition and MMP-2, MMP-9 levels in the hippocampus of rats after hypoxia. *Pharmacological Reports: PR*, 64(3), 536–45.

Caraceni, A., Zecca, E., Bonezzi, C., Arcuri, E., Tur, R. Y., Maltoni, M., ... De Conno, F. (2004). Gabapentin for Neuropathic Cancer Pain: A Randomized Controlled Trial From the Gabapentin Cancer Pain Study Group. *Journal of Clinical Oncology*, 22(14), 2909–2917.

Casarosa, S., Fode, C., & Guillemot, F. (1999). *Mash1 and neurogenesis in the telencephalon*. *Development*, 126(3), 525-534.

Cash, H., Steiner, U., Heidenreich, A., Klotz, T., Albers, P., Melchior, S., ... PRINCE investigators. (2018). Intermittent vs continuous docetaxel therapy in

patients with metastatic castration-resistant prostate cancer - a phase III study (PRINCE). *BJU International*, 122(5), 774-782.

Cassidy, J. W., Caldas, C., & Bruna, A. (2015). Maintaining Tumor Heterogeneity in Patient-Derived Tumor Xenografts. *Cancer Research*, 75(15), 2963–8.

Castro, D. S., Martynoga, B., Parras, C., Ramesh, V., Pacary, E., Johnston, C., ... Guillemot, F. (2011). A novel function of the proneural factor *Ascl1* in progenitor proliferation identified by genome-wide characterization of its targets. *Genes & Development*, 25(9), 930–45.

Castro, D. S., Skowronska-Krawczyk, D., Armant, O., Donaldson, I. J., Parras, C., Hunt, C., ... Guillemot, F. (2006). Proneural bHLH and Brn Proteins Coregulate a Neurogenic Program through Cooperative Binding to a Conserved DNA Motif. *Developmental Cell*, 11(6), 831–844.

Castro, E., Goh, C., Olmos, D., Saunders, E., Leongamornlert, D., Tymrakiewicz, M., ... Eeles, R. (2013). Germline *BRCA* Mutations Are Associated With Higher Risk of Nodal Involvement, Distant Metastasis, and Poor Survival Outcomes in Prostate Cancer. *Journal of Clinical Oncology*, 31(14), 1748–1757.

Chang, J. C. (2016). Cancer stem cells. *Medicine*, 95, S20–S25.

Chang, K.-H., Ercole, C. E., & Sharifi, N. (2014). Androgen metabolism in prostate cancer: from molecular mechanisms to clinical consequences. *British Journal of Cancer*, 111(7), 1249–54.

Chang, K.-H., Li, R., Papari-Zareei, M., Watumull, L., Zhao, Y. D., Auchus, R. J., & Sharifi, N. (2011). Dihydrotestosterone synthesis bypasses testosterone to drive castration-resistant prostate cancer. *Proceedings of the National Academy of Sciences*, 108(33), 13728–13733.

Chang, Y.-T., Lin, T.-P., Campbell, M., Pan, C.-C., Lee, S.-H., Lee, H.-C., ... Chang, P.-C. (2017). REST is a crucial regulator for acquiring EMT-like and stemness phenotypes in hormone-refractory prostate cancer.

Chen, R., Zeng, X., Zhang, R., Huang, J., Kuang, X., Yang, J., ... Li, B. (2014). Cav1.3 channel $\alpha 1D$ protein is overexpressed and modulates androgen receptor transactivation in prostate cancers. *Urologic Oncology*, 32(5), 524–36.

Chen, Y.-F., Chou, C.-Y., Wilkins, R. J., Ellory, J. C., Mount, D. B., & Shen, M.-R. (2009). Motor Protein-Dependent Membrane Trafficking of KCl Cotransporter-4 Is Important for Cancer Cell Invasion. *Cancer Research*, 69(22), 8585–8593.

Chevalier, S., Defoy, I., Lacoste, J., Hamel, L., Guy, L., Bégin, L. R., & Aprikian, A. G. (2002). Vascular endothelial growth factor and signaling in the prostate: more than angiogenesis. *Molecular and Cellular Endocrinology*, 189(1–2), 169–79.

Chiu, M.-H., Liu, H.-S., Wu, Y.-H., Shen, M.-R., & Chou, C.-Y. (2014). SPAK mediates KCC3-enhanced cervical cancer tumorigenesis. *FEBS Journal*, 281(10), 2353–2365.

- Cohen, R. J., Shannon, B. A., Phillips, M., Moorin, R. E., Wheeler, T. M., & Garrett, K. L. (2008). Central zone carcinoma of the prostate gland: a distinct tumor type with poor prognostic features. *The Journal of Urology*, *179*(5), 1762–1767.
- Conteduca, V., Aieta, M., Amadori, D., & De Giorgi, U. (2014). Neuroendocrine differentiation in prostate cancer: Current and emerging therapy strategies. *Critical Reviews in Oncology/Hematology*, *92*(1), 11–24.
- Corpet, F. (1988). Multiple sequence alignment with hierarchical clustering. *Nucleic Acids Research*, *16*(22), 10881–90.
- Costigan, M., Scholz, J., & Woolf, C. J. (2009). Neuropathic Pain: A Maladaptive Response of the Nervous System to Damage. *Annual Review of Neuroscience*, *32*(1), 1–32.
- Cox, M. E., Deeble, P. D., Lakhani, S., & Parsons, S. J. (1999). Acquisition of neuroendocrine characteristics by prostate tumor cells is reversible: implications for prostate cancer progression. *Cancer Research*, *59*(15), 3821–30.
- Crabtree, J. S., & Miele, L. (2016). Neuroendocrine tumors: current therapies, notch signaling, and cancer stem cells. *Journal of Cancer Metastasis and Treatment*, *2*(8), 279.
- Creyghton, M. P., Cheng, A. W., Welstead, G. G., Kooistra, T., Carey, B. W., Steine, E. J., ... Jaenisch, R. (2010). Histone H3K27ac separates active from poised enhancers and predicts developmental state. *Proceedings of the National Academy of Sciences*, *107*(50), 21931–21936.
- Crook, J. M., O'Callaghan, C. J., Duncan, G., Dearnaley, D. P., Higano, C. S., Horwitz, E. M., ... Klotz, L. (2012). Intermittent Androgen Suppression for Rising PSA Level after Radiotherapy. *New England Journal of Medicine*, *367*(10), 895–903.
- Danza, G., Di Serio, C., Rosati, F., Lonetto, G., Sturli, N., Kacer, D., ... Tarantini, F. (2012). Notch signaling modulates hypoxia-induced neuroendocrine differentiation of human prostate cancer cells. *Molecular Cancer Research: MCR*, *10*(2), 230–8.
- DaSilva, J., Gioeli, D., Weber, M., Parsons, S. (2009). The neuroendocrine-derived peptide, PTHrP, promotes prostate cancer cell growth by stabilizing the androgen receptor. *Cancer Research*, *69*(18), 7402-7411.
- De Marzo, A. M., Platz, E. A., Sutcliffe, S., Xu, J., Grönberg, H., Drake, C. G., ... Nelson, W. G. (2007). Inflammation in prostate carcinogenesis. *Nature Reviews. Cancer*, *7*(4), 256–69.
- de Torres, I., Castellvi, J., Landolfi, S., Fernandez, S., Alana, L., Paciucci, R., & Ramon, S. (2010). PTOV-1 overexpression in neuroendocrine tumors: a new molecular marker. *7th Annual ENETS Conference*, 79.
- Deeble, P. D., Murphy, D. J., Parsons, S. J., & Cox, M. E. (2001). Interleukin-6-

and cyclic AMP-mediated signaling potentiates neuroendocrine differentiation of LNCaP prostate tumor cells. *Molecular and Cellular Biology*, 21(24), 8471–82.

Dehm, S., Tindall, D. (2011). Alternatively spliced androgen receptor variants. *Endocrine Related Cancer*, 18(5) 183-96.

Demelash, A., Rudrabhatla, P., Pant, H. C., Wang, X., Amin, N. D., McWhite, C. D., ... Linnoila, R. I. (2012). Achaete-scute homologue-1 (ASH1) stimulates migration of lung cancer cells through Cdk5/p35 pathway. *Molecular Biology of the Cell*, 23(15), 2856–66.

Deng, X., Elzey, B. D., Poulson, J. M., Morrison, W. B., Ko, S.-C., Hahn, N. M., ... Hu, C.-D. (2011). Ionizing radiation induces neuroendocrine differentiation of prostate cancer cells in vitro, in vivo and in prostate cancer patients. *American Journal of Cancer Research*, 1(7), 834–44.

Deng, X., Liu, H., Huang, J., Cheng, L., Keller, E. T., Parsons, S. J., & Hu, C.-D. (2008). Ionizing radiation induces prostate cancer neuroendocrine differentiation through interplay of CREB and ATF2: implications for disease progression. *Cancer Research*, 68(23), 9663–70.

Di Sant'Agnese, P. A. (1992). Neuroendocrine differentiation in carcinoma of the prostate. Diagnostic, prognostic, and therapeutic implications. *Cancer*, 70(S1), 254–268.

Dixon, C., Sah, P., Lynch, J. W., & Keramidas, A. (2014). GABAA receptor α and γ subunits shape synaptic currents via different mechanisms. *The Journal of Biological Chemistry*, 289(9), 5399–411.

Dutt, S. S., & Gao, A. C. (2009). Molecular mechanisms of castration-resistant prostate cancer progression. *Future Oncology (London, England)*, 5(9), 1403–13.

Dwight, Z., Palais, R., & Wittwer, C. T. (2011). uMELT: prediction of high-resolution melting curves and dynamic melting profiles of PCR products in a rich web application. *Bioinformatics*, 27(7), 1019–1020.

Epstein, J. I., Egevad, L., Amin, M. B., Delahunt, B., Srigley, J. R., & Humphrey, P. A. (2015). The 2014 International Society of Urological Pathology (ISUP) Consensus Conference on Gleason Grading of Prostatic Carcinoma. *The American Journal of Surgical Pathology*, 1.

Esposito, S., Russo, M. V, Airoidi, I., Tupone, M. G., Sorrentino, C., Barbarito, G., ... Di Carlo, E. (2015). SNAI2/Slug gene is silenced in prostate cancer and regulates neuroendocrine differentiation, metastasis-suppressor and pluripotency gene expression. *Oncotarget*, 6(19), 17121–34.

Fallon, M., Hoskin, P. J., Colvin, L. A., Fleetwood-Walker, S. M., Adamson, D., Byrne, A., ... Laird, B. J. A. (2016). Randomized Double-Blind Trial of Pregabalin Versus Placebo in Conjunction With Palliative Radiotherapy for Cancer-Induced Bone Pain. *Journal of Clinical Oncology*, 34(6), 550–556.

- Farach, A., Ding, Y., Lee, M., Creighton, C., Delk, N. A., Ittmann, M., ... Ayala, G. E. (2016). Neuronal trans-differentiation in prostate cancer cells. *The Prostate*, 76(14), 1312-1325.
- Feldman, B. J., & Feldman, D. (2001). The development of androgen-independent prostate cancer. *Nature Reviews. Cancer*, 1(1), 34–45.
- Fernández-García, E. M., Vera-Badillo, F. E., Perez-Valderrama, B., Matos-Pita, A. S., & Duran, I. (2014). Immunotherapy in prostate cancer: review of the current evidence. *Clinical & Translational Oncology*, 17(5), 339-357.
- Foley, C., & Mitsiades, N. (2016). Moving Beyond the Androgen Receptor (AR): Targeting AR-Interacting Proteins to Treat Prostate Cancer. *Hormones and Cancer*, 7(2), 84–103.
- Friedman, R. (2016). Drug resistance in cancer: molecular evolution and compensatory proliferation. *Oncotarget*, 7(11), 11746–55.
- Fritschy, J.-M., Meskenaite, V., Weinmann, O., Honer, M., Benke, D., & Mohler, H. (1999). GABA_B -receptor splice variants GB1a and GB1b in rat brain: developmental regulation, cellular distribution and extrasynaptic localization. *European Journal of Neuroscience*, 11(3), 761–768.
- Frolund, B., Ebert, B., Kristiansen, U., Liljefors, T., & Krogsgaard-Larsen, P. (2002). GABA-A Receptor Ligands and their Therapeutic Potentials. *Current Topics in Medicinal Chemistry*, 2(8), 817–832.
- Gale, J. D., & Houghton, L. A. (2011). Alpha 2 Delta ($\alpha(2)\delta$) Ligands, Gabapentin and Pregabalin: What is the Evidence for Potential Use of These Ligands in Irritable Bowel Syndrome. *Frontiers in Pharmacology*, 2, 28.
- Gallagher, S. R., & Desjardins, P. R. (2006). Quantitation of DNA and RNA with Absorption and Fluorescence Spectroscopy. In *Current Protocols in Molecular Biology*. Hoboken, NJ, USA: John Wiley & Sons, Inc.
- Gangisetty, O., & Reddy, D. (2009). THE Optimization of TaqMan Real-Time RT-PCR Assay for Transcriptional Profiling of GABA-A Receptor Subunit Plasticity. *Journal of Neuroscience Methods*, 181(1), 58-66.
- Gao, B.-X., Stricker, C., & Ziskind-Conhaim, L. (2001). Transition From GABAergic to Glycinergic Synaptic Transmission in Newly Formed Spinal Networks. *Journal of Neurophysiology*, 86(1), 492–502.
- Gao, L., Schwartzman, J., Gibbs, A., Lisac, R., Kleinschmidt, R., Wilmot, B., ... Alumkal, J. (2013). Androgen Receptor Promotes Ligand-Independent Prostate Cancer Progression through c-Myc Upregulation. *PLoS ONE*, 8(5), e63563.
- Gao, Z., Ure, K., Ding, P., Nashaat, M., Yuan, L., Ma, J., ... Hsieh, J. (2011). The master negative regulator REST/NRSF controls adult neurogenesis by restraining the neurogenic program in quiescent stem cells. *The Journal of Neuroscience: The Official Journal of the Society for Neuroscience*, 31(26), 9772–86.

Garnier, J.-M., Sharp, P. P., & Burns, C. J. (2014). BET bromodomain inhibitors: a patent review. *Expert Opinion on Therapeutic Patents*, 24(2), 185–199.

Gassmann, M., & Bettler, B. (2012). Regulation of neuronal GABAB receptor functions by subunit composition. *Nature Reviews Neuroscience*, 13(6), 380–394.

Gater, A., Abetz-Webb, L., Battersby, C., Parasuraman, B., McIntosh, S., Nathan, F., & Piault, E. C. (2011). Pain in castration-resistant prostate cancer with bone metastases: a qualitative study. *Health and Quality of Life Outcomes*, 9, 88.

Gathirua-Mwangi, W. G., & Zhang, J. (2014). Dietary factors and risk for advanced prostate cancer. *European Journal of Cancer Prevention : The Official Journal of the European Cancer Prevention Organisation (ECP)*, 23(2), 96–109.

Giachino, C., Barz, M., Tchorz, J. S., Tome, M., Gassmann, M., Bischofberger, J., ... Taylor, V. (2014). GABA suppresses neurogenesis in the adult hippocampus through GABAB receptors. *Development*, 141(1), 83–90.

Gianelli, G., Falk-Marzillier, J., Schiraldi, O., Stetler-Stevenson, W., Quaranta, V. (1997). Induction of cell migration by matrix metalloprotease-2 cleavage of laminin-5. *Science*, 227(5323), 225–228.

Gillotin, S., Davies, J. D., & Philpott, A. (2018). Subcellular localisation modulates ubiquitylation and degradation of Ascl1. *Scientific Reports*, 8(1), 4625.

Glass, A. S., Cary, K. C., & Cooperberg, M. R. (2013). Risk-based prostate cancer screening: who and how? *Current Urology Reports*, 14(3), 192–8.

Goa, K. L., & Sorkin, E. M. (1993). Gabapentin. *Drugs*, 46(3), 409–427.

Goetz, M. P., Kalari, K. R., Suman, V. J., Moyer, A. M., Yu, J., Visscher, D. W., ... Boughey, J. C. (2017). Tumor Sequencing and Patient-Derived Xenografts in the Neoadjuvant Treatment of Breast Cancer. *Journal of the National Cancer Institute*, 109(7).

Gomella, L. (2009). Effective testosterone suppression for prostate cancer: is there a best castration therapy?. *Reviews in Urology*, 11(2), 52-60.

Grigore, A. D., Ben-Jacob, E., & Farach-Carson, M. C. (2015). Prostate cancer and neuroendocrine differentiation: more neuronal, less endocrine? *Frontiers in Oncology*, 5, 37.

Grossfeld, G. D., Small, E. J., Lubeck, D. P., Latini, D., Broering, J. M., & Carroll, P. R. (2001). Androgen deprivation therapy for patients with clinically localized (stages T1 to T3) prostate cancer and for patients with biochemical recurrence after radical prostatectomy. *Urology*, 58(2), 56–64.

Guardavaccaro, D., Frescas, D., Dorrello, N. V., Peschiaroli, A., Multani, A. S., Cardozo, T., ... Pagano, M. (2008). Control of chromosome stability by the β -TrCP–REST–Mad2 axis. *Nature*, 452(7185), 365–369.

Gudmundsson, J., Besenbacher, S., Sulem, P., Gudbjartsson, D. F., Olafsson, I., Arinbjarnarson, S., ... Stefansson, K. (2010). Genetic correction of PSA values using sequence variants associated with PSA levels. *Science Translational Medicine*, 2(62), 62-92.

Guillemot, F., & Hassan, B. A. (2017). Beyond proneural: emerging functions and regulations of proneural proteins. *Current Opinion in Neurobiology*, 42, 93–101.

Gumireddy, K., Li, A., Kossenkov, A. V., Sakurai, M., Yan, J., Li, Y., ... Huang, Q. (2016). The mRNA-edited form of GABRA3 suppresses GABRA3-mediated Akt activation and breast cancer metastasis. *Nature Communications*, 7, 10715.

Gudem, G., Van Loo, P., Kremeyer, B., Alexandrov, L. B., Tubio, J. M. C., Papaemmanuil, E., ... Bova, G. S. (2015). The evolutionary history of lethal metastatic prostate cancer. *Nature*, 520, 353-357.

Gupta, A., Yu, X., Case, T., Paul, M., Shen, M. M., Kaestner, K. H., & Matusik, R. J. (2013). Mash1 expression is induced in neuroendocrine prostate cancer upon the loss of Foxa2. *The Prostate*, 73(6), 582–589.

Gut, P., Czarnywojtek, A., Fischbach, J., Bączyk, M., Ziemnicka, K., Wrotkowska, E., ... Ruchała, M. (2016). Chromogranin A - unspecific neuroendocrine marker. Clinical utility and potential diagnostic pitfalls. *Archives of Medical Science : AMS*, 12(1), 1–9.

Hager, S., Ackermann, C. J., Joerger, M., Gillessen, S., & Omlin, A. (2016). Anti-tumour activity of platinum compounds in advanced prostate cancer—a systematic literature review. *Annals of Oncology*, 27(6), 975–984.

Hamilton, W., Sharp, D. J., Peters, T. J., & Round, A. P. (2006). Clinical features of prostate cancer before diagnosis: a population-based, case-control study. *The British Journal of General Practice : The Journal of the Royal College of General Practitioners*, 56(531), 756–62.

Hammerstrom, A. E., Cauley, D. H., Atkinson, B. J., & Sharma, P. (2011). Cancer immunotherapy: sipuleucel-T and beyond. *Pharmacotherapy*, 31(8), 813–28.

Hartmann, A.-M., & Nothwang, H. G. (2014). Molecular and evolutionary insights into the structural organization of cation chloride cotransporters. *Frontiers in Cellular Neuroscience*, 8, 470.

Hashimoto, K., Shindo, T., Tabata, H., Tanaka, T., Hashimoto, J., Inoue, R., & Shimizu, T. (2017). Serum Testosterone Level is a Useful Biomarker to Aid Optimal Treatment Selection in Men with Castration-Resistant Prostate Cancer. *Japanese Journal of Clinical Oncology*, 41(3), 405-410

He, Y., Hooker, E., Yu, E.-J., Wu, H., Cunha, G. R., & Sun, Z. (2018). An Indispensable Role of Androgen Receptor in Wnt Responsive Cells During Prostate Development, Maturation, and Regeneration. *Stem Cells*, 36(6), 891–902.

He, Y., Lu, J., Ye, Z., Hao, S., Wang, L., Kohli, M., ... Huang, H. (2018). Androgen

receptor splice variants bind to constitutively open chromatin and promote abiraterone-resistant growth of prostate cancer. *Nucleic Acids Research*, 46(4), 1895-1911.

Hedblom, E., & Kirkness, E. F. (1997). A novel class of GABAA receptor subunit in tissues of the reproductive system. *The Journal of Biological Chemistry*, 272(24), 15346–50.

Heidenreich, A., Bastian, P. J., Bellmunt, J., Bolla, M., Joniau, S., van der Kwast, T., ... European Association of Urology. (2014). EAU Guidelines on Prostate Cancer. Part II: Treatment of Advanced, Relapsing, and Castration-Resistant Prostate Cancer. *European Urology*, 65(2), 467–479.

Hendrich, J., Tran Van Minh, A., Heblich, F., Nieto-Rostro, M., Watschinger, K., Striessnig, J., ... Tsien, R. W. (2008). Pharmacological disruption of calcium channel trafficking by the alpha2delta ligand gabapentin. *Proceedings of the National Academy of Sciences of the United States of America*, 105(9), 3628-3633.

Henke, R. M., Meredith, D. M., Borromeo, M. D., Savage, T. K., & Johnson, J. E. (2009). Ascl1 and Neurog2 form novel complexes and regulate Delta-like3 (Dll3) expression in the neural tube. *Developmental Biology*, 328(2), 529–540.

Hill, D. R., & Bowery, N. G. (1981). 3H-baclofen and 3H-GABA bind to bicuculline-insensitive GABA B sites in rat brain. *Nature*, 290(5802), 149–52.

Ho-Kim, M. A., Tremblay, R. R., & Dube, J. Y. (1981). Binding of Methyltrienolone to Glucocorticoid Receptors in Rat Muscle Cytosol. *Endocrinology*, 109(5), 1418–1423.

Hoffman-Censits, J., & Kelly, W. K. (2013). Enzalutamide: A Novel Antiandrogen for Patients with Castrate-Resistant Prostate Cancer. *Clinical Cancer Research*, 19(6), 1335–1339.

Honarmand, A., Safavi, M., & Zare, M. (2011). Gabapentin: An update of its pharmacological properties and therapeutic use in epilepsy. *Journal of Research in Medical Sciences*, 16(8), 1062–9.

Horoszewicz, J. S., Leong, S. S., Kawinski, E., Karr, J. P., Rosenthal, H., Chu, T. M., ... Murphy, G. P. (1983). LNCaP Model of Human Prostatic Carcinoma. *Cancer Research*, 43(4).

Hsu, Y.-M., Chou, C.-Y., Chen, H. H. W., Lee, W.-Y., Chen, Y.-F., Lin, P.-W., ... Shen, M.-R. (2007). IGF-1 upregulates electroneutral K-Cl cotransporter KCC3 and KCC4 which are differentially required for breast cancer cell proliferation and invasiveness. *Journal of Cellular Physiology*, 210(3), 626–636.

Hu, C.-D., Choo, R., & Huang, J. (2015). Neuroendocrine differentiation in prostate cancer: a mechanism of radioresistance and treatment failure. *Frontiers in Oncology*, 5, 90.

Hu, R., Lu, C., Mostaghel, E. A., Yegnasubramanian, S., Gurel, M., Tannahill, C., ... Luo, J. (2012). Distinct transcriptional programs mediated by the ligand-

dependent full-length androgen receptor and its splice variants in castration-resistant prostate cancer. *Cancer Research*, 72(14), 3457–62.

Hu, Y., Ippolito, J. E., Garabedian, E. M., Humphrey, P. A., & Gordon, J. I. (2002). Molecular Characterization of a Metastatic Neuroendocrine Cell Cancer Arising in the Prostates of Transgenic Mice. *Journal of Biological Chemistry*, 277(46) 44462-44474.

Huggins, C. (1941). Studies on Prostatic Cancer. *Archives of Surgery*, 43(2), 209.

Humphrey, P. A. (2004). Gleason grading and prognostic factors in carcinoma of the prostate. *Modern Pathology*, 17(3), 292–306.

Hussain, M., Tangen, C. M., Berry, D. L., Higano, C. S., Crawford, E. D., Liu, G., ... Thompson, I. M. (2013). Intermittent versus Continuous Androgen Deprivation in Prostate Cancer. *New England Journal of Medicine*, 368(14), 1314–1325.

Inglefield, J. R., & Schwartz-Bloom, R. D. (1999). Fluorescence Imaging of Changes in Intracellular Chloride in Living Brain Slices. *Methods*, 18(2), 197–203.

Ippolito, J. E., Merritt, M. E., Bäckhed, F., Moulder, K. L., Mennerick, S., Manchester, J. K., ... Gordon, J. I. (2006). Linkage between cellular communications, energy utilization, and proliferation in metastatic neuroendocrine cancers. *Proceedings of the National Academy of Sciences of the United States of America*, 103(33), 12505–10.

Ippolito, J. E., & Piwnica-Worms, D. (2014). A fluorescence-coupled assay for gamma aminobutyric acid (GABA) reveals metabolic stress-induced modulation of GABA content in neuroendocrine cancer. *PloS One*, 9(2), e88667.

Isgro, M. A., Bottoni, P., & Scatena, R. (2015). Neuron-Specific Enolase as a Biomarker: Biochemical and Clinical Aspects. *Advances in Experimental Medicine and Biology*, 867, 125–143.

Ishibashi, M., Ang, S. L., Shiota, K., Nakanishi, S., Kageyama, R., & Guillemot, F. (1995). Targeted disruption of mammalian hairy and Enhancer of split homolog-1 (HES-1) leads to up-regulation of neural helix-loop-helix factors, premature neurogenesis, and severe neural tube defects. *Genes & Development*, 9(24), 3136–48.

Ishii, J., Sato, H., Sakaeda, M., Shishido-Hara, Y., Hiramatsu, C., Kamma, H., ... Yazawa, T. (2013). POU domain transcription factor BRN2 is crucial for expression of ASCL1, ND1 and neuroendocrine marker molecules and cell growth in small cell lung cancer. *Pathology International*, 63(3), 158–168.

Iwafuchi-doi, M., Donahue, G., Kakumanu, A., Lee, D., Kaestner, K. H., ... Pugh, B. F. (2016). The Pioneer Transcription Factor FoxA Maintains an Accessible Nucleosome Configuration at Enhancers Article The Pioneer Transcription Factor FoxA Maintains an Accessible Nucleosome Configuration at Enhancers for Tissue-Specific Gene Activation. *Molecular Cell*, 62(1), 79–91.

Iwafuchi-Doi, M., & Zaret, K. S. (2014). Pioneer transcription factors in cell

reprogramming. *Genes & Development*, 28(24), 2679–92.

Iwakiri, M., Mizukami, K., Ikonovic, M. D., Ishikawa, M., Abrahamson, E. E., DeKosky, S. T., & Asada, T. (2009). An immunohistochemical study of GABA A receptor gamma subunits in Alzheimer's disease hippocampus: relationship to neurofibrillary tangle progression. *Neuropathology*, 29(3), 263–9.

Jacob, T. C., Moss, S. J., & Jurd, R. (2008). GABA(A) receptor trafficking and its role in the dynamic modulation of neuronal inhibition. *Nature Reviews. Neuroscience*, 9(5), 331–43.

Jagla, M., Fève, M., Kessler, P., Lapouge, G., Erdmann, E., Serra, S., ... Céraline, J. (2007). A Splicing Variant of the Androgen Receptor Detected in a Metastatic Prostate Cancer Exhibits Exclusively Cytoplasmic Actions. *Endocrinology*, 148(9), 4334–4343.

Jahn, J. L., Giovannucci, E. L., & Stampfer, M. J. (2015). The high prevalence of undiagnosed prostate cancer at autopsy: implications for epidemiology and treatment of prostate cancer in the Prostate-specific Antigen-era. *International Journal of Cancer*, 137(12), 2795–802.

James, N. D., de Bono, J. S., Spears, M. R., Clarke, N. W., Mason, M. D., Dearnaley, D. P., ... Sydes, M. R. (2017). Abiraterone for Prostate Cancer Not Previously Treated with Hormone Therapy. *New England Journal of Medicine*, 377(4), 338–351.

James, N. D., Sydes, M. R., Clarke, N. W., Mason, M. D., Dearnaley, D. P., Spears, M. R., ... Parmar, M. K. B. (2016). Addition of docetaxel, zoledronic acid, or both to first-line long-term hormone therapy in prostate cancer (STAMPEDE): survival results from an adaptive, multiarm, multistage, platform randomised controlled trial. *The Lancet*, 387(10024), 1163–1177.

Johnston, G. (2014). Muscimol as an ionotropic GABA receptor agonist. *Neurochemical Research*, 39(10), 1942-1947.

Johnston, S. J., & Carroll, J. S. (2015). Transcription factors and chromatin proteins as therapeutic targets in cancer. *Biochimica et Biophysica Acta - Reviews on Cancer*, 18852(2), 183-192.

Jones, D., Noble, M., Wedge, S. R., Robson, C. N., & Gaughan, L. (2017). Aurora A regulates expression of AR-V7 in models of castrate resistant prostate cancer. *Scientific Reports*, 7(1), 40957.

Jones, D., Wade, M., Nakjang, S., Chaytor, L., Grey, J., Robson, C. N., & Gaughan, L. (2015). FOXA1 regulates androgen receptor variant activity in models of castrate-resistant prostate cancer. *Oncotarget*, 6(30), 29782–94.

Juarranz, M. G., Bolaños, O., Gutiérrez-Cañas, I., Lerner, E. A., Robberecht, P., Carmena, M. J., ... Rodríguez-Henche, N. (2001). Neuroendocrine differentiation of the LNCaP prostate cancer cell line maintains the expression and function of VIP and PACAP receptors. *Cellular Signalling*, 13(12), 887–894.

Justus, C., Leffler, N., Ruiz-Echevarria, M., Yang, L. (2014). In vitro migration and invasion assays. *Journal of Visual Experiments*, (88), 51046.

Kahle, K. T., Khanna, A. R., Alper, S. L., Adragna, N. C., Lauf, P. K., Sun, D., & Delpire, E. (2015). K-Cl cotransporters, cell volume homeostasis, and neurological disease. *Trends in Molecular Medicine*, 21(8), 513–23.

Kahle, K. T., Staley, K. J., Nahed, B. V, Gamba, G., Hebert, S. C., Lifton, R. P., & Mount, D. B. (2008). Roles of the cation–chloride cotransporters in neurological disease. *Nature Clinical Practice Neurology*, 4(9), 490–503.

Kaighn, M. E., Narayan, K. S., Ohnuki, Y., Lechner, J. F., & Jones, L. W. (1979). Establishment and characterization of a human prostatic carcinoma cell line (PC-3). *Investigative Urology*, 17(1), 16–23.

Kamiya, N., Akakura, K., Suzuki, H., Isshiki, S., Komiyama, A., Ueda, T., & Ito, H. (2003). Pretreatment serum level of neuron specific enolase (NSE) as a prognostic factor in metastatic prostate cancer patients treated with endocrine therapy. *European Urology*, 44(3), 309–14.

Kammerer, M., Rassner, M. P., Freiman, T. M., & Feuerstein, T. J. (2011). Effects of antiepileptic drugs on GABA release from rat and human neocortical synaptosomes. *Naunyn-Schmiedeberg's Archives of Pharmacology*, 384(1), 47–57.

Karantanos, T., Corn, P. G., & Thompson, T. C. (2013). Prostate cancer progression after androgen deprivation therapy: mechanisms of castrate resistance and novel therapeutic approaches. *Oncogene*, 32(49), 5501–11.

Kasim, M., Heß, V., Scholz, H., Persson, P. B., & Föhling, M. (2016). Achaete-Scute Homolog 1 Expression Controls Cellular Differentiation of Neuroblastoma. *Frontiers in Molecular Neuroscience*, 9, 156.

Katsogiannou, M., Ziouziou, H., Karaki, S., Andrieu, C., Henry de Villeneuve, M., & Rocchi, P. (2015). The hallmarks of castration-resistant prostate cancers. *Cancer Treatment Reviews*, 41(7), 588–597.

Kaufmann, O., Georgi, T., & Dietel, M. (1997). Utility of 123C3 monoclonal antibody against CD56 (NCAM) for the diagnosis of small cell carcinomas on paraffin sections. *Human Pathology*, 28(12), 1373–8.

Kenfield, S. A., Stampfer, M. J., Chan, J. M., & Giovannucci, E. (2011). Smoking and prostate cancer survival and recurrence. *JAMA*, 305(24), 2548–55.

Khozhaï, L. I., & Il'icheva, N. V. (2017a). Establishment of the GABAergic Neural Network in the Ventrolateral Part of the Solitary Tract Nucleus in Normal Conditions and in Prenatal Serotonin Deficiency in Rats. *Neuroscience and Behavioral Physiology*, 47(7), 846–850.

Khozhaï, L. I., & Il'icheva, N. V. (2017b). Formation of GABAergic Neural Networks in the Böttinger Complex in Rats in the Early Postnatal Period in Normal Conditions and with Prenatal Deficiency of Endogenous Serotonin.

Neuroscience and Behavioral Physiology, 47(6), 641–645.

Kibbe, W. A. (2007). OligoCalc: an online oligonucleotide properties calculator. *Nucleic Acids Research*, 35, 43–46.

Kim, J., & Coetzee, G. A. (2004). Prostate specific antigen gene regulation by androgen receptor. *Journal of Cellular Biochemistry*, 93(2), 233–241.

Klausberger, T., Ehya, N., Fuchs, K., Fuchs, T., Ebert, V., Sarto, I., & Sieghart, W. (2001). Detection and binding properties of GABA(A) receptor assembly intermediates. *The Journal of Biological Chemistry*, 276(19), 16024–32.

Klotz, L. H., Herr, H. W., Morse, M. J., & Whitmore, W. F. (1986). Intermittent endocrine therapy for advanced prostate cancer. *Cancer*, 58(11), 2546–50.

Klotz, L., Zhang, L., Lam, A., Nam, R., Mamedov, A., & Loblaw, A. (2010). Clinical Results of Long-Term Follow-Up of a Large, Active Surveillance Cohort With Localized Prostate Cancer. *Journal of Clinical Oncology*, 28(1), 126–131.

Komatsu, Y. (1996). GABAB receptors, monoamine receptors, and postsynaptic inositol trisphosphate-induced Ca²⁺ release are involved in the induction of long-term potentiation at visual cortical inhibitory synapses. *The Journal of Neuroscience*, 16(20), 6342–52.

Komiya, A., Suzuki, H., Imamoto, T., Kamiya, N., Nihei, N., Naya, Y., ... Fuse, H. (2009). Neuroendocrine differentiation in the progression of prostate cancer. *International Journal of Urology: Official Journal of the Japanese Urological Association*, 16(1), 37–44.

Komiya, A., Yasuda, K., Watanabe, A., Fujiuchi, Y., Tsuzuki, T., & Fuse, H. (2013). The prognostic significance of loss of the androgen receptor and neuroendocrine differentiation in prostate biopsy specimens among castration-resistant prostate cancer patients. *Molecular and Clinical Oncology*, 1(2), 257–262.

Kong, D., Sethi, S., Li, Y., Chen, W., Sakr, W. A., Heath, E., & Sarkar, F. H. (2015). Androgen receptor splice variants contribute to prostate cancer aggressiveness through induction of EMT and expression of stem cell marker genes. *The Prostate*, 75(2), 161–74.

Koninckx, M., Marco, J. L., Pérez, I., Faus, M. T., Alcolea, V., & Gómez, F. (2019). Effectiveness, safety and cost of abiraterone acetate in patients with metastatic castration-resistant prostate cancer: a real-world data analysis. *Clinical and Translational Oncology*, 21(3), 314–323.

Krause, W. C., Shafi, A. A., Nakka, M., & Weigel, N. L. (2014). Androgen receptor and its splice variant, AR-V7, differentially regulate FOXA1 sensitive genes in LNCaP prostate cancer cells. *The International Journal of Biochemistry & Cell Biology*, 54, 49–59.

Lai, E. C. (2004). Notch signaling: control of cell communication and cell fate. *Development*, 131(5), 965–973.

- Lang, S., Frame, F., & Collins, A. (2009). Prostate cancer stem cells. *The Journal of Pathology*, 217(2), 299–306.
- Lanneau, C., Green, A., Hirst, W. D., Wise, A., Brown, J. T., Donnier, E., ... Pangalos, M. N. (2001). Gabapentin is not a GABAB receptor agonist. *Neuropharmacology*, 41(8), 965–975.
- Lapuk, A. V, Wu, C., Wyatt, A. W., McPherson, A., McConeghy, B. J., Brahmabhatt, S., ... Collins, C. C. (2012). From sequence to molecular pathology, and a mechanism driving the neuroendocrine phenotype in prostate cancer. *The Journal of Pathology*, 227(3), 286–297.
- Larry Goldenberg, S., Bruchofsky, N., Gleave, M. E., Sullivan, L. D., & Akakura, K. (1995). Intermittent androgen suppression in the treatment of prostate cancer: A preliminary report. *Urology*, 45(5), 839–845.
- Laurie, D. J., Wisden, W., & Seeburg, P. H. (1992). The distribution of thirteen GABAA receptor subunit mRNAs in the rat brain. III. Embryonic and postnatal development. *The Journal of Neuroscience*, 12(11), 4151–72.
- Lee, C.-L., & Kuo, H.-C. (2017). Pathophysiology of benign prostate enlargement and lower urinary tract symptoms: Current concepts. *Ci Ji Yi Xue Za Zhi = Tzu-Chi Medical Journal*, 29(2), 79–83.
- Lee, L. F., Guan, J., Qiu, Y., & Kung, H. J. (2001). Neuropeptide-induced androgen independence in prostate cancer cells: roles of nonreceptor tyrosine kinases Etk/Bmx, Src, and focal adhesion kinase. *Molecular and Cellular Biology*, 21(24), 8385–97.
- Lenhart, R., Kirov, S., Desilva, H., Cao, J., Lei, M., Johnston, K., ... Wee, S. (2015). Sensitivity of Small Cell Lung Cancer to BET Inhibition Is Mediated by Regulation of ASCL1 Gene Expression. *Molecular Cancer Therapeutics*, 14(10), 2167–2174.
- Leung, J. K., & Sadar, M. D. (2017). Non-Genomic Actions of the Androgen Receptor in Prostate Cancer. *Frontiers in Endocrinology*, 8, 2.
- Li, K., & Xu, E. (2008). The role and the mechanism of gamma-aminobutyric acid during central nervous system development. *Neuroscience Bulletin*, 24(3), 195–200.
- Li, Q., Zhang, C. S., & Zhang, Y. (2016). Molecular aspects of prostate cancer with neuroendocrine differentiation. *Chinese Journal of Cancer Research = Chung-Kuo Yen Cheng Yen Chiu*, 28(1), 122–9.
- Li, Y.-H., Liu, Y., Li, Y.-D., Liu, Y.-H., Li, F., Ju, Q., ... Li, G.-C. (2012a). GABA stimulates human hepatocellular carcinoma growth through overexpressed GABAA receptor theta subunit. *World Journal of Gastroenterology*, 18(21), 2704–11.
- Liang, H., Studach, L., Hullinger, R. L., Xie, J., & Andrisani, O. M. (2014). Down-regulation of RE-1 silencing transcription factor (REST) in advanced prostate

cancer by hypoxia-induced miR-106b~25. *Experimental Cell Research*, 320(2), 188–199.

Lin, T.-P., Chang, Y.-T., Lee, S.-Y., Campbell, M., Wang, T.-C., Shen, S.-H., ... Chang, P.-C. (2016). REST reduction is essential for hypoxia-induced neuroendocrine differentiation of prostate cancer cells by activating autophagy signaling. *Oncotarget*, 7(18), 26137-26151.

Liang, C., Park, A., Guan, J. (2007). In vitro scratch assay: a convenient and inexpensive method for analysis of cell migration in vitro. *Nature Protocols*, 2(2), 329-333.

Liu, Y., Guo, F., Dai, M., Wang, D., Tong, Y., Huang, J., ... Li, G. (2009). Gammaaminobutyric Acid A Receptor Alpha 3 Subunit is Overexpressed in Lung Cancer. *Pathology & Oncology Research*, 15(3), 351–358.

Livak, K. J., & Schmittgen, T. D. (2001). Analysis of relative gene expression data using real-time quantitative PCR and the 2^{(-Delta Delta C(T))} Method. *Methods (San Diego, Calif.)*, 25(4), 402–8.

Lu-Yao, G. L., Albertsen, P. C., Moore, D. F., Shih, W., Lin, Y., DiPaola, R. S., ... Yao, S.-L. (2009). Outcomes of localized prostate cancer following conservative management. *JAMA*, 302(11), 1202–9.

Lu, C., & Luo, J. (2013). Decoding the androgen receptor splice variants. *Translational Andrology and Urology*, 2(3).

Lu, X., Zhang, S., Lu, Y., Xiu, X., & Sun, X. (2007). The significance of K-Cl cotransport1 expression in cervical cancer tissues. *Zhonghua Yi Xue Za Zhi*, 87(17), 1156–9.

Lukasiewicz, P. D. (1996). GABAC receptors in the vertebrate retina. *Molecular Neurobiology*, 12(3), 181–194.

Luke, M. C., & Coffey, D. S. (1994). Human Androgen Receptor Binding to the Androgen Response Element of Prostate Specific Antigen. *Journal of Andrology*, 15(1), 41–51.

Madersbacher, S., Alcaraz, A., Emberton, M., Hammerer, P., Ponholzer, A., Schröder, F. H., & Tubaro, A. (2011). The influence of family history on prostate cancer risk: implications for clinical management. *BJU International*, 107(5), 716–21.

Mäkinen, M. E.-L., Ylä-Outinen, L., & Narkilahti, S. (2018). GABA and Gap Junctions in the Development of Synchronized Activity in Human Pluripotent Stem Cell-Derived Neural Networks. *Frontiers in Cellular Neuroscience*, 12, 56.

Marangos, P. J., & Schmechel, D. E. (1987). Neuron Specific Enolase, A Clinically Useful Marker for Neurons and Neuroendocrine Cells. *Annual Review of Neuroscience*, 10(1), 269–295.

Marks, L. S. (2004). 5alpha-reductase: history and clinical importance. *Reviews*

in Urology, 6(9), S11-21.

Marmigère, F., Rage, F., & Tapia-Arancibia, L. (2003). GABA-glutamate interaction in the control of BDNF expression in hypothalamic neurons. *Neurochemistry International*, 42(4), 353–8.

Martín-Orozco, R. M., Almaraz-Pro, C., Rodríguez-Ubreva, F. J., Cortés, M. A., Ropero, S., Colomer, R., ... Colás, B. (2007). EGF prevents the neuroendocrine differentiation of LNCaP cells induced by serum deprivation: the modulator role of PI3K/Akt. *Neoplasia*, 9(8), 614–24.

Mazurier, N., Parain, K., Parlier, D., Pretto, S., Hamdache, J., Vernier, P., ... Perron, M. (2014). *Ascl1* as a Novel Player in the *Ptf1a* Transcriptional Network for GABAergic Cell Specification in the Retina. *PLoS ONE*, 9(3), e92113.

McKeithen, D., Graham, T., Chung, L. W. K., & Odero-Marah, V. (2010). Snail transcription factor regulates neuroendocrine differentiation in LNCaP prostate cancer cells. *The Prostate*, 70(9), 982–92.

McNeal, J. E. (1968). Regional morphology and pathology of the prostate. *American Journal of Clinical Pathology*, 49(3), 347–57.

Meder, L., König, K., Ozretic, L., Schultheis, A. M., Ueckerth, F., Ade, C. P., ... Buettner, R. (2016). NOTCH, ASCL1, p53 and RB alterations define an alternative pathway driving neuroendocrine and small cell lung carcinomas. *International Journal of Cancer*, 138(4), 927–938.

Migliaccio, A., Castoria, G., Di Domenico, M., de Falco, A., Bilancio, A., Lombardi, M., ... Auricchio, F. (2000). Steroid-induced androgen receptor-oestradiol receptor beta-*Src* complex triggers prostate cancer cell proliferation. *The EMBO Journal*, 19(20), 5406–5417.

Migliaccio, A., Varricchio, L., De Falco, A., Castoria, G., Arra, C., Yamaguchi, H., ... Auricchio, F. (2007). Inhibition of the SH3 domain-mediated binding of *Src* to the androgen receptor and its effect on tumor growth. *Oncogene*, 26(46), 6619–6629.

Miller, P. S., & Aricescu, A. R. (2014). Crystal structure of a human GABAA receptor. *Nature*, 512(7514), 270–5.

Miller, P. S., & Smart, T. G. (2010). Binding, activation and modulation of Cys-loop receptors. *Trends in Pharmacological Sciences*, 31(4), 161–174.

Miller, W. L., & Auchus, R. J. (2011). The Molecular Biology, Biochemistry, and Physiology of Human Steroidogenesis and Its Disorders. *Endocrine Reviews*, 32(1), 81–151.

Mingorance-Le Meur, A., & O'Connor, T. P. (2009). Neurite consolidation is an active process requiring constant repression of protrusive activity. *The EMBO Journal*, 28(3), 248–60.

Minuk, G. Y., Zhang, M., Gong, Y., Minuk, L., Dienes, H., Pettigrew, N., ... Sun,

- D. (2007). Decreased hepatocyte membrane potential differences and GABA α - β 3 expression in human hepatocellular carcinoma. *Hepatology*, 45(3), 735–745.
- Mirosevich, J., Gao, N., Gupta, A., Shappell, S. B., Jove, R., & Matusik, R. J. (2006). Expression and role of Foxa proteins in prostate cancer. *Prostate*, 66(10), 1013–1028.
- Miyashita, N., Horie, M., Suzuki, H., Yoshihara, M., Djureinovic, D., Persson, J., ... Nagase, T. (2018). TAn integrative analysis of transcriptome and epigenome features of ASCL1-Positive lung adenocarcinomas. *Journal of Thoracic Oncology*, 13(11) 1676-1691.
- Mohammed, H., Taylor, C., Brown, G. D., Papachristou, E. K., Carroll, J. S., & D'Santos, C. S. (2016). Rapid immunoprecipitation mass spectrometry of endogenous proteins (RIME) for analysis of chromatin complexes. *Nature Protocols*, 11(2), 316–326.
- Montori, S., Dos Anjos, S., Poole, A., Regueiro-Purrinos, M. M., Llorente, I. L., Darlison, M. G., ... Martinez-Villayandre, B. (2012). Differential effect of transient global ischaemia on the levels of GABA(A) receptor subunit mRNAs in young and older rats. *Neuropathology and applied Neurobiology*, 38(7), 710-722.
- Mooradian, A. D., Morley, J. E., & Korenman, S. G. (1987). Biological Actions of Androgens. *Endocrine Reviews*, 8(1), 1–28.
- Moraska, A. R., Atherton, P. J., Szydlo, D. W., Barton, D. L., Stella, P. J., Rowland, K. M., ... Loprinzi, C. L. (2010). Gabapentin for the management of hot flashes in prostate cancer survivors: a longitudinal continuation Study-NCCTG Trial N00CB. *The Journal of Supportive Oncology*, 8(3), 128–32.
- Mottet, N., Bellmunt, J., Bolla, M., Joniau, S., Mason, M., Matveev, V., ... Heidenreich, A. (2011). *EAU Guidelines on Prostate Cancer. Part II: Treatment of Advanced, Relapsing, and Castration-Resistant Prostate Cancer. European Urology* (59).
- Mottet, N., Van Damme, J., Loulidi, S., Russel, C., Leitenberger, A., & Wolff, J. M. (2012). Intermittent hormonal therapy in the treatment of metastatic prostate cancer: a randomized trial. *BJU International*, 110(9), 1262–1269.
- Mulligan, M. K., Wang, X., Adler, A. L., Mozhui, K., Lu, L., & Williams, R. W. (2012). Complex Control of GABA(A) Receptor Subunit mRNA Expression: Variation, Covariation, and Genetic Regulation. *PLoS ONE*, 7(4), e34586.
- Myers, R. P. (2000). Structure of the adult prostate from a clinician's standpoint. *Clinical Anatomy*, 13(3), 214–5.
- Nagakawa, O., Ogasawara, M., Fujii, H., Murakami, K., Murata, J., Fuse, H., & Saiki, I. (1998). Effect of prostatic neuropeptides on invasion and migration of PC-3 prostate cancer cells. *Cancer Letters*, 133(1), 27–33.
- Nagakawa, Y., Aoki, T., Kasuya, K., Tsuchida, A., & Koyanagi, Y. (2002). Histologic features of venous invasion, expression of vascular endothelial growth

factor and matrix metalloproteinase-2 and matrix metalloproteinase-9, and the relation with liver metastasis in pancreatic cancer. *Pancreas*, 24(2), 169–78.

Nagase, H., & Woessner, J. F. (1999). Matrix metalloproteinases. *The Journal of Biological Chemistry*, 274(31), 21491–4.

Nakamura, Y., Suzuki, T., Igarashi, K., Kanno, J., Furukawa, T., Tazawa, C., ... Sasano, H. (2006). PTOV1: a novel testosterone-induced atherogenic gene in human aorta. *The Journal of Pathology*, 209(4), 522–531.

Napoleone, P., Bronzetti, E., Cavallotti, C., & Amenta, F. (1990). Predominant epithelial localization of type A gamma-aminobutyric acid receptor sites within rat seminal vesicles and prostate glands. *Pharmacology*, 41(1), 49–56.

Neelands, T. R., Zhang, J., & Macdonald, R. L. (1999). GABA A Receptors Expressed in Undifferentiated Human Teratocarcinoma NT2 Cells Differ from Those Expressed by Differentiated NT2-N Cells. *Journal of Neuroscience*, 19(16), 7057-7065.

Nelson, A. W., Tilley, W. D., Neal, D. E., & Carroll, J. S. (2014). Estrogen receptor beta in prostate cancer: Friend or foe? *Endocrine-Related Cancer*, 21(4), 219–234.

Nelson, B. R., Hartman, B. H., Ray, C. A., Hayashi, T., Bermingham-McDonogh, O., & Reh, T. A. (2009). Acheate-scute like 1 (Ascl1) is required for normal delta-like (Dll) gene expression and notch signaling during retinal development. *Developmental Dynamics : An Official Publication of the American Association of Anatomists*, 238(9), 2163–78.

Neman, J., Termini, J., Wilczynski, S., Vaidehi, N., Choy, C., Kowolik, C. M., ... Jandial, R. (2014). Human breast cancer metastases to the brain display GABAergic properties in the neural niche. *Proceedings of the National Academy of Sciences*, 111(3), 984–989.

Nimmich, M. L., Heidelberg, L. S., & Fisher, J. L. (2009). RNA editing of the GABA(A) receptor alpha3 subunit alters the functional properties of recombinant receptors. *Neuroscience Research*, 63(4), 288–93.

Nishikawa, E., Osada, H., Okazaki, Y., Arima, C., Tomida, S., Tatematsu, Y., ... Takahashi, T. (2011). miR-375 is activated by ASH1 and inhibits YAP1 in a lineage-dependent manner in lung cancer. *Cancer Research*, 71(19), 6165–73.

Noordzij, M. A., van Steenbrugge, G. J., van der Kwast, T. H., & Schröder, F. H. (1995). Neuroendocrine cells in the normal, hyperplastic and neoplastic prostate. *Urological Research*, 22(6), 333–41.

North, A. J. (2006). Seeing is believing? A beginners' guide to practical pitfalls in image acquisition. *The Journal of Cell Biology*, 172(1).

Nuñez, J. L., & McCarthy, M. M. (2008). Androgens predispose males to GABAA-mediated excitotoxicity in the developing hippocampus. *Experimental Neurology*, 210(2), 699–708.

- Obin, M., Mesco, E., Gong, X., Haast, A. L., Joseph, J., & Taylor, A. (1999). Neurite Outgrowth in PC12 Cells Distinguishing the roles of ubiquitylation and ubiquitin-dependent proteolysis. *Journal of Biological Chemistry*, *274*(17), 11789–11795.
- Obrietan, K., Gao, X., Van Den Pol, A. N., Gao, X.-B., & van den Pol, A. N. (2002). Excitatory Actions of GABA Increase BDNF Expression via a MAPK-CREB-Dependent Mechanism-A Positive Feedback Circuit in Developing Neurons Excitatory actions of GABA increase BDNF expression via a MAPK-CREB-dependent mechanism-a positive feedback circuit in developing hypothalamic neurons. *J Neurophysiol*, *88*, 1005–1015.
- Ohlson, J., Pedersen, J. S., Haussler, D., & Ohman, M. (2007). Editing modifies the GABA(A) receptor subunit alpha3. *RNA*, *13*(5), 698–703.
- Oliver, R. T. D., Williams, G., Paris, A. M. I., & Blandy, J. P. (1997). Intermittent androgen deprivation after PSA-complete response as a strategy to reduce induction of hormone-resistant prostate cancer. *Urology*, *49*(1), 79–82.
- Olsen, R. W., & Sieghart, W. (2008). International Union of Pharmacology. LXX. Subtypes of gamma-aminobutyric acid(A) receptors: classification on the basis of subunit composition, pharmacology, and function. Update. *Pharmacological Reviews*, *60*(3), 243–60.
- Orr, B., Grace, O. C., Vanpoucke, G., Ashley, G. R., & Thomson, A. A. (2009). A role for notch signaling in stromal survival and differentiation during prostate development. *Endocrinology*, *150*(1), 463–72.
- Osada, H., Tatematsu, Y., Yatabe, Y., Horio, Y., & Takahashi, T. (2005). ASH1 gene is a specific therapeutic target for lung cancers with neuroendocrine features. *Cancer Research*, *65*(23), 10680–5.
- Osada, H., Tomida, S., Yatabe, Y., Tatematsu, Y., Takeuchi, T., Murakami, H., ... Takahashi, T. (2008). Roles of achaete-scute homologue 1 in DKK1 and E-cadherin repression and neuroendocrine differentiation in lung cancer. *Cancer Research*, *68*(6), 1647–55.
- Palapattu, G. S., Sutcliffe, S., Bastian, P. J., Platz, E. A., De Marzo, A. M., Isaacs, W. B., & Nelson, W. G. (2005). Prostate carcinogenesis and inflammation: emerging insights. *Carcinogenesis*, *26*(7), 1170–81.
- Pallotto, M., & Deprez, F. (2014). Regulation of adult neurogenesis by GABAergic transmission: signaling beyond GABAA-receptors. *Frontiers in Cellular Neuroscience*, *8*, 166.
- Papachristou, E. K., Kishore, K., Holding, A. N., Harvey, K., Roumeliotis, T. I., Chilamakuri, C. S. R., ... Carroll, J. S. (2018). A quantitative mass spectrometry-based approach to monitor the dynamics of endogenous chromatin-associated protein complexes. *Nature Communications*, *9*(1), 2311.
- Paquette, A. J., Perez, S. E., & Anderson, D. J. (2000). Constitutive expression of the neuron-restrictive silencer factor (NRSF)/REST in differentiating neurons

disrupts neuronal gene expression and causes axon pathfinding errors in vivo. *Proceedings of the National Academy of Sciences of the United States of America*, 97(22), 12318–23.

Parimi, V., Goyal, R., Poropatich, K., & Yang, X. J. (2014). Neuroendocrine differentiation of prostate cancer: a review. *American Journal of Clinical and Experimental Urology*, 2(4), 273–85.

Park, N. I., Guilhamon, P., Desai, K., McAdam, R. F., Langille, E., O'Connor, M., ... Dirks, P. B. (2017). ASCL1 Reorganizes Chromatin to Direct Neuronal Fate and Suppress Tumorigenicity of Glioblastoma Stem Cells. *Cell Stem Cell*, 21(2), 209–224.e7.

Patrawala, L., Calhoun, T., Schneider-Broussard, R., Li, H., Bhatia, B., Tang, S., ... Tang, D. G. (2006). Highly purified CD44+ prostate cancer cells from xenograft human tumors are enriched in tumorigenic and metastatic progenitor cells. *Oncogene*, 25(12), 1696–708.

Pawar, A., Gollavilli, P. N., Wang, S., & Asangani, I. A. (2018). Resistance to BET Inhibitor Leads to Alternative Therapeutic Vulnerabilities in Castration-Resistant Prostate Cancer. *Cell Reports*, 22(9), 2236–2245.

Pedrosa, A.-R., Trindade, A., Carvalho, C., Graça, J., Carvalho, S., Peleteiro, M. C., ... Duarte, A. (2015). Endothelial Jagged1 promotes solid tumor growth through both pro-angiogenic and angiocrine functions. *Oncotarget*, 6(27), 24404–24423.

Peltopuro, P., Kala, K., & Partanen, J. (2010). Distinct requirements for Ascl1 in subpopulations of midbrain GABAergic neurons. *Developmental Biology*, 343(1–2), 63–70.

Peng, X., Xu, X., Wang, Y., Hawke, D. H., Yu, S., Han, L., ... Mills, G. B. (2018). A-to-I RNA Editing Contributes to Proteomic Diversity in Cancer. *Cancer Cell*, 33(5), 817–828.e7.

Peran, M., Hooper, H., Rayner, S. L., Stephenson, F. A., & Salas, R. (2004). GABAA receptor $\alpha 1$ and $\alpha 6$ subunits mediate cell surface anchoring in cultured cells. *Neuroscience Letters*, 364(2), 67–70.

Perlmutter, M. A., & Lepor, H. (2007). Androgen deprivation therapy in the treatment of advanced prostate cancer. *Reviews in Urology*, 9 Suppl 1, S3-8.

Price, T. T., Burness, M. L., Sivan, A., Warner, M. J., Cheng, R., Lee, C. H., ... Sipkins, D. A. (2016). Dormant breast cancer micrometastases reside in specific bone marrow niches that regulate their transit to and from bone. *Science Translational Medicine*, 8(340), 340ra73.

Prolo, L. M., Li, A., Morgens, D., Reimer, R., Bassik, M., & Grant, G. A. (2017). 137 Novel Genome-wide CRISPR Screen for Glioblastoma Invasion. *Neurosurgery*, 64(CN_suppl_1), 232–232.

Puthenkalam, R., Hieckel, M., Simeone, X., Suwattanasophon, C., Feldbauer, R.

V, Ecker, G. F., & Ernst, M. (2016). Structural Studies of GABAA Receptor Binding Sites: Which Experimental Structure Tells us What? *Frontiers in Molecular Neuroscience*, 9, 44.

Qian, H. (1995). GABAC Receptors in the Vertebrate Retina. *Molecular Neurobiology*, 12(3), 181-194

Rada-Iglesias, A., Bajpai, R., Swigut, T., Brugmann, S. A., Flynn, R. A., & Wysocka, J. (2011). A unique chromatin signature uncovers early developmental enhancers in humans. *Nature*, 470(7333), 279–283.

Rao, V. R., Perez-Neut, M., Kaja, S., & Gentile, S. (2015). Voltage-gated ion channels in cancer cell proliferation. *Cancers*, 7(2), 849–75.

Rapa, I., Ceppi, P., Bollito, E., Rosas, R., Cappia, S., Bacillo, E., ... Volante, M. (2008). Human ASH1 expression in prostate cancer with neuroendocrine differentiation. *Modern Pathology: An Official Journal of the United States and Canadian Academy of Pathology, Inc*, 21(6), 700–7.

Rapa, I., Volante, M., Migliore, C., Farsetti, A., Berruti, A., Vittorio Scagliotti, G., ... Papotti, M. (2013). Human ASH-1 promotes neuroendocrine differentiation in androgen deprivation conditions and interferes with androgen responsiveness in prostate cancer cells. *The Prostate*, 73(11), 1241–9.

Raposo, A. A. S. F., Vasconcelos, F. F., Drechsel, D., Marie, C., Johnston, C., Dolle, D., ... Castro, D. S. (2015). Ascl1 Coordinately Regulates Gene Expression and the Chromatin Landscape during Neurogenesis. *Cell Reports*, 10(9), 1544-1556.

Ranna, M., Sinkkonen, S. T., Möykkynen, T., Uusi-Oukari, M., & Korpi, E. R. (2006). Impact of ϵ and θ subunits on pharmacological properties of $\alpha 3\beta 1$ GABA A receptors expressed in *Xenopus* oocytes.

Rech, T. H., Vieira, S. R. R., Nagel, F., Brauner, J. S., & Scalco, R. (2006). Serum neuron-specific enolase as early predictor of outcome after in-hospital cardiac arrest: a cohort study. *Critical Care (London, England)*, 10(5), 133.

Reyes, E. E., Kunovac, S. K., Duggan, R., Kregel, S., & Vander Griend, D. J. (2013). Growth kinetics of CD133-positive prostate cancer cells. *The Prostate*, 73(7), 724–33.

Ristorcelli, E., Beraud, E., Mathieu, S., Lombardo, D., & Verine, A. (2009). Essential role of Notch signaling in apoptosis of human pancreatic tumoral cells mediated by exosomal nanoparticles. *International Journal of Cancer*, 125(5), 1016–1026.

Ritta, M. N., Campos, M. B., & Calandra, R. S. (1987). Effect of GABA and benzodiazepines on testicular androgen production. *Life Sciences*, 40(8), 791–8.

Robinson, J. L. L., & Carroll, J. S. (2012). FoxA1 is a key mediator of hormonal response in breast and prostate cancer. *Frontiers in Endocrinology*, 3(MAY), 1–6.

Roderfeld, M., Graf, J., Giese, B., Salguero-Palacios, R., Tschuschner, A., Müller-Newen, G., & Roeb, E. (2007). Latent MMP-9 is bound to TIMP-1 before secretion. *Biological Chemistry*, 388(11), 1227–34.

Rose, M. A., & Kam, P. C. A. (2002). Gabapentin: Pharmacology and its use in pain management. *Anaesthesia*, 57(5), 451–462.

Rudin, C. M., Pietanza, M. C., Bauer, T. M., Ready, N., Morgensztern, D., Glisson, B. S., ... SCRX16-001 investigators. (2017). Rovalpituzumab tesirine, a DLL3-targeted antibody-drug conjugate, in recurrent small-cell lung cancer: a first-in-human, first-in-class, open-label, phase 1 study. *The Lancet. Oncology*, 18(1), 42–51.

Ryan, C. J., Smith, M. R., Fizazi, K., Saad, F., Mulders, P. F. A., Sternberg, C. N., ... Rathkopf, D. E. (2015). Abiraterone acetate plus prednisone versus placebo plus prednisone in chemotherapy-naïve men with metastatic castration-resistant prostate cancer (COU-AA-302): final overall survival analysis of a randomised, double-blind, placebo-controlled phase 3 study. *The Lancet Oncology*, 16(2), 152–60.

Rybak, A. P., Ingram, A. J., & Tang, D. (2013). Propagation of Human Prostate Cancer Stem-Like Cells Occurs through EGFR-Mediated ERK Activation. *PLoS ONE*, 8(4), e61716.

Saad, F., Chi, K. N., Finelli, A., Hotte, S. J., Izawa, J., Kapoor, A., ... Fleshner, N. E. (2015). The 2015 CUA-CUOG Guidelines for the management of castration-resistant prostate cancer (CRPC). *Canadian Urological Association Journal = Journal de l'Association Des Urologues Du Canada*, 9(3–4), 90–6.

Sarkar, D., Singh, S. K., Mandal, A. K., Agarwal, M. M., Mete, U. K., Kumar, S., ... Prasad, R. (2011). Plasma chromogranin A: Clinical implications in patients with castrate resistant prostate cancer receiving docetaxel chemotherapy. *Cancer Biomarkers*, 8(2), 81–87.

Satoh, T., Uemura, H., Tanabe, K., Nishiyama, T., Terai, A., Yokomizo, A., ... Akaza, H. (2014). A phase 2 study of abiraterone acetate in Japanese men with metastatic castration-resistant prostate cancer who had received docetaxel-based chemotherapy. *Japanese Journal of Clinical Oncology*, 44(12), 1206–15.

Sauer, C. G., Roemer, A., & Grobholz, R. (2006). Genetic analysis of neuroendocrine tumor cells in prostatic carcinoma. *The Prostate*, 66(3), 227–234.

Scher, H., & Kelly, W. (1993). Flutamide withdrawal syndrome: its impact on clinical trials in hormone-refractory prostate cancer. *J. Clin. Oncol.*, 11(8), 1566–1572.

Schmechel, D., Marangos, P. J., & Brightman, M. (n.d.). Neurone-specific enolase is a molecular marker for peripheral and central neuroendocrine cells. *Nature*, 276(5690), 834–6.

Schneider, C. A., Rasband, W. S., & Eliceiri, K. W. (2012). NIH Image to ImageJ: 25 years of image analysis. *Nature Methods*, 9(7), 671–675.

- Scholl, U. I., Goh, G., Stölting, G., de Oliveira, R. C., Choi, M., Overton, J. D., ... Lifton, R. P. (2013). Somatic and germline CACNA1D calcium channel mutations in aldosterone-producing adenomas and primary aldosteronism. *Nature Genetics*, 45(9), 1050–4.
- Seruga, B., & Tannock, I. F. (2008). Intermittent androgen blockade should be regarded as standard therapy in prostate cancer. *Nature Clinical Practice Oncology*, 5(10), 574–576.
- Serwanski, D. R., Miralles, C. P., Christie, S. B., Mehta, A. K., Li, X., & De Blas, A. L. (2006). Synaptic and nonsynaptic localization of GABA_A receptors containing the alpha5 subunit in the rat brain. *The Journal of Comparative Neurology*, 499(3), 458–70.
- Seshi, B., True, L., Carter, D., & Rosai, J. (1988). Immunohistochemical characterization of a set of monoclonal antibodies to human neuron-specific enolase. *The American Journal of Pathology*, 131(2), 258–69.
- Sflomos, G., Dormoy, V., Metsalu, T., Vilo, J., Ayyanan, A., Correspondence, C. B., ... Brisken, C. (2016). A Preclinical Model for ER α -Positive Breast Cancer Points to the Epithelial Microenvironment as Determinant of Luminal Phenotype and Hormone Response. *Cancer Cell*, 29, 407–422.
- Shen, M. M., & Abate-Shen, C. (2010). Molecular genetics of prostate cancer: new prospects for old challenges. *Genes & Development*, 24(18), 1967–2000.
- Shen, R., Dorai, T., Szaboles, M., Katz, a E., Olsson, C. a, & Buttyan, R. (1997). Transdifferentiation of cultured human prostate cancer cells to a neuroendocrine cell phenotype in a hormone-depleted medium. *Urologic Oncology*, 3(2), 67–75.
- Shi, J., & Vakoc, C. R. (2014). The mechanisms behind the therapeutic activity of BET bromodomain inhibition. *Molecular Cell*, 54(5), 728–36.
- Shiozaki, A., Nako, Y., Ichikawa, D., Konishi, H., Komatsu, S., Kubota, T., ... Otsuji, E. (2014). Role of the Na⁺/K⁺/2Cl⁻ cotransporter NKCC1 in cell cycle progression in human esophageal squamous cell carcinoma. *World Journal of Gastroenterology*, 20(22), 6844–59.
- Shiozaki, A., Takemoto, K., Ichikawa, D., Fujiwara, H., Konishi, H., Kosuga, T., ... Otsuji, E. (2014). The K-Cl cotransporter KCC3 as an independent prognostic factor in human esophageal squamous cell carcinoma. *BioMed Research International*, 2014, 936401.
- Shore, N. D., & Crawford, E. D. (2010). Intermittent androgen deprivation therapy: redefining the standard of care? *Reviews in Urology*, 12(1), 1–11.
- Shukla, S., Cyrta, J., Murphy, D. A., Walczak, E. G., Ran, L., Agrawal, P., ... Chen, Y. (2017). Aberrant Activation of a Gastrointestinal Transcriptional Circuit in Prostate Cancer Mediates Castration Resistance. *Cancer Cell*, 1–15.
- Sigel, E., & Steinmann, M. E. (2012). Structure, Function, and Modulation of GABA_A Receptors. *Journal of Biological Chemistry*, 287(48), 40224–40231.

Simon, D. B., Karet, F. E., Hamdan, J. M., Pietro, A. Di, Sanjad, S. A., & Lifton, R. P. (1996). Bartter's syndrome, hypokalaemic alkalosis with hypercalciuria, is caused by mutations in the Na–K–2Cl cotransporter NKCC2. *Nature Genetics*, 13(2), 183–188.

Singh, S., Gauthier, S., & Labrie, F. (2000). Androgen Receptor Antagonists (Antiandrogens) Structure-Activity Relationships. *Current Medicinal Chemistry*, 7(2), 211–247.

Smith, J. R., Chipps, T. J., Ilias, H., Pan, Y., & Appukuttan, B. (2012). Expression and regulation of activated leukocyte cell adhesion molecule in human retinal vascular endothelial cells. *Experimental Eye Research*, 104, 89–93.

Soghomonian, J. J., & Martin, D. L. (1998). Two isoforms of glutamate decarboxylase: why? *Trends in Pharmacological Sciences*, 19(12), 500–5.

Somasundaram, K., Reddy, S. P., Vinnakota, K., Britto, R., Subbarayan, M., Nambiar, S., ... Rao, M. R. S. (2005). Upregulation of ASCL1 and inhibition of Notch signaling pathway characterize progressive astrocytoma. *Oncogene*, 24(47), 7073–7083.

Solorzano, S., Imaz-Rosshandler, I., Camacho-Arroyo, I., Garcia-Tobilla, P., Morales-Montor, G., Salazar, P., Arena-Ortiz, M., Rodriguez-Dorantes, M. (2018). GABA promotes gastrin-releasing peptide secretion in NE/NE-like cells: Contribution to prostate cancer progression. *Scientific Reports*, 8(1) 10272.

Sriuranpong, V., Borges, M. W., Strock, C. L., Nakakura, E. K., Watkins, D. N., Blaumueller, C. M., ... Ball, D. W. (2002). Notch signaling induces rapid degradation of achaete-scute homolog 1. *Molecular and Cellular Biology*, 22(9), 3129–39.

Steiger, J. L., & Russek, S. J. (2004). GABAA receptors: building the bridge between subunit mRNAs, their promoters, and cognate transcription factors. *Pharmacology & Therapeutics*, 101(3), 259–281.

Steinberg, G. D., Carter, B. S., Beaty, T. H., Childs, B., & Walsh, P. C. (1990). Family history and the risk of prostate cancer. *The Prostate*, 17(4), 337–47.

Stone, K. R., Mickey, D. D., Wunderli, H., Mickey, G. H., & Paulson, D. F. (1978). Isolation of a human prostate carcinoma cell line (DU 145). *International Journal of Cancer*, 21(3), 274–81.

Succol, F., Fiumelli, H., Benfenati, F., Cancedda, L., & Barberis, A. (2012). Intracellular chloride concentration influences the GABAA receptor subunit composition. *Nature Communications*, 3, 738.

Svensson, C., Ceder, J., Iglesias-Gato, D., Chuan, Y.-C., Pang, S. T., Bjartell, A., ... Flores-Morales, A. (2014). REST mediates androgen receptor actions on gene repression and predicts early recurrence of prostate cancer. *Nucleic Acids Research*, 42(2), 999–1015.

Symmans, W. F., Fiterman, D. J., Anderson, S. K., Ayers, M., Rouzier, R.,

Dunmire, V., ... Puzstai, L. (2005). A single-gene biomarker identifies breast cancers associated with immature cell type and short duration of prior breastfeeding. *Endocrine Related Cancer*, 12(4), 1059–1069.

Szklarczyk, D., Gable, A. L., Lyon, D., Junge, A., Wyder, S., Huerta-Cepas, J., ... Mering, C. von. (2019). STRING v11: protein–protein association networks with increased coverage, supporting functional discovery in genome-wide experimental datasets. *Nucleic Acids Research*, 47(D1), D607–D613.

Takeda, K., Kermani, P., Anastasia, A., Obinata, Y., Hempstead, B. L., & Kurihara, H. (2013). BDNF protects human vascular endothelial cells from TNF α -induced apoptosis. *Biochemistry and Cell Biology*, 91(5), 341–349.

Takehara, A., Hosokawa, M., Eguchi, H., Ohigashi, H., Ishikawa, O., Nakamura, Y., & Nakagawa, H. (2007). γ -Aminobutyric Acid (GABA) Stimulates Pancreatic Cancer Growth through Overexpressing GABAA Receptor Subunits. *Cancer Research*, 67(20), 9704–9712.

Tamura, M., Gu, J., Danen, E. H., Takino, T., Miyamoto, S., & Yamada, K. M. (1999). PTEN interactions with focal adhesion kinase and suppression of the extracellular matrix-dependent phosphatidylinositol 3-kinase/Akt cell survival pathway. *The Journal of Biological Chemistry*, 274(29), 20693–703.

Tawadros, T., Alonso, F., Jichlinski, P., Clarke, N., Calandra, T., Haefliger, J.-A., & Roger, T. (2013). Release of macrophage migration inhibitory factor by neuroendocrine-differentiated LNCaP cells sustains the proliferation and survival of prostate cancer cells. *Endocrine-Related Cancer*, 20(1), 137–49.

Taylor, C. P. (1997). Mechanisms of action of gabapentin. *Revue Neurologique*, 153(1), 39-45.

Taylor, C. P., Gee, N. S., Su, T.-Z., Kocsis, J. D., Welty, D. F., Brown, J. P., ... Singh, L. (1998). A summary of mechanistic hypotheses of gabapentin pharmacology. *Epilepsy Research*, 29(3), 233–249.

Taylor, C. P., Vartanian, M. G., Andruszkiewicz, R., & Silverman, R. B. (1992). 3-alkyl GABA and 3-alkylglutamic acid analogues: two new classes of anticonvulsant agents. *Epilepsy Research*, 11(2), 103–110.

Terry, S., & Beltran, H. (2014). The many faces of neuroendocrine differentiation in prostate cancer progression. *Frontiers in Oncology*, 4, 60.

Tisell, L. E., & Salander, H. (1975). The lobes of the human prostate. *Scandinavian Journal of Urology and Nephrology*, 9(3), 185–91.

Tomlins, S. A., Laxman, B., Varambally, S., Cao, X., Yu, J., Helgeson, B. E., ... Chinnaiyan, A. M. (2008). Role of the TMPRSS2-ERG gene fusion in prostate cancer. *Neoplasia*, 10(2), 177–88.

Tretter, V., Ehya, N., Fuchs, K., & Sieghart, W. (1997). Stoichiometry and assembly of a recombinant GABAA receptor subtype. *The Journal of Neuroscience : The Official Journal of the Society for Neuroscience*, 17(8), 2728–

37.

Tu, S.-M., & Lin, S.-H. (2012). Prostate cancer stem cells. *Clinical Genitourinary Cancer*, *10*(2), 69–76.

Tyagi, N., Lominadze, D., Gillespie, W., Moshal, K. S., Sen, U., Rosenberger, D. S., ... Tyagi, S. C. (2007). Differential expression of γ -aminobutyric acid receptor A (GABAA) and effects of homocysteine. *Clinical Chemical Laboratory Medicine*, *45*(12), 1777–84.

Unger, J. M., Hershman, D. L., Till, C., Tangen, C. M., Barlow, W. E., Ramsey, S. D., ... Thompson, I. M. (2018). Using Medicare Claims to Examine Long-term Prostate Cancer Risk of Finasteride in the Prostate Cancer Prevention Trial. *JNCI: Journal of the National Cancer Institute*, *110*(11), 1208–1215.

Unni, E., Sun, S., Nan, B., McPhaul, M. J., Cheskis, B., Mancini, M. A., & Marcelli, M. (2004). Changes in Androgen Receptor Nongenotropic Signaling Correlate with Transition of LNCaP Cells to Androgen Independence. *Cancer Research*, *64*(19), 7156–7168.

Vale, C. L., Burdett, S., Rydzewska, L. H. M., Albiges, L., Clarke, N. W., Fisher, D., ... STOpCaP Steering Group. (2016). Addition of docetaxel or bisphosphonates to standard of care in men with localised or metastatic, hormone-sensitive prostate cancer: a systematic review and meta-analysis of aggregate data. *The Lancet. Oncology*, *17*(2), 243–256.

Valero, M. L., Mello de Queiroz, F., Stühmer, W., Viana, F., & Pardo, L. A. (2012). TRPM8 Ion Channels Differentially Modulate Proliferation and Cell Cycle Distribution of Normal and Cancer Prostate Cells. *PLoS ONE*, *7*(12), e51825.

Vander-Griend, D., Litvinov, I., Isaacs, J. (2014). Conversion of androgen receptor signalling from a growth suppressor in normal prostate epithelial cells to an oncogene in prostate cancer cells involves a gain of function in c-Myc regulation. *International Journal of Biological Sciences*, *10*(6), 627-642.

Vasconcelos, F. F., & Castro, D. S. (2014). Transcriptional control of vertebrate neurogenesis by the proneural factor *Ascl1*. *Frontiers in Cellular Neuroscience*, *8*, 412.

Vedula, S. S., Li, T., & Dickersin, K. (2013). Differences in reporting of analyses in internal company documents versus published trial reports: comparisons in industry-sponsored trials in off-label uses of gabapentin. *PLoS Medicine*, *10*(1), e1001378.

Verma, A., St Onge, J., Dhillon, K., & Chorneyko, A. (2014). PSA density improves prediction of prostate cancer. *The Canadian Journal of Urology*, *21*(3), 7312–21.

Vierbuchen, T., Ostermeier, A., Pang, Z. P., Kokubu, Y., Südhof, T. C., & Wernig, M. (2010). Direct conversion of fibroblasts to functional neurons by defined factors. *Nature*, *463*(7284), 1035–1041.

Vlachostergios, P. J., & Papandreou, C. N. (2015a). Targeting neuroendocrine prostate cancer: molecular and clinical perspectives. *Frontiers in Oncology*, 5, 6.

von Amsberg, G., Stroelin, P., Bokemeyer, C., & Steuber, T. (2014). [Current treatment concepts for castration resistant prostate cancer]. *Deutsche Medizinische Wochenschrift*, 139(41), 2086–90.

Wadhwa, E., & Nicolaidis, T. (2016). Bromodomain Inhibitor Review: Bromodomain and Extra-terminal Family Protein Inhibitors as a Potential New Therapy in Central Nervous System Tumors. *Cureus*, 8(5), e620.

Wang, C.-Y., Shahi, P., Huang, J. T. W., Phan, N. N., Sun, Z., Lin, Y.-C., ... Werb, Z. (2017). Systematic analysis of the achaete-scute complex-like gene signature in clinical cancer patients. *Molecular and Clinical Oncology*, 6(1), 7–18.

Wang, C., Peng, G., Huang, H., Liu, F., Kong, D.-P., Dong, K.-Q., ... Sun, Y.-H. (2018). Blocking the Feedback Loop between Neuroendocrine Differentiation and Macrophages Improves the Therapeutic Effects of Enzalutamide (MDV3100) on Prostate Cancer. *Clinical Cancer Research*, 24(3), 708–723.

Wang, H.-Y., Juo, L.-I., Lin, Y.-T., Hsiao, M., Lin, J.-T., Tsai, C.-H., ... Lu, P.-J. (2012). WW domain-containing oxidoreductase promotes neuronal differentiation via negative regulation of glycogen synthase kinase 3 β . *Cell Death and Differentiation*, 19(6), 1049–1059.

Wang, X.-D., Leow, C. C., Zha, J., Tang, Z., Modrusan, Z., Radtke, F., ... Gao, W.-Q. (2010). Notch signaling is required for normal prostatic epithelial cell proliferation and differentiation. *Developmental Biology*, 290, 66–80.

Wang, X.-D., Shou, J., Wong, P., French, D. M., & Gao, W.-Q. (2004). Notch1-expressing Cells Are Indispensable for Prostatic Branching Morphogenesis during Development and Re-growth Following Castration and Androgen Replacement. *Journal of Biological Chemistry*, 279(23), 24733–24744.

Wapinski, O. L., Lee, Y., Chen, A. C., Dahmane, N., Wernig, M., & Chang, H. Y. (2017). Rapid Chromatin Switch in the Direct Reprogramming of Fibroblasts to Neurons. *Cell Reports*, 20, 3236–3247.

Wapinski, O. L., Vierbuchen, T., Qu, K., Lee, Q. Y., Chanda, S., Fuentes, D. R., ... Wernig, M. (2013). Hierarchical Mechanisms for Direct Reprogramming of Fibroblasts to Neurons. *Cell*, 155(3), 621–635.

Warnier, M., Roudbaraki, M., Derouiche, S., Delcourt, P., Bokhobza, A., Prevarskaya, N., & Mariot, P. (2015). CACNA2D2 promotes tumorigenesis by stimulating cell proliferation and angiogenesis. *Oncogene*, 34(42), 5383–5394.

Watanabe, M., Maemura, K., Oki, K., Shiraishi, N., Shibayama, Y., & Katsu, K. (2006). Gamma-aminobutyric acid (GABA) and cell proliferation: focus on cancer cells. *Histology and Histopathology*, 21(10), 1135–41.

Westbrook, T. F., Martin, E. S., Schlabach, M. R., Leng, Y., Liang, A. C., Feng, B., ... Elledge, S. J. (2005). A genetic screen for candidate tumor suppressors

identifies REST. *Cell*, 121(6), 837–48.

Whiting, P. J., McKernan, R. M., & Wafford, K. A. (1995). Structure and pharmacology of vertebrate GABAA receptor subtypes. *International Review of Neurobiology*, 38, 95–138.

Wilkinson, G., Dennis, D., & Schuurmans, C. (2013). Proneural genes in neocortical development. *Neuroscience*, 253, 256–273.

Wilson, J. D. (2011). The Critical Role of Androgens in Prostate Development. *Endocrinology and Metabolism Clinics of North America*, 40(3), 577–590.

Wong, R. O. L., & Ghosh, A. (2002). Activity-dependent regulation of dendritic growth and patterning. *Nature Reviews Neuroscience*, 3(10), 803–812.

Woodward, R. M., Polenzani, L., & Miledi, R. (1993). Characterization of bicuculline/baclofen-insensitive (rho-like) gamma-aminobutyric acid receptors expressed in *Xenopus* oocytes. II. Pharmacology of gamma-aminobutyric acidA and gamma-aminobutyric acidB receptor agonists and antagonists. *Molecular Pharmacology*, 43(4), 609–25.

Wu, C. L., Chou, Y. H., Chang, Y. J., Teng, N. Y., Hsu, H. L., & Chen, L. (2012). Interplay between cell migration and neurite outgrowth determines SH2B1??-enhanced neurite regeneration of differentiated PC12 cells. *PLoS ONE*, 7(4).

Wu, W., Yang, Q., Fung, K.-M., Humphreys, M. R., Brame, L. S., Cao, A., ... Lin, H.-K. (2014). Linking γ -aminobutyric acid A receptor to epidermal growth factor receptor pathways activation in human prostate cancer. *Molecular and Cellular Endocrinology*, 383(1–2), 69–79.

Wylie, L. A., Hardwick, L. J. A., Papkovskaia, T. D., Thiele, C. J., & Philpott, A. (2015). Ascl1 phospho-status regulates neuronal differentiation in a *Xenopus* developmental model of neuroblastoma. *Disease Models & Mechanisms*, 8(5),

Xia, D., Lai, D. V., Wu, W., Webb, Z. D., Yang, Q., Zhao, L., ... Lin, H.-K. (2018). Transition from androgenic to neurosteroidal action of 5 α -androstane-3 α , 17 β -diol through the type A γ -aminobutyric acid receptor in prostate cancer progression. *The Journal of Steroid Biochemistry and Molecular Biology*, 178, 89–98.

Xia, S., He, C., Zhu, Y., Wang, S., Li, H., Zhang, Z., ... Liu, J. (2017). GABA_B R-Induced EGFR Transactivation Promotes Migration of Human Prostate Cancer Cells. *Molecular Pharmacology*, 92(3), 265–277.

Xing, N., Qian, J., Bostwick, D., Bergstralh, E., & Young, C. Y. (2001). Neuroendocrine cells in human prostate over-express the anti-apoptosis protein survivin. *The Prostate*, 48(1), 7–15.

Yadav, S. S., Li, J., Stockert, J. A., Herzog, B., O'connor, J., Garzon-Manco, L., ... Yadav, K. K. (2017). Induction of Neuroendocrine Differentiation in Prostate Cancer Cells by Dovitinib (TKI-258) and its Therapeutic Implications. *Translational Oncology*, 10, 357–366.

Yang, N., Chanda, S., Marro, S., Ng, Y.-H., Janas, J. A., Haag, D., ... Wernig, M. (2017). Generation of pure GABAergic neurons by transcription factor programming. *Nature Methods*, 14(6), 621–628.

Ye, J., Coulouris, G., Zaretskaya, I., Cutcutache, I., Rozen, S., & Madden, T. L. (2012). Primer-BLAST: a tool to design target-specific primers for polymerase chain reaction. *BMC Bioinformatics*, 13(1), 134.

Yogeeswari, P., Ragavendran, J., & Sriram, D. (2006). An Update on GABA Analogs for CNS Drug Discovery. *Recent Patents on CNS Drug Discovery*, 1(1), 113–118.

Young, S. Z., & Bordey, A. (2009). GABA's control of stem and cancer cell proliferation in adult neural and peripheral niches. *Physiology (Bethesda, Md.)*, 24, 171–85.

Yu, J., Yu, J., Mani, R.-S., Cao, Q., Brenner, C. J., Cao, X., ... Chinnaiyan, A. M. (2010). An integrated network of androgen receptor, polycomb, and TMPRSS2-ERG gene fusions in prostate cancer progression. *Cancer Cell*, 17(5), 443–54.

Yuan, T.-C., Veeramani, S., Lin, F.-F., Kondrikou, D., Zelivianski, S., Igawa, T., ... Lin, M.-F. (2006). Androgen deprivation induces human prostate epithelial neuroendocrine differentiation of androgen-sensitive LNCaP cells. *Endocrine-Related Cancer*, 13(1), 151–67.

Yuan, T.-C., Veeramani, S., & Lin, M.-F. (2007). Neuroendocrine-like prostate cancer cells: neuroendocrine transdifferentiation of prostate adenocarcinoma cells. *Endocrine-Related Cancer*, 14(3), 531–47.

Zaret, K. S., & Carroll, J. S. (2011). Pioneer transcription factors: establishing competence for gene expression. *Genes & Development*, 25(21), 2227–41.

Zarif, J. C., Lamb, L. E., Schulz, V. S., Nollet, E. A., & Miranti, C. K. (2015). Androgen receptor non-nuclear regulation of prostate cancer cell invasion mediated by Src and matriptase. *Oncotarget*, 6(9), 6862–76.

Zarnowska, E. D., Keist, R., Rudolph, U., & Pearce, R. A. (2009). GABAA receptor alpha5 subunits contribute to GABAA,slow synaptic inhibition in mouse hippocampus. *Journal of Neurophysiology*, 101(3), 1179–91.

Zhang, K., & Waxman, D. J. (2010). PC3 prostate tumor-initiating cells with molecular profile FAM65Bhigh/MFI2low/LEF1low increase tumor angiogenesis. *Molecular Cancer*, 9, 319.

Zhang, K., & Waxman, D. J. (2013). Impact of tumor vascularity on responsiveness to antiangiogenesis in a prostate cancer stem cell-derived tumor model. *Molecular Cancer Therapeutics*, 12(5), 787–98.

Zhang, S., Wu, X., Jiang, T., Lu, Y., Ma, L., Liang, M., & Sun, X. (2009). The up-regulation of KCC1 gene expression in cervical cancer cells by IGF-II through the ERK1/2MAPK and PI3K/AKT pathways and its significance. *European Journal of Gynaecological Oncology*, 30(1), 29–34.

Zhang, W., Girard, L., Zhang, Y.-A., Haruki, T., Papari-Zareei, M., Stastny, V., ... Gazdar, A. F. (2018). Small cell lung cancer tumors and preclinical models display heterogeneity of neuroendocrine phenotypes. *Translational Lung Cancer Research*, 7(1), 32–49.

Zhang, X., Coleman, I. M., Brown, L. G., True, L. D., Kollath, L., Lucas, J. M., ... Morrissey, C. (2015). SRRM4 Expression and the Loss of REST Activity May Promote the Emergence of the Neuroendocrine Phenotype in Castration-Resistant Prostate Cancer. *Clinical Cancer Research: An Official Journal of the American Association for Cancer Research*, 21(20), 4698–708.

Zhang, X., Zhang, R., Zheng, Y., Shen, J., Xiao, D., Li, J., ... Zhang, H. (2013). Expression of gamma-aminobutyric acid receptors on neoplastic growth and prediction of prognosis in non-small cell lung cancer. *Journal of Translational Medicine*, 11, 102.

Zhang, Y., Zheng, D., Zhou, T., Song, H., Hulsurkar, M., Su, N., ... Li, W. (2018). Androgen deprivation promotes neuroendocrine differentiation and angiogenesis through CREB-EZH2-TSP1 pathway in prostate cancers. *Nature Communications*, 9(1), 4080.

Zheleznova, N. N., Sedelnikova, A., & Weiss, D. S. (2009). Function and modulation of delta-containing GABA(A) receptors. *Psychoneuroendocrinology*, 34 Suppl 1, S67-73.

Zhu, Y., Liu, C., Cui, Y., Nadiminty, N., Lou, W., & Gao, A. C. (2014). Interleukin-6 induces neuroendocrine differentiation (NED) through suppression of RE-1 silencing transcription factor (REST). *The Prostate*, 74(11), 1086–94.

Zou, M., Toivanen, R., Mitrofanova, A., Floch, N., Hayati, S., Sun, Y., ... Abate-Shen, C. (2017). Transdifferentiation as a Mechanism of Treatment Resistance in a Mouse Model of Castration-Resistant Prostate Cancer. *Cancer Discovery*, 7(7), 736–749.

Zvejniece, L., Vavers, E., Svalbe, B., Veinberg, G., Rizhanova, K., Liepins, V., ... Dambrova, M. (2015). R-phenibut binds to the $\alpha 2\text{-}\delta$ subunit of voltage-dependent calcium channels and exerts gabapentin-like anti-nociceptive effects. *Pharmacology Biochemistry and Behavior*, 137, 23–29.

APPENDIX

8.1 Investigation of androgen receptor splice variants induced by AD

LNCaP cells which were maintained in AD conditions (AD and V) showed robust expression of a lower molecular weight band in the AR immunoblot, this is approximately 95 kDa (Fig. 4.4). Differentiated LNCaP cells which had 1 nM R1881 re-introduced to their culture conditions lost expression of this additional band (Fig. 4.4).

This prompted investigation of possible AR splice variants that may have been targeted by the AR antibody SC-815. The antibody used in this study was confirmed by the manufacturer (Santa Cruz Biotechnology, USA) to target amino acids in the region 869-919 at the C-Terminus of human androgen receptor (accession: P10275) which encodes exons 5-8 of the full-length AR protein, comprising the ligand binding domain. The manufacturer was not willing to give the precise peptide sequence of the immunogen. Consulting the literature and the Ensembl genome browser 91, identified 18 known AR splice variants (Fig. 8.1), of which AR-45 and AR-23 retain exons 5-8 and therefore could be targeted by the SC-815 antibody. However, only AR-45 is truncated (at the N-terminus) and therefore a lower molecular weight than the full-length AR protein. However, AR-45 is reported to be 45 kDa (Lu & Luo, 2013), whereas the additional immunoblot band identified in this study is approximately 95 kDa. A previous study has demonstrated that AR-23 is of a higher molecular weight than the endogenous LNCaP AR protein, thereby ruling out the possibility that the additional band is AR-23 (Jagla *et al.*, 2007). This analysis would suggest that the additional bands observed in the immunoblot are likely to be protein degradation products, rather than an AR splice variant. Ideally, an antibody targeting the highly conserved N-terminus of AR (such as sc-816, widely used in the literature (He *et al.*, 2018)) could be used to better investigate the potential induction of AR splice variants by AD and their likely identity, however this was not completed during this project.

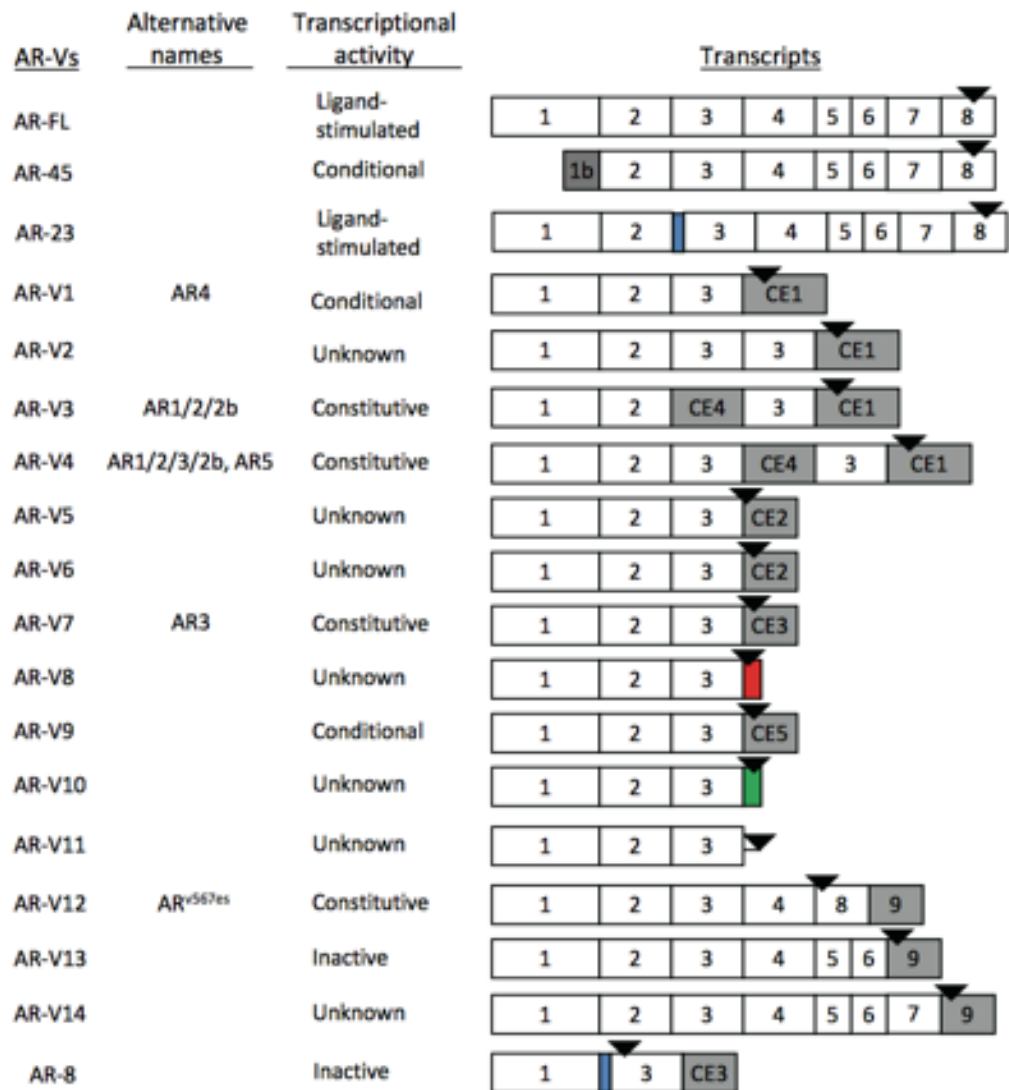


Figure 8.1. Diagram displaying known androgen receptor splice variants and their exon composition adapted from Lu and Luo, 2013.